Optimizing Lightweight Concrete Mix Design: Balancing Ecological and Technical Attributes for Sustainable Construction

Timo Niels Haller

Vollständiger Abdruck der von der Fakultät für Bauingenieurwesen und Umweltwissenschaften der Universität der Bundeswehr München zur Erlangung des akademischen Grades eines

Doktor-Ingenieurs (Dr.-Ing.)

angenommenen Dissertation.

Gutachter/Gutachterin:

1. Univ.-Prof. Dr.-Ing. Karl-Christian Thienel
2. Prof. Dr.-Ing. Harald Garrecht, Universität Stuttgart
3. Prof. Dr.-Ing Andrea Kustermann, Hochschule München

Die Dissertation wurde am 18.06.2025 bei der Universität der Bundeswehr München eingereicht und durch die Fakultät für Bauingenieurwesen und Umweltwissenschaften am 17.11.2025 angenommen. Die mündliche Prüfung fand am 17.11.2025 statt.

Abstract

Modern construction faces the dual pressures of environmental responsibility and technological advancement. This research focuses on lightweight concretes designed for monolithic exterior walls that inherently meet thermal requirements without additional insulation. These concretes are well positioned to address the present challenges by offering a unique combination of low density, thermal efficiency, and potential for material circularity. The experimental findings are based on three fundamental case studies, each exploring different strategies for optimizing lightweight concrete technologies under real-world conditions and providing empirically based solutions for their integration into modern construction practices.

While pumping is well established for normal concrete, the porous, lightweight aggregates of lightweight concrete present unique challenges. For the first time, it has been demonstrated that infra-lightweight concrete can be successfully pumped using piston, eccentric screw, and rotor pump, provided that the mix design is optimized and handling is carefully managed. The rotor pump proved most efficient, minimizing mechanical abrasion and preserving workability. Key properties, including compressive strength, flexural strength, and modulus of elasticity, remained consistent, confirming that pumping does not compromise material integrity.

The combination of lightweight concrete with an open structure and steel frameworks presents an innovative solution for prefabricated wall elements that meet modern energy requirements. The concrete mix is optimized for maximum density reduction to achieve low thermal conductivity, while providing sufficient lateral support for the slender steel structure, which is susceptible to buckling. Key concrete performance parameters such as strength, modulus of elasticity, shrinkage, creep, and sustained loading behavior aligned with normative guidelines. Mechanical tests demonstrated that the composite elements achieved three times the load capacity of standalone steel sections. The study also confirmed the scalability of this design from laboratory testing to factory production.

Recycling of infra-lightweight concrete addresses existing limitations in recycling standards and presents viable pathways for sustainable construction. The recycled products have been evaluated for their suitability in new concrete formulations and their potential to sequester CO_2. The mix design of the recycled concrete uses 100 % recycled material as the aggregate source and was optimized to replicate the properties of the original concrete, achieving the same strength class while maintaining the lowest possible density and thermal conductivity. Test results showed mechanical properties and thermal conductivity comparable to the original concrete. Accelerated carbonation tests on recycled material revealed significant CO_2 absorption, capturing up to 30 % of the original emissions and achieving a 50 % reabsorption rate relative to cement emissions.

The multi-generational reuse of materials through recycling and recarbonation highlights the circular potential of lightweight concretes. Integrating the recarbonation potential into life cycle assessments presents a viable approach toward net-zero concrete production, while reducing resource consumption and construction waste.

Future work is needed to refine material classification and standardization to facilitate wider adoption of these innovative lightweight concretes. Aligning material properties with existing standards and developing tailored guidelines for pumping, composite systems, and recycling practices will be critical. This will positively impact regulatory acceptance, industrial scalability, and the long-term promotion of circular design practices.

Kurzfassung

Das moderne Bauwesen steht vor der Herausforderung technologischen Fortschritt mit ökologischen Ansprüchen zu verbinden. Gegenstand der Untersuchungen sind Leichtbetone für monolithische Außenwände, die bereits ohne zusätzliche Dämmstoffe die thermischen Anforderungen erfüllen können. Die experimentellen Ergebnisse basieren auf drei Fallstudien, die unterschiedliche Strategien zur Optimierung von Leichtbetontechnologien unter realen Bedingungen untersuchen und empirisch fundierte Lösungen für die Baupraxis liefern.

Während das Pumpen von Normalbeton in der Praxis etabliert ist, stellen die porösen und leichten Gesteinskörnungen von Leichtbetonen besondere Herausforderungen dar. Erstmals konnte gezeigt werden, dass Infraleichtbeton mit Kolben-, Exzenterschnecken- und Rotorpumpen erfolgreich gepumpt werden kann, sofern das Mischungsdesign optimiert und die Handhabung sorgfältig optimiert werden. Die Rotorpumpe erwies sich als die effizienteste Methode, da sie den mechanischen Abrieb minimiert und die Verarbeitbarkeit beibehält. Wesentliche Eigenschaften wie Druckfestigkeit und Elastizitätsmodul blieben konstant, was bestätigt, dass das Pumpen die Materialintegrität nicht beeinträchtigt.

Die Kombination von haufwerksporigem Leichtbeton mit Stahlblechrahmen bietet eine neue Konstruktionsmethode für vorgefertigte Wandelemente mit hoher thermischer Leistungsfähigkeit. Dafür wurde der Leichtbeton auf eine minimale Dichte optimiert, um eine möglichst geringe Wärmeleitfähigkeit zu erreichen. Die Tragfähigkeit wird durch die laterale Unterstützung schlanker, knickgefährdeter Stahlblechrahmen gewährleistet. Leistungsparameter wie Festigkeit, Elastizitätsmodul, Schwinden, Kriechen und Dauerlastverhalten erfüllen normativen Anforderungen. Mechanische Tests zeigten, dass die Verbundbauteile die dreifache Tragfähigkeit der einzelnen Stahlprofile erreichen. Die Übertragbarkeit dieser Bauweise von Laborversuchen in die industrielle Fertigung wurde bestätigt.

Durch das Recycling von Infraleichtbeton konnte gezeigt werden, dass bestehenden normativen Beschränkungen überwunden werden können. Die charakteristischen Eigenschaften der Recyclingprodukte wurden hinsichtlich ihrer Eignung für neue Betonrezepturen und des Potenzials zur CO_2-Bindung untersucht. Der Recyclingbeton substituiert 100 % der leichten Gesteinskörnung durch rezyklierte Materialien. Das Mischungsdesign wurde so optimiert, dass die Eigenschaften des Originalbetons mit gleicher Festigkeitsklasse und Wärmeleitfähigkeit erreicht werden. Beschleunigte Karbonatisierungsversuche ergaben eine signifikante CO_2-Aufnahme, wobei bis zu 30 % der Emissionen aus der ursprünglichen Betonproduktion resorbiert wurden, was etwa 50 % der durch den Zementanteil verursachten Emissionen entspricht. Die generationenübergreifende Wiederverwendung von Materialien durch Recycling und Rekarbonatisierung unterstreicht das zirkuläre Potenzial von Leichtbetonen. Die Einbeziehung des Rekarbonisierungspotenzials in die Ökobilanz ist ein praktikabler Ansatz für eine Netto-Null-Betonproduktion.

Zukünftige Arbeiten sind erforderlich, um die Materialklassifizierung und -normung zu verfeinern und so eine breitere Anwendung von Leichtbetonen zu ermöglichen. Die Anpassung der Materialeigenschaften an bestehende Normen sowie maßgeschneiderte Richtlinien für Pumpen, Verbundsysteme und Recyclingverfahren sind entscheidend für behördliche Akzeptanz, industrielle Skalierbarkeit und langfristige Förderung zirkulärer Bauweisen.

Table of contents

Abstract I

Kurzfassung II

Table of contents III

Glossary V

List of Figures VI

1 Introduction 1

1.1 Background 1

1.2 Key content of the thesis 2

2 State of knowledge 3

2.1 Classification of lightweight concretes and their unique aggregates 3

2.1.1 Structural lightweight concrete (LC) 4

2.1.2 Lightweight aggregate concrete (LAC) 5

2.1.3 Infra-lightweight concrete (ILC) 5

2.2 Selected challenges of lightweight concrete technologies 7

2.2.1 Unique challenges in pumping lightweight concretes 7

2.2.2 Recycling lightweight concretes 7

2.2.3 CO_2 sequestration in cementitious materials 9

3 Summary of materials and methods applied 10

3.1 Materials and methodology of case studies 10

3.1.1 Pumpability of ILC 10

3.1.2 Combination of optimized LAC with sheet steel framework 11

3.1.3 Recycling of ILC for material circularity 13

3.2 Experimental Methods 14

3.2.4 Determination of LWA properties 14

3.2.5 Fresh concrete properties 14

3.2.6 Dry density and thermal conductivity 14

3.2.7 Load-bearing behavior 14

3.2.8 Deformation behavior 15

3.2.9 Determination of CO_2 absorption and maximum capacity 15

3.2.10 Scanning electron microscopy (SEM) 16

4 Main results 17

4.1 Rationalizing concrete placement in modern construction 17

4.1.1 Pumping of ILC with highly porous aggregates 17
4.1.2 Effects of pumping on the fresh state behavior of ILC 18
4.1.3 Effects of pumping on hardened concrete properties 19
4.2 Thermal optimization in novel prefabricated wall elements 20
4.2.1 Material optimization for thermal and structural efficiency 21
4.2.2 Evaluating the structural integrity of the composite system 24
4.3 Advancing circular practices in lightweight concrete recycling 26
4.3.1 Evaluating RLCA properties for recycled concrete design 26
4.3.2 Consistency in mix design and balancing strength and density 27
4.3.3 Evaluating the mechanical properties of RILC 29
4.3.4 CO_2 sequestration potential of RLCA 31
4.4 Reflections on advancing lightweight concrete innovations 34

5 Conclusion 36

6 References 37

7 Publications 46

7.1 Lightweight Concrete – From Basics to Innovations 46
7.2 Challenges on pumping infra-lightweight concrete based on highly porous aggregates 71
7.3 Optimized Building Envelope: Lightweight Concrete with Integrated Steel Framework 86
7.4 Renewable construction with lightweight concrete – Reclaimed recycled material system with CO_2-absorption 107

8 Appendix 126

Glossary

NC	Normal-weight concrete
LC	Lightweight concrete
LAC	Lightweight aggregate concrete
LAC+	Optimized lightweight aggregate concrete
ILC	Infra-lightweight concrete
RC	Recycled concrete
RILC	Recycled infra-lightweight concrete
LWA	Lightweight aggregate
RCA	Recycled concrete aggregate
RLCA	Recycled lightweight concrete aggregate
ITZ	Interfacial transition zone
TGA	Thermogravimetric analysis
FTIR	Fourier-transform infrared spectroscopy
LECA	Lightweight expanded clay aggregate
TP_K	Piston pump
TP_S	Eccentric screw pump
TP_P	Rotor pump
TP_K_{LWA}	LWA extracted after pumping test with TP_K
TP_S_{LWA}	LWA extracted after pumping test with TP_S
TP_P_{LWA}	LWA extracted after pumping test with TP_P
ICP-OES	Inductively coupled plasma optical emission spectrometry
SEM	Scanning electron microscope
LCA	Life cycle assessment
GWP	Global warming potential
CDW	Construction and demolition waste
ILC_{Origin}	Original concrete serving as a reference benchmark for RILC
LWA_{Origin}	Original LWA serving as a reference benchmark for RLCA

List of Figures

Figure 1: Cross-sections of structural lightweight concrete (LC) with a dense matrix structure (left), lightweight aggregate concrete (LAC) with open pore structure (middle), and infra-lightweight concrete (ILC) with a porous matrix filling the open pore structure (right)..... 6
Figure 2: Schematic representation of the transportation mechanisms for the different pumps, highlighting their material flow and operational principles..... 11
Figure 3: Prefabricated wall construction with sheet steel framework in an optimized LAC envelope. Top left: Cross-section with Sigma-Profile. Bottom left: Wall with optimized LAC and embedded steel framework. Right: CAD model illustrating the building with new wall elements..... 12
Figure 4: Schematic representation of the study methodology for recycling ILC. 13
Figure 5: Particle size distributions across 20 size classes (400 – 4500 µm). A: Reference LWA ($Reference_{LWA}$) compared to as-delivered LWA ($Delivered_{LWA}$). B,C,D: Reference LWA compared to LWA after pumping: TP_K_{LWA} (B), TP_S_{LWA} (C), and TP_P_{LWA} (D). 18
Figure 6: Left: Dry density and compressive strength of reference and pumped cube specimens, including data from project-related approvals for completed construction projects with the same ILC using a concrete bucket for placement. Right: Compressive strength shown in box format with statistical indicators..... 20
Figure 7: Cross-section of optimized LAC. Series 3 (right) exhibits significantly higher porosity compared to Series 2 (left), which closely resembles conventional LAC with its open-pore structure..... 21
Figure 8: Left: Dry density and compressive strength of three extended test series from precast plants. Right: Compressive strength presented in box format with statistical indicators..... 22
Figure 9: Strains during shrinkage and creep for test series 2 (left), Relative load capacity ($\sigma_{sustained}/\sigma_m$) of compressive strength under sustained loading (right)..... 24
Figure 10: Comparison of test specimens for the composite system. Left: Plain steel profiles connected by spot-welded horizontal U-profiles. Right: Identical steel profiles embedded in LAC+. Compression tests shown before (A-D) and after (E-F) the test. 25
Figure 11: Composite test results for plain sheet steel (top) and composite specimens (bottom), featuring load-displacement diagrams (left) and box plots with statistical indicators (right).Note the different scaling. 25
Figure 12: RLCA at three magnification levels: (left) petri dish with 4 – 8 mm particles, highlighting one RLCA particle; (middle) closer view distinguishing porous matrix and LWA; (right) SEM image showing the RLCA particle embedded in the RILC..... 26
Figure 13: Particle density and water absorption of RLCA, subdivided by grain fractions, compared to the particle density of ILC's original aggregates (expanded glass) to illustrate the density increase. Results are differentiated between storage conditions (~20 °C / 65% relative humidity) and oven-dry conditions (mass constancy at 105 °C). 27
Figure 14: Results of mix design optimization for RILC production to replicate ILC_{Origin}. Left: Fresh concrete density compared to calculated density and average density across all batches, with yield shown on the secondary y-axis. Right: Relationship between dry

density and compressive strength of 100 mm cubes for RILC (blue) compared to preliminary tests (red) targeting the density and compressive strength of ILC_{Origin}.28

Figure 15: Compressive strength tests on RILC cylinders. Top left: Compressive strength as a function of dry density. Top right: Stress-strain curves and box plot showing statistical variation in compressive strength results. Bottom left: Ultimate strain in compression tests as a function of dry density. Bottom right: Modulus of elasticity as a function of compressive strength. 30

Figure 16: Relative load capacity ($\sigma_{sustained}/\sigma_m$) of compressive strength under sustained loading for ILC_{Origin} (left) and RILC (right)..... 31

Figure 17: (Left) CO_2 uptake of three RLCA fractions after conditioning (0 days) and after 3, 7, and 10 days of CO_2 exposure, compared with literature data on RCA. (Right) RLCA uptake under natural and accelerated conditions, relative to its absorption capacity, reference GWP [135], and target recarbonation goal (acc. to [94]). 32

1 Introduction

1.1 Background

Modern life in the 21st century occurs in the built environment and is characterized by concrete and steel. The expansion and maintenance of the construction sector both require vast amounts of natural resources and generate significant CO_2 emissions, making the building industry one of the largest global contributors to carbon emissions. Cement production alone accounts for a substantial share of this impact, with estimates ranging between 5 – 8 % of global anthropogenic CO_2 emissions, depending on the source and methodology used to calculate these figures [1–4]. Consequently, there is an urgent need to explore alternative and innovative construction methods to reduce environmental harm and energy consumption [3,5]. Efforts concentrate on several key areas:

Clinker-reduced and alternative binder systems constitute a significant priority to reduce reliance on energy- and CO_2-intensive clinker production, significantly lowering CO_2 emissions while improving material properties and durability [6,7]. This can be achieved by using supplementary cementitious materials such as fly ash [8], ground granulated blast furnace slag [9], calcined clay [10], silica fume [11] and limestone powder [12]. Additionally, alternative binders like magnesium silicate cement [13], calcium sulfoaluminate cement [14] and alkali-activated materials [15,16] have been developed to further reduce environmental impact. **Innovative construction** techniques aim to enhance material efficiency, customization, and construction speed. Examples include structural designs like multifunctional graded (e.g. weight optimized) construction elements [17], hollow-core systems [18], additive manufacturing [19,20], and the development of novel building materials like infra-lightweight concrete [21,22]. Rationalizing construction processes, such as optimized concrete pumping [23,24], enhances efficiency, reduces material waste, and minimizes system failures. **Energy optimization in cement production** is a response to rising energy costs and stringent environmental standards, which have driven cement producers worldwide to optimize production processes. Strategies include fuel optimization using biomass and waste-derived fuels [25,26], implementing heat recovery systems in cement kilns [27], and lowering kiln temperatures with mineralizers [28]. **Carbon sequestration** techniques to offset CO_2 emissions during the production and lifecycle of building materials are increasingly explored. These include carbon capture and storage [29,30], carbonation curing in precast concrete to sequester CO_2 [31], and incorporating carbon-rich materials like biochar into concrete mixes [32]. **Reuse and recycling** of construction and demolition waste offers significant potential to reduce landfill use, conserve natural resources, and enhance material circularity [5,33,34]. Strategies also include designing modular components for easier reuse at the end of their lifecycle [35] and employing high-performance or self-healing concrete to extend the lifespan of structures [36,37]. The **digital transformation** of the construction industry offers several emerging research fields beyond traditional domains. Life cycle assessment (LCA) supports informed decision-making to assess and minimize environmental impact [38]. Applications in machine learning and artificial intelligence range from enhancing structural design and optimizing material usage to predicting the lifespan of infrastructure and improving energy efficiency [39]. In addition, building information modelling [40–42] and digital twins [43] facilitate real-time collaboration, lifecycle management, and predictive maintenance.

Lightweight concretes, with their combination of low density and high thermal efficiency, are in a unique position to address some of the challenges associated with the efforts described above. However, gaps in standards, production methods, and application techniques present barriers that require extensive research.

Therefore, this thesis explores the role of lightweight concrete in sustainable construction, focusing on balancing technical performance and ecological impact to meet modern building requirements. Specifically, the associated challenges include improving process efficiency, enhancing energy performance in building envelopes, reducing CO_2 emissions along the life cycle, and promoting the reuse of building materials through recycling.

The following chapter will outline the key content of this research and its contribution to advancing sustainable construction practices.

1.2 Key content of the thesis

The overarching goal of this thesis is to investigate how lightweight concretes can achieve an optimal balance between technical and environmental aspects through innovative applications and methodologies. The primary application area is monolithic exterior walls that do not need additional thermal insulation layers due to their inherently superior thermal properties.

The theoretical background of lightweight concrete technologies is organized in **Chapter 2** and is based on a comprehensive review article of Thienel et al. [22] that explores the evolution of lightweight concretes from their historical foundations to modern innovations. Furthermore, it highlights selected challenges in today's research efforts. **Chapter 3** provides an overview of the materials used and the methodological approach, together with information on specific experimental methods employed.

The experimental research is based on three fundamental case studies [44–46], each addressing different strategies for optimizing lightweight concrete technologies in the context of sustainable construction, testing them under real-world conditions, and providing solutions for their integration into modern construction practice:

1. **Pumpability of lightweight concrete with highly porous aggregates [44]**: Investigating strategies to enable and optimize the pumping of infra-lightweight concrete and to maintain material consistency, minimize segregation, and preserve the integrity of the concrete mix during application.
2. **Combination of lightweight aggregate concrete with steel frameworks [45]**: Evaluating design criteria for a novel construction method that combines lightweight aggregate concrete with steel frameworks, to minimize thermal conductivity while ensuring structural stability.
3. **Recycling of infra-lightweight concrete for material circularity [46]**: Exploring methods for recycling infra-lightweight concrete to promote material circularity, reduce CO_2 emissions, and preserve structural performance, contributing to sustainable construction practices.

The main findings of these studies are discussed in **Chapter 4**. Based on these findings, **Chapter 4.4** reflects on the balance between environmental and technical attributes for sustainable lightweight concrete. **Chapter 5** presents a concise summary of the thesis's key findings. **Chapter 7** contains the peer-reviewed publications of the case studies and the review article.

2 State of knowledge

The primary source of information for **Chapter 2.1** is the review paper by Thienel et al. [22] (see **Chapter 7.1**), which provides the basic context for the discussion of lightweight concrete and some of its specific types and their particular material properties. In the following **Chapter 2.2**, selected topics on lightweight concrete are presented. These topics provide concentrated information on specific challenges addressed in each fundamental case study, while a broader context can be found in the respective case studies.

2.1 Classification of lightweight concretes and their unique aggregates

The defining characteristic of lightweight concrete is its low density, distinguishing it from normal-weight concrete (NC). This reduction in density is achieved through the introduction of a pore system, accomplished via porous lightweight aggregates (LWA) (e.g. structural lightweight concrete), the inclusion of air voids within the binder (e.g. aerated or foamed concrete), or the intentional omission of finer aggregate grains (e.g. no-fines concrete). Combinations of these methods are also common [22].

Lightweight concretes can be further categorized based on their intended use (e.g., structural, insulating, or sound absorbing concrete), production method (e.g., foam concrete, autoclaved aerated concrete, precast lightweight concrete), or defining properties such as density, strength, and type of LWA used (e.g. LECA (lightweight expanded clay aggregate) concrete, perlite concrete). The numerous definitions and classifications of lightweight concrete, many of which lack standardization, often lead to misunderstandings in research and practice [22].

In this thesis, *'lightweight concrete'* refers to the overarching category, while specific types are explicitly named where necessary.

The roots of lightweight concrete date back to ancient Rome, as exemplified by structures like the Pantheon, which demonstrate the early use of natural LWA in *'opus caementicium'*. The availability of natural LWA is geographically limited because it is obtained from volcanic rock and mechanically processed through washing, crushing, and screening. Pumice, tuff, lava slag, and perlite are classic examples of this category [22,47]. The industrial production of LWA in the 19th and 20th centuries marked a significant turning point, enabling the widespread manufacture of industrial LWA [22,47,48]. Compared to natural LWA, industrially produced LWA offer consistent quality and composition, which are significant advantages [22,49].

Industrially produced LWA are manufactured by expanding natural mineral materials such as clay, shale, slate in a rotary kiln, or originate from industrial by-products like fly ash and blast-furnace slag [49,50]. The expansion process is based on gas formation reactions within a certain temperature range when the material reaches a plastic state. This stage is reached, when a glassy phase of sufficient viscosity forms to trap the evolving gases within the material, resulting in a highly porous, nearly spherical pellet [49,51]. The desired aggregate size can be achieved by granulating the raw material before firing or by crushing the material post-firing.

Defining the properties of LWA, particularly their density, is essential for differentiating them from normal aggregates. According to EN 13055 [52], LWA are of mineral origin and can be derived from natural origin, manufactured from natural materials, manufactured from by-products of industrial processes, recycled source materials, or by-products of industrial processes [52,53]. They are defined as having a particle density below 2000 kg/m³ or a bulk loose density below 1200 kg/m³ [52].

Modern LWA are available with a variety of properties including low density, excellent thermal and sound insulation, high fire resistance, and chemical stability [22,47,49]. These properties make LWA an excellent building material and contribute to the status of lightweight concrete as a highly versatile and effective building material.

2.1.1 Structural lightweight concrete (LC)

In the 1990s, national standards and regulations were revised to establish lightweight concrete as an equal alternative to NC [22]. In Europe, structural lightweight concrete (LC) suitable for reinforced applications is covered by EN 206 [54] and its use is regulated by EN 1992-1-1 [55]. According to these standards, LC has an oven-dry density range of 800 to 2000 kg/m³ and is categorized into density classes with 200 kg/m³ intervals. The minimum strength class is LC 8/9, and the highest strength class is LC 80/88, corresponding to characteristic compressive cylinder strengths of 8 N/mm² and 80 N/mm², respectively. However, a free combination of density and strength is not possible; every given LC strength class must be explicitly paired with a corresponding density class [22].

LC is characterized by a dense structure (see **Figure 1**), similar to NC. The reduced density is achieved by partially or entirely replacing normal-weight aggregates with LWA. Most LC utilize coarse LWA in combination with normal-weight sand. Although fine LWA can also be used, they require precise water absorption management [22].

Any binder material can be used for producing LC. However, when exclusively using LWA, binders with lower specific heat are recommended. The low thermal conductivity of LC can lead to significant core temperature increases during hydration in structural elements [22,47]. The raw material and manufacturing process of LWA defines the interconnectivity of open and closed pores, resulting in different pore size distributions [22,49]. The high porosity and low density of LWA have significant implications for LC mix design. The porous character of LWA presents challenges, such as water absorption from the cement paste, which can stiffen the fresh concrete or cause microcracking and reduce durability [22]. To address this challenge, LC mix designs must incorporate LWA water absorption, either through adjusted water additions or pre-wetting of the aggregates [22,47]. The water absorbed by LWA can partly be drawn out during the subsequent stages of hydration by the rising capillary action of the hardening cement paste, thereby providing internal curing of the LC [56]. Unlike NC, well-designed LC lacks a distinct interfacial transition zone (ITZ) due to binder infiltration into the porous LWA during mixing. This infiltration allows hydration products to grow within and into the LWA, enhancing mechanical interlocking and particle strength. The extent of infiltration depends on the microstructure and surface characteristics of the specific LWA [57]. Additionally, the water absorbed by LWA contributes to internal curing during hydration, a concept widely utilized in high-strength NC [22,56,58].

The mix design of LC requires an adequate balance of desired strength and reduced density. For LC used in heat-insulating applications, thermal conductivity becomes a crucial factor. In LC, the load-bearing behavior differs from NC due to the typically lower stiffness and strength of the LWA compared to the cement matrix. Initially, load transfer is similar to NC, with compressive stresses running through the mortar between the aggregates. As hydration progresses, the matrix may become stiffer than the LWA, leading to a redistribution of internal forces. The compressive stresses bypass the weaker aggregates, inducing tensile stresses in the matrix that can initiate cracking. Once matrix cracking occurs, tensile loads are gradually transferred to the aggregates. When the LWA tensile strength is exceeded, grain fracture

defines the failure, marking the *'limit strength'* of the LC. Up to this threshold, LC strength largely corresponds to the matrix strength. Beyond this point, further increases in strength require significant improvements in matrix strength as the aggregates contribute less to load transfer. The strength limit is thus determined by the properties of the LWA: the higher its strength, the higher the compressive strength of the LC that can be achieved. This concept is illustrated in **Chapter 7.1** (**Figure 5**), showing how different LWA types influence the upper strength limit of LC [22,59].

2.1.2 Lightweight aggregate concrete (LAC)

Lightweight aggregate concrete (LAC) with an open structure exhibits distinct characteristics compared to dense LC. It is specifically regulated for prefabricated reinforced components under EN 1520 [60]. LAC structure is defined by the voids between LWA particles, which result from omitting or reducing certain particle sizes. These voids remain in the structure after compaction, with the cement paste volume reduced to the extent that particles are only connected at specific points [22,47,61,62], as detailed in **Figure 1**.

LAC is predominantly produced using coarse LWA, leading to its synonym *'no-fines concrete'*, although *'low-fines concrete'* would be a more accurate description [61]. This open structure differentiates LAC significantly from dense LC in terms of concrete technology. LAC is primarily used in wall blocks, load-bearing and thermally insulating wall elements, and non-load-bearing components such as noise barriers and drainage concrete [45,63].

Modern advancements in concrete technology, including innovative admixtures, additives, and manufacturing processes, coupled with the availability of even lighter LWA such as expanded glass, have expanded the application range of LAC. These innovations have enabled the production of external wall elements with low densities and excellent thermal insulation properties, eliminating the need for additional insulation layers [45,61].

According to EN 1520 [60], LAC has an oven-dry density range of 400 to 2000 kg/m³ and is categorized into density classes with 200 kg/m³ intervals for densities below 1000 kg/m³ and 100 kg/m³ intervals for densities above 1000 kg/m³. The minimum strength class is LAC 2, and the maximum strength class is LAC 25, corresponding to characteristic strengths of 2 N/mm² and 25 N/mm², respectively, measured using drill core specimens as the reference.

2.1.3 Infra-lightweight concrete (ILC)

Over the past two decades, there has been a growing interest in reducing concrete density while maintaining sufficient strength [21,22]. Monolithic structures with fair-faced concrete in the lowest strength and density classes have gained popularity in Europe. These structures offer the possibility of constructing finished walls in a single operation, eliminating the need for additional insulation or multi-layer wall systems [21,22,64]. The appeal of monolithic lightweight concrete walls lies in their ability to support creative, easily formable architectural designs that leverage the aesthetic potential of fair-faced concrete [22,65].

At the forefront is the development of infra-lightweight concrete (ILC) [21,22,65–68]. Similar materials are referred to in the literature under terms such as *'Warmbeton'* [69], or *'ultra-lightweight concrete'* [70–72]. ILC is characterized by dry densities below 800 kg/m³, aligning with the lower density limit for LC defined by EN 206 [54]. Based on this, the term *'infra'*, derived from the Latin preposition meaning *'below'*, distinguishes ILC from conventional LC [67].

The mix design of ILC seeks to balance reduced density, sufficient strength, and low thermal conductivity. LWA play a critical role in reducing density, with expanded clay and expanded

glass being the only aggregates currently used for ILC [21,22,65]. Binder materials typically include cements with low heat of hydration, often combined with supplementary cementitious materials such as fly ash, ground granulated blast furnace slag, or limestone [21,65]. These combinations help mitigate the high core hydration temperatures that can develop in thick components (50 - 60 cm) due to the low heat capacity and thermal conductivity of the ILC [21,22,65].

Admixtures commonly used in NC are also applicable to ILC. However, due to the density disparity between binder and LWA, ILC is particularly susceptible to segregation and bleeding [21,22,65]. This has led to a focus on admixtures that stabilize the balance between LWA, binder particles, and finely distributed air bubbles within the cement paste. Superplasticizers, stabilizers, and air-entraining agents are the most commonly used admixtures in ILC mix design [21,22,65].

Visually, ILC exhibits a closed internal structure, attributed to the finely dispersed, artificially introduced air voids within the cement paste, and therefore resembles LC more closely than LAC (see **Figure 1**). However, due to its high porosity —exceeding 10% of the total volume— ILC does not meet the structural criteria of structural LC [73]. Furthermore, LC standards [54] do not regulate densities below 800 kg/m³, which is the target density range for thermal-insulating concrete elements. Conversely, the regulatory orientation of ILC towards LAC standards offers an established structural design framework for precast elements under EN 1520 [60]. This framework serves as the basis for adapting the standard to ready-mix concrete applications and developing site conformity guidelines. These adaptations have already been included in several project-specific approvals [22,44,74] and is scheduled for formal introduction through a technical guideline by the German Committee for Reinforced Concrete (DAfStb) [22].

The working group for this technical guideline is currently proposing density classes ranging from 400 to 800 kg/m³ and strength classes from ILC 2 to ILC 15, corresponding to characteristic compressive strengths of 2 N/mm² to 15 N/mm², based on cubes as reference specimen type. Furthermore, the working group notes that no differences in terms of specimen shape (cubic or cylindric) are to be expected.

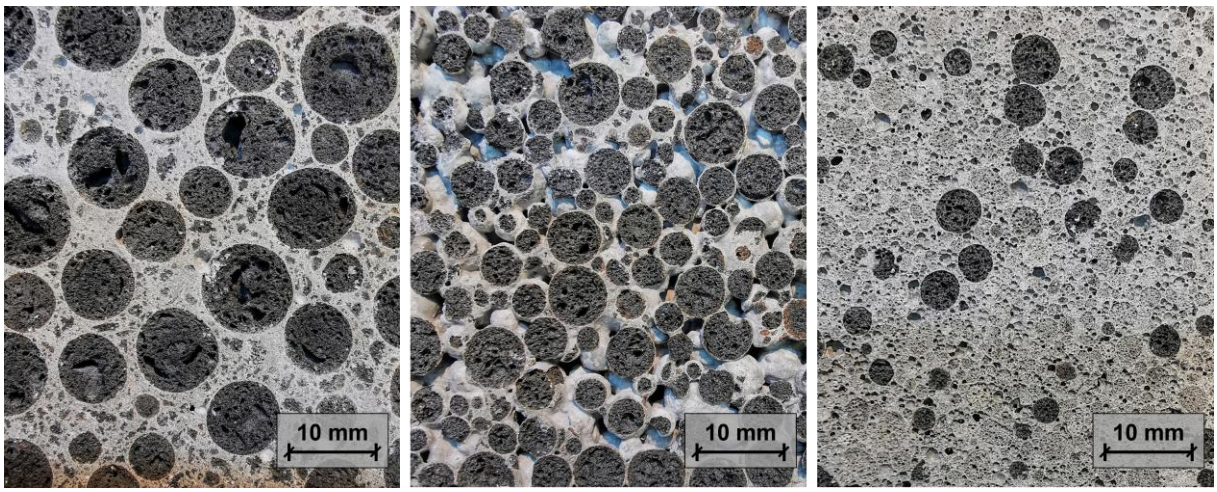

Figure 1: Cross-sections of structural lightweight concrete (LC) with a dense matrix structure (left), lightweight aggregate concrete (LAC) with open pore structure (middle), and infra-lightweight concrete (ILC) with a porous matrix filling the open pore structure (right).

2.2 Selected challenges of lightweight concrete technologies

The following sections briefly summarize key information related to the case studies conducted. A more comprehensive contextual discussion on these topics can be found in each case study (see **Chapter 7**).

2.2.1 Unique challenges in pumping lightweight concretes

Modern construction requires continuous optimization to improve cost efficiency, time management, quality, safety and resource consumption and to survive in a highly competitive industry. Concrete pumping has become an indispensable method of improving site efficiency and rationalizing construction workflows. Advances in machinery and concrete technology have made it possible to pump fresh concrete efficiently, even in confined spaces. For successful pumping, the fresh concrete's properties and external factors such as the pipework geometry and equipment performance must be considered [23,24].

Although it is not a directly measurable physical property, the term *'pumpability'* is often used in the literature to describe the ability of concrete to be pumped through pipes without compromising its fresh and hardened properties [23,24,75–77]. This ability depends on the deformation behavior of the fresh concrete under pressure, which is influenced by the rheological properties and the formation of a *'lubricant layer'* along the pipe walls. This sliding layer, composed of cement, water, fine aggregates, and admixtures, is essential for reducing friction and maintaining consistent pressure during pumping [23,24,75–77].

Pumping is widely used for placing fresh NC on construction sites [23,24], but lightweight concretes present unique challenges due to their porous LWA [78]. While pumping NC is well-supported by guidelines, the representation of lightweight concretes in regulatory frameworks remains limited, with the pumping process frequently perceived as complex or impractical [79]. Key challenges include the following [78]:

- **Water and cement paste absorption**: During pumping, water and cement paste may be squeezed into the porous LWA, reducing the flowability of the fresh concrete and increasing pipe friction.
- **Volume reduction**: Pressing water into the LWA reduces the volume of the fresh concrete, resulting in elastic compression of the concrete column in the pipeline that impairs the pressure transfer in the pipeline.
- **Air compression and expansion**: The air in the pores of the LWA can be compressed during pumping. As the pumping pressure decreases, the compressed air expands and expels the water, causing segregation of the fresh concrete and potentially causing problems to the ITZ in the hardened concrete.

These phenomena can lead to segregation, reduced workability, blockages, and diminished strength and durability in hardened concrete.

2.2.2 Recycling lightweight concretes

Recycling and reuse of construction and demolition waste (CDW) is a central part of circular economy in the building industry. Studies estimate that CDW is the largest source of waste, and its volume is continuously rising [80–83]. Despite efforts to reuse CDW, a major part is disposed of in landfills or used in roads or earthworks. The share of CDW used as recycled concrete aggregates (RCA) in concrete production is comparatively low. In Germany, itis estimated to be less than 1 % [84].

Recycling and reuse of NC has been widely researched and is increasingly being used in practice. A major challenge in reusing coarse RCA is the adherent mortar, which lowers mechanical performance efficiency in general and results in higher water absorption and higher density compared to the natural aggregates [29,85,86].

In contrast to NC, the recycling and reuse of lightweight concrete faces several restrictions. DIN 4226-101 [87] divides RCA (> 2 mm) into 4 types according to their material composition, whereby only type 1 and 2 are permitted for use in concrete following EN 206-1/DIN 1045-2 [54,88]. For RCA derived from lightweight concrete, in the following referred to *'Recycled Lightweight Concrete Aggregate'* (RLCA), the reuse in structural concrete is limited to less than 10 % for type 1 and less than 30 % for type 2 RCA. As additional criteria for type 1 and 2 RCA, the minimum particle density is 2000 kg/m³, and the maximum water absorption is limited to 10 or 15 % by mass respectively. Therefore, lightweight concrete with its particular low density, such as those described in **Chapter 2.1** and utilized for monolithic wall constructions, is explicitly excluded from normative reuse. In addition, the reuse of RLCA in structural LC is not permitted at all according to DIN 1045-2 [88].

Research on recycling products derived from lightweight concrete is limited and focusses on reducing natural resource consumption and studying the effect of RLCA on concrete properties. A research program founded by the European Union [89] performed laboratory leaching-tests on RLCA derived from laboratory LC and found that they fulfill environmental requirements. Furthermore, a mixture of recycled concrete and brickwork was used to replicate the RLCA and produce recycled concrete. As a result, this recycled concrete had a density approximately 200 kg/m³ lower than the reference concrete with conventional aggregates and a strength class of B35 (equivalent to C30/37 in the current standard [54]), with a 50 kg/m^3 increase in cement content. Kümmel [90] examined the recycling of structural LC, assessing technical, ecological, and economical criteria. The analysis revealed that RLCA demonstrates high flakiness and an unfavorable shape when processed with a jaw crusher. Contrary to RCA, it was observed that RLCA density decreases with increasing particle size. Concrete produced with RLCA met compressive strength requirements when its increased water absorption was considered in mix design. A reduced modulus of elasticity was attributed to a weaker ITZ, and the higher shrinkage and creep values were attributed to the higher porosity and the presence of cracks in RLCA. Bogas et al. [91,92] investigated recycled concrete with varying substitution rates of RLCA derived from LC and LAC, observing that the density of RLCA was up to 60 % higher than the original LWA. The recycled concrete exhibited a higher compressive strength, accompanied by a 10 % increased density. However, the durability properties, including drying shrinkage, capillary and immersion water absorption, carbonation, and chloride resistance, declined with increasing RLCA substitution rates. Furthermore, an elevated modulus of elasticity was observed, which was attributed to the greater stiffness of the RLCA compared to the original LWA. This finding contrasts the observations reported by Kümmel [90]. Huang et al. [93] proposed a novel procedure to separate LWA and cement paste without significant damage by applying freezing and thawing cycles on used lightweight concrete derived from the Nanjing Yangtze River Bridge. The RLCA obtained through this process showed comparable density, but lower water absorption, due to adhering cement paste, compared to the original LWA. While the compressive strength demonstrated no significant change after 28 days with 10 % and 20 % replacement compared to reference concretes, a replacement level of 30 % resulted in a 14 % increase in compressive strength. Microstructural analyses indicated that the ITZ between the new cement matrix and the RLCA without old cement paste coverage

exhibited the highest strength, while the weakest ITZ was observed between the RLCA with remaining cement paste coverage and the new cement paste.

2.2.3 CO_2 sequestration in cementitious materials

The VDZ roadmap [94] outlines the cement industry's objective to attain climate neutrality by the year 2050. This objective can be accomplished through the implementation of a series of measures, including the capture of 20 % of the emissions from clinker production through the process of '*recarbonation'*. The underlying process of carbonation is a result of the chemical conversion of calcium hydroxide into calcium carbonate [95,96]. In the context of recycling and reuse strategies, the carbonation of RCA (and RLCA) is of significant interest, as in the course of demolition and mechanical processing of concrete structures, a larger surface area is exposed for carbonation [97,98]. The main parameters affecting the carbonation of recycled materials are the type of material, the proportion of carbonatable material (e.g. non-hydrated cement residues, calcium hydroxide, calcium silicate hydrates, sulfate-free and sulfate-containing alumina hydrates [83]), the initial carbonation state, porosity, and particle size [98]. The quantity of carbon dioxide absorbed by the carbonation of RCA can be accounted for in part D of the LCA. Research focusing on the targeted carbonation of concrete and its recycled materials is designated as *'CO_2-mineralization'*, '*CO_2-curing'*, or *'Forced carbonation'*. Fang [98] developed a fundamental model for CO_2 absorption kinetics under different ambient conditions, like temperature, relative humidity, CO_2 concentration, pressure conditions, and exposure time. A variety of strategies have been studied to maximize CO_2 absorption. These strategies include optimizing the media in which the RCA is exposed to CO_2, such as different gases (e.g. biogenetic CO_2 [99] or aqueous medium [100]), pressure chambers, flow containers [98], pressurized autoclave [83], or technological integration in cement plants [101,102]. Furthermore, pretreatment of carbonation material through pre-soaking in solutions, slurries, or emulsions has also been identified as a promising method for maximizing CO_2 absorption [102,103]. Researchers have studied the effect of the change in the physical properties of RCA through carbonation. The related research focuses on reducing the water absorption behavior and removing or strengthening the adherent cement paste on RCA [30]. This objective can be achieved, for example, by exploiting the underlying mechanism of calcium carbonate microcrystal formation in the pores of RCA, which can densify the cement matrix and result in improved material properties [29,30,103,104]. Infante Gomes et al. [105] provided a comprehensive overview of the impact of CO_2-curation on the properties of carbonated RCA through a meta-analysis. A further research topic is the increased reactivity of carbonated recycled fines when utilized as alternative cementitious constituents [106,107].

In order to consider the absorption of CO_2 in LCA, it is necessary to quantify experimentally the CO_2 uptake potential of the RCA. Therefore, several attempts [97,98,104,108–112] have been made to examine the CO_2 uptake in RCA under various carbonation conditions, quantified via thermogravimetric analysis (TGA) and mass control. Key factors include aggregate type, pre-conditioning, exposure duration, and environmental conditions. **Table 1** in **Chapter 7.4** details the findings. CO_2 uptake of RCA in these studies ranged from 3.7 to 71 kg of CO_2 per ton of RCA. The different methods for determining CO_2 uptake, and variability in RCA properties such as carbonatable material content, initial carbonation progress, and porosity make it difficult to compare directly RCA samples. However, there is agreement that targeted carbonation of RCA can be implemented on an industrial scale [101,102]. Therefore, advancements in CO_2 sequestration technology hold great promise and offer significant potential for integration with recycling lightweight concrete.

3 Summary of materials and methods applied

Chapter 3.1 offers a comprehensive overview of the materials and methodologies employed in each case study. Additionally, **Chapter 3.2** provides detailed information regarding specific experimental methods.

3.1 Materials and methodology of case studies

3.1.1 Pumpability of ILC

A large-scale field test was conducted to address the challenges associated with pumping lightweight concrete containing porous LWA. The ILC investigated in this study was produced using a truck-mounted plant. The ILC was classified in a project-related approval referencing EN 1520 [60]. The ILC complies with strength class LAC 4 and has a characteristic dry density of 570 kg/m³ with an associated thermal conductivity ($\lambda_{10,dry}$) of 0.125 W/(m·K) according to EN 12664 [113]. **Table 1** provides an overview of the characteristics of the project-related approval of the ILC.

Table 1: Summary of the characteristic material properties of the ILC used.

Maximum grain size [mm]	4
Compaction class (EN 206 [54])	C4
Strength Class (EN 1520 [60])	LAC 4
Characteristic compressive strength [N/mm²]	5
Density class (EN 1520 [60])	0.6
Characteristic dry density [kg/m³]	570
Flexural strength [N/mm²]	0.9
Modulus of elasticity [N/mm²]	3900
Thermal conductivity $\lambda_{10,dry}$ (EN 12664 [113])) [W/(m·K)]	0.125
Thermal conductivity $\lambda_{23/80}$ (EN 12664 [113])) [W/(m·K)]	0.143

The ILC incorporates expanded glass in 1 – 2 mm and 2 – 4 mm fractions as LWA, according to EN 13055 [52]. The binder material is composed of slag cement CEM III/A 42.5 N according to EN 197–1 [114] and condensed silica fume in suspension according to EN 13263–1 [115]. The additives used in the mixture include a polycarboxylate ether-based superplasticizer, an air-entraining agent, and micropolymer fibers, as specified in EN 14889–2 [116].

Three commonly used pump types –piston, eccentric screw, and rotor– were evaluated under practical conditions. The piston pump (TP_K) operates with two hydraulic cylinders in reciprocating motion. The reciprocating movement of the pistons creates pressure differentials in the pipework and therefore suction and discharge of the fresh concrete. The eccentric screw pump (TP_S) utilizes a helical rotor rotating within a stator, creating radially moving spaces for continuous concrete conveyance. The rotor pump (TP_P) employs radially rotating pressure rollers that deform a flexible hose, thereby creating a suction effect within the hose, which continuously draws in the fresh concrete. The basic operation of each pump type is shown schematically in **Figure 2**.

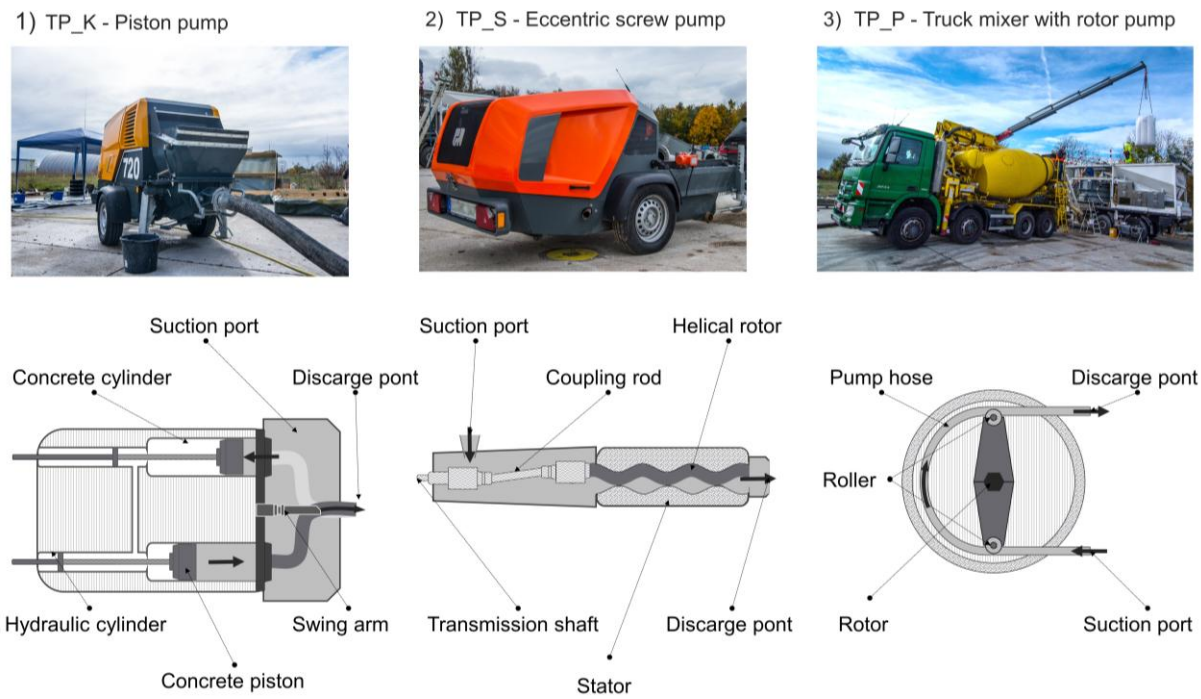

Figure 2: Schematic representation of the transportation mechanisms for the different pumps, highlighting their material flow and operational principles.

Approximately 4 m³ of ILC were pumped per pump type, with varying pipe diameters (100 – 125 mm), lengths (13 – 20 m), and applied pressures (0.2 – 2.0 N/mm²) to replicate real-world scenarios. Samples were collected before (reference) and after the pumping operations (TP_K, TP_S, TP_P). These samples were then used in an experimental study to ascertain whether the pressurization of fresh concrete during the pumping process exerts an influence on fresh and hardened ILC properties.

Details presenting the first-ever study investigating the pumpability of an ILC can be found in **Chapter 7.2**. The key findings are summarized in **Chapter 4.1**.

3.1.2 Combination of optimized LAC with sheet steel framework

A new prefabricated construction method for wall elements aims to provide an alternative solution to meet the growing market demand for affordable, rapidly constructed, and durable buildings. The method involves the combination of a thin-walled sheet steel frame and thermally optimized LAC to produce prefabricated wall elements.

The primary load-bearing function of the wall elements is provided by cold-formed steel profiles. These profiles are vertically arranged at defined intervals and connected at the top and bottom with non-load-bearing U-profiles through spot welding. The steel frame can be individually prepared to accommodate technical installations, window openings, and connecting elements. The optimized LAC is then poured into the formwork, encapsulating the steel frame. Due to their length and slenderness, the vertical sigma-profiles are susceptible to buckling. To mitigate the risk of stability failure, the surrounding LAC provides lateral bracing, preventing stability failure. **Figure 3** schematically illustrates the construction method.

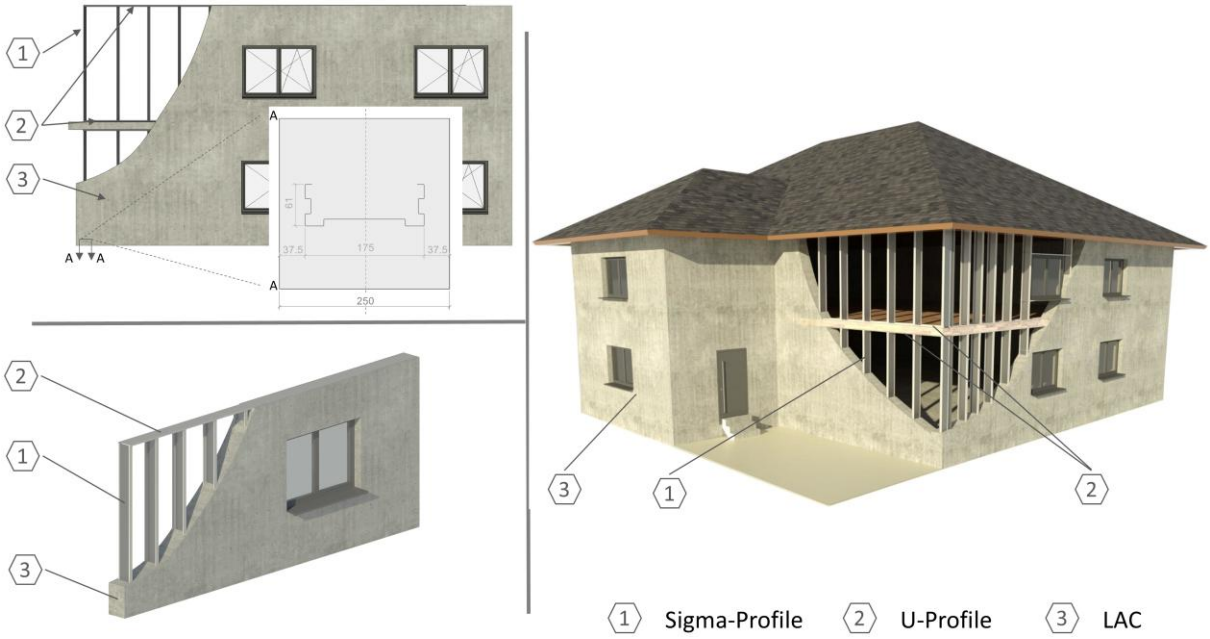

Figure 3: Prefabricated wall construction with sheet steel framework in an optimized LAC envelope. Top left: Cross-section with Sigma-Profile. Bottom left: Wall with optimized LAC and embedded steel framework. Right: CAD model illustrating the building with new wall elements.

The optimized LAC, characterized by a dry density below 400 kg/m³ and a correspondingly low strength, falls below the normative limits of EN 1520 [60]. Nonetheless, its properties remain comparable to those of conventional LAC. In order to distinguish it from standard materials, this optimized LAC is referred to as *'LAC+'* in subsequent sections. The wall elements are intended to be assembled on-site by filling profile joints with mortar and using additional mechanical connectors, as is standard procedure in precast construction practices.

The following key objectives are critical for the successful realization of this construction method:

- **Reduce thermal conductivity:** LAC+ is engineered for minimal thermal conductivity to meet modern energy efficiency regulations without requiring additional insulation layers. This is achieved primarily by reducing material density and increasing the air void content of the concrete matrix.
- **Maintain structural integrity:** While the LAC+ contributes to the thermal and structural-physical properties, the embedded steel frame ensures the primary load-bearing capacity. The concrete envelope stabilizes the thin-walled steel profiles and prevents buckling under load.
- **Feasibility and scalability:** The feasibility of producing these wall elements must be demonstrated at scale, transitioning from laboratory development to full-scale manufacturing in precast plants.

The case study demonstrating the application and effectiveness of this construction method can be found in **Chapter 7.3**. The key findings are summarized in **Chapter 4.2**.

3.1.3 Recycling of ILC for material circularity

The recycling potential of ILC is explored by converting end-of-life elements into RLCA. To manufacture RLCA, larger elements (4 x 2 x 0.5 m) were manually crushed, followed by subsequent mechanical crushing to a particle size of approximately < 32 mm using a laboratory jaw crusher. The crushed material was then screened and graded into different particle size groups: < 1 mm ($RLCA_{fine}$), 1 – 2 mm ($RLCA_{1–2}$), 2 – 4 mm ($RLCA_{2–4}$), 4 – 8 mm ($RLCA_{4–8}$) and 8 – 16 mm ($RLCA_{8–16}$).

The mechanical, thermal, and CO_2 absorption properties of RLCA are evaluated to determine their suitability for new concrete formulations and to evaluate their CO_2 absorption potential. The primary objective is to restore the properties of the original ILC *'ILC_{Origin}'* in a new generation of *'Recycled Infra-Lightweight Concrete'* (RILC). ILC_{Origin} was produced as part of a study into the pumpability of ILC [44] (see **Chapter 3.1.1**), in which its characteristic properties were evaluated. These properties will serve as a reference for evaluating the performance of the RILC developed in this experimental setup.

The mix design of RILC is optimized to replicate the properties of ILC_{Origin} solely using RLCA as LWA and achieving the same strength class while maintaining the lowest possible density and thermal insulation hereby. To ensure compatibility with structural applications, parameters influenced by RLCA properties –such as strength, modulus of elasticity, and sustained loading behavior– are also investigated. These parameters are crucial for validating the efficiency of the recycling process and ensuring comparable performance with the primary product ILC_{Origin}.

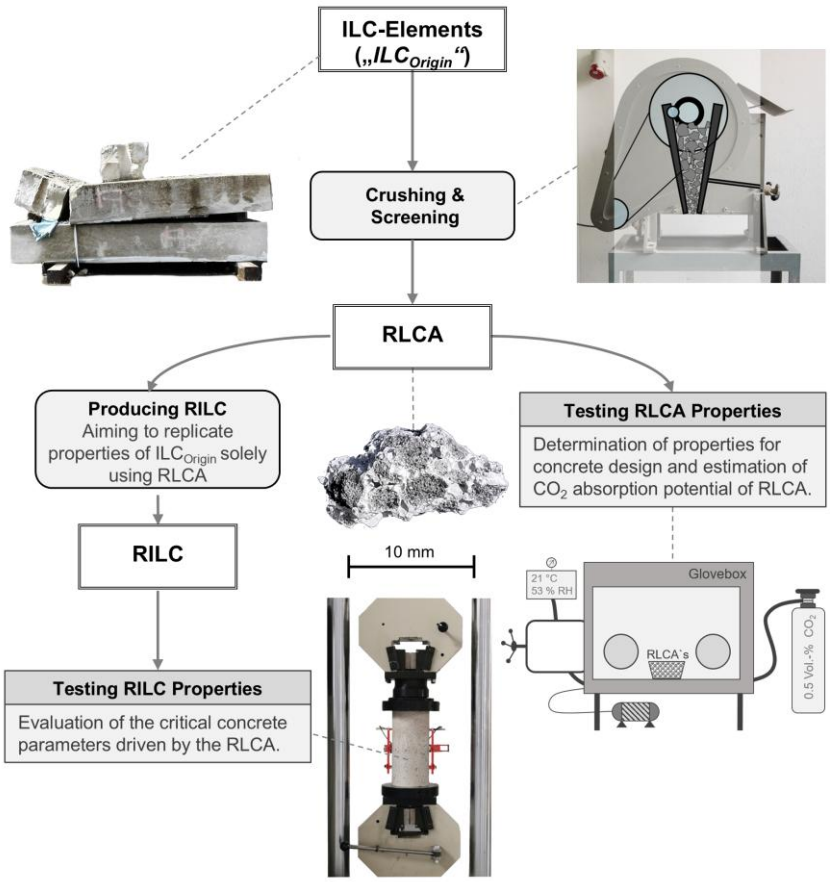

Figure 4: Schematic representation of the study methodology for recycling ILC.

The case study demonstrating the application and effectiveness of recycling ILC can be found in **Chapter 7.4**. The main findings are summarized in **Chapter 4.3**.

3.2 Experimental Methods

3.2.4 Determination of LWA properties

Densities and water absorption

Particle density and water absorption were determined by using the pycnometer method as specified in EN 1097-6 [117]. For finer particles (< 1 mm), measurements followed the procedures specified in EN 1097-6 (Annex D) [117], which is tailored for lightweight, open-porous aggregates predominantly < 1 mm and accounting for more than 50 % of the sample weight. Loose bulk density was measured following EN 1097-3 [118].

Particle size distribution

The particle size distribution of the LWA was analyzed using a photo-optical particle characterization system (BeVision D2, 3P Instruments GmbH & Co. KG, Odelzhausen, Germany). This system employs two parallel digital cameras to capture and analyze particles ranging from 30 µm to 10 mm. LWA were recovered during the pumping study by sieving and washing the mixes. Each sample was measured at least twice to ensure reproducibility. The particle size distribution was evaluated for as-delivered LWA ($Delivered_{LWA}$), LWA extracted from the mixes before pumping ($Reference_{LWA}$), and LWA recovered after pumping for each pumping equipment (TP_K_{LWA}, TP_S_{LWA}, and TP_P_{LWA}).

3.2.5 Fresh concrete properties

The consistency of the fresh concrete was evaluated by using the slump test following EN 12350-2 [119]. The degree of compactability was determined by following EN 12350-4 [120], and the air content was measured by using the pressure equalization method outlined in EN 12350-7 [121]. Fresh concrete density for all specimens was assessed following EN 12350-6 [122].

3.2.6 Dry density and thermal conductivity

Dry density was measured following EN 992 [123]. Thermal conductivity was evaluated using the transient plane source method (TPS 2200, Hot Disk, Gothenburg, Sweden) given in EN ISO 22007-2 [124]. Before measurements, specimens were dried to achieve mass constancy and then cooled to a stable temperature of 23 °C. During the cooling process, samples were stored in an airtight container with silica gel to preserve dryness. Thermal conductivity measurements were performed on at least three specimens per sample to ensure accuracy and reproducibility.

3.2.7 Load-bearing behavior

Compressive and flexural strength

Compressive strength tests were conducted after 28 days on cubes, cylinders, and drilled cores, following EN 1354 [125]. Flexural strength was evaluated using a four-point bending test on each of three beams (100 × 100 × 500 mm) with a span of 300 mm, performed after 28 days following EN 1521 [126].

Sustained loading

The sustained loading behavior of concrete was assessed using cylindrical specimens subjected to a steadily increasing load at a low rate until failure, typically over 6 – 7 hours. Specimens were pre-conditioned in a standard climate (20 °C, 65 % relative humidity) to

achieve equilibrium moisture content. Deformation was recorded using inductive displacement transducers aligned with the loading direction.

The reduction coefficient (α) for long-term compressive strength effects was calculated as the ratio of the ultimate load to the average compressive strength at the reference age. This methodology has been applied to study aerated concrete, NC, LAC, and ILC and is widely cited in the literature [45,79,127–129]. Results were compared with reduction coefficients from building codes, such as EN 1992-1-1 [55] and EN 1520 [60], to contextualize material performance.

Composite strength

The composite strength of specimens, consisting of a sheet steel column embedded in LAC+, was investigated to evaluate the load-bearing behavior of a novel wall element construction method as described in **Chapter 3.1.2**.

Representative composite specimens were fabricated in a precast plant to study the stabilizing effect of LAC+ on sheet steel profiles under compression. The specimens measured 580 mm in height with a 250 × 250 mm cross-section and featured a sheet steel framework embedded in LAC+, with a concrete cover of 37.5 mm on the wide side of the sigma profiles. U-profiles were integrated at the top and bottom of the specimens to ensure effective load transfer and proper fixing within the formwork. Specimens were subjected to compressive loading until failure, and their load-bearing performance was compared to that of plain sheet steel profiles. The technical specifications of the sigma profile are summarized in **Chapter 7.3** (**Table 1**).

3.2.8 Deformation behavior

The modulus of elasticity was determined on drill cores or cast cylinders (h/d = 300/150 mm) after 28 days, following EN 1352 [130].

Shrinkage and creep deformations were determined on drill cores following DAfStb Booklet 422 [131] in a controlled climate chamber (20 °C, 65 % relative humidity). Shrinkage deformation was recorded using displacement gauges, with length changes recorded at fixed intervals up to 460 days. For creep measurements, three drill cores were subjected to a constant stress equal to one-third of their average 28-day compressive strength.

Deformations were measured using three displacement gauges, starting at 30 days of concrete age and recorded at specified intervals up to 460 days.

3.2.9 Determination of CO_2 absorption and maximum capacity

The CO_2 absorption and maximum capacity of ILC was evaluated by TGA (STA 449 F3 Jupiter, Netzsch-Gerätebau GmbH, Selb, Germany) coupled with Fourier-transform infrared spectroscopy (FTIR, Nicolet iS10, ThermoFisher Scientific, Waltham, Massachusetts, USA). Samples were prepared in three particle size fractions (< 1 mm, 2 – 4 mm, and 8 – 16 mm) and conditioned in a glovebox (Sylatech, Walzbach, Germany) under a controlled N_2 atmosphere (21 °C, 53 ± 5 % relative humidity) to stabilize their initial mass. Subsequently, the samples were exposed to a nitrogen atmosphere containing 0.5 % CO_2 by volume for 10 days.

Coupled TGA-FTIR analyses were conducted at four time points (0, 3, 7, and 10 days) to monitor mass loss attributed to CO_2 release, distinguishing it from H_2O, over a temperature range of 300 – 1000 °C (see **Chapter 7.4**, **Appendix A**). The mass loss corresponding to CO_2 release was linked to calcium carbonate decomposition, enabling the calculation of CO_2 uptake.

The maximum CO_2 absorption capacity was determined following the method of Greve-Dierfeld et al. [132], which relates absorption potential to the CaO content of the recycled material. CaO content was quantified via inductively coupled plasma optical emission spectrometry (ICP-OES, Varian 720 ES spectrometer, Agilent Technologies, Santa Clara, CA, USA) after melt fusion (see **Table 6** in **Chapter 7.4**). The carbonatable CaO fraction ($m_{CaO\text{-}CO2}$) was calculated by subtracting contributions from LWA and calcium sulfate. LWA content was estimated using Na_2O levels, assuming negligible cement-derived Na_2O, while SO_3 content was used to correct for calcium sulfate contributions.

3.2.10 Scanning electron microscopy (SEM)

The SEM analysis was performed using a Zeiss EVO® LS 15 microscope (Evo LS 15, Zeiss, Oberkochen, Germany) operated at an acceleration voltage of 20 kV. The analyses were carried out on broken samples coated with 15 nm gold.

4 Main results

The following main results are based on three fundamental case studies, each addressing a different strategy for optimizing lightweight concrete technologies. The research explores the pumpability of ILC to ensure consistency and minimize segregation, examines the integration of optimized LAC with steel frameworks to balance thermal and structural performance, and investigates ILC recycling methods to increase material circularity and reduce environmental impact, providing practical solutions for modern construction. **Chapter 4.4** reflects these findings in the context of balancing environmental and technical attributes for sustainable lightweight concretes.

4.1 Rationalizing concrete placement in modern construction

While pumping is a well-established method for placing normal concrete, lightweight concrete poses unique challenges due to its porous LWA. This study examines how mix design, rheology, and pumping parameters affect pumpability, intending to improve practical guidelines and increase the efficiency of lightweight concrete applications in construction. The challenge of successful ILC pumping is addressed in a comprehensive case study [44], which can be found in **Chapter 7.4**.

4.1.1 Pumping of ILC with highly porous aggregates

For each pump, several pumping runs were performed with different pumping pressures, equipment settings, and partial adjustments of water and additives. The following characteristics were found for each type of pump with adjustment parameters to improve the process:

Piston pump (TP_K):

- Observed effects: Cyclical material transport reduced flowability due to the removal of water or cement paste from the fresh concrete, resulting in stiffer fresh concrete and potential pipe blockages at high pressures.
- Control measures: A shorter stroke length reduces suction effects; lower pressure minimizes fresh concrete compression and a gradual increase in flow rate assists in steady pumping.

Eccentric screw pump (TP_S):

- Observed effects: Significant variations in fresh density and slump flow at both low and high pump pressures, with increased susceptibility to segregation.
- Control measures: Reduced rotor-stator gap minimizes damage, maintaining low pressure prevents segregation, and optimized rotor speeds for balanced flow.

Rotor pump (TP_P):

- Observed effects: The pump delivered a smooth and consistent flow with minimal impact on fresh concrete properties.
- Control measures: Controlled air supply in the suction port enhances material flow, pressure regulation prevents blockages, and optimized roller speed yields consistent flow rates.

While all three pumps demonstrated the capability to pump ILC, a careful evaluation of the impact of the pumping process on both the fresh and hardened concrete properties is essential to ensure that the final product meets established standards within acceptable limits.

4.1.2 Effects of pumping on the fresh state behavior of ILC

The varying pumping methods exert different mechanical and pressure forces on the fresh concrete, which can significantly impact the porous LWA. Consequently, the impact of pumping is crucial, given that the LWA constitutes over 70 % of the mix volume and is essential for the fresh and hardened concrete properties of the ILC. Key considerations include how this will affect the water absorption of the LWA under compression, and how the LWA will resist mechanical abrasion.

Exceeding the particle strength of the LWA can compromise the integrity of the fresh concrete, resulting in increased water absorption and subsequently reduced workability. **Figure 5** provides the particle size distribution of the LWA as-delivered ($Delivered_{LWA}$), as well as the LWA taken from the fresh concrete before ($Reference_{LWA}$) and after pumping (TP_K_{LWA}, TP_S_{LWA} and TP_P_{LWA}) It reveals a uniform shift toward finer sizes after pumping, reflecting the mechanical abrasion of the LWA. This shift is further validated by quantitative metric functions, as detailed in **Table 4** in **Chapter 7.2**. It is apparent from this figure, that the piston (TP_K) and the rotor pump (TP_P) caused less damage compared to the screw pump (TP_S).

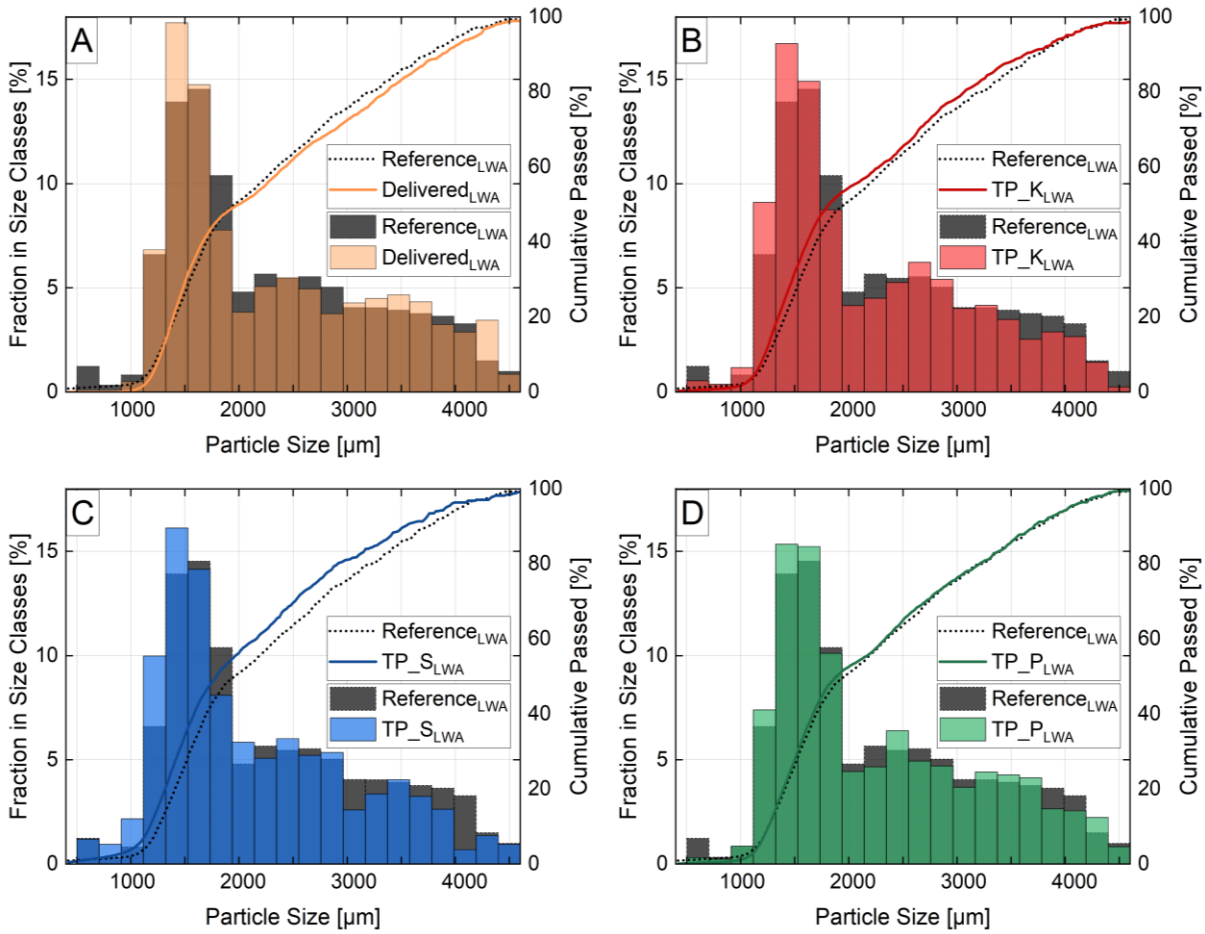

Figure 5: Particle size distributions across 20 size classes (400 – 4500 µm). A: Reference LWA ($Reference_{LWA}$) compared to as-delivered LWA ($Delivered_{LWA}$). B, C, D: Reference LWA compared to LWA after pumping: TP_K_{LWA} (B), TP_S_{LWA} (C), and TP_P_{LWA} (D).

To ascertain the impact of altered particle size distribution on fresh concrete, it is essential to examine the properties of both fresh and hardened concrete. Fresh concrete test results showed an increase in fresh density for all pump types, with values increasing by 2 – 5 %. Simultaneously, the workability, measured by the slump flow, decreased after pumping. The

rotor pump caused a minimal reduction in slump flow of only 2 %, while the piston and screw pumps led to significant reductions of 12 % and 30 %, respectively. The observed increase in fresh concrete density and decrease in slump flow can be attributed to the enhanced absorption capacity of the LWA under pump pressure and the associated abrasion. When the particle strength of the LWA is exceeded, the aggregates become damaged, exposing their enclosed pores. This damage reduces the aggregate volume and increases fresh concrete density. Furthermore, the broken surface structure of the LWA exposes the internal pores, which increases their absorption capacity. These changes allow the LWA to suck water or cement paste from the fresh concrete, leading to reduced workability.
Despite these changes, all the ILC conveyed maintained their compactability and were subsequently qualified as Class C4 according to EN 12350-4 [120]. Accurate determination of air content is essential but challenging because the pressure method cannot distinguish between air voids in cement paste and air-filled pores in LWA. However, its reproducibility allows qualitative comparisons between pumping operations and the reference. The results indicate no significant differences in air void content due to pumping.
The fresh concrete properties are summarized for each pump type in **Table 2** together with the unpumped reference.

Table 2: Summary of fresh concrete properties for ILC before pumping (Reference) and after pumping (TP_K, TP_S, TP_P).

Property	Reference	TP_K	TP_S	TP_P
Fresh Density [kg/m³]	694	705	723	730
Slump Flow [mm]	490	430	360	480
Degree of Compactability [-]	1.0	1.0	1.0	1.0
Air Content [Vol.-%]	24	25	22	24

4.1.3 Effects of pumping on hardened concrete properties

As highlighted in the literature (see **Chapter 2.2.1**), the pumping process can adversely affect the properties of the hardened concrete through various transport phenomena. Combined with the abrasive effects on the LWA, it is crucial to assess whether the mechanical and compressive forces applied during pumping could lead to structural damage, strength reduction, or reduced durability in the hardened concrete.

Figure 6 (right) shows that the compressive strength of the pumped ILC is close to the reference value. The compressive strength of TP_K and TP_P showed a smaller coefficient of variation, 5 % and 3 % respectively, compared to the reference value of 7 %. In contrast, the coefficient of variation of the compressive strength of TP_S is 12 % compared to the reference value. The higher variation is also observed for fresh and dry density and reflects the observed challenges of pumping pressure and abrasion in TP_S on fresh concrete. The change in compressive strength after pumping is crucial, since the load transfer of ILC primarily occurs through the granular structure of the LWA, rather than the matrix, as known for NC [21,68]. This makes the granular structure highly susceptible to changes induced by pumping, such as the alterations in particle size distribution presented in the previous section. **Figure 6** (left) contextualizes the study's strength and density tests by comparing the dry density and compressive strength with data from project-related approvals on completed construction projects using the same ILC and a concrete bucket for placement [44]. As can be seen from the figure, the dry density and compressive strength of the pumped specimens fit in well with the overall picture of the samples from structures. By calculating the normative values following EN 1520 [60], it was confirmed that the pumped ILC achieves the same classifications as the

reference, including strength class LAC 4 with a characteristic strength of 4 N/mm² and density class 0.6 with a dry density of 600 kg/m³ or less. Furthermore, the findings on the flexural strength and modulus of elasticity, as outlined in **Table 3**, demonstrate comparable material behavior across pump types, thereby suggesting that the pumping process does not significantly influence the material's characteristics.

Thermal conductivity, which is closely linked to dry density, is significantly influenced by the pore volume and pore size distribution in the hardened concrete. If pores are enlarged or destroyed during pumping –due to abrasive effects on the LWA or suppression of air void formation– the thermal conductivity could increase. However, the experimental results presented in **Table 3** do not indicate a significant increase in thermal conductivity due to the pumping process.

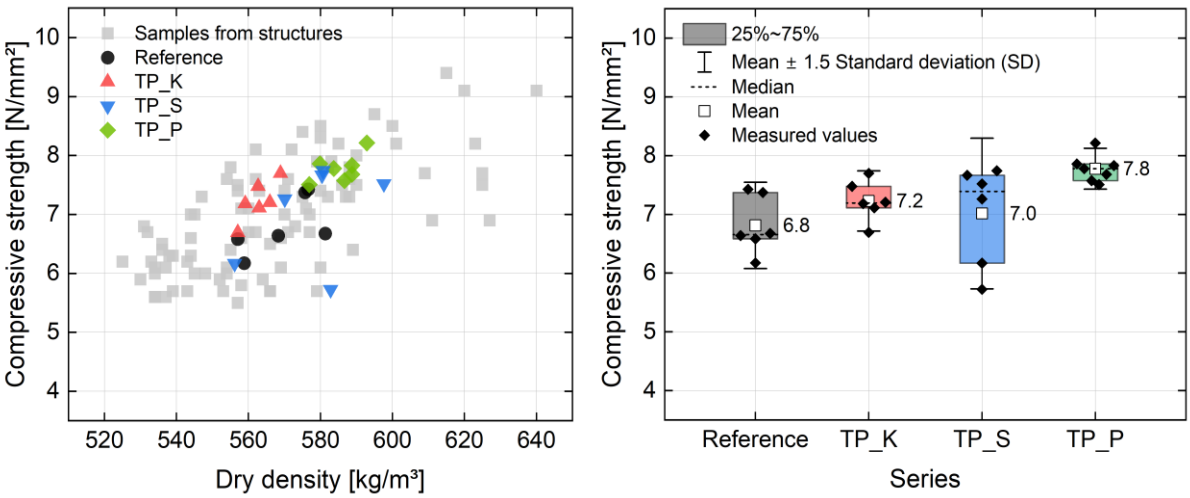

Figure 6: Left: Dry density and compressive strength of reference and pumped cube specimens, including data from project-related approvals for completed construction projects with the same ILC using a concrete bucket for placement. Right: Compressive strength is shown in box format with statistical indicators.

Table 3: Summary of hardened concrete properties for ILC before pumping (Reference) and after pumping (TP_K, TP_S, TP_P).

Property	Reference	TP_K	TP_S	TP_P
Hardened Density [kg/m³]	681	690	709	715
Dry Density [kg/m³]	570	563	578	586
Compressive Strength [N/mm²]	6.8	7.2	7.0	7.8
Flexural Strength [N/mm²]	1.0	1.0	1.1	0.9
Modulus of Elasticity [N/mm²]	3,367	3,379	3,289	2,960
Thermal Conductivity [W/(m·K)]	0.154	0.152	0.155	0.167

4.2 Thermal optimization in novel prefabricated wall elements

Stricter requirements for thermal insulation in the field of construction have driven the development of innovative and energy-efficient building methods. These advancements aim to meet stringent energy regulations, such as the *'Gebäudeenergiegesetz' [133]*, while ensuring sustainability and practicality in design and application. Wall elements, in particular, are critical for achieving these goals as they play a central role in thermal performance and overall structural integrity. The underlying study on the challenging process of thermal optimization of LAC is detailed in [45] (see **Chapter 7.3**).

4.2.1 Material optimization for thermal and structural efficiency

The optimization of the LAC+ focused on iteratively refining its composition, including adjustments to the proportions of LWA, binder paste, and foam. The primary goal was to maximize thermal efficiency while maintaining sufficient strength to stabilize the thin-walled steel framework. The key parameter in achieving this goal is the reduction of material density, as lower density directly correlates with reduced thermal conductivity. This reduction in density was maximized by a porosification of the binder paste. The porosification was achieved by introducing fine air bubbles into the binder paste using a foam generator that uses water and air pressure in conjunction with a foaming additive. The properties of the foam were controlled by adjusting the air and water pressure and the dosage of the foaming agent. Once produced, the foam was mixed into the fresh concrete, where the foamed cement paste filled voids between LWA particles. Successful porosification stabilizes the granular structure of the LWA, allowing for further reduction in density while also minimizing convective heat transfer through voids. However, the porosification process required precise control of foam quality and quantity. Insufficient foam led to incomplete void filling, resulting in poor porosification. Conversely, excessive foam disrupted the granular structure, weakening the load-transfer mechanisms characteristic of LAC+. These effects are illustrated in **Figure 7**, comparing partial porosification (left) to complete porosification (right) in LAC+.

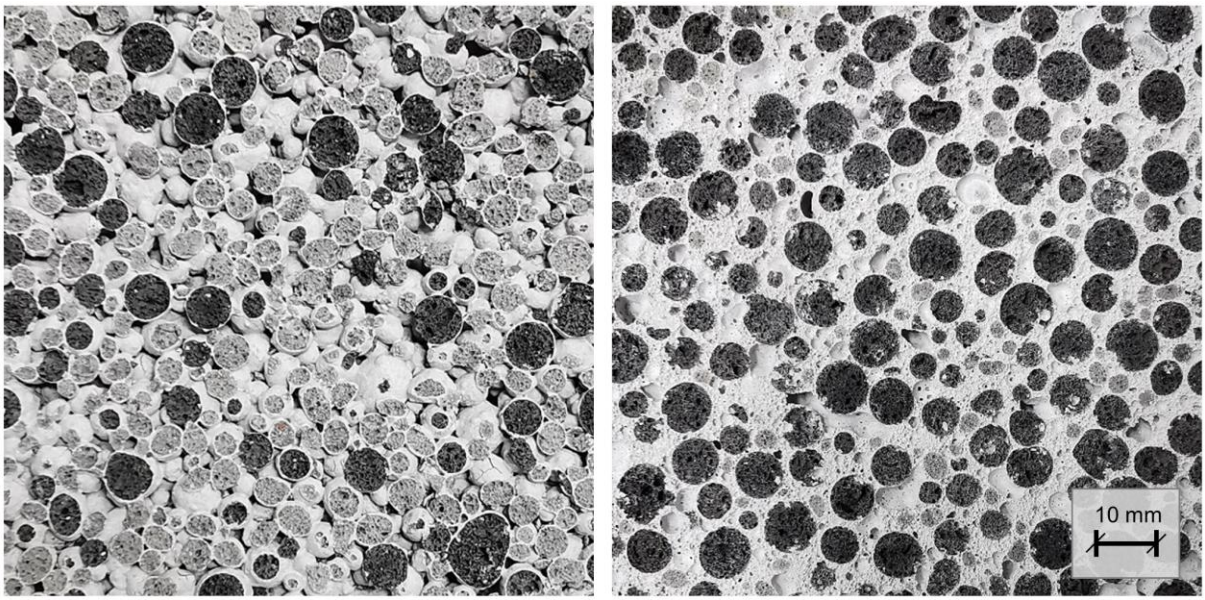

Figure 7: Cross-section of optimized LAC. Series 3 (right) exhibits significantly higher porosity compared to Series 2 (left), which closely resembles conventional LAC with its open-pore structure.

The first two test series, manufactured in two different precast plants, achieved the target dry density of 400 kg/m³ with an average compressive strength of 1.1 N/mm². However, the high standard deviations of 0.11 N/mm² (Series 1) and 0.12 N/mm² (Series 2), resulting in variation coefficients of 11 % and 12 %, respectively, reflected the challenges of transferring laboratory results to factory-scale production. In this context, the challenges associated with scaling the optimized LAC+ mix design to precast production were as follows:

- **Raw material variability:** Storage conditions for LWA influenced its moisture content, affecting water absorption during mixing. Open-air storage, as observed at manufacturer 1, introduced greater variability compared to covered silos at manufacturer 2.

- **Compaction methods:** Vibrating roller compaction at manufacturer 1 provided more uniform results compared to the shaking compaction used at manufacturer 2, which occasionally caused uneven foam distribution and LWA aggregation.
- **Foam sensitivity:** The externally mixed foam used for porosification was highly sensitive to dosage, mixing time, and temperature, leading to the variability of the final LAC+ properties.
- **Mix design adjustment:** Balancing strength and thermal conductivity within the target density range required precise adjustments, particularly given the challenges outlined above.

In the third test series, these insights led to improved outcomes. The dry density was reduced to 360 kg/m³ while compressive strength increased to 1.2 N/mm², and the coefficient of variation dropped significantly to 4 %. The difference in dry density between the heaviest and lightest specimens was only 22 kg/m³, indicating high uniformity. In terms of thermal conductivity, the first two test series achieved values of 0.118 and 0.121 W/(m·K) respectively. The further improvement described for test series 3 resulted in a further reduction in thermal conductivity of 0.09 W/(m·K). Assuming a realistic wall thickness of 50 cm, neglecting the influence of embedded steelwork and using measured rather than designed values, the U-value for series 1 and 2 is 0.23 (m^2·K)/W, and 0.17 (m^2·K)/W for series 3. This is well below the current maximum U-value for external walls (for new buildings, reference building method) according to reference values in Gebäudeenergiegesetz [133] of 0.28 (m^2·K)/W. Furthermore, the measured values are competitive and suitable for energy-efficient building envelopes, even when an expected tightening of the requirements is taken into account, for example, a further reduction of 20 % to 0.21 (m^2·K)/W, as proposed by Lösch [65]. In order to classify the measured values, it must be taken into account that in Germany there are no fixed requirements for the thermal resistance of individual building components, as the transmission heat loss refers to the entire surface of the building envelope. Therefore, the required U-value can be achieved not only by adjusting the thickness of the external wall, but also by considering the thermal performance of other buidling components (e.g. windows, roof, etc.) [65]. **Figure 8** shows the results of the experimental investigation into material optimization, highlighting the relationship between dry density and compressive strength in three comprehensive series of tests carried out in two precast plants.

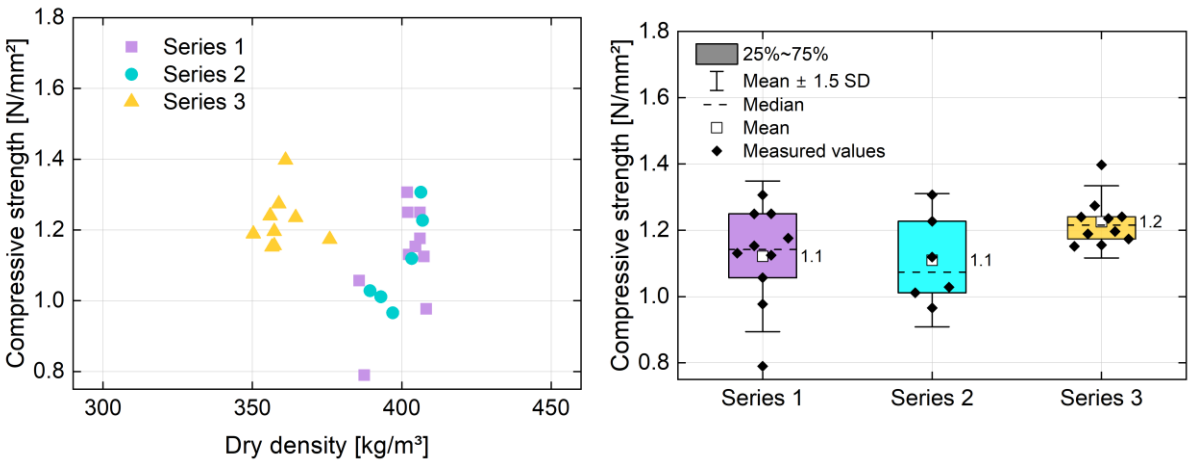

Figure 8: Left: Dry density and compressive strength of three extended test series from precast plants. Right: Compressive strength presented in box format with statistical indicators.

In addition to the closely linked parameters of dry density, thermal conductivity, and compressive strength, further evaluation of deformation-related properties was required to assess their influence on the interactions between LAC+ and the steel frame in the composite system.

The deformation-related properties of LAC+ are of particular interest because they affect crack formation, stress development, and the bond between LAC+ and the steel framework, as well as ensure the long-term performance and durability of the composite system. These time-dependent deformations can arise from load-independent processes, such as shrinkage, or load-dependent processes, such as creep, modulus of elasticity, and sustained loading.

- **Modulus of elasticity:** The normative estimation of the modulus of elasticity, based on EN 1520 [60] and calculated using a constant factor (see **Chapter 7.4, Formula 3**), yields values of 1,016 N/mm², 1,106 N/mm² and 1,240 N/mm² for test series 1, 2 and 3, respectively. However, experimentally determined values, as presented in **Table 4**, were consistently lower. This discrepancy is attributed to the increased porosity of the cement paste, which reduces matrix stiffness and deformation resistance.
- **Shrinkage and creep:** Empirical data for LAC with a foamed matrix are limited, particularly within the density ranges examined here. A prior study [61] exhibited comparable shrinkage values for LAC without fines and LAC with a foamed matrix, approximately 0.6 mm/m at a density of 600 kg/m³. LAC with a foamed matrix tend to exhibit higher specific creep values compared to conventional lightweight concrete, which improves relaxation potential and reduces the risk of shrinkage cracking [61]. EN 1520 [60] recommends a shrinkage value of 0.75 mm/m (at 45 ± 5% relative humidity) and a final creep value of 2.0. The experimental results for LAC+, shown in **Figure 9** (left), align well with these standards, with shrinkage measured at - 0.62 mm/m and final creep deformation at - 0.96 mm/m (final creep value: 1.55).
- **Sustained loading:** This parameter measures the reduction in compressive strength under long-term service loads and identifies a critical microstructural threshold where irreversible damage may occur. For LAC+, the coefficient for long-term effects was experimentally determined to be 0.81, slightly below the normative reduction value of 0.85 (EN 1520 [60]). However, this remains within acceptable limits for structural applications. The standard also recommends reducing this value to 0.80 when the compression zone narrows in the direction of the most heavily compressed fibers. The relative load capacity of compressive strength under sustained loading for test series 3 is shown in **Figure 9** (right).

Table 4 provides a comprehensive summary of the performance evaluation results, highlighting the key material properties across the three test series. Some entries are missing due to the extensive test matrix and methodological effort, focusing on the most critical specimens (e.g. sustained loading, series 3). **Figure 9** illustrates the experimental findings for these properties, offering a detailed view of the deformation behavior under both load-independent (shrinkage) and load-dependent conditions (creep and sustained loading).

Table 4: Overview of mechanical parameters for three test series of optimized LAC+.

Parameter	Series 1 (precast plant 2)	Series 2 (precast plant 1)	Series 3 (precast plant 1)
Dry density [kg/m³]	400	407	358
Thermal conductivity [W/(m·K)]	0.118	0.121	0.092
Mean compressive strength [N/mm²]	1.12	1.11	1.23
Modulus of elasticity [N/mm²]	969	1,046	878
Sustained loading factor α [-]	-	-	0.81
Shrinkage[1] [mm/m]	-	-0.62	-
Creep[1] [mm/m]	-	-0.96	-

[1]Measurement started 30 days after concreting.

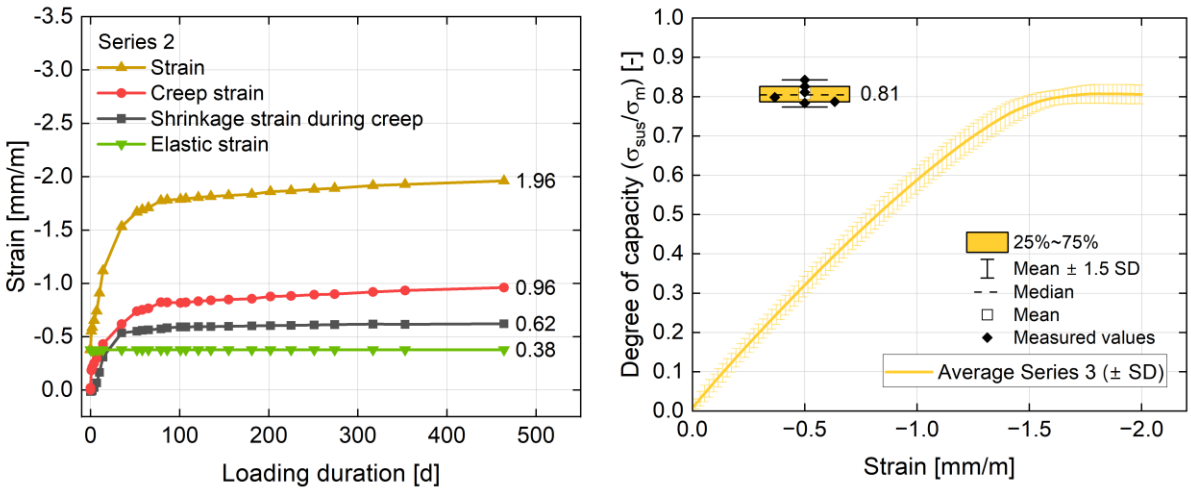

Figure 9: Strains during shrinkage and creep for test series 2 (left), relative load capacity ($\sigma_{sustained}/\sigma_m$) of compressive strength under sustained loading (right).

4.2.2 Evaluating the structural integrity of the composite system

The integration of the steel framework into the LAC+ matrix is an essential prerequisite for forming stable and functional wall elements. The surrounding LAC+, despite its relatively low strength, must effectively prevent buckling of the vertical steel profiles, which are vulnerable to stability failure. To validate the structural performance of the composite system, a test program compared the load-bearing behavior of a standalone steel profile with that of an identical steel profile embedded in LAC+. **Figure 10** illustrates the specimens. The left side (A,B,E,F) of the figure shows the pure steel profile, while the right side (C,D,G,H) displays the composite profile. The failure modes are visibly distinct. The pure steel profile failed due to buckling, while the composite specimen failed due to spalling of the LAC+, which destabilized the steel frame and caused its ultimate failure. The top portion (A,B,C,D) of the figure shows the specimens before testing, and the bottom portion (E,F,G,H) shows the post-test deformation.

Figure 10: Comparison of test specimens for the composite system. Left: Four plain steel profiles connected by spot-welded horizontal U-profiles. Right: Four identical steel profiles embedded in LAC+. Specimens are shown before (A-D) and after (E-H) the test.

The experimental results demonstrate that embedding steel profiles within LAC+ significantly enhances their load-bearing capacity. The composite samples achieved an ultimate load of 170 kN, over three times higher than the load-bearing capacity of the standalone steel profile (52 kN) and more than 50 % higher than the maximum compressive load capacity specified by the manufacturer (110 kN, see **Chapter 7.3**, **Table 1**). These findings confirm that the composite strength of the steel profiles and the LAC+ matrix effectively prevents stability failure due to buckling. **Figure 11** provides a detailed summary of the test results, with box diagrams and load-displacement curves comparing the compression test outcomes for both the steel profiles and the composite specimens.

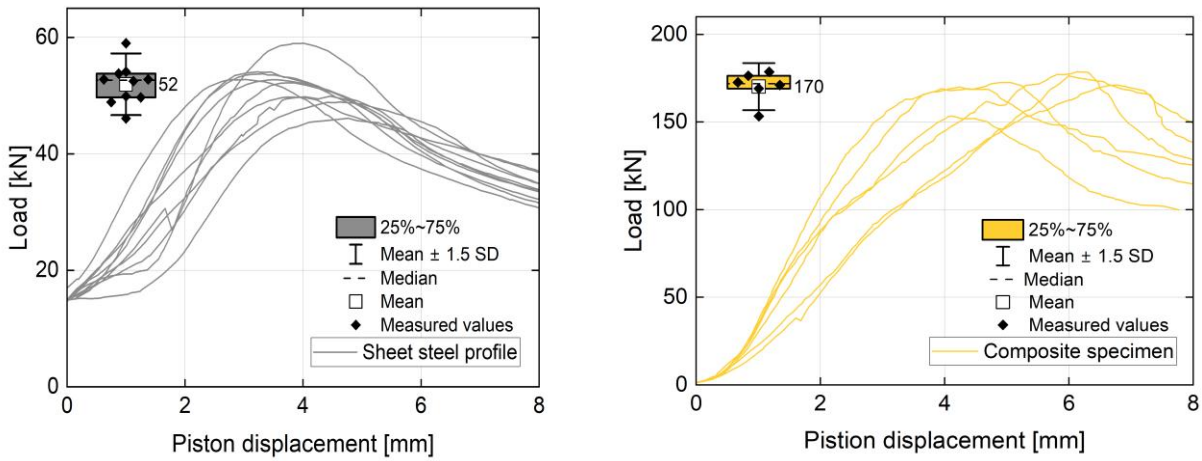

Figure 11: Composite test results for plain sheet steel (left) and composite specimens (right). The figure includes load–displacement curves alongside box plots summarizing key statistical parameters. Note: the y-axis are scaled differently between the two charts to better highlight characteristic trends within each test group.

4.3 Advancing circular practices in lightweight concrete recycling

The transition towards sustainable construction requires innovative approaches to minimize waste and reduce carbon emissions. Lightweight concretes face specific recycling challenges because existing concrete recycling standards do not account for their unique properties. These limitations are effectively addressed in a comprehensive case study [46], which develops methods to recycle the most challenging type of lightweight concrete –ILC– and reintroduce it into the construction cycle, contributing to the broader goal of net-zero concrete production.

4.3.1 Evaluating RLCA properties for recycled concrete design

The mechanical processing of lightweight concretes distinguishes significantly from NC. While crushing NC, cracks traverse through the weak ITZ between the cement matrix and the aggregates, resulting in RCA composed predominantly of normal-weight aggregate with adherent mortar. In contrast, well-designed lightweight concrete lacks an ITZ, which leads to cracks also propagating through the LWA. Therefore, the mechanical processing of lightweight concrete results in an agglomerate structure of the RLCA. The agglomerate structure distinctly differentiates RLCA from recycled products of NC. The RLCA is composed of varying proportions of partially fractured LWA and adhering mortar, which determines their characteristic properties. **Figure 12** presents RLCA at three magnification levels, illustrating its agglomerate structure. (Left) A petri dish containing RLCA particles of the 4 – 8 mm fraction is shown at 100 mm scale, with a single particle highlighted in blue. (Middle) A closer view at 10 mm scale isolates the RLCA particle, revealing the distinction between the porous cement matrix and the LWA, as well as the characteristic agglomerate structure. (Right) At 1 mm scale, a SEM image captures the internal structure of the recycled concrete, showing the incorporation of the RLCA particle within the surrounding matrix.

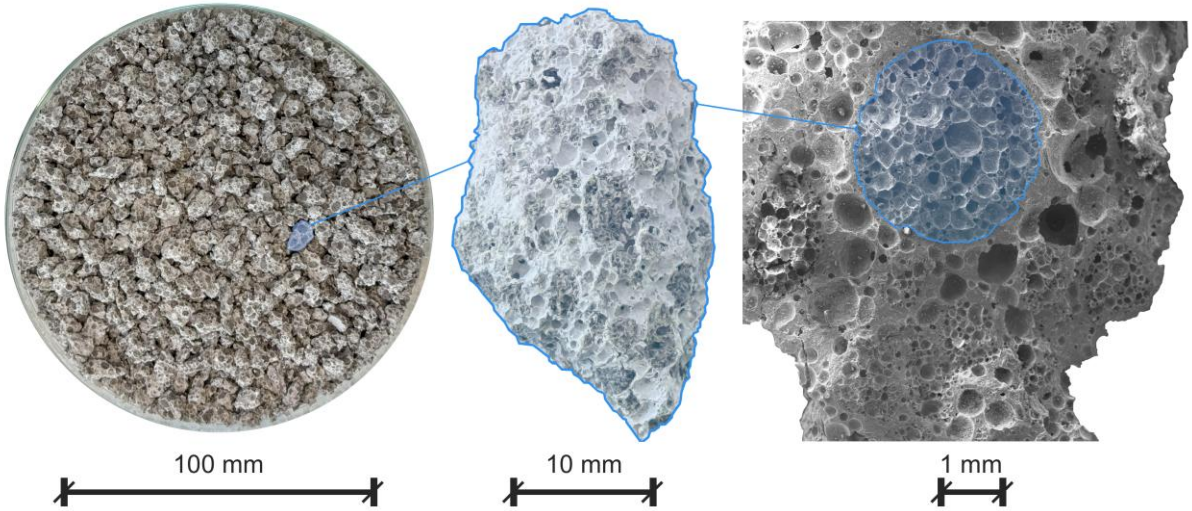

Figure 12: RLCA at three magnification levels: (left) petri dish with 4 – 8 mm particles, highlighting one RLCA particle; (middle) closer view distinguishing porous matrix and LWA; (right) SEM image showing the RLCA particle embedded in the RILC.

The challenge of incorporating uniquely structured RLCA into concrete is therefore to adjust the mix design and to carefully classify different batches of recycled material to account for the greater variation in material properties. These properties, such as higher porosity and water absorption, are essential in replicating the mix design of ILC_{Origin} in the production of RILC. **Figure 13** shows the particle density and water absorption of RLCA across different grain size

groups, compared to the LWA originally used in ILC_{Origin}, conditioned in two distinct environments: 20 °C / 65 % relative humidity (storage condition) and oven-dried at 105 °C until constant mass (dry condition). The particle density of RLCA ranges between 730 and 1,590 kg/m³, with significant differences observed among the grain size groups. The $RLCA_{fine}$ group exhibits a substantially higher particle density –at least 500 kg/m³ heavier on average than the coarser RLCA fractions. This is attributed to the pronounced agglomerate structure of RLCA, where larger particles contain a higher proportion of LWA with relatively low density, while the $RLCA_{fine}$ fraction consists of more fragmented LWA with reduced pore volume, resulting in higher particle density. Consequently, particle density decreases with increasing particle size. These trends align with findings reported in the literature [40–42]. Compared to the original LWA (LWA_{Origin}) used in ILC_{Origin}, which has particle densities of approximately 345 kg/m³ for similar particle size groups, RLCA shows an increase in particle density by a factor of 2.6. This poses challenges in achieving the same density for RILC as the original ILC_{Origin}, given the substantial density increase in RLCA. The water absorption of RLCA ranges between 27 % and 60 % by weight, with significantly higher values observed under oven-dry conditions. Notably, water absorption of RLCA in storage condition exhibits considerable fluctuations, likely due to differences in initial moisture content. Given that moisture exchange with surrounding air is more extensive at the surface of ILC_{Origin} elements, it can be assumed that RLCA from these regions undergo a greater degree of exchange than RLCA from the internal regions. Storage conditions, such as free weathering versus controlled environments, may also influence these variations. These findings are in line with the findings of Smeplass [134], who investigated the phenomenon of water absorption in LWA at varying initial moisture states.

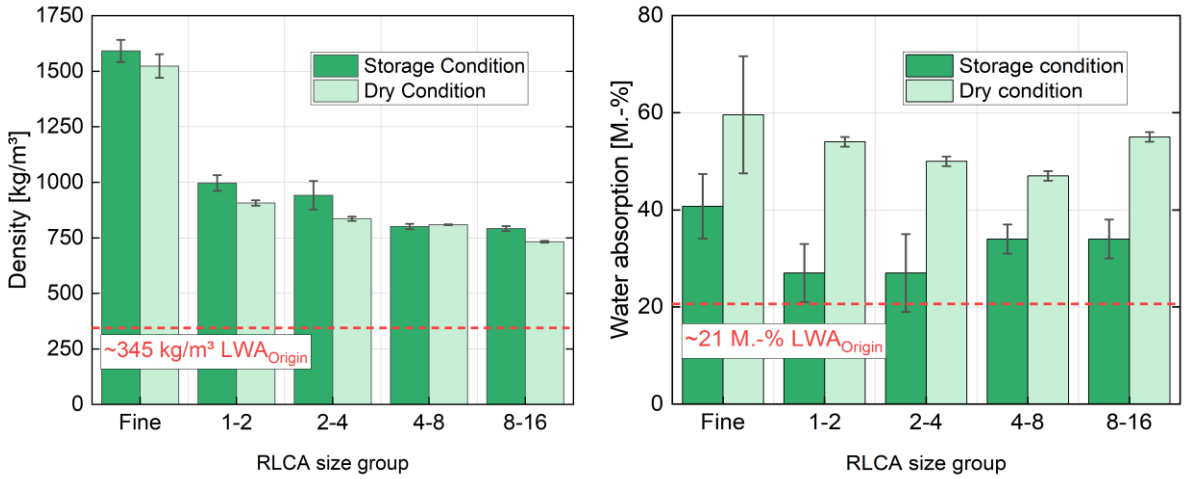

Figure 13: Particle density and water absorption of RLCA, subdivided by grain fractions, compared to the particle density of ILC's original aggregates (expanded glass) to illustrate the density increase. Results are differentiated between storage conditions (~20 °C / 65% relative humidity) and oven-dry conditions (mass constancy at 105 °C).

The accurate evaluation of RLCA water absorption is crucial, as uncontrolled water absorption from the concrete matrix can result in microcrack formation. These microcracks negatively impact achievable strength and compromise the durability of the hardened concrete [22].

4.3.2 Consistency in mix design and balancing strength and density

The mix design for RILC addresses specific challenges arising from RLCA properties, such as density variations, water absorption, and the effectiveness of air-entraining agents. To maintain consistency, the fresh concrete density and yield are continuously monitored throughout the

mixing process. **Figure 14** (left) summarizes the test results, showing an average fresh concrete density of 1,078 kg/m³ across nine batches, with a maximum deviation of 77 kg/m³. This closely aligns with the calculated mix design density of 1,088 kg/m³. The measured yield ranged from 92 % to 102 % of the calculated volume, confirming reproducibility and consistency despite the inherent variability of RLCA. Furthermore, the results validate the suitability of test methods described in EN 1097-6 [117] (Appendix C and Appendix D), originally designed for LWA, for determining density and water absorption in RLCA to achieve a successful mix design composition.

Figure 14 (right) gives an idea of the effort needed within the iterative mix design process aimed at replicating ILC_{Origin} properties, targeting a maximum dry density of 800 kg/m³ and a minimum compressive strength of 5.6 N/mm². Importantly, the results also indicate that the compressive strength of RILC is not limited to that of ILC_{Origin} but even can surpass it significantly. In the RILC test series (blue), an average dry density of 750 kg/m³ was determined, based on testing of 16 cylinders across different batches with a small coefficient of variation of 2 %. Thermal conductivity, measured on oven-dried specimens, averaged 0.159 W/(m·K), representing only a 3.3 % increase despite a 31.6 % higher dry density compared to ILC_{Origin}. This value remains well below the normative estimate of 0.205 W/(m·K) for that density according to EN 1520 [60].

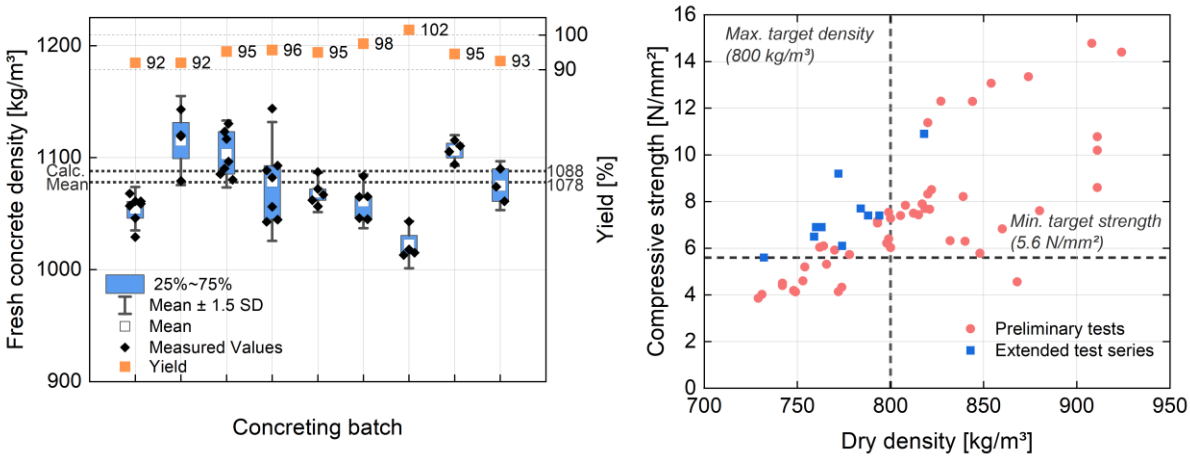

Figure 14: Results of mix design optimization for RILC production to replicate ILC_{Origin}. Left: Fresh concrete density compared to calculated density and average density across all batches, with yield shown on the secondary y-axis. Right: Relationship between dry density and compressive strength of 100 mm cubes for RILC (blue) compared to preliminary tests (red) targeting the density and compressive strength of ILC_{Origin}.

A potential explanation for the minimal increase in thermal conductivity observed in RILC lies in its more porous cement paste matrix compared to that of ILC_{Origin}. The higher porosity of the matrix results from the composition of the mixture. Specifically, the higher particle density of the RLCA compared to the original LWA had to be compensated for in order to fall below the maximum target density. This was achieved by a lower cement content and increased foaming agent addition. The resulting higher porosity might minimize convective heat transfer. However, more research is needed to understand the factors that influence thermal performance.

4.3.3 Evaluating the mechanical properties of RILC

To ensure that RILC can fulfill the same structural functions as ILC_{Origin}, its mechanical performance was verified experimentally. These tests evaluated compressive strength, modulus of elasticity, stress-strain relationships, and behavior under sustained loading.

The following section focuses on different evaluation aspects of the same test series to assess the mechanical performance of RILC. **Figure 15** (A) illustrates the relationship between dry density and compressive strength for RILC. Similar to classic LC and LAC, the compressive strength of RILC increases with rising dry density. Based on the same test series, the compressive strength results, shown in **Figure 15** (B), reveal a mean value of 7.1 N/mm² across nine cylinders from different batches, with a standard deviation of 0.9 N/mm². This slightly exceeds the mean compressive strength of ILC_{Origin}, which is 6.8 N/mm². The higher compressive strength of RILC can primarily be attributed to its increased dry density. However, the relatively moderate strength gain, despite this higher density, results from a trade-off between increased porosity and reduced cement content. This adjustment is necessary due to the significantly higher particle density of RLCA compared to the original LWA, which alters the overall mix composition and binder-to-aggregate ratio. Therefore, despite a 32 % increase in dry density, the thermal conductivity of RILC increased by only 3.3 %, highlighting its continued suitability for thermal insulation. In addition, for both RILC and ILC_{Origin}, the characteristic compressive strength, calculated according to EN 1520 [60], is 5 N/mm², meeting structural requirements and achieving a key objective of the recycling approach.

The stress-strain curves of RILC associated with the compressive strength tests are shown in **Figure 15** (B). These curves demonstrate an initial linear elastic behavior, followed by minimal plastic deformation, which leads to earlier failure compared to NC. **Figure 15** (C) plots ultimate strains as a function of dry density, showing that lower dry density results in reduced ultimate strains. This limited plastic deformation and elongation at failure, also observed in ILC by Hückler et al. [68], both appear to be characteristic of very lightweight concretes rather than being a direct result of the recycling process or the use of RLCA. However, the reduced elongation at failure requires careful structural design to mitigate the risk of brittle failure.

The modulus of elasticity as a function of compressive strength is shown in **Figure 15** (D). RILC has a mean modulus of elasticity of 3,750 N/mm² with a standard deviation of 385 N/mm², closely matching the estimated value of 3,730 N/mm² according to EN 1520 [60]. This value is slightly higher than the modulus of elasticity for ILC_{Origin} (3,370 N/mm²), primarily due to the higher dry density and compressive strength of RILC. These results demonstrate that the use of RLCA in RILC allows for moduli of elasticity comparable to those of LAC with conventional LWA.

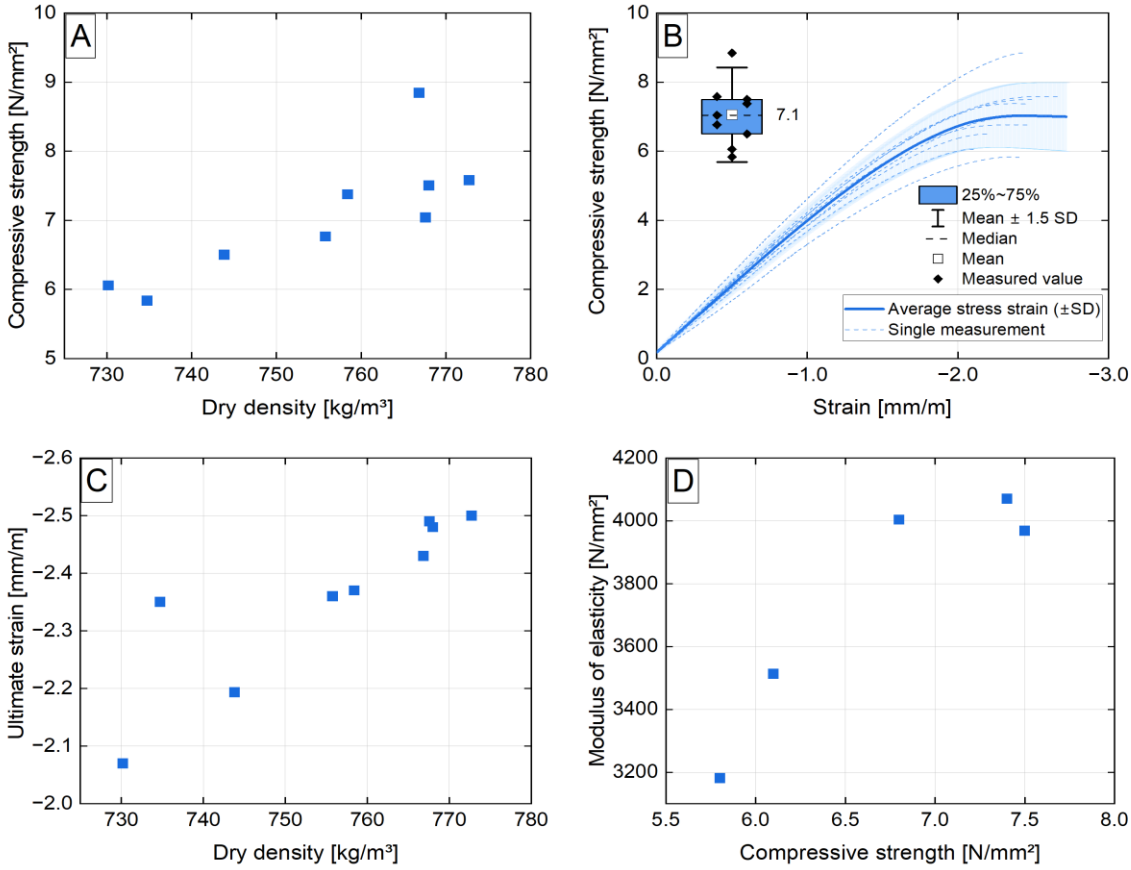

Figure 15: Compressive strength tests on RILC cylinders. A: Compressive strength as a function of dry density. B: Stress-strain curves and box plot showing statistical variation in compressive strength results. C: Ultimate strain in compression tests as a function of dry density. D: Modulus of elasticity as a function of compressive strength.

The experimental determination of the ratio of compressive strength under sustained loading ($\sigma_{sustained}$) to its 28-day compressive strength (σ_m) is indicative of the load-bearing behavior of the concrete under permanent stress in its installed state (see **Chapter 3.2.7**). The stress-strain curves for both RILC and ILC_{Origin} under sustained loading are shown in **Figure 16**. RILC exhibits an initial linear relationship between longitudinal strain and applied stress, transitioning into a plateau with slight plastic deformation at higher stresses. This behavior mirrors that of ILC_{Origin}, though RILC displays more pronounced plastic deformation. The reduction factor, α, which is defined by the relative load capacity of $\sigma_{sustained}$ and σ_m at ultimate load, was determined to be 0.80 for RILC and 0.84 for ILC_{Origin}. These values fall within the normative range of 0.75 to 0.85 for LC and LAC as specified by EN 1992-1-1 [55] national annex and EN 1520 [60], resp. For practical design, a conservative reduction factor of, for example, α = 0.75 is recommended to avoid overestimating load-bearing capacity. Similar results were reported by Schlaich et al. [79], who derived a reduction coefficient of α = 0.78 for ILC.

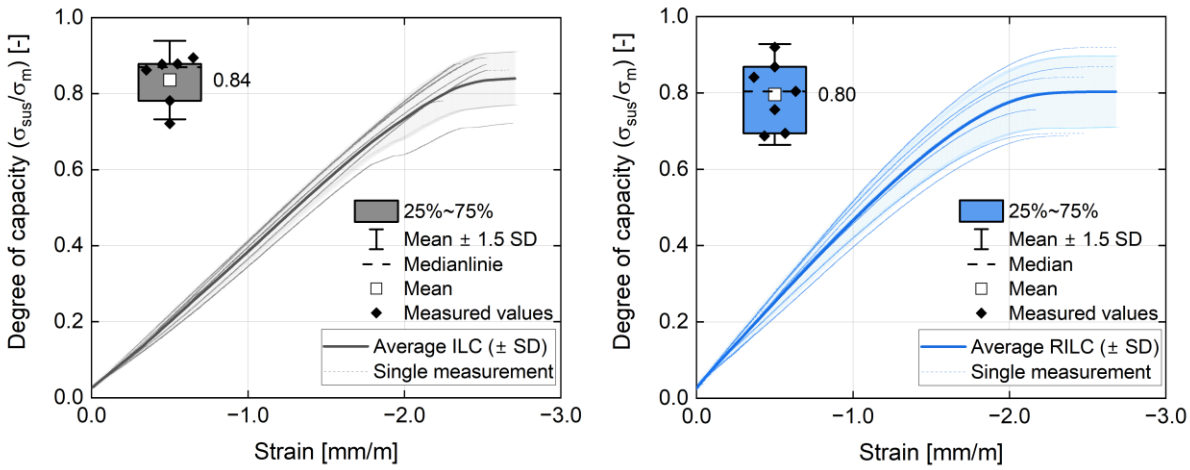

Figure 16: Relative load capacity ($\sigma_{sustained}/\sigma_m$) of compressive strength under sustained loading for ILC_{Origin} (left) and RILC (right).

The experimental findings on RILC are summarized in **Table 5** and compared with the reference value of ILC, along with a relative percentage change. It can be concluded that RILC behaves predictably under sustained compressive loading, and its mechanical properties align with the standards commonly applied to lightweight concretes. This confirms its suitability for structural applications.

Table 5: Summarized results for performance parameters of RILC and ILC_{Origin}

Property	**ILC_{Origin}**	**RILC**	**Change in RILC vs. ILC_{Origin}**
Dry density [kg/m³]	570[1]	750	+ 31.6 %
Compressive strength [N/mm²]	6.8[1]	7.1	+ 4.4 %
Thermal conductivity [W/(m·K)]	0.154[1]	0.159	+ 3.3 %
Modulus of elasticity [N/mm²]	3,370[1]	3,750	+ 11.4 %
Sustained loading factor α [-]	0.84	0.80	- 4.8 %

[1]Values determined in [44].

4.3.4 CO_2 sequestration potential of RLCA

To integrate CO_2 absorption into the LCA, it is necessary to quantify the CO_2 absorption of the RLCA and to compare it to the process-related emissions from recycling and carbonation, as well as to the Global Warming Potential (GWP) of the source material (ILC_{Origin}).
As illustrated in **Figure 17** (left), CO_2 uptake was measured for three RLCA particle size groups immediately after conditioning (0 days) and after 3, 7, and 10 days of controlled CO_2 exposure (0.5 vol.-% CO_2). The value of 0 days reflects the natural carbonation of RLCA, which was extracted from ILC_{Origin} 32 months before testing. The data reveals that finer RLCA fractions exhibit a faster carbonation rate in the initial period (3 days), a trend that slows down between 3 and 7 days and slightly reverses by 10 days. This early acceleration is primarily attributed to the larger specific surface area of finer RLCA fractions and, to a lesser extent, their slightly higher binder content (see **Table 9** in **Chapter 7.4**). The total CO_2 uptake values for $RLCA_{fine}$, $RLCA_{2-4}$, and $RLCA_{8-16}$ were 138 kg CO_2/t_{RLCA}, 128 kg CO_2/t_{RLCA}, and 123 kg CO_2/t_{RLCA}, respectively. Comparing these results with other studies on CO_2-update of RCA [97,98,104,108–112] remains challenging due to the variations in exposure conditions and materials analyzed. Variations in aggregate type, carbonatable material content, pre-conditioning, exposure duration, and environmental conditions —such as CO_2 concentration,

pressure, temperature, and humidity— contribute to this variability (see **Table 1** in **Chapter 7.4**) and highlight the need for a standardized methodology. **Figure 17** (Right) illustrates CO_2 uptake in relation to the theoretical capacity and compares it to the GWP of ILC. These values are given per cubic meter of ILC, which corresponds to approximately 680 kg of RLCA. The maximum theoretical carbonation capacity, calculated based on the available CaO content (see **Table 6** in **Chapter 7.4**), is highest for $RLCA_{fine}$ at 140 kg/m³, followed by $RLCA_{2-4}$ at 132 kg/m³ and $RLCA_{8-16}$ at 131 kg/m³. This similarity suggests minimal binder accumulation in finer RLCA fractions, likely due to the random fragmentation of LWA and cement paste during recycling. The relative utilization of the theoretical carbonation capacity for the investigated fractions is 68 %, 66 %, and 64 % respectively.

In the context of LCA, the initial GWP of ILC must be considered. Richter [135] estimates a GWP range of 255 to 295 kg CO_2/m³, with cement alone contributing 180 kg CO_2/m³ for ILC. These estimates account for a wide range of available ILC types produced with varying types and proportions of cement and LWA. The range is highlighted in **Figure 17** (left) to contextualize the results of the accelerated carbonation tests. To enable a direct comparison, the CO_2 uptake determined through accelerated carbonation can be expressed per cubic meter. This results in 94 kg CO_2/m³ for $RLCA_{fine}$, 87 kg CO_2/m³ for $RLCA_{2-4}$ and 84 kg CO_2/m³ for $RLCA_{8-16}$. Based on these values, accelerated carbonation reduces the initial GWP of ILC by 33 – 37 %, depending on the aggregate fraction. With respect to the VDZ Scenario 2050 [94], the objective is to attain net-zero CO_2 emissions. Achieving this objective involves a multifaceted approach, including the capture of 20 % of cement production emissions through a recarbonation process. Given that the cement contributes 180 kg CO_2/m³ to the total emissions of ILC [135], the aforementioned objective would be achieved at CO_2 uptake values above 36 kg CO_2/m³, as illustrated in **Figure 17** (Right). According to this classification, it can be stated that ILC_{Origin} has already absorbed 20 kg CO_2/m³ after 32 months and under natural conditions. This corresponds to approximately 11 % CO_2 reabsorption and therefore slightly more than half of the targeted 20 % recarbonation. With regard to the accelerated CO_2 uptake of RLCA, the reabsorption rate associated with cement emissions exhibits an even higher range, varying from 47 % to 52 %.

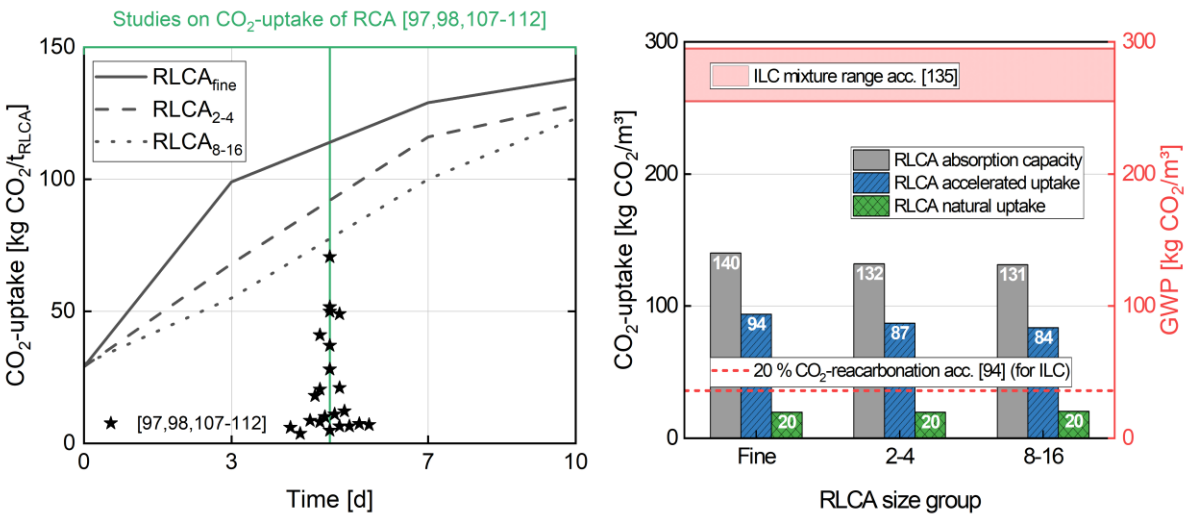

Figure 17: (Left) CO_2 uptake of three RLCA fractions after conditioning (0 days) and after 3, 7, and 10 days of CO_2 exposure, compared with literature data on RCA. (Right) RLCA uptake under natural and accelerated conditions, relative to its absorption capacity, reference GWP [135], and target recarbonation goal (acc. to [94]).

However, the recarbonation effect must be offset against the process-related emissions from recycling and the accelerated carbonation process itself. According to Kuroda and Kikuchi [97], the CO_2 equivalent emissions of the recycling process are equivalent to 4.4 kg CO_2 per cubic meter. Additionally, the large-scale study, titled *'FastCarb'* [102], provides quantifiable data on total CO_2 emissions resulting from industrial carbonation process. This study estimates the amount of CO_2 emissions to be 11 kg CO_2-eq/t_{RLCA}, with the carbonation process itself contributing only 0.9 kg CO_2-eq/t_{RLCA}, while the remaining emissions were attributed to transportation and infrastructure.

Assuming these values apply to ILC, emissions for accelerated carbonation of 7.5 kg CO_2-eq/m³ can be estimated. Therefore, the average CO_2 uptake of ILC_{Origin} over three fractions of 88 kg CO_2/m³ is offset by the estimated process-related emissions of 4.4 kg CO_2-eq/m³ for recycling and 7.5 kg CO_2-eq/m³ for accelerated carbonation, resulting in an effective recarbonation of 75.9 kg CO_2-eq/m³. Accordingly, the revised GWP (*'$GWP_{ILC,revised}$'*) of ILC_{Origin} is 179 kg CO_2-eq/m³, representing a 30 % reduction through accelerated carbonation.

These results demonstrate that recarbonation can be a valuable complementary measure in the decarbonization of concrete. In particular, its integration with recycling strategies provides an efficient method of CO_2 sequestration. When recycled ILC is reused as RLCA, material cycles are closed and the demand for primary aggregates is reduced.

However, the reabsorption rate of ILC is not representative of NC, and recarbonation alone cannot offset the substantial emissions from cement production. In particular, most of the GWP stems from the process-related CO_2 emissions released during the calcination of limestone. Consequently, further measures are therefore essential. These include the development of low-clinker or low-carbon cements, the use of alternative raw materials with lower energy demand, and the use of carbon capture, utilization, and storage technologies. To ensure implementation, these technical solutions need to be supported by market transformation and robust policy frameworks, as highlighted in the cement industry roadmaps [94,136].

4.4 Reflections on advancing lightweight concrete innovations

The research presented in this thesis evidences the potential of lightweight concretes to contribute to sustainable construction by balancing technical performance and ecological impact. By focusing on monolithic exterior walls that do not depend on additional insulation, the studies addressed key challenges and provided innovative solutions for practical applications. Through optimizing pumping processes, integrating steel frameworks, and recycling ILC, this work offers a pathway for advancing lightweight concrete technologies to meet modern construction demands.

Bridging innovation and sustainability in lightweight concrete

At the crossroads of technical innovation and ecological responsibility, this research highlights the role of lightweight concrete in addressing pressing environmental challenges.

- Pumping studies [44] proved that highly porous ILC can be pumped without compromising material integrity, enabling efficient construction processes with reduced labor and faster project timelines.
- The combination of LAC+ with a steel framework [45] introduced a novel prefabrication method, offering competitive thermal performance and structural stability for energy-efficient designs.
- Recycling ILC into RLCA and the fabrication of RILC with RLCA [46] demonstrated material circularity by maintaining near-original properties while reducing natural resource consumption, construction waste, and CO_2 emissions.

Enhancing technical performance

This research addressed critical technical challenges, improving both thermal efficiency and structural integrity to meet modern building requirements.

- ILC retained its thermal and mechanical properties post-pumping, supporting efficient construction processes.
- LAC+ combined low thermal conductivity with stabilized steel frameworks, preventing buckling and enhancing load capacity.
- RILC demonstrated comparable compressive strength and thermal performance to the original ILC, confirming the viability of recycling without performance loss.

These findings underscore the practicality of lightweight concrete as an efficient material for monolithic exterior wall elements.

Advancing standards for broader adoption

A significant barrier to the broader integration of the investigated lightweight concretes is their exclusion from existing standards, necessitating reliance on project-specific approvals and limiting accessibility. This thesis contributes to broader adaption by aligning the properties of ILC, LAC+, and RILC with existing frameworks, such as EN 1520 [60] and EN 13055 [52], and demonstrates compliance through experimental studies.

Key insights include:

- **Density and strength relationships:** The studied concretes exhibit density and strength trends similar to those observed in LAC. Lightweight concrete mix designs resembling LAC and containing high air content (> 10 % by volume) exceeding the classification thresholds for LC, disqualifying them as LC [73].

- **Modulus of elasticity:** Empirical estimates of modulus of elasticity aligned closely with experimentally determined values. This was observed despite variations in stiffness among the LWA examined. However, the normative estimates represent average ratios for approved LWA and do not account for the specific properties of individual LWA.
- **Properties of RLCA:** RLCA properties were assessed as LWA, providing precise performance parameters for lightweight concrete design. Consequently, applying standards, such as EN 1097-6 [117], for LWA is more appropriate than using recycled aggregate standards [87].
- **Stress-strain properties:** The stress-strain behavior of the studied concretes under compression, sustained loading, shrinkage, and creep are in line with normative ranges for LAC. These results further support the inclusion of these concretes in regulatory systems, as their long-term mechanical performance meets established expectations.

Future research work

While this thesis highlights the potential of lightweight concretes to balance technical and ecological aspects, further research is required to refine methods, address experimental gaps, and expand the applications of these materials. Aligning novel material concepts (ILC, LAC+, RILC) with standards like EN 1520 [60] will require comprehensive material test data sets covering a wider range of density-strength combinations under different environmental conditions. Specific recommendations include:

- **Pumpability optimization:** Identification of mix design parameters —such as admixture combinations, water-binder ratio, and LWA pre-saturation levels— that secure pumpability without compromising performance. Development and testing of specialized pumping equipment tailored to lightweight concrete to minimize LWA damage and segregation during transport. Evaluation of challenges associated with pumping ILC at industrial scales, including long-distance and high-rise applications.
- **Composite systems:** Expansion of studies on composite elements to examine the impact of varying concrete properties, steel profile types, and geometries, as well as the effects of different concrete cover thicknesses on load distribution and structural behavior. Inclusion of strength evaluations of wall specimens to better simulate real-world conditions and develop robust design concepts for composite systems.
- **Forced carbonation:** Extension of the ILC recycling approach to other types of lightweight concrete to enhance versatility. Optimization of carbonation process to maximize CO_2 uptake and integrate findings into LCA. This would provide a more comprehensive evaluation of the environmental benefits and potential of circular lightweight concretes.
- **Circular ILC approach:** Tests have confirmed that RILC can fulfill structural functions similar to ILC_{Origin}. In the mix design, 100 % LWA is replaced by RLCA, and the cement content is reduced by 20 kg to meet the density requirements. This results in a combined reduction of 69 (58 plus 11) kg CO_2-eq/m³, respectively, compared to ILC_{Origin}. $GWP_{ILC,revised}$ is reduced by 19 % by assuming that the process-related emissions from recycling and carbonization are attributed to the previous generation. The GWP for cement and LWA is based on LCA data maintained by the German Federal Ministry of Housing, Urban Development and Construction [137,138]. Therefore, multi-generational reuse of ILC, including recycling and forced carbonation, is well suited for monolithic exterior walls.

5 Conclusion

The construction industry faces increasing pressures to adopt sustainable practices. Concrete, a cornerstone of modern construction, significantly impacts this ecological footprint, necessitating innovative approaches to reduce resource consumption and CO_2 emissions. Lightweight concretes are well-positioned to address the present challenges by offering a unique combination of sufficient strength, low density, thermal efficiency, and potential for material circularity.

It has been demonstrated for the first time that ILC can be pumped using three different pump types —piston pump, eccentric screw pump, and rotor pump— provided that mixture composition is optimized, and careful handling is applied. The rotor pump proved to be the most efficient, causing minimal abrasion to the LWA and preserving the workability of fresh concrete. In contrast, the eccentric screw pump caused significant LWA damage, resulting in higher fresh concrete density and reduced slump flow. Compressive strength and modulus of elasticity remained constant after pumping. Therefore, the same classification of characteristic properties can be made as for an ILC placed with a bucket. These findings underline the importance of preliminary tests and site-specific adjustments to optimize pumping processes, ensuring the technical and ecological viability of ILC for practical applications.

A novel mix design for LAC+ successfully reduced dry density to achieve low thermal conductivity while maintaining sufficient strength for structural applications. The integration of a thin-walled steel framework into LAC+ resulted in composite wall elements that exhibited superior load capacity, thereby achieving a performance that was three times greater than that of standalone steel sections. This combination provides an innovative solution for prefabricated wall elements that meet modern energy efficiency requirements. The study also confirmed the scalability and feasibility of this construction method through factory-scale production. Key performance parameters such as strength, modulus of elasticity, shrinkage, creep, and sustained loading behavior aligned with normative guidelines, further validate the practicality of this approach. These findings demonstrate the potential of LAC+ with steel frameworks to contribute to energy-efficient building envelopes.

A novel approach to recycling ILC addressed limitations in current standards and introduced RLCA as a viable component for the production of RILC. RLCA exhibited unique characteristics, including an agglomerate structure, densities up to three times higher than those of the original LWA, and water absorption rates that exceeded established normative guidelines. However, the RLCA was successfully incorporated into the RILC, resulting in mechanical properties and thermal conductivity comparable to the original ILC. Despite a significant increase in dry density, the thermal conductivity of RILC increased only slightly, underscoring its continued suitability for thermal insulation. Furthermore, accelerated carbonation tests revealed a significant CO_2 absorption, capturing up to 30 % of the original emissions produced by ILC. The circular approach not only reduced construction waste but also promoted material circularity and lowered the carbon footprint with ILC production. The results confirmed that monolithic wall elements could be constructed using RILC with RLCA as the sole LWA, without compromising performance.

These findings collectively prove that lightweight concretes can meet the dual demands of technical performance and ecological sustainability. By optimizing their design, production, and application, lightweight concretes provide a viable pathway for reducing the carbon footprint of the construction industry while maintaining modern performance standards.

6 References

[1] Barcelo L, Kline J, Walenta G, Gartner E. Cement and carbon emissions. Mater Struct 2014;47(6):1055–65. https://doi.org/10.1617/s11527-013-0114-5.

[2] Andrew RM. Global CO_2 emissions from cement production. Earth Syst. Sci. Data 2018;10(1):195–217. https://doi.org/10.5194/essd-10-195-2018.

[3] Oh D-Y, Noguchi T, Kitagaki R, Park W-J. CO2 emission reduction by reuse of building material waste in the Japanese cement industry. Renewable and Sustainable Energy Reviews 2014;38:796–810. https://doi.org/10.1016/j.rser.2014.07.036.

[4] Ali MB, Saidur R, Hossain MS. A review on emission analysis in cement industries. Renewable and Sustainable Energy Reviews 2011;15(5):2252–61. https://doi.org/10.1016/j.rser.2011.02.014.

[5] Akhtar A, Sarmah AK. Construction and demolition waste generation and properties of recycled aggregate concrete: A global perspective. Journal of Cleaner Production 2018;186:262–81. https://doi.org/10.1016/j.jclepro.2018.03.085.

[6] Scrivener KL, John VM, Gartner EM. Eco-efficient cements: Potential economically viable solutions for a low-CO2 cement-based materials industry. Cement and Concrete Research 2018;114:2–26. https://doi.org/10.1016/j.cemconres.2018.03.015.

[7] Lothenbach B, Scrivener K, Hooton RD. Supplementary cementitious materials. Cement and Concrete Research 2011;41(12):1244–56. https://doi.org/10.1016/j.cemconres.2010.12.001.

[8] Ghosh SK (ed.). Circular Economy and Fly Ash Management. Singapore: Springer Singapore Pte. Limited; 2020.

[9] Özbay E, Erdemir M, Durmuş Hİ. Utilization and efficiency of ground granulated blast furnace slag on concrete properties – A review. Construction and Building Materials 2016;105:423–34. https://doi.org/10.1016/j.conbuildmat.2015.12.153.

[10] Hanein T, Thienel K-C, Zunino F, Marsh ATM, Maier M, Wang B et al. Clay calcination technology: state-of-the-art review by the RILEM TC 282-CCL. Mater Struct 2022;55(1):1–29. https://doi.org/10.1617/s11527-021-01807-6.

[11] Ganesh Babu K, Surya Prakash PV. Efficiency of silica fume in concrete. Cement and Concrete Research 1995;25(6):1273–83. https://doi.org/10.1016/0008-8846(95)00120-2.

[12] Rudić O, Ukrainczyk N, Krüger M, Tritthart J, Juhart J. Efficiency of limestone in clinker-reduced binders: Consideration of water-binder ratio, capillary porosity and compressive strength. Construction and Building Materials 2023;386:131594. https://doi.org/10.1016/j.conbuildmat.2023.131594.

[13] Li X, Fu Q, Lv Y, Leng D, Jiang D, He C et al. Influence of curing conditions on hydration of magnesium silicate hydrate cement. Construction and Building Materials 2022;361:129648. https://doi.org/10.1016/j.conbuildmat.2022.129648.

[14] Winnefeld F, Lothenbach B. Hydration of calcium sulfoaluminate cements — Experimental findings and thermodynamic modelling. Cement and Concrete Research 2010;40(8):1239–47. https://doi.org/10.1016/j.cemconres.2009.08.014.

[15] Provis JL. Geopolymers and other alkali activated materials: why, how, and what? Mater Struct 2014;47(1-2):11–25. https://doi.org/10.1617/s11527-013-0211-5.

[16] Singh NB, Middendorf B. Geopolymers as an alternative to Portland cement: An overview. Construction and Building Materials 2020;237:117455. https://doi.org/10.1016/j.conbuildmat.2019.117455.

[17] Wörner M, Schmeer D, Schuler B, Pfinder J, Garrecht H, Sawodny O et al. Gradientenbetontechnologie. Beton- und Stahlbetonbau 2016;111(12):794–805. https://doi.org/10.1002/best.201600056.

[18] Liu F, Battini J-M, Pacoste C, Granberg A. Experimental and Numerical Dynamic Analyses of Hollow Core Concrete Floors. Structures 2017;12:286–97. https://doi.org/10.1016/j.istruc.2017.10.001.

[19] Baran E. Effects of cast-in-place concrete topping on flexural response of precast concrete hollow-core slabs. Engineering Structures 2015;98:109–17. https://doi.org/10.1016/j.engstruct.2015.04.017.
[20] Bos FP, Menna C, Pradena M, Kreiger E, Da Silva WL, Rehman AU et al. The realities of additively manufactured concrete structures in practice. Cement and Concrete Research 2022;156:106746. https://doi.org/10.1016/j.cemconres.2022.106746.
[21] Elshahawi M, Hückler A, Schlaich M. Infra lightweight concrete: A decade of investigation (a review). Structural Concrete 2021;22(S1):E152-E168. https://doi.org/10.1002/suco.202000206.
[22] Thienel K-C, Haller T, Beuntner N. Lightweight Concrete—From Basics to Innovations. Materials 2020;13(5):1120. https://doi.org/10.3390/ma13051120.
[23] Feys D, Schutter G de, Fataei S, Martys NS, Mechtcherine V. Pumping of concrete: Understanding a common placement method with lots of challenges. Cement and Concrete Research 2022;154:106720. https://doi.org/10.1016/j.cemconres.2022.106720.
[24] Mikhalev D, Fakhrayee Nejad S, Ng S, Bose B, Schryver R de, Brunčič A et al. Practical Insights and Advances in Concrete Pumping. RILEM Tech Lett 2024;9:1–9. https://doi.org/10.21809/rilemtechlett.2024.198.
[25] Rahman A, Rasul MG, Khan M, Sharma S. Impact of Alternative Fuels on the Cement Manufacturing Plant Performance: An Overview. Procedia Engineering 2013;56:393–400. https://doi.org/10.1016/j.proeng.2013.03.138.
[26] Kääntee U, Zevenhoven R, Backman R, Hupa M. Cement manufacturing using alternative fuels and the advantages of process modelling. Fuel Processing Technology 2004;85(4):293–301. https://doi.org/10.1016/S0378-3820(03)00203-0.
[27] Mirhosseini M, Rezania A, Rosendahl L. Power optimization and economic evaluation of thermoelectric waste heat recovery system around a rotary cement kiln. Journal of Cleaner Production 2019;232:1321–34. https://doi.org/10.1016/j.jclepro.2019.06.011.
[28] Renó MLG, Torres FM, Da Silva RJ, Santos, José Joaquim Conceição Soares, Melo, Mirian de Lourdes Noronha Motta. Exergy analyses in cement production applying waste fuel and mineralizer. Energy Conversion and Management 2013;75:98–104. https://doi.org/10.1016/j.enconman.2013.05.043.
[29] Zajac M, Skocek J, Ben Haha M, Deja J. CO2 Mineralization Methods in Cement and Concrete Industry. Energies 2022;15(10):3597. https://doi.org/10.3390/en15103597.
[30] Shi C, Li Y, Zhang J, Li W, Chong L, Xie Z. Performance enhancement of recycled concrete aggregate – A review. Journal of Cleaner Production 2016;112:466–72. https://doi.org/10.1016/j.jclepro.2015.08.057.
[31] Monkman S, Shao Y. Integration of carbon sequestration into curing process of precast concrete. Can. J. Civ. Eng. 2010;37(2):302–10. https://doi.org/10.1139/L09-140.
[32] Senadheera SS, Gupta S, Kua HW, Hou D, Kim S, Tsang DC et al. Application of biochar in concrete – A review. Cement and Concrete Composites 2023;143:105204. https://doi.org/10.1016/j.cemconcomp.2023.105204.
[33] Butera S, Christensen TH, Astrup TF. Life cycle assessment of construction and demolition waste management. Waste Manag 2015;44:196–205. https://doi.org/10.1016/j.wasman.2015.07.011.
[34] Vázquez E (ed.). Progress of Recycling in the Built Environment: Final report of the RILEM Technical Committee 217-PRE. Dordrecht: Springer; 2013.
[35] Zhuang G-L, Shih S-G, Wagiri F. Circular economy and sustainable development goals: Exploring the potentials of reusable modular components in circular economy business model. Journal of Cleaner Production 2023;414:137503. https://doi.org/10.1016/j.jclepro.2023.137503.

[36] van Belleghem B, van den Heede P, van Tittelboom K, Belie N de. Quantification of the Service Life Extension and Environmental Benefit of Chloride Exposed Self-Healing Concrete. Materials 2016;10(1). https://doi.org/10.3390/ma10010005.
[37] Hossain MR, Sultana R, Patwary MM, Khunga N, Sharma P, Shaker SJ. Self-healing concrete for sustainable buildings. A review. Environ Chem Lett 2022;20(2):1265–73. https://doi.org/10.1007/s10311-021-01375-9.
[38] Marinković S, Carević V, Dragaš J. The role of service life in Life Cycle Assessment of concrete structures. Journal of Cleaner Production 2021;290:125610. https://doi.org/10.1016/j.jclepro.2020.125610.
[39] Völker C, John E, Firdous R, Hirsch T, Kaczmarek D, Ziesak K et al. Beyond Theory: Pioneering AI-Driven Materials Design in the Sustainable Building Material Lab. In: p. 274–282.
[40] Shelote KM, Bala A, Gupta S. An overview of mechanical, permeability, and thermal properties of silica fume concrete using bibliographic survey and building information modelling. Construction and Building Materials 2023;385(3):131489. https://doi.org/10.1016/j.conbuildmat.2023.131489.
[41] Yin X, Liu H, Chen Y, Al-Hussein M. Building information modelling for off-site construction: Review and future directions. Automation in Construction 2019;101(3):72–91. https://doi.org/10.1016/j.autcon.2019.01.010.
[42] Teichmann L, Resta LF, Hein H, Dinga GT, Ramadan Z, Bögle A et al. Sustainable development in listed districts: CO 2 neutral World Heritage Speicherstadt Hamburg. Bauphysik 2024;46(3):127–34. https://doi.org/10.1002/bapi.202400015.
[43] Chacón R, Posada H, Ramonell C, Jungmann M, Hartmann T, Khan R et al. Digital twinning of building construction processes. Case study: A reinforced concrete cast-in structure. Journal of Building Engineering 2024;84(3):108522. https://doi.org/10.1016/j.jobe.2024.108522.
[44] Haller T, Beuntner N, Gutsch H, Thienel K-C. Challenges on pumping infra-lightweight concrete based on highly porous aggregates. Journal of Building Engineering 2023;65(5):105761. https://doi.org/10.1016/j.jobe.2022.105761.
[45] Haller T, Beuntner N, Thienel K-C. Optimized Building Envelope: Lightweight Concrete with Integrated Steel Framework. Materials 2024;17(6). https://doi.org/10.3390/ma17061278.
[46] Haller T, Scherb S, Beuntner N, Thienel K-C. Renewable construction with lightweight concrete – Reclaimed recycled material systems with CO2-absorption. Construction and Building Materials 2025;466:140339. https://doi.org/10.1016/j.conbuildmat.2025.140339.
[47] Chandra S, Berntsson L. Lightweight Aggregate Concrete. Elsevier; 2002.
[48] Slate Institute. Lightweight Concrete: History, Applications; 1971.
[49] Bernhardt M. Development of high performance lightweight aggregates: Norges teknisk-naturvitenskapelige universitet, Fakultet for naturvitenskap og teknologi, Institutt for materialteknologi; Norges teknisk-naturvitenskapelige universitet, Fakultet for naturvitenskap og teknologi, Institutt for materialteknologi.
[50] Manufacturing processes of artificial lightweight aggregates from fly ash. International Journal of Cement Composites and Lightweight Concrete 1986;8(3):191–9. https://doi.org/10.1016/0262-5075(86)90040-0.
[51] CHARLES M. RILEY. Relation of Chemical Properties to the Bloating of Clays. Journal of the American Ceramic Society 1951;34(4):121–8. https://doi.org/10.1111/j.1151-2916.1951.tb11619.x.
[52] DIN EN 13055:2016-11, Leichte Gesteinskörnungen; Deutsche Fassung EN_13055:2016. Berlin: DIN Media GmbH. https://doi.org/10.31030/2505101.

[53] Nadesan MS, Joy A. Production of Lightweight Aggregates for Construction Industry from Industrial Byproducts: A Review. In: Reddy KR, Pancharathi RK, Reddy NG, Arukala SR, editors. Advances in Sustainable Materials and Resilient Infrastructure. Singapore: Springer Singapore; 2022, p. 253–264.
[54] DIN EN 206:2021-06, Beton_- Festlegung, Eigenschaften, Herstellung und Konformität; Deutsche Fassung EN_206:2013+A2:2021. Berlin: DIN Media GmbH. https://doi.org/10.31030/3198971.
[55] DIN EN 1992-1-1:2011-01, Eurocode_2: Bemessung und Konstruktion von Stahlbeton- und Spannbetontragwerken_- Teil_1-1: Allgemeine Bemessungsregeln und Regeln für den Hochbau; Deutsche Fassung EN_1992-1-1:2004_+ AC:2010. Berlin: DIN Media GmbH. https://doi.org/10.31030/1723945.
[56] Lura P. Autogenous Deformation and Internal Curing of Concrete [Dissertation]. Delft: TU Delft; 2003.
[57] Zhang M, Gjørv O. Characteristics of Lightweight Aggregates for High-Strength Concrete. MJ 1991;88(2). https://doi.org/10.14359/1924.
[58] Proceedings / International Symposium on Structural Lightweight Aggregate Concrete: Sandefjord, Norway, 20 - 24 June 1995. Oslo: Norwegian Concrete Association; 1995.
[59] Guide for Structural Lightweight-Aggregate Concrete ACI 213 R-03 Reported by ACI Committee 213: American Concrete Institute; 2003.
[60] DIN EN 1520:2011-06, Vorgefertigte Bauteile aus haufwerksporigem Leichtbeton und mit statisch anrechenbarer oder nicht anrechenbarer Bewehrung; Deutsche Fassung EN_1520:2011. Berlin: DIN Media GmbH. https://doi.org/10.31030/1720849.
[61] Thienel K-C. Precast elements of lightweight concrete with a porous matrix. BFT International 2000(66):62–72.
[62] Schumacher K, Saßmannshausen N, Pritzel C, Trettin R. Lightweight aggregate concrete with an open structure and a porous matrix with an improved ratio of compressive strength to dry density. Construction and Building Materials 2020;264:120167. https://doi.org/10.1016/j.conbuildmat.2020.120167.
[63] Wu G, Feng D-C, Wang C-L. Novel Precast Concrete Structure Systems. Singapore: Springer Nature Singapore; 2023.
[64] Thienel K-C, Peck M. Die Renaissance leichter Betone in der Architektur. Zement + Beton 2010(4):2–9.
[65] Lösch C, Rieseberg P, Schlaich M, Leibinger R. Building with Infra-lightweight Concrete. De Gruyter; 2020.
[66] Schulze J, Breit W. Experimentalgebäude aus Infraleichtbeton – monolithisch und hochwärmedämmend. Beton und Stahlbetonbau 2016;111(6):377–84. https://doi.org/10.1002/best.201600015.
[67] Schlaich M, Zareef ME. Infraleichtbeton. Beton und Stahlbetonbau 2008;103(3):175–82. https://doi.org/10.1002/best.200700605.
[68] Hückler A, Schlaich M. Zur Biegung von Infraleichtbetonbauteilen – Werkstoff-, Verbund-, Trag- und Verformungsverhalten. Beton- und Stahlbetonbau 2017;112(5):282–92. https://doi.org/10.1002/best.201700008.
[69] Schließer A. Warmbeton Mischungsentwicklung mit verbesserter Übertragbarkeit in den Realmaßstab. Stuttgart: Universität Stuttgart; 2019.
[70] Sikora P, Rucinska T, Stephan D, Chung S-Y, Abd Elrahman M. Evaluating the effects of nanosilica on the material properties of lightweight and ultra-lightweight concrete using image-based approaches. Construction and Building Materials 2020;264:120241. https://doi.org/10.1016/j.conbuildmat.2020.120241.
[71] Yu QL, Spiesz P, Brouwers H. Ultra-lightweight concrete: Conceptual design and performance evaluation. Cement and Concrete Composites 2015;61(2):18–28. https://doi.org/10.1016/j.cemconcomp.2015.04.012.

[72] Spiesz PR, Hunger M (eds.). Structural ultra-lightweight concrete – from laboratory research to field trials.
[73] DIBt Mitteilungen 2002. Herstellung und Verwendung von Schaumbeton (Production and use of foamed concrete); 2002.
[74] Holcim GmbH. Außenwände aus hochwärmedämmendem, haufwerksporigem Infraleichtbeton LAC4 (Exterior walls made of highly thermal insulating, opem porous infra-lightweight concrete LAC4)(29-4112.55-4-107); 1019.
[75] Cui W., Tang Q.-W., Song H.-F. Effects of Viscosity on Pumping Concrete Behavior Using Computational Fluid Dynamics Method. MJ 2021;118(2):117–26. https://doi.org/10.14359/51729329.
[76] Li H, Sun D, Wang Z, Huang F, Yi Z, Yang Z et al. A Review on the Pumping Behavior of Modern Concrete. ACT 2020;18(6):352–63. https://doi.org/10.3151/jact.18.352.
[77] Secrieru E. Pumping behaviour of modern concretes – characterisation and prediction [Dissertation]: Technische Universität Dresden.
[78] Norden G, Thienel K-C. Pumping of lightweight aggregate concrete based on expanded clay in Europe. In: Helland S, editor. Second International Symposium on Structural Lightweight Aggregate Concrete: 18 - 22 June 2000, Kristiansand, Norway ; [proceedings. Oslo: Helli Grafisk AS; 2000.
[79] Schlaich M, Hückler A, Lösch C. Infraleichtbeton (ILC). In: Beton Kalender 2021. Wiley; 2021, p. 907–952.
[80] Kim. An experimental study on structural concrete containing recycled aggregates and powder from construction and demolition waste. Materials 2022.
[81] Kim J. Construction and demolition waste management in Korea: recycled aggregate and its application. Clean Techn Environ Policy 2021;23(8):2223–34. https://doi.org/10.1007/s10098-021-02177-x.
[82] Yang H, Xia J, Thompson JR, Flower RJ. Urban construction and demolition waste and landfill failure in Shenzhen, China. Waste Manag 2017;63:393–6. https://doi.org/10.1016/j.wasman.2017.01.026.
[83] A. Müller. Progresses and challenges in recycling of construction and demolition waste 2023.
[84] Verein Deutscher Zementwerke e. V. Ressourcen der Zukunft für Zement und Beton. Düsseldorf, Germany; 2022.
[85] Scheidt. Einfluss der Wasseraufnahme von rezyklierten Gesteinskörnungen auf den Wasserzementwert von R-Beton. Beton 2020;70(4):2.
[86] Juan MS de, Gutiérrez PA. Study on the influence of attached mortar content on the properties of recycled concrete aggregate. Construction and Building Materials 2009;23(2):872–7. https://doi.org/10.1016/j.conbuildmat.2008.04.012.
[87] DIN 4226-101, Rezyklierte Gesteinskörnungen für Beton nach DIN EN 12620 – Teil 101: Typen und geregelte gefährliche Substanzen (Recycled aggregates for concrete in accordance with DIN EN 12620 – Part 101: Types and regulated dangerous substances), 2017, p. 11; 4226.
[88] DIN 1045-2, Tragwerke aus Beton, Stahlbeton und Spannbeton – Teil 2: Beton (Concrete, reinforced and prestressed concrete structures – Part 2: Concrete), Beuth-Verlag, Berlin, Germany, 2023, p. 62; 1045.
[89] Kouwenhoven. Economic Design and Construction with Light Weight Aggregate Concrete 2000.
[90] Kümmel. Ökobilanzierung von Baustoffen am Beispiel des Recyclings von Konstruktionsleichtbeton. Fak. ät Bauing. - und Vermess., Univ. ät Stuttg., Stuttg. 2000:169.

[91] Bogas JA, Brito J de, Cabaço J. Long-term behaviour of concrete produced with recycled lightweight expanded clay aggregate concrete. Construction and Building Materials 2014;65:470–9. https://doi.org/10.1016/j.conbuildmat.2014.05.003.
[92] Bogas JA, Brito J de, Figueiredo JM. Mechanical characterization of concrete produced with recycled lightweight expanded clay aggregate concrete. Journal of Cleaner Production 2015;89:187–95. https://doi.org/10.1016/j.jclepro.2014.11.015.
[93] Huang L, Yang Z, Li Z, Xu Y, Yu L. Recycling of the end-of-life lightweight aggregate concrete (LWAC) with a novel approach. Journal of Cleaner Production 2020;275:123099. https://doi.org/10.1016/j.jclepro.2020.123099.
[94] Verein Deutscher Zementwerke e.V. Dekarbonisierung von Zement und Beton – Minderungspfade und Handlungsstrategien: Eine CO_2-Roadmap für die deutsche Zementindustrie. [March 06, 2025]; Available from: https://vdz.info/dekarbonisierung.
[95] Groves GW, Brough A, Richardson IG, Dobson CM. Progressive Changes in the Structure of Hardened C 3 S Cement Pastes due to Carbonation. Journal of the American Ceramic Society 1991;74(11):2891–6. https://doi.org/10.1111/j.1151-2916.1991.tb06859.x.
[96] Papadakis. Fundamental modeling and experimental investigation of concrete carbonation. Materials 1991;88:363.
[97] Kikuchi T, Kuroda Y. Carbon Dioxide Uptake in Demolished and Crushed Concrete. ACT 2011;9(1):115–24. https://doi.org/10.3151/jact.9.115.
[98] Fang X, Xuan D, Poon CS. Empirical modelling of CO2 uptake by recycled concrete aggregates under accelerated carbonation conditions. Mater Struct 2017;50(4). https://doi.org/10.1617/s11527-017-1066-y.
[99] Rosa L, Becattini V, Gabrielli P, Andreotti A, Mazzotti M. Carbon dioxide mineralization in recycled concrete aggregates can contribute immediately to carbon-neutrality. Resources, Conservation and Recycling 2022;184:106436. https://doi.org/10.1016/j.resconrec.2022.106436.
[100] Ho H-J, Iizuka A, Shibata E, Tomita H, Takano K, Endo T. Utilization of CO2 in direct aqueous carbonation of concrete fines generated from aggregate recycling: Influences of the solid–liquid ratio and CO2 concentration. Journal of Cleaner Production 2021;312:127832. https://doi.org/10.1016/j.jclepro.2021.127832.
[101] Wang T, Yi Z, Song J, Zhao C, Guo R, Gao X. An industrial demonstration study on CO2 mineralization curing for concrete. iScience 2022;25(5):104261. https://doi.org/10.1016/j.isci.2022.104261.
[102] Izoret L, Pernin T, Potier J-M, Torrenti J-M. Impact of Industrial Application of Fast Carbonation of Recycled Concrete Aggregates. Applied Sciences 2023;13(2):849. https://doi.org/10.3390/app13020849.
[103] Ouyang K, Shi C, Chu H, Guo H, Song B, Ding Y et al. An overview on the efficiency of different pretreatment techniques for recycled concrete aggregate. Journal of Cleaner Production 2020;263:121264. https://doi.org/10.1016/j.jclepro.2020.121264.
[104] Xuan D, Zhan B, Poon CS. Assessment of mechanical properties of concrete incorporating carbonated recycled concrete aggregates. Cement and Concrete Composites 2016;65:67–74. https://doi.org/10.1016/j.cemconcomp.2015.10.018.
[105] Infante Gomes R, Brazão Farinha C, Veiga R, Brito J de, Faria P, Bastos D. CO2 sequestration by construction and demolition waste aggregates and effect on mortars and concrete performance - An overview. Renewable and Sustainable Energy Reviews 2021;152:111668. https://doi.org/10.1016/j.rser.2021.111668.
[106] Skocek J, Zajac M, Ben Haha M. Carbon Capture and Utilization by mineralization of cement pastes derived from recycled concrete. Scientific Reports 2020;10(1):5614. https://doi.org/10.1038/s41598-020-62503-z.

[107] Gholizadeh-Vayghan A, Snellings R. Beneficiation of recycled concrete fines through accelerated carbonation. Mater Struct 2022;55(7). https://doi.org/10.1617/s11527-022-01985-x.
[108] Sereng M, Djerbi A, Metalssi OO, Dangla P, Torrenti J-M. Improvement of Recycled Aggregates Properties by Means of CO2 Uptake. Applied Sciences 2021;11(14):6571. https://doi.org/10.3390/app11146571.
[109] Leemann. Accelerated carbonation of recycled concrete aggregates and its implications for the production of recycling concrete. J. Build. Eng. 2023;79.
[110] Kaddah. Complementary use of thermogravimetric analysis and oven to assess the composition and bound CO2 content of recycled concrete aggregates. Dev. Built Environ. 2023;15.
[111] Dündar. The effects of various operational- and materials-oriented parameters on the carbonation performance of low-quality recycled concrete aggregate. J. Build. Eng. 2023;68.
[112] Bastos D, Brazão Farinha C, Maia Pederneiras C, Veiga R, Bogas JA, Infante Gomes R et al. Pathway to Carbon Neutrality in the Cement Industry: CO2 Uptake by Recycled Aggregates from Construction and Demolition Waste. Applied Sciences 2024;14(12):5224. https://doi.org/10.3390/app14125224.
[113] DIN EN 12664:2001-05, Wärmetechnisches Verhalten von Baustoffen und Bauprodukten_- Bestimmung des Wärmedurchlasswiderstandes nach dem Verfahren mit dem Plattengerät und dem Wärmestrommessplatten-Gerät_- Trockene und feuchte Produkte mit mittlerem und niedrigem Wärmedurchlasswiderstand; Deutsche Fassung EN_12664:2001. Berlin: DIN Media GmbH. https://doi.org/10.31030/9057702.
[114] DIN EN 197-1:2011-11, Zement_- Teil_1: Zusammensetzung, Anforderungen und Konformitätskriterien von Normalzement; Deutsche Fassung EN_197-1:2011. Berlin: DIN Media GmbH. https://doi.org/10.31030/1758792.
[115] DIN EN 13263-1:2009-07, Silikastaub für Beton_- Teil_1: Definitionen, Anforderungen und Konformitätskriterien; Deutsche Fassung EN_13263-1:2005+A1:2009. Berlin: DIN Media GmbH. https://doi.org/10.31030/1517699.
[116] DIN EN 14889-2:2006-11, Fasern für Beton_- Teil_2: Polymerfasern_- Begriffe, Festlegungen und Konformität; Deutsche Fassung EN_14889-2:2006. Berlin: DIN Media GmbH. https://doi.org/10.31030/9708447.
[117] DIN EN 1097-6:2022-05, Prüfverfahren für mechanische und physikalische Eigenschaften von Gesteinskörnungen_- Teil_6: Bestimmung der Rohdichte und der Wasseraufnahme; Deutsche Fassung EN_1097-6:2022. Berlin: DIN Media GmbH. https://doi.org/10.31030/3290441.
[118] DIN EN 1097-3:1998-06, Prüfverfahren für mechanische und physikalische Eigenschaften von Gesteinskörnungen_- Teil_3: Bestimmung von Schüttdichte und Hohlraumgehalt; Deutsche Fassung EN_1097-3:1998. Berlin: DIN Media GmbH. https://doi.org/10.31030/7464084.
[119] DIN EN 12350-2:2019-09, Prüfung von Frischbeton_- Teil_2: Setzmaß; Deutsche Fassung EN_12350-2:2019. Berlin: DIN Media GmbH. https://doi.org/10.31030/3045704.
[120] DIN EN 12350-4:2019-09, Prüfung von Frischbeton_- Teil_4: Verdichtungsmaß; Deutsche Fassung EN_12350-4:2019. Berlin: DIN Media GmbH. https://doi.org/10.31030/3045712.
[121] DIN EN 12350-7:2022-05, Prüfung von Frischbeton_- Teil_7: Luftgehalt_- Druckverfahren; Deutsche Fassung EN_12350-7:2019_+ AC:2022. Berlin: DIN Media GmbH. https://doi.org/10.31030/3334083.

[122] DIN EN 12350-6:2019-09, Prüfung von Frischbeton_- Teil_6: Frischbetonrohdichte; Deutsche Fassung EN_12350-6:2019. Berlin: DIN Media GmbH. https://doi.org/10.31030/3045731.
[123] DIN EN 992:1995-09, Bestimmung der Trockenrohdichte von haufwerksporigem Leichtbeton; Deutsche Fassung EN_992:1995. Berlin: DIN Media GmbH. https://doi.org/10.31030/2820215.
[124] DIN EN ISO 22007-2:2022-09, Kunststoffe_- Bestimmung der Wärmeleitfähigkeit und der Temperaturleitfähigkeit_- Teil_2: Transientes ebenes Wärmequellenverfahren (Hot-Disc-Verfahren) (ISO_22007-2:2022); Deutsche Fassung EN_ISO_22007-2:2022. Berlin: DIN Media GmbH. https://doi.org/10.31030/3340784.
[125] DIN EN 1354:2005-09, Bestimmung der Druckfestigkeit von haufwerksporigem Leichtbeton; Deutsche Fassung EN_1354:2005. Berlin: DIN Media GmbH. https://doi.org/10.31030/9646792.
[126] DIN EN 1521:1996-12, Bestimmung der Biegezugfestigkeit von haufwerksporigem Leichtbeton; Deutsche Fassung EN_1521:1996. Berlin: DIN Media GmbH. https://doi.org/10.31030/7312334.
[127] Raue E, Tartsch E. Bewertung der Dauerstandfestigkeit von Porenbeton und Normalbeton auf der Basis von Kurzzeitversuchen. DAMA 2006;10(4):140–8. https://doi.org/10.1002/dama.200600280.
[128] Tartsch E. Bewertung der Dauerstandfestigkeit von dampfgehärtetem Porenbeton auf der Grundlage von Kurzzeitversuchen. Weimar: Bauhaus-Universitat Weimar; 2008.
[129] Tasevski D, Ruiz MF, Muttoni A. Compressive Strength and Deformation Capacity of Concrete under Sustained Loading and Low Stress Rates. ACT 2018;16(8):396–415. https://doi.org/10.3151/jact.16.396.
[130] DIN EN 1352:1997-02, Bestimmung des statischen Elastizitätsmoduls unter Druckbeanspruchung von dampfgehärtetem Porenbeton und von haufwerksporigem Leichtbeton; Deutsche Fassung EN_1352:1996. Berlin: DIN Media GmbH. https://doi.org/10.31030/7312272.
[131] Bunke N (ed.). Prüfung von Beton: Empfehlungen und Hinweise als Ergänzung zu DIN 1048. Berlin: Beuth; 1991.
[132] Greve-Dierfeld S von, Lothenbach B, Vollpracht A, Wu B, Huet B, Andrade C et al. Understanding the carbonation of concrete with supplementary cementitious materials: a critical review by RILEM TC 281-CCC. Mater Struct 2020;53(6):1. https://doi.org/10.1617/s11527-020-01558-w.
[133] Bundeministerium für Wohnen, Stadtentwicklung und Bauwesen. GEG - Gesetz zur Einsparung von Energie und zur Nutzung erneuerbarer Energien zur Wärme- und Kälteerzeugung in Gebäuden*; 2020.
[134] Smeplass S. Moisture in Light Weight Aggregates - Practical Consequences for the Production Properties of Light Weight Aggregate Concrete. In: Helland S, Holand S, Smeplass S, editors. Second International Conference on Structural Lightweight Aggregate Concrete, Norwegian Concrete Association; 2000, p. 844–854.
[135] A.R. Richter, Thomas, Zement-Merkblatt Betontechnik B14 - Infraleichtbeton, in: I.B. GmbH (Ed.), 2022; 2022.
[136] CEMBUREAU. Cementing the European Green Deal. REACHING CLIMATE NEUTRALITY ALONG THE CEMENT AND CONCRETE VALUE CHAIN BY 2050. Brussels, Belgium; 2020.
[137] Sphera Solutions GmbH. Produktfluss-Datensatz: Expanded glass (de) - OEKOBAU.DAT. [March 09, 2025]; Available from: https://oekobaudat.de/OEKOBAU.DAT/datasetdetail/process.xhtml?uuid=dad163a2-a15b-48e0-a763-6142445b5d42&version=20.24.070&stock=OBD_2024_I&lang=de.

[138] Verein Deutscher Zementwerke e. V. Prozess-Datensatz: Hochofenzement CEM III/A (de): EPD-VDZ-20220154-IAG1-DE. [March 09, 2025]; Available from: https://oekobaudat.de/OEKOBAU.DAT/resource/sources/c8b5e79a-f9a3-4cf0-a385-fa7332e611e7/Hochofenzement_CEM_IIIA_16003.pdf?version=00.01.000.

7 Publications

7.1 Lightweight Concrete – From Basics to Innovations

Reprint:

Published in “Materials”

Materials 2020, 13(5), 1120; doi: 10.3390/ma13051120

Authors: K.-Ch. Thienel, T. Haller, N. Beuntner

materials

MDPI

Review

Lightweight Concrete—From Basics to Innovations

Karl-Christian Thienel *, Timo Haller and Nancy Beuntner

Institute for Construction Materials, Universität der Bundeswehr München, Werner-Heisenberg-Weg 39, 85579 Neubiberg, Germany; timo.haller@unibw.de (T.H.); nancy.beuntner@unibw.de (N.B.)

* Correspondence: christian.thienel@unibw.de; Tel.: +49-89-6004-2512

Received: 15 January 2020; Accepted: 28 February 2020; Published: 3 March 2020

check for updates

Abstract: Lightweight concrete has a history of more than two-thousand years and its technical development is still proceeding. This review starts with a retrospective that gives an idea of the wide range of applications covered by lightweight concrete during the last century. Although lightweight concrete is well known and has proven its technical potential in a wide range of applications over the past decades, there are still hesitations and uncertainties in practice. For that reason, lightweight aggregate properties and the various types of lightweight concrete are discussed in detail with a special focus on current standards. The review is based on a background of 25 years of practical and theoretical experience in this field. One of the main challenges in designing lightweight concrete is to adapt most of design, production and execution rules since they often deviate from normal weight concrete. Therefore, aspects are highlighted that often are the cause of misunderstandings, such as nomenclature or the informational value of certain tests. Frequently occurring problems regarding the mix design and production of lightweight concrete are addressed and the unintended consequences are described. A critical view is provided on some information given in existing European concrete standards regarding the mechanical properties of structural lightweight concrete. Finally, the latest stage of development of very light lightweight concretes is presented. Infra-lightweight concrete is introduced as an innovative approach for further extending the range of applications of lightweight concrete by providing background knowledge and experiences from case records.

Keywords: lightweight concrete; lightweight aggregate concrete; infra-lightweight concrete; LC; LAC; ILC; lightweight aggregate; LWA; production; mix design

1. Introduction

Lightweight concretes are not a modern achievement of concrete technology. They have been known since ancient times and are basically the predecessors of today's concrete. The first European references of lightweight concrete were built two thousand years ago during the early Roman Empire. The Pantheon in Rome, Italy, was built ca. 128 A.D. and can be cited as one of the best-known examples. It has amazed engineers from various disciplines over hundreds of years and has impressively demonstrated the systematic use of various natural lightweight aggregates in opus caementitium [1]. After the collapse of the Roman Empire, the use of lightweight concrete was limited due to the low availability and variability of natural, volcanic aggregates. The development and production of industrially produced lightweight aggregate in the 19th and 20th centuries marked a historic turning point for material technology [2,3].

Initially, the use of the expanded aggregates was reserved for the Navy of the United States of America. The associated U.S. Emergency Fleet Building Corporation established a shipbuilding program with the U.S. entry into World War I. In 1918, Atlantis was the first ship to emerge from this program and fourteen lightweight concrete ship hulls were built in total. During World War II, these early experiences led to the deployment of 104 supply ships, with cargo capacities ranging from 3200 to 140,000 tons [4].

Its successful use in shipbuilding has enabled the introduction of lightweight concrete in structural engineering. The first commercial plant to produce expanded aggregates has been established in 1920 in Kansas, USA. The uniform quality and composition of the industrially produced aggregates have proved to be advantageous over aggregates from natural origin [3].

During the 1920s, several bridges were built using expanded slate as aggregate in lightweight concrete. Fifty years later, more than 200 lightweight concrete bridges have been constructed in the United States and Canada [5]. In the middle of the 20th century, the use of lightweight concrete in structural engineering intensified. It led to multi-story high-rise buildings such as the Prudential Plaza Building or the Marina City Towers in Chicago. However, lightweight concrete was predominantly used for structural reasons and a conscious adaptation of lightweight concrete by the architecture remained largely limited to individual cases [6].

As consequence of the oil crisis in 1973, Germany has reconsidered its political position with regard to energy consumption. In order to become more independent of energy imports, the Energy Saving Act [7] was implemented as a logical consequence. Among other things, the efficient use of energy in buildings has become a political obligation. As one of the consequences, monolithic exterior walls made of lightweight concrete with an economical thickness no longer met the increased thermal insulation requirements.

Since the 1990s, the technical regulations for building with concrete in Germany have been revised. The use of lightweight concretes has experienced an upswing due to these new regulations, as well as the ongoing developments in both technology and science. However, the number of examples carried out remained comparatively low. Recent developments aim on a further reduction of the concrete density, while maintaining a sufficient and as high as possible strength. Within the last years, monolithic structures made of fair faced lightweight concretes in the lowest strength and density classes have gained popularity in Europe. These structures provide the construction of a finished wall in one operation and, thus, prevent the use of multi-layer wall structures [6]. The decision in favor of a massive lightweight concrete wall is usually based on the desire to design an individual architecture that can be shaped easily, while exploiting the design possibilities of exposed concrete. Moreover, the physical properties of lightweight concrete, such as low density, favorable building physics and high fire resistance are the main characteristics of a promising material [8–11] as well as its excellent durability [12–17].

The latest stage in this development includes the so-called infra-lightweight concrete (ILC) [18]. Other researchers refer to similar material approaches under terms like Warmbeton [19], Architekturleichtbeton [20] or ultra-lightweight concrete [21]. ILC aims at fulfilling both structural specifications and thermal insulation requirements. ILC offers possibilities for monolithic wall design, meeting current regulations for energy consumption in buildings without using additional insulation material. Despite the technological point of view, building regulations are still a challenge for the application of ILC in practice. ILC is not yet a standardized building material and thus far, it is necessary to obtain a project-related or a technical approval. However, it is possible to order ILC commercially.

This paper focuses on structural lightweight concrete (LC) based on mineral lightweight aggregate (LWA). The basic constituents of LC, their interactions and influence on mechanical properties and durability can differ significantly from normal weight concrete (NC). This justifies increasing attention and the necessity to adjust most of the design, production and execution rules compared to NC. Therefore, this work provides a basic overview of the main constituents, their properties and the associated special features in mix design and production. Frequently occurring problems, missing or questionable information in some European standards are highlighted. In addition, this paper gives an outlook on the latest developments in the field of ILC. The aim of this publication is to consolidate the basic understanding of design criteria, to promote a better understanding in the practical application of lightweight concrete and to establish ILC in construction practice.

2. Description of Lightweight Aggregate and Lightweight Concrete

2.1. Lightweight Aggregate

Lightweight aggregates (LWA) are specified in international standards like EN 13055 [22], ASTM C330M [23], ASTM C331M [24], and ASTM C332 [25]. The ASTM standards distinguish between LWA for structural lightweight concrete [23], LWA for the application in masonry lightweight concrete [24] and LWA for insulating concrete [25]. The European standard EN 13055 holds amongst others for LWA to be used for any type of lightweight concrete. The standards mentioned, however, do consider only LWA of mineral origin. EN 13055 lists LWA not by their common name, but defines their sources. LWA can be of natural origin, manufactured from natural materials, manufactured from by-products of industrial processes or from recycled source materials, or by-products of industrial processes [22]. The ASTM standards have an explicit list of LWA covered: "Two general types of lightweight aggregates are covered by this specification: aggregates prepared by expanding, pelletizing, or sintering products such as blast-furnace slag, clay, diatomite, fly ash, shale, or slate; and aggregates prepared by processing natural materials, such as pumice, scoria, or tuff" [23]. In addition, lightweight "aggregates consisting of end products of coal or coke combustion" are listed in ASTM C331M [24]. Literature, e.g., [26–29], provides details about the various types of LWA, their properties and typical production processes.

Besides their origin, the definition of the aggregate properties, mainly the density, is important in order to distinguish between normal weight and lightweight aggregate. ASTM C330M [23] and ASTM C331M [24] give upper limits for the loose bulk density 1120 kg/m^3 for fine LWA, 880 kg/m^3 for coarse LWA and 1040 kg/m^3 for the combination of fine and coarse LWA. Additionally, it should be possible to produce structural lightweight concrete with LWA conforming ASTM C330M as given in Table 1, where compressive strength is determined on cylindrical specimens [30].

Table 1. Compressive strength and splitting tensile strength requirements for LWA [24].

Calculated Equilibrium Density max, kg/m^3	Average 28-day Splitting Tensile Strength, min, MPa	Average 28-day Compressive Strength, min, MPa
All Lightweight Aggregate		
1760	2.2	28
1680	2.1	21
1600	2.0	17
Combination of Normal Weight and Lightweight Aggregate		
1840	2.3	28
1760	3.1	21
1680	2.1	17

The possible range of LWA types and applications is further defined in EN 13055. Restrictions apply to loose bulk density (ρ_s) (≤1200 kg/m^3) and particle density (ρ_k) (≤2000 kg/m^3). Thus the standard covers even very light LWA like expanded perlite and exfoliated vermiculite which both are rather used in mortar and plaster or for "concrete not exposed to the weather, in which the prime consideration is the thermal insulating property of the resulting concrete" [25].

The use of any other LWA than the ones given above requires project-related or technical approval before being considered for any standardized lightweight concrete in practice or is limited for research purpose only. This holds, e.g., for cold-bound LWA [31] or any organic material like wood chips, rubber crumbs, plastic beads, or expanded polystyrene (EPS). Another major field of interest includes the use of recycling products as LWA. The potential base materials, such as rice husk ash [32], dredged silt [33], and polyethylene terephthalate waste [34], are some examples of the numerous possibilities. The following text will consider only lightweight concrete produced with LWA covered by the aggregate standards mentioned [22–25].

The crushing resistance according to EN 13055 [22] is often used to select or compare coarse LWA for lightweight concrete. It has to be noted that this approach ignores completely the background of the crushing resistance test: it is intended for production control only and shall provide information for conformity control. This test method is originally part of a Soviet standard [35]. The crushing resistance is determined at a compaction of 20%, while in concrete the maximum strain in compression is 3.5 mm/m. Thus, using this test for any other purpose than conformity control is a crude misunderstanding of the underlying principles and the intention of the test. A note in EN 13055 points out that "there is no simple relationship between the crushing resistance of lightweight aggregate and the properties at its end use" [22].

2.2. Lightweight Concrete

There are several definitions of lightweight concrete, which often leads to a lack of precision when referring to lightweight concrete. Deviations exist for strength, density and the type of lightweight concrete covered. ACI 213R-14 "Guide for Structural Lightweight-Aggregate Concrete" [36] specifies a minimum cylinder strength of 17 MPa and an equilibrium density between 1120 and 1920 kg/m^3 for structural lightweight concrete (SLC) and without any strength requirement an equilibrium density between 800 and 2240 kg/m^3 for specified density concrete (SDC). SLC with compressive strength of 40 MPa at 28 days is classified as high strength lightweight concrete.

In Europe, structural lightweight concrete (LC) is covered as material in EN 206 [37] and its application is regulated in EN 1992 [38]. Minimum strength class is LC8/9 referring to a characteristic cylinder strength of 8 MPa and a characteristic cube strength of 9 MPa [37]. The design standard [38] requests a minimum strength class of LC12/13 [37]. Due to a lack of practical experience, a technical approval is mandatory in Germany for strength classes LC70/77 and LC80/88. LC has an oven dry density of $800 \geq \rho_d \leq 2000$ kg/m^3. The density range is divided into density classes with a span of 200 kg/m^3. A free and unrestricted combination of strength and density classes is not possible [39]. However, Figure 1 shows that specific LC strength classes require certain density classes (D) for a proper definition. Compared to other types of lightweight concrete, LC has a dense cement matrix and its surface can hardly be distinguished from normal weight concrete (NC). The lightweight aggregates become visible only on a damaged or cut surface (Figure 2a).

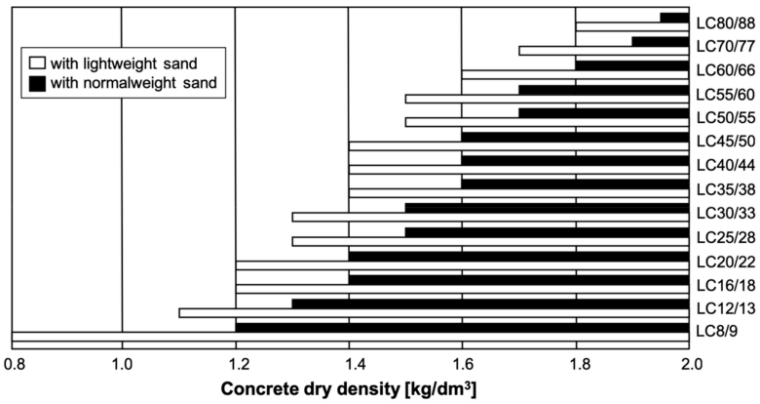

Figure 1. Correlation between strength classes and necessary dry density for LC [40,41].

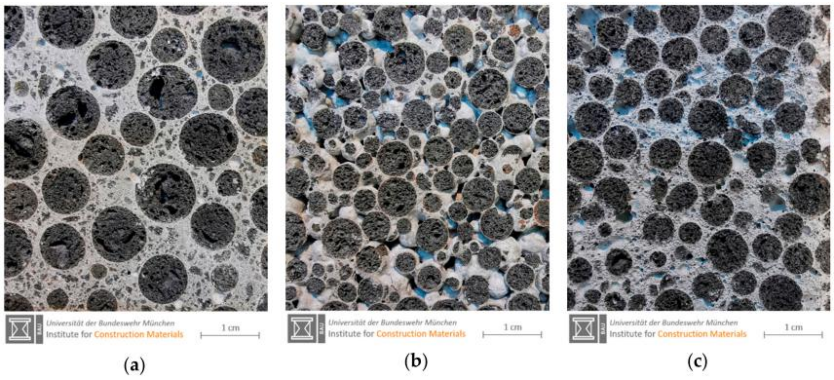

Figure 2. (**a**) Image of structural lightweight concrete (LC) with a dense matrix structure; (**b**) Image of the lightweight aggregate concrete (LAC) with open pore structure; (**c**) Image of LAC with a porous matrix filling the open pore structure. All three types of lightweight concrete are based on expanded clay from one producer as LWA.

Care should be taken when referring to terms like lightweight aggregate concrete (LWAC), all-lightweight aggregate concrete (ALWAC) or sand lightweight aggregate concrete (SLAWC) since these terms are not specified in standards and often subject to individual definitions. Hence, any reference to such unspecified definitions may result in an incorrect or at least an incomplete statement.

Lightweight aggregate concrete with open structure (LAC) differs significantly from the aforementioned lightweight concrete (LC). Its properties are defined in EN 1520 [42]. The dry density of LAC ranges from $400 \geq \rho_d \leq 2000$ kg/m^3. EN 1520 covers strength classes LAC 2 to LAC 25, which are based on the characteristic strength [MPa] of 100-mm cores drilled from LAC elements. LAC is used for structural elements like loadbearing walls, roof elements, slabs and beams, and for non-structural components like noise barriers. Some properties of LAC can be improved significantly when the open structure is filled with a porous matrix (aerated cement paste) [43]. Figure 2 gives an idea of two different LAC types in comparison with a structural LC. LAC is characterized by defined voids between the aggregates that remain in the structure after compaction (Figure 2b). These voids are created by limiting the cement paste content to the amount required for binding the aggregates at the points of contact. There is no standardized definition regarding the minimum pore volume threshold to consider a concrete as "open porous". A planned pore volume of about 10% by volume can be assumed, which is the upper limit for structural concrete when adding air-entraining agent (LP concrete) [44]. Hence, the distinction must be made on the basis of the volumetric mix design.

A recent kind of lightweight concrete was developed initially for an application outside building industry. This very light lightweight concrete was intended for sandwich ship hulls. The underlying concept for design of ships and marine structures was developed by using sandwich plates composed of steel skins with a very low density lightweight concrete as core material [45]. Schlaich adopted this type of lightweight concrete and established infra-lightweight concrete as a non-standardized lightweight concrete [18,46]. ILC has a dry density of less than 800 kg/m^3. Its compressive strength is less or equal than LC8/9 [47,48]. ILC provides a fair faced concrete surface and enables monolithic external concrete walls without additional insulation. Its structure after compaction rather complies with a LAC with a porous matrix (aerated cement paste) (Figure 2c) than with a LC. Thus far, the standards for structural concrete [37,38] have been applied for the design of ILC. In doing so, the design rules were extrapolated towards lower densities. This could be accomplished with a project-related approval [48].

New approaches are now initiated at Universität der Bundeswehr München in cooperation with several industrial partners. The basic idea is combining the initial design concept of ILC with the technical regulations laid down in EN 1520 [42]. The actual challenge is establishing rules for

conformity on site. This is already part of a first project-related approval [49] and shall be transferred into a European technical approval (ETA).

3. Constituents, Mix Design and Production of Lightweight Concrete

3.1. Other Constituents in Lightweight Concrete than LWA

3.1.1. Normal Aggregate

Most LC use a combination of lightweight coarse aggregate and normal weight sand. The decision depends among others on the requirements regarding specified strength and density, thermal conductivity and the market price of the aggregates. The quality and availability of LWA gradings are further factors that influence the optimum ratio of normal weight aggregate and LWA. Especially fine LWA often are available as crushed material only, resulting in a high water demand and affecting workability characteristics. The requirements for normal weight sand are the same as for their use in NC.

3.1.2. Binder Materials

LC can be produced with any cement available. For LC made with LWA it is highly recommended to use a cement with a modest specific heat release, like blast furnace cement, or cements in combination with fly ash, calcined clay, granulated blast furnace slag or limestone. These LC have a low thermal conductivity which could lead to high temperatures in the core of the construction element [50] during hydration exceeding the critical limit for delayed ettringite formation at 60 °C–70 °C [51]. The addition of SCM is discussed controversially. Demirboga and Gül [52] observed a reduction of strength when using microsilica and fly ash which also reduced thermal conductivity by about 15%, while Chung et al. [53] found improved mechanical and thermal properties due the use of fly ash or limestone powder. Shafigh et al. [54] investigated the addition of fly ash and limestone powder as well and noted that the latter improved the compressive strength of lightweight concrete in the early and late ages. Abd Elrahman et al. [55] performed experimental investigations on the influence of nanosilica, which improved strength and transport properties significantly.

3.1.3. Water

Any kind of water used in normal concrete production can be used for LC as well. This includes recycling water [56].

3.1.4. Admixtures

Any admixture used in normal concrete production can be used for LC as well. The compatibility with the binder and LWA used should be checked beforehand, as for NC. This holds especially for LWA that may have different surface charges compared to normal weight aggregate. Initially dry or only prewetted LWA will absorb parts of liquid admixtures if these are added too early to the mix (see Section 3.2). ACI 304R-00 [57] recommends the use of presaturated LWA to avoid absorption of the admixtures into the LWA. Delayed addition of liquid admixtures will reduce the problem [26].

3.2. Producing LC

3.2.1. Mix Design of LC

The mix design for LC differs fundamentally from NC due to the dominant impact of the LWA used [55,58–62]. Proportioning of LC must consider the boundary conditions like strength, density and durability, but also takes into account the casting situation and equipment. Detailed considerations can be found in [36]. When designing for a certain strength, a coarse LWA must be selected which has sufficient strength capacity. In the case of doubt local LWA producers should be asked for their

advice [36]. The strength of selected coarse LWA sets the ceiling for the LC strength. The threshold above which the LWA is decisive and the strength of the matrix becomes a secondary factor for the potential LC strength is called strength limit (see Section 4.2) [62–64]. Above this strength limit, binder content and water to binder ratio play a secondary role in LC. However, they also determine the durability properties of LC and thus have to be chosen properly (e.g., according to DIN 1045-2 [65]). The type of sand has a major impact on thermal conductivity. Replacing normal weight sand with lightweight sand reduces in a typical LC the dry density by approximately 200 kg/m^3. At the same time, compressive strength is lowered as well depending on the type of lightweight sand selected.

Mix design of LC should always disclose the water added to account for the water absorption of the LWA, although the water will not increase the LC volume [66,67]. The w_{60} value indicates the water absorbed by coarse LWA within 60 minutes and is a common parameter in practice [68]. This experimental value, however, does not respect the actual moisture stage of the coarse LWA, which in turn has an impact on the effective water absorption [66,69,70]. It is even more important to account for the high water absorption of fine LWA. It ranges from 25 to 40 wt% [27] and must be considered in mix design at least to a certain extent. Thus far, there exists only one proposal related to this topic [40] which recommends to consider 70% of the water absorption measured according to DIN V 18004 [71]. This test method will be adopted in the next version of EN 1097-6. Ignoring the water absorption will cause an uncontrolled uptake of water from the matrix by the LWA and especially by the lightweight sand. This will consequently lead to the formation of serious microcracks in the matrix (Figure 3) which reduce the achievable strength and jeopardize the durability. Since the absorption takes place during the plastic stage of the LC matrix, it cannot be compensated by later internal curing effects [72].

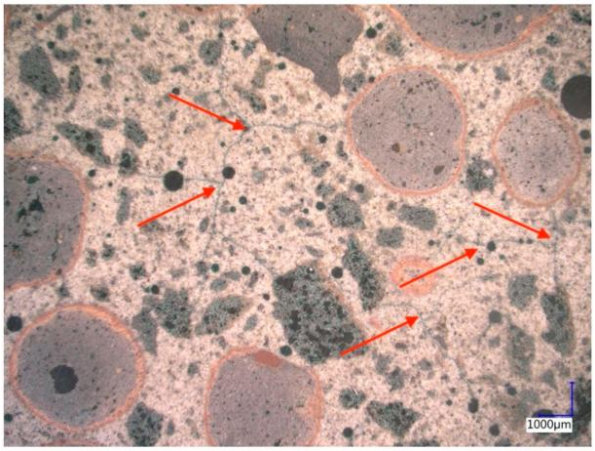

Figure 3. Severe formation of microcracks in the matrix (marked with red arrows) of a high strength LC due to water absorption of fine and coarse LWA (Courtesy: Andrea Kustermann).

Any mix design for LC must be given in dm^3/m^3 based on volumetric share of the constituents. The weight is an inaccurate measure for LC. Nevertheless, this weight information shall be provided together with the particle densities used in the mix design. By doing so, the air void content must be given as well. It is often missing in mix designs. Measurements of the air void content following ASTM C 173 [73] must always be double-checked considering the yield [74] and the density achieved. Other methods [75] will not provide correct information about the air void content since one cannot distinguish between air voids in the paste and air entrapped in the LWA. This method can be used on site for conformity control.

3.2.2. Mixing and Delivery of LC

The dosage of the LWA should be volumetric wherever possible. Since in most concrete plants gravimetric weighing is available only, the moisture content and absorption of the LWA [69] as well as their loose bulk density must be checked at appropriate intervals and changes taken into account to adjust the dosing. All other components are measured as usual.

During mixing, the LWA are filled in first. Up to two thirds of the required mixing water and the water compensating the absorption are added to the running mixer and mixed in for about 30 seconds. This is particularly important when lightweight sand is used as it absorbs a relatively large amount of water. If LWA is prewetted, it should be as uniform as possible [36]. Next, the cement is given into the mixer, followed by the remaining mixing water. Powdery additives are added along with the cement. If silica fume is used, it should go either as powder with other dry additives or as slurry together with the remaining mixing water. As mentioned beforehand in Section 3.1.4, admixtures should be added as late as possible and in the best case with the remaining mixing water to prevent uncontrollable absorption into LWA. The minimum mixing time of structural lightweight concrete, after the addition of all constituents, should be prolonged from a range of 30 to 60 s up to 90 s, compared to NC.

Structural lightweight concrete is preferably produced in a compulsory mixer. If possible, the mixer blades should have a plastic lining in order to avoid unnecessary crushing of the LWA, especially in the case of very light LWA. In concrete plants, up to 5–10% of the very light coarse LWA can be crushed. In the laboratory, this grain fragmentation is between 3% and 5%, in some laboratory mixers also significantly higher. Water absorption of LWA and LC density both rise due to the LWA fragmentation. Workability will be reduced due to the higher water absorption of the crushed LWA.

The fresh LC should be checked for unit weight and yield [74]. One option is the comparison of the fresh density with the density in the mix design. A second method requires an accurate job in the laboratory. The effective volume of the trial batch should be verified. When compacted, the combined volume achieved can be checked against the intended volume. The initial mix design must be corrected by the yield factor. Due to all the uncertainties, the yield may vary by ±5 to ±10% by volume for LC. The latter holds for LC made with coarse and fine LWA. Here, the tests available for particle density of fine LWA [68,71] will provide non-suitable values since they do not account for the real water absorption in a mixer [76].

As a result of the water absorption of the lightweight aggregates, the duration of transport and placing has a greater impact on the workability of LC than on that of NC. The degree of compactability [77] should be used to assess the workability and compare different LC. The values of the flow table test [78] can be misleading, as the weight of the aggregates acts as the main driving force in this test. With LC, different flow consistencies can therefore be determined for apparently identical workability, depending on the density of LWA used.

3.2.3. Placing and Handling of LC

Structural lightweight concrete does require the same placing techniques as used for NC [36]. LC is mainly placed on the construction site by using buckets, which is one reason for its restrained use. In the USA, however, the pumping of LC is common practice thanks to the use of water-saturated LWA. The obvious advantage comes along with higher density and increased transport costs. In the meantime, technology of LC in Europe has progressed so far that even LC with only pre-wetted LWA, can be pumped accurately [41].

When pumping LC with non-water saturated LWA, the water in cement paste is pressed out by the pumping pressure and ingresses together with fine particles into the pores of air-filled LWA [79]. This, in turn, compresses the volume of LC and as consequence, the consistency of LC declines due to the reduced water content left in the paste. As soon as the pressure on the fresh LC drops at the end of the pump line or—depending on the design of the pump—in the pump line, the air within the LWA pores and the LC itself can relax and expand. The air trapped in the pores of the LWA forces again the water out of the LWA. This often leads to segregation effects of the LC and can indicate pumping fails.

Such behavior can even occur despite a previous, longer lasting (e.g., 24 h) water storage of the LWA. It can be remedied by specially adapted, almost self-compacting LC mix designs. A suitability test including a pumping test is always recommended before pumping on construction sites.

Even if the pumping of LC has been successful, it may have negatively affected the quality of the hardened concrete [69]. The cause is again the water squeezed into the pores of the LWA during pumping. After relaxation, the water is displaced by the air, which was beforehand trapped and compressed inside the aggregate during the pumping process. As a consequence, a water seam forms around the LWA and a porous ring remains after hardening. A comparable effect can occur if the LC is not remixed at the construction site before placing [80].

3.3. Mixing and Delivery of ILC

Infra-lightweight concrete combines LC with several ideas used for LAC with a porous matrix. Thus, the mix design approach is similar as for LC. In order to reduce density and thermal conductivity, the air void content exceeds the limitation of 10% by volume for LC [44]. The necessary workability for placing this concrete on site is maintained by adding sufficient air entraining admixture, without jeopardizing the intended fair faced surface quality [18,48]. For mixing, transport, and placing, the same rules apply as for LC. Pumping will most likely destroy the air void system and was thus far omitted in all executed projects.

4. Microstructure of LC and Resulting Consequences

4.1. Interface between LWA and Matrix

The microstructure of LC differs significantly from that of NC. The latter represents a 3-phase system of aggregate, matrix and the interfacial transition zone (ITZ) around the aggregate [81,82]. In contrast to NC, there is no ITZ in LC when correctly composed (Figure 4). This is due to four mechanisms:

1. The LWA absorbs water during mixing. Together with the mixing water, parts of the binder components infiltrate the porous LWA. The hydration products therefore do not only grow towards the outer LWA surface, but also to a limited extent towards the inside of the LWA (Figure 4). The resulting increase in particle strength is associated with an increase in bulk density and a loss of binder component in the matrix. The intrusion of binder components into the LWA provides an advantage, but it is more economical to keep them in the matrix [83].
2. Some expanded clays exhibit reactive clinker phases, such as Gehlenite (C_2AS), on the outer shell of the coarse aggregate. These LWA can therefore react with the binder components to a limited extent [84]. With regard to reactive LWA surfaces, there is greater research interest in the impact of cold-bound aggregates [85] as mentioned above (see Section 2.1), as well as in LWA synthesized by cementing and geopolymerization [86].
3. The LWA surface is rough and porous and permits very good mechanical interlocking [29].
4. As mentioned beforehand, the water absorbed by the lightweight aggregate is available for optimum internal post-treatment in the course of the hydration. This property is partly used in high strength normal concretes [87–89].

The absence of a pronounced ITZ affects load-bearing behavior and durability [15,90–93]. It is particularly important for the composition and mixing of LC when silica fume is part of the mix design. In high strength NC, the addition of silica fume is intended above all to improve the ITZ (e.g., [81,94–96]). In order to bring it to the surface of the normal weight aggregate of NC, the silica suspension is added to the mixer immediately after the aggregate has been added to the mixer. In LC, the silica suspension would partly be lost in the LWA and is therefore added later to the mix (see Section 3.2.2) to improve the quality of the matrix.

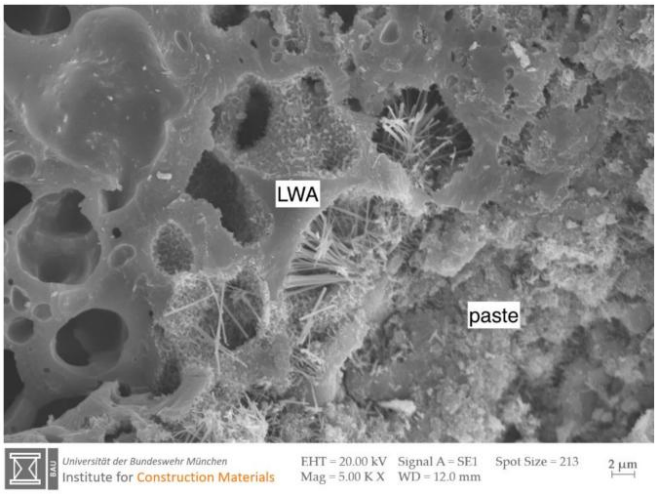

Figure 4. SEM image of the interfacial transition zone in lightweight concrete between an expanded clay aggregate and the paste. Hydration products are visible inside the outer LWA pores [97].

4.2. Load-bearing Behavior of LC

The strength of the mortar matrix determines the strength of NC. Therefore, a uniform relationship between the concrete and matrix compressive strength can be established. Mortar strength is characterized by the w/c ratio and the standard compressive strength of the cement.

In the case of LC, the LWA are often less solid and less stiff than the matrix, depending on the density of the LWA. The LWA is therefore decisive for the strength of the lightweight concrete structure. As a result, the concrete strength may lag behind the compressive strength of the matrix [29,98].

At young age, the strength of LC and NC initially develops simultaneously [99,100]. Under compressive loading, the main compressive stress trajectories run in a concentrated manner from coarse particle to coarse particle. The mortar layers transmit the compressive forces and are predominantly subjected to compressive loading. At right angles to the direction of loading, tensile stresses arise due to the deflection of the compression trajectories. This, in turn, does also stress the adhesive bond between aggregate and matrix. As in NC, adhesive cracks and finally fracture occur below a limit strength that depends on the LWA properties [100,101].

As hydration progresses, the stiffness and strength of the matrix can exceed that of the LWA. In this case, the internal flow of forces changes [29,100]. The main compressive stresses run around the LWA. The mortar layers are subjected to compressive stress. Tensile stresses arise above and below the LWA at right angles to the compression trajectories, i.e., approximately at right angles to the direction of loading. If the tensile stresses exceed the matrix tensile strength, cracks form there. The tensile forces are gradually transferred to the LWA until their tensile strength and thereby finally the strength capacity of the LC is reached. The threshold above which the LWA strength capacity becomes the strength determining factor for LC is known as strength limit ($f_{lc,lim}$) [29].

Up to a level, which dependents on the strength capacity of the LWA, strength of LC does more or less coincide with the matrix strength to a certain level. Above this level, the strength of LC increases disproportionately less with an increase in matrix strength [102,103]. In Figure 5, "lightweight aggregate 1" could for instance represent an expanded clay with $\rho_s \sim 350$ kg/m^3 and "lightweight aggregate 2" an expanded clay with $\rho_s \sim 600$ kg/m^3.

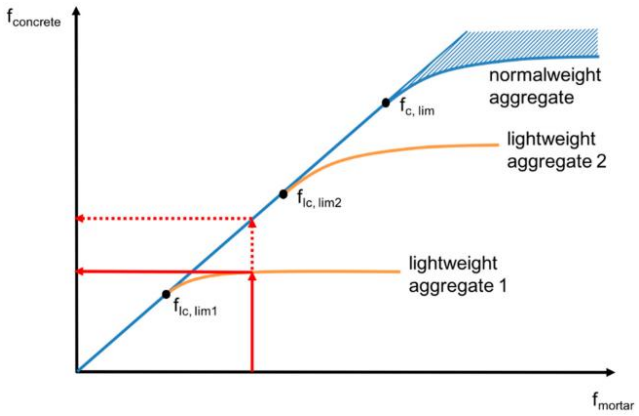

Figure 5. Explanation of limit strength ($f_{lc,lim}$) of different types of lightweight and normal weight aggregate [64].

Since the lightweight aggregates contribute increasingly less to the load transfer above the limit strength, the matrix strength must be drastically enhanced to further increase the concrete strength. This procedure is not economically meaningful and it is better to select a stronger LWA instead. The ultimate LC strength depends on the LWA used: The stronger the LWA, the higher the ultimate strength of the LC.

For a mortar strength below the limit strength, the strength of LC differs only slightly from the matrix strength, i.e., it corresponds approximately with that of a NC of the same strength. This is important with respect to strength classes and conversion factors (see Section 4.3). The ultimate strength is reached when stiffness of the matrix exceeds that of the aggregate, so that the grains participate increasingly less in the transmission of forces according to their volume fraction [29].

4.3. Conversion Factors for LC

4.3.1. Conversion Factors for Different Specimen Sizes and Shapes

The load bearing behavior of LC has an impact on conversion factors applied for different specimen shapes and sizes [104–106]. The cylinder strength is always considered being the reference for uniaxial compression [36,38]. Nevertheless, cubes are the most common and sometimes the only test specimens in many European countries, e.g., Austria [107], Belgium [108], Germany [109], The Netherlands [110], and U.K. [111]. Originally, standards always used identical conversion factors for NC and LC. For the first time Model Code 90 [112] assumed the possibility of deviating factors for LC and NC. "If national standards require different types of specimens or different storage conditions up to the time of testing, conversion factors which have been verified by tests have to be applied." These deviating conversion factors are based on the recommendation given in [113]: "For LWAC the cylinder strength shall be the only reference strength. The cube strengths specified in Table 2.1.1 [of Model Code 90, the authors] are thus not valid." To the best knowledge of the authors, the tests recommended have not been performed. With the introduction of EN 206 and EN 1992, the conversion factor between 15-cm cubes and 30/15-cm cylinders was 1.23 for NC and 1.10 for LC. The preceding Section 4.2 on load-bearing behavior of LC pointed out the difference between the behavior of LC below and above the limit strength ($f_{lc,lim}$). For economic reasons, most LC in practice will have a design strength below $f_{lc,lim}$. Thus, their behavior is dominated by the matrix as it is the case for NC and the conversion factors between different specimen sizes are expected to be the same for LC and NC. This was confirmed in a series of tests involving more than 200 mix designs with various types of LWA, covering the strength

range between 15 and 70 MPa and densities between 950 and 1700 kg/m^3 [64,114]. Figure 6 gives the resulting conversion factors between 15-cm cubes and 30/15 cm cylinders for different testing ages and curing conditions. These and other results [115] cast severe doubts to whether a deviating conversion factor between cylinders and cubes for LC is reasonable and correct. The actual conversion factor in [37,38] for LC (i.e., 1.10) may lead to a faulty anticipation of the cylinder strength, and in some cases to an incorrect declaration of strength classes, if cubes are used as only specimen type [64,114].

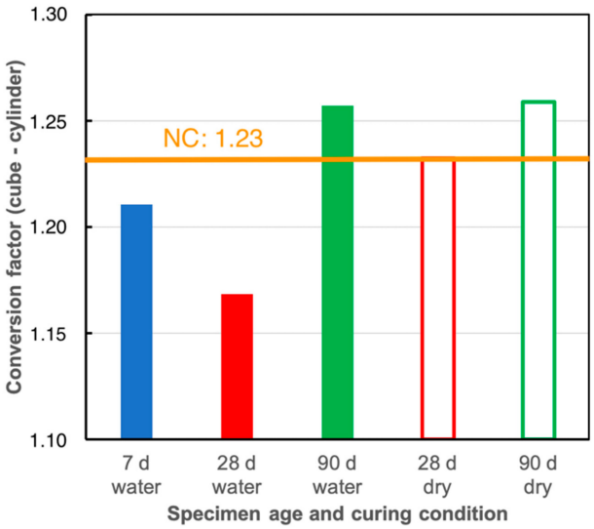

Figure 6. Conversion factors between 150-mm cubes and 300/150-mm cylinders for LC tested at 7 d, 28 d and 90 d. The specimens were cured under water [116] or in a climate room (20 °C/65% relative humidity) following the German national annex to [116] [64].

4.3.2. Conversion Factors for Different Curing Conditions

Figure 7 shows conversion factors between various types of LC specimens cured under water until testing or cured under water for seven days and subsequently in a controlled climate chamber at 20 °C/65% relative humidity [64]. The conversion factor for NC (0.96) does not distinguish between various specimen types or sizes. The impact of curing determined for LC depends on the type of specimen and the age of testing [117]. Cylinders do not exhibit any effect at 28 d, but at 90 d. Strength of cubes is more sensitive against curing conditions due to the faster drying of the corners. Here, a clear effect can be observed at 28 d. Strength values of small cubes (100 mm) are more sensitive than those measured on bigger cubes (150 mm and 200 mm) as the effect of corner drying on the cube is more severe for smaller samples. At 90 d, the curing impact leads to a conversion factor of 0.96 for both LC specimen shapes, which is the one used for NC.

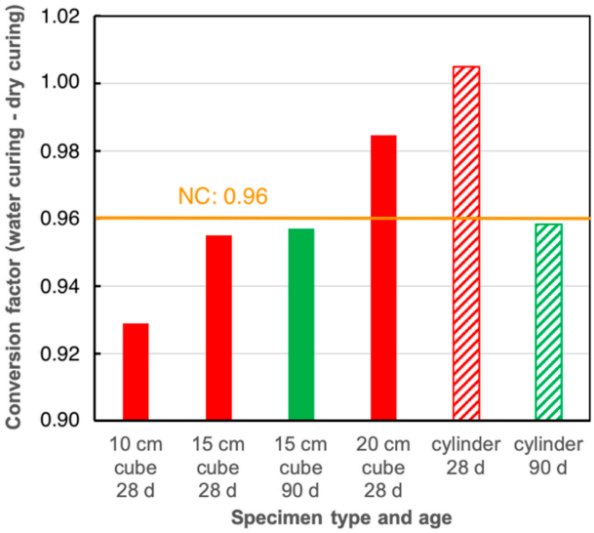

Figure 7. Conversion factors between specimens cured under water [116] or in a climate room (20 °C/65% relative humidity) following the German national annex to [116] for different specimens sizes, shapes and testing ages [64].

5. Application Areas of LC and ILC Depending on Strength, Density and Thermal Conductivity

5.1. Application Areas of LC

LC is suitable for a wide range of applications due to its versatility. Much information is available for LC made with coarse LWA and normal weight sand since it is quite common worldwide. The most interesting and challenging LC structures are bridges [5,118–129] and offshore platforms [13,130–132]. A broad range of LC projects is described in [41,113]. In the following, the focus will be on LC made with coarse LWA and lightweight sand as they provide additionally interesting thermal insulation properties. For this approach, three fields are identified in Figure 8 [6]. A similar designation is given by Dilli et al. [133]. Further information on the correlation between compressive strength and density of LC covering a wide range of mix designs and LWA types are available from databases [33,134,135].

- A concrete dry density in the range between 1.3 and 1.6 kg/dm^3 is aimed for highly stressed facades of office buildings with many and wide window and door openings. They demand for a higher compressive strength in combination with a reduced thermal conductivity of the LC.
- Less stressed facades with higher requirements regarding thermal insulation are built with LC densities in the range between 1.0 and 1.3 kg/dm^3. These walls often have a thickness of 50 cm in order to fulfill legal requirements regarding building physics.
- The third field of LC with a dry density < 1.0 kg/dm^3 represents the most innovative part these days in central Europe. These very light LC offer the best thermal insulation for monolithic concrete and are increasingly used for exclusive private houses. The architect Gartmann developed a fair faced LC for the monolithic exterior walls of his private house [136]. His idea has been adopted by other architects and developed further by concrete technologists. Since the thermal insulation requirements demand rather thick walls, the achievable strength usually provides sufficient load bearing capacity for single- or two-story houses.

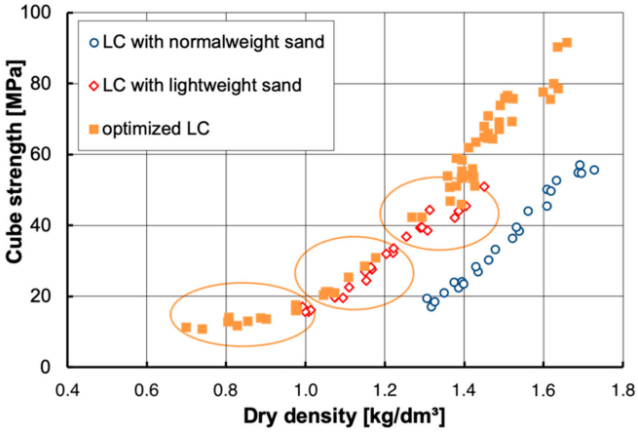

Figure 8. Correlation between 28-day cube strength and dry density for lightweight concretes with different compositions [6].

5.2. *Extending the Application Area of ILC*

A new approach is needed since building physics requirements ask for thermal insulation properties, which cannot be accomplished within the limits defined in the standards for structural lightweight concrete. Some ILC exhibit a dry concrete density below 800 kg/m^3 and thus are no longer covered by existing LC standards [48]. Schlaich and his co-workers (Technical University Berlin, Germany) have extrapolated the application rules for LC below the existing limits for strength values and densities in DIN EN 1992 and established design rules for infra-lightweight concretes (ILC) [137–139].

Recently, another approach to extend the application range of ILC was started at Universität der Bundeswehr München, Germany. Since the mix design of ILC is rather close to LAC, due to the high air void content (see Section 2.2), it was self-evident to adopt the relevant standard EN 1520 [42] for cast-in-place concrete. The advantage of using EN 1520 as basis for structural design is the possibility to cover even dry densities as low as 400 kg/m^3. At the same time, mean strength can be reduced to less than 4 MPa which corresponds with strength class LAC 2 [42]. Figure 10 is a blow-up of Figure 8 and displays additionally the values of executed projects with very light LC and those of the first two ILC projects [18,48]. It shows also the average values obtained within the first two projects following the new LAC-based approach in comparison with LAC data published earlier [43]. The first two ILC projects that follow this LAC-based approach achieved dry densities of 600 kg/m^3 and less on site and strength values suitable for LAC 4 [49].

The new LAC based approach is very successful with respect to the thermal insulation properties of the LAC based ILC. Figure 9 displays measured and design values of the thermal conductivity of projects as well as values laid down in technical approvals [140,141]. The data of the new ILCs will open new opportunities for the producers in an interesting market. An overview with thermal conductivity values of LC and a focus on dry densities above 1400 kg/m^3 is given in [142].

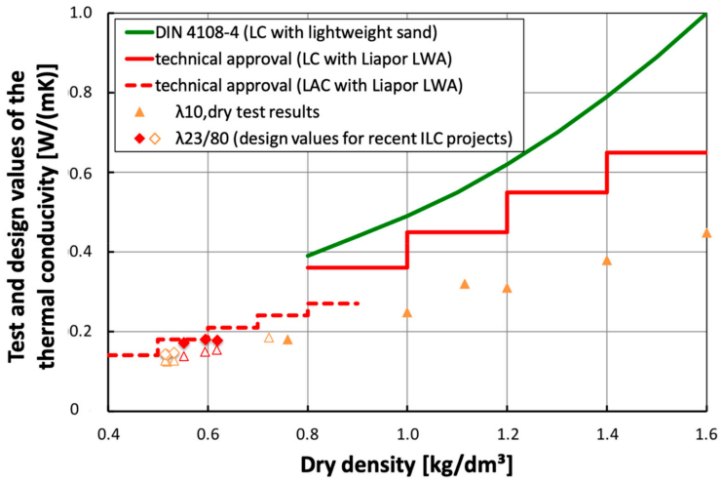

Figure 9. Correlation between thermal conductivity and dry density for LC, LAC taken from technical approvals [140,141], data published for several LC and two ILC projects [18,48] as well as for most recent LAC-based ILC projects [49].

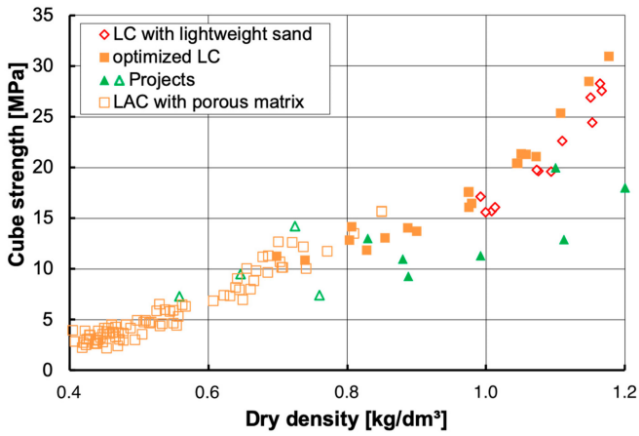

Figure 10. Correlation between 28-day cube strength and dry density for lightweight concretes (LC) with lightweight sand [143], lightweight aggregate concrete (LAC) with porous matrix different compositions [43], data for two ILC projects [18,48] and most recent LAC-based ILC projects [49].

Another very important challenge for ILC is maintaining the appearance of a fair faced concrete which is mandatory for meeting the expectations of future house owners and architects. It is not possible to classify the surface quality according to the same technical and design criteria as applied for NC, such as defined in [144]. Although ILC clients expect or even demand a rather "vivid" surface texture [143] (Figure 11), special considerations are necessary regarding a suitable conformity concept and durability for ILC. Thus, ILC requires a project-related approval or a technical approval.

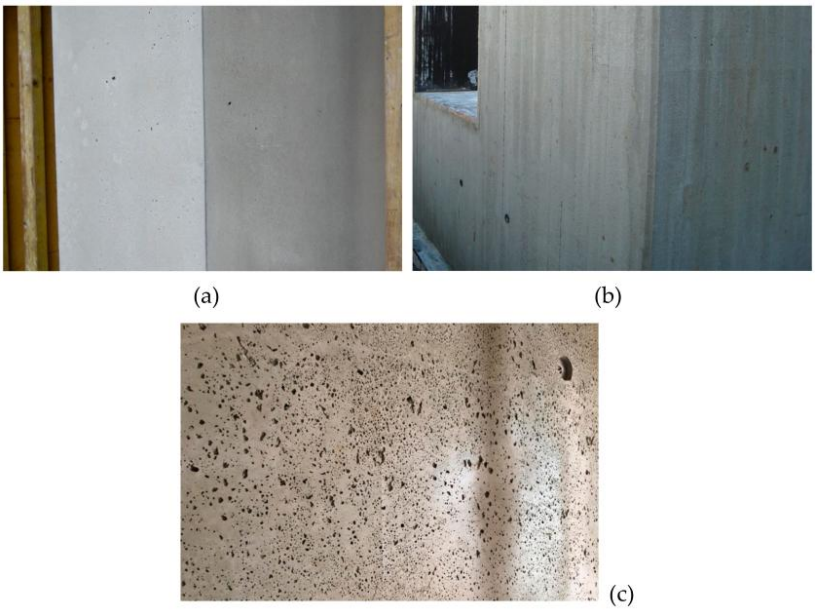

Figure 11. Surface texture of executed ILC projects. Perfectly smooth surface (**a**); rough saw surface (**b**); porous (vivid) surface (**c**) (courtesy: Björn Callsen and Werner Rothenbacher)

Currently there are two deviating ILC approaches under investigation in close cooperation with concrete producers. The first one is a conventional course of action: the ILC is produced in a concrete plant, delivered in a conventional mixing truck and placed on site with a concrete bucket. Quite often, architects who are interested in using ILC for their projects fail finding a concrete producer willing or capable to provide ILC. Since the request for LC is low in most regions, common concrete plants are not equipped for the production of LC or even ILC or suffer from a lack of silo capacity. Both dilemma can be solved with the second approach: the ILC is produced under controlled conditions on site by means of a tailored truck-mounted concrete plant (Figure 12).

Figure 12. Truck-mounted concrete plant for ILC (courtesy: Björn Callsen).

Despite the lack of a basis for production and execution rules for lightweight concretes below a dry density of 800 kg/m^3, the increased interest of clients and architects has led to the construction of various single and multi-family houses. Figure 13 shows a map that gives the locations of ILC construction

projects carried out in Germany until the end of 2019. It was necessary to obtain a project-related approval for these projects. The experience from construction and ongoing research projects can form the basis for the further development of design criteria and promote the establishment of very light LC in new fields of application. Future work will focus on the development ILC with competitive thermal insulation properties while maintaining appropriate design and durability specifications.

Figure 13. Map of Germany showing locations where ILC-projects have been realized until end 2019.

6. Conclusions

Lightweight concrete is an extremely versatile material, which can be used for a wide range of applications. Although lightweight concrete has been in use for two millennia, there are still uncertainties, which were addressed in this review paper. Clear definitions were given for the different types of lightweight concrete and information was provided about crucial topics regarding lightweight aggregate properties as well as mix design, testing and classification of structural lightweight concrete. Several issues represent key information in the state-of-the-art of lightweight concrete.

Infra-lightweight concretes (ILC) constitute an innovative development with very low dry densities (<800 kg/m^3) and respectable thermal insulation properties. ILC is the answer to a new and unexploited area of application. Future research is an essential precondition for the development of a reliable design and construction methodology to ensure production quality and to prepare a European standardization concept.

Author Contributions: Conceptualization, K.-C.T., T.H., N.B.; writing—original draft preparation, K.-C.T., T.H.; writing—review and editing, K.-C.T., T.H., N.B. All authors have read and agreed to the published version of the manuscript.

Funding: This research received no external funding.

Acknowledgments: The authors like to thank Björn Callsen, Holcim GmbH, Germany and Werner Rothenbacher, Schwenk KG, Germany for letting us participate in their projects and for providing project photos (Figures 11 and 12). The authors like to thank Andrea Kustermann, University of Applied Sciences Munich, Germany for providing a microstructure photo of LC (Figure 3).

Conflicts of Interest: The authors declare no conflict of interest.

References

1. Lamprecht, H.-O. *Opus Caementitium: Bautechnik der Römer*, 5th ed.; Beton-Verlag GmbH: Düsseldorf, Germany, 1996; p. 264. ISBN 3-7640-0350-2.
2. Chandra, S.; Berntsson, L. *Lightweight Aggregate Concrete*, 1st ed.; Noyes Publications: Norwich, UK, 2002; p. 450. ISBN 978-0815514862.
3. Expanded Clay and Slate Institute. *Lightweight Concrete History Applications Economics*; Expanded Clay and Slate Institute (ESCSI): Salt Lake City, UT, USA, 1971.
4. Holm, T.A. Performance ol Structural Lightweight Concrete in a Marine Environment. In Proceedings of the Performance of Concrete in Marine Environments, St. New Brunswick, NB, Canada, 1 August 1980; pp. 589–608.
5. Raithby, K.D.; Lydon, F.D. Lightweight concrete in highway bridges. *Int. J. Cem. Compos. Lightweight Concr.* **1981**, *3*, 133–146. [CrossRef]
6. Thienel, K.-C.; Peck, M. Die Renaissance leichter Betone in der Architektur. *DETAIL* **2007**, *47*, 522–534.
7. Bundesregierung. *Verordnung Über Einen Energiesparenden Wärmeschutz bei Gebäuden (Wärmeschutzverordnung-WärmeschutzV)*; Bundesregierung (German Federal Government): Berlin, Germany, 1977; p. 11.
8. Cavalline, T.L.; Castrodale, R.W.; Freeman, C.; Wall, J. Impact of Lightweight Aggregate on Concrete Thermal Properties. *ACI Mater. J.* **2017**, *114*, 945–956. [CrossRef]
9. Fares, H.; Toutanji, H.; Pierce, K.; Noumowé, A. Lightweight Self-Consolidating Concrete Exposed to Elevated Temperatures. *J. Mater. Civil Eng.* **2015**, *27*, 04015039. [CrossRef]
10. Roberz, F.; Loonen, R.C.G.M.; Hoes, P.; Hensen, J.L.M. Ultra-lightweight concrete: Energy and comfort performance evaluation in relation to buildings with low and high thermal mass. *Energy Build.* **2017**, *138*, 432–442. [CrossRef]
11. Samson, G.; Phelipot-Mardelé, A.; Lanos, C. A review of thermomechanical properties of lightweight concrete. *Mag. Concr. Res.* **2017**, *69*, 201–216. [CrossRef]
12. Liu, X.; Chia, K.S.; Zhang, M.-H. Development of lightweight concrete with high resistance to water and chloride-ion penetration. *Cem. Concr. Compos.* **2010**, *32*, 757–766. [CrossRef]
13. Helland, S.; Aarstein, R.; Maage, M. In-field performance of North Sea offshore platforms with regard to chloride resistance. *Struct. Concr.* **2010**, *11*, 15–24. [CrossRef]
14. Lotfy, A.; Hossain, K.M.A.; Lachemi, M. Transport and Durability Properties of Self-Consolidating Concrete Using Three Types of Lightweight Aggregates. *ACI Mater. J.* **2016**, *113*, 679–690. [CrossRef]
15. Real, S.; Bogas, J.A.; Ferrer, B. Service life of reinforced structural lightweight aggregate concrete under chloride-induced corrosion. *Mater. Struct.* **2016**, *50*, 17. [CrossRef]
16. Thomas, M.; Bremner, T. Performance of lightweight aggregate concrete containing slag after 25years in a harsh marine environment. *Cem. Concr. Res.* **2012**, *42*, 358–364. [CrossRef]
17. Vaysburd, A.M. Durability of Lightweight Concrete and its Connections with the Composition of Concrete, Design and Construction Methods. In Proceedings of the ACI SP 136-Structural Lightweight Aggregate Concrete Performance, Detroit, MI, USA, 14 November 1991; pp. 295–318.
18. Schlaich, M.; Zareef, M.E. Infraleichtbeton (Infra-Lightweight Concrete). *Beton Stahlbetonbau* **2008**, *103*, 175–182. [CrossRef]
19. Schließer, A.E. Warmbeton-Mischungsentwicklung mit Verbesserter Übertragbarkeit in den Realmaßstab. Ph.D. Thesis, Universität Stuttgart, Stuttgart, Germany, 2019; p. 197. [CrossRef]
20. Schulze, J.; Breit, W. Experimentalgebäude aus Infraleichtbeton–monolithisch und hochwärmedämmend. *Beton Stahlbetonbau* **2016**, *111*, 377–384. [CrossRef]
21. Yu, Q.L.; Spiesz, P.; Brouwers, H.J.H. Ultra-lightweight concrete: Conceptual design and performance evaluation. *Cem. Concr. Compos.* **2015**, *61*, 18–28. [CrossRef]
22. DIN EN 13055. *Leichte Gesteinskörnungen (Lightweight Aggregates)*; Beuth-Verlag: Berlin, Germany, 2016; p. 58.
23. ASTM C330M-17a. *Standard Specification for Lightweight Aggregates for Structural Concrete*; ASTM International: West Conshohocken, PA, USA, 2017. [CrossRef]
24. ASTM C331M-17. *Standard Specification for Lightweight Aggregates for Concrete Masonry Units*; ASTM International: West Conshohocken, PA, USA, 2017. [CrossRef]

25. ASTM C332-17. *Standard Specification for Lightweight Aggregates for Insulating Concrete*; ASTM International: West Conshohocken, PA, USA, 2017. [CrossRef]
26. Sveindottir, E.L.; Maage, M.; Poot, S.; Hansen, E.A.; Bennenk, H.W.; Helland, S.; Norden, G.; Kwint, E.; Milencovic, A.; Smeplass, S.; et al. LWAC Material Properties-State-of-the-Art. *Brite Euram Proj. Euro Lightcon* **1998**, *111*. [CrossRef]
27. Sveindottir, E.L.; Maage, M.; Poot, S.; Hansen, E.A.; Bennenk, H.W.; Helland, S.; Norden, G.; Kwint, E.; Milencovic, A.; Smeplass, S.; et al. Light Weight Aggregates-Datasheets. *Brite Euram Proj. Euro Lightcon.* **1997**, *132*. [CrossRef]
28. Pauw, A. Structural Lightweight Aggregate Concrete (Concrete Technology, Structural Design). In Proceedings of the 8th IABSE Congress, New York, NY, USA, 9–14 September 1968; pp. 541–557. [CrossRef]
29. Faust, T. *Leichtbeton im Konstruktiven Ingenieurbau*; Ernst & Sohn: Berlin, Germany, 2003; p. 307. ISBN 3-433-01613-5.
30. ASTM C39M-16. *Standard Test Method for Compressive Strength of Cylindrical Concrete Specimens*; ASTM International: West Conshohocken, PA, USA, 2016. [CrossRef]
31. Tajra, F.; Elrahman, M.A.; Stephan, D. The production and properties of cold-bonded aggregate and its applications in concrete: A review. *Constr. Build. Mater.* **2019**, *225*, 29–43. [CrossRef]
32. Ling, I.H.; Teo, D.C.L. Properties of EPS RHA lightweight concrete bricks under different curing conditions. *Constr. Build. Mater.* **2011**, *25*, 3648–3655. [CrossRef]
33. Wang, H.Y.; Tsai, K.C. Engineering properties of lightweight aggregate concrete made from dredged silt. *Cem. Concr. Compos.* **2006**, *28*, 481–485. [CrossRef]
34. Akçaözoğlu, S.; Ulu, C. Recycling of waste PET granules as aggregate in alkali-activated blast furnace slag/metakaolin blends. *Constr. Build. Mater.* **2014**, *58*, 31–37. [CrossRef]
35. Государственного Комитета Совета МинистровСссрПо ДеламСтроительства (State Committee of the Council of Ministers of the USSR on Construction). *GOST 9758-77 ЗаполнителиПористые Неорганические для Бетона. Методы Испытаний(Porous Inorganic Aggregates for Concrete. Test Methods)*; State Committee of the Council of Ministers of the USSR on Construction: Moscow, Russia, 1971; p. 49.
36. ACI Committee 213. *ACI 213R-14 Guide for Structural Lightweight-Aggregate Concrete*; American Concrete Institute: Farmington Hills, MI, USA, 2014; p. 53.
37. DIN EN 206. *Concrete-Specification, Performance, Production and Conformity*; Beuth Verlag: Berlin, Germany, 2013; p. 96.
38. DIN EN 1992-1-1. *Eurocode 2: Design of Concrete Structures-Part 1-1: General Rules and Rules for Buildings*; Beuth-Verlag: Berlin, Germany, 2011; p. 241.
39. DIN 4219-1. *Teil 1: Leichtbeton und Stahlleichtbeton mit Geschlossenem Gefüge-Anforderungen an den Beton, Herstellung und Überwachung*; Beuth-Verlag: Berlin, Germany, 1979; p. 4.
40. Thienel, K.-C. Besonderheiten bei Leichtbeton in DIN FB 100. In *Heft 526 Erläuterungen zu den Normen DIN EN 206-1, DIN 1045-2, DIN EN 13670, DIN 1045-3, DIN 1045-4 und DIN EN 12620*, 2nd ed.; Deutscher Stahlbeton, A., Ed.; Beuth Verlag: Berlin, Germany, 2011; Volume 422, pp. 80–84. ISBN 978-3-410-65196-3.
41. Thienel, K.-C. Application of Lightweight Concrete. In *Nordic Mini-Seminar: Structural Lightweight Aggregate Concrete*; Øverli, J.A., Zivkovic, J., Eds.; Nordic Concrete Federation: Trondheim, Norway, 2019; pp. 6–9. ISBN 978-82-8208-066-8.
42. DIN EN 1520. *Vorgefertigte Bauteile aus Haufwerksporigem Leichtbeton und mit Statisch Anrechenbarer oder Nicht Anrechenbarer Bewehrung (Prefabricated Reinforced Components of Lightweight aggregate Concrete with Open Structure with Structural and Non-Structural Reinforcement)*; Beuth Verlag: Berlin, Germany, 2011; p. 119.
43. Thienel, K.-C. Precast elements of lightweight concrete with a porous matrix. *BFT Int.* **2000**, *66*, 62–72.
44. Deutsches Institut für Bautechnik. Herstellung und Verwendung von Schaumbeton (Production and use of foamed concrete). *DIBt Mitt.* **2002**, *33*, 185.
45. Bergan, P.G.; Bakken, K.; Thienel, K.-C. Analysis and Design of Sandwich Structures Made of Steel and Lightweight Concrete. In *III European Conference on Computational Mechanics*; Motasoares, C.A., Martins, J.A.C., Rodrigues, H.C., Ambrósio, J.C., Pina, C.A.B., Motasoares, C.M., Pereira, E.B.R., Eds.; Springer: Berlin/Heidelberg, Germany, 2006; ISBN 978-1-4020-4994-1.
46. Lösch, C.; Rieseberg, P. *Infraleichtbeton*; Fraunhofer IRB Verlag: Stuttgart, Germany, 2018; p. 214. ISBN 978-3-8167-9931-3.

47. Lösch, C.; Hückler, A.; Schlaich, M. Infraleichtbeton. *Bauphysik* **2019**, *41*, 1–6. [CrossRef]
48. Callsen, B.; Thienel, K.-C. Besondere Aspekte bei der Entwicklung und Ausführung eines hochwärmedämmenden Hochleistungs-Leichtbetons mit sehr niedriger Betonrohdichte. *Beton* **2017**, *67*, 128–134.
49. HOLCIM GmbH. *Außenwände aus Hochwärmedämmendem, Haufwerksporigem Infraleichtbeton LAC4 (Exterior Walls Made of Highly Thermal Insulating, Open Porous Infra-Lightweight Concrete LAC4)*; Bayerisches Staatsministerium für Verkehr, Bau und Wohnen: München, Germany, 2019; p. 10.
50. Held, M. Hochfester Konstruktions-Leichtbeton. *Beton* **1996**, *46*, 411–415.
51. Taylor, H.F.W. *Cement Chemistry*, 2th ed.; Thomas Telford Ltd.: London, UK, 1997; p. 459. ISBN 9780727725929.
52. Demirboğa, R.; Gül, R. Thermal conductivity and compressive strength of expanded perlite aggregate concrete with mineral admixtures. *Energy Build.* **2003**, *35*, 1155–1159. [CrossRef]
53. Chung, S.-Y.; Abd Elrahman, M.; Stephan, D. Effect of Different Gradings of Lightweight Aggregates on the Properties of Concrete. *Appl. Sci.* **2017**, *7*, 585. [CrossRef]
54. Shafigh, P.; Nomeli, M.A.; Alengaram, U.J.; Mahmud, H.B.; Jumaat, M.Z. Engineering properties of lightweight aggregate concrete containing limestone powder and high volume fly ash. *J. Clean. Prod.* **2016**, *135*, 148–157. [CrossRef]
55. Abd Elrahman, M.; Chung, S.-Y.; Stephan, D. Effect of different expanded aggregates on the properties of lightweight concrete. *Mag. Concr. Res.* **2019**, *71*, 95–107. [CrossRef]
56. DIN EN 1008. *Zugabewasser für Beton-Festlegung für die Probenahme, Prüfung und Beurteilung der Eignung von Wasser, Einschließlich bei der Betonherstellung Anfallendem Wasser, als Zugabewasser für Beton (Mixing Water for Concrete-Specification for Sampling, Testing and Assessing the Suitability of Water, Including Water Recovered from Processes in the Concrete Industry, as Mixing Water for Concrete)*; Beuth-Verlag GmbH: Berlin, Germany, 2002; p. 18.
57. ACI Committee 304. *ACI 304R-00 Guide for Measuring, Mixing, Transporting, and Placing Concrete*; American Concrete Institute: Farmington Hills, MI, USA, 2002; p. 41.
58. Dhir, K.; Mays, R.G.C.; Chua, H.C. Lightweight structural concrete with Aglite aggregate: Mix design and properties. *Int. J. Cem. Compos. Lightweight Concr.* **1984**, *6*, 249–261. [CrossRef]
59. Videla, C.; López, M. Mixture proportioning methodology for structural sand-lightweight concrete. *ACI Mater. J.* **2000**, *97*, 281–289.
60. Nepomuceno, M.C.S.; Pereira-de-Oliveira, L.A.; Pereira, S.F. Mix design of structural lightweight self-compacting concrete incorporating coarse lightweight expanded clay aggregates. *Constr. Build. Mater.* **2018**, *166*, 373–385. [CrossRef]
61. Lotfy, A.; Hossain, K.M.A.; Lachemi, M. Mix design and properties of lightweight self-consolidating concretes developed with furnace slag, expanded clay and expanded shale aggregates. *J. Sustain. Cem. Based Mater.* **2015**, *5*, 297–323. [CrossRef]
62. Ke, Y.; Beaucour, A.L.; Ortola, S.; Dumontet, H.; Cabrillac, R. Influence of volume fraction and characteristics of lightweight aggregates on the mechanical properties of concrete. *Constr. Build. Mater.* **2009**, *23*, 2821–2828. [CrossRef]
63. Grübl, P. Modell zur Quantitativen Beschreibung der Bruchvorgänge in Gefügedichtem Leichtbeton unter Kurzzeitbelastung. Ph.D. Thesis, Technische Hochschule München, München, Germany, 1976.
64. Thienel, K.-C.; Sposito, R. Effects of Specimen Shape, Size, Age and Curing on Compressive Strength Values Obtained for Structural Lightweight Concrete/ЗАВИСИМОСТЬПОКАЗАТЕЛЕЙПРОЧНОСТИ ЛЕГКОГО КОНСТРУКЦИОННОГО БЕТОНА ПРИСЖАТИИ ОТϕОРМЫ, РАЗМЕРОВ, ВОЗРАСТА И УСЛОВИЙ ТВЕРДЕНИЯ ОБРАЗЦОВ. ALITinform: Cement. Concrete. *Dry Mix.* **2017**, *47*, 26–46.
65. DIN 1045-2. *Tragwerke aus Beton, Stahlbeton und Spannbeton–Teil 2: Beton–Festlegung, Eigenschaften, Herstellung und Konformität–Anwendungsregeln zu DIN EN 206-1 (Concrete, reinforced and prestressed concrete structures–Part 2: Concrete–Specification, Properties, Production and Conformity–Application Rules for DIN EN 206-1)*; Beuth-Verlag: Berlin, Germany, 2008; p. 62.
66. Bogas, J.A.; Gomes, A.; Gomes, M.G. Estimation of water absorbed by expanding clay aggregates during structural lightweight concrete production. *Mater. Struct.* **2012**, *45*, 1565–1576. [CrossRef]
67. Domagała, L. The Effect of Lightweight Aggregate Water Absorption on the Reduction of Water-cement Ratio in Fresh Concrete. *Procedia Eng.* **2015**, *108*, 206–213. [CrossRef]

68. DIN EN 1097-6. *Prüfverfahren für Mechanische und Physikalische Eigenschaften von Gesteinskörnungen-Teil 6: Bestimmung der Rohdichte und der Wasseraufnahme (Tests for Mechanical and Physical Properties of Aggregates-Part 6: Determination of Particle Density and Water Absorption)*; Beuth-Verlag: Berlin, Germany, 2013; p. 51.
69. Smeplass, S. Moisture in Light Weight Aggregates-Practical Consequences for the Production Properties of Light Weight Aggregate Concrete. In *Proceedings of the Second International Conference on Structural Lightweight Aggregate Concrete, Kristiansand, Norway, 18–22 June 2000*; Helland, S., Holand, I., Smeplass, S., Eds.; Norwegian Concrete Association: Oslo, Norway, 2000; pp. 844–854. ISBN 9788291341378.
70. Fernández-Fanjul, A.; Tenza-Abril, A.J.; Baeza-Brotons, F. A new methodology for determining water absorption of lightweight, normal-weight and heavyweight aggregates in a viscous medium. *Constr. Build. Mater.* **2018**, *165*, 596–607. [CrossRef]
71. DIN V 18004. *Anwendung von Bauprodukten in Bauwerken-Prüfverfahren für Gesteinskörnungen nach DIN V 20000-103 und DIN V 20000-104*; Beuth-Verlag: Berlin, Germany, 2004; p. 14.
72. Lura, P.; Jensen, O.M.; Igarashi, S.-I. Experimental observation of internal water curing of concrete. *Mater. Struct.* **2007**, *40*, 211–220. [CrossRef]
73. ASTM C173M-16. *Standard Test Method for Air Content of Freshly Mixed Concrete by the Volumetric Method*; ASTM International: West Conshohocken, PA, USA, 2016. [CrossRef]
74. ACI Committee 211. *ACI 211.9R-18 Guide to Selecting Proportions for Pumpable Concrete*; American Concrete Institute: Farmington Hills, MI, USA, 2018; p. 13.
75. DIN EN 12350-7. *Prüfung von Frischbeton-Teil 7: Luftgehalte-Druckverfahren (Testing fresh concrete-Part 7: Air Content-Pressure Methods)*; Beuth-Verlag: Berlin, Germany, 2019; p. 26.
76. Thienel, K.-C. Heavy Lifter–Konstruktion und Bautechnik. *Beton* **2011**, *61*, 224–229.
77. DIN EN 12350-4. *Prüfung von Frischbeton-Teil 4: Verdichtungsmaß (Testing Fresh Concrete–Part 4: Degree of Compactability)*; Beuth-Verlag: Berlin, Germany, 2019; p. 10.
78. DIN EN 12350-5. *Prüfung von Frischbeton-Teil 5: Ausbreitmaß (Testing fresh Concrete– Part 5: Flow Table Test)*; Beuth-Verlag: Berlin, Germany, 2019; p. 12.
79. Norden, G.; Thienel, K.-C. Pumping of Lightweight Aggregate Concrete Based on Expanded Clay in Europe. In *Proceedings of the Second International Conference on Structural Lightweight Aggregate Concrete, Kristiansand, Norway, 18–22 June 2000*; Concrete, S., Holand, I., Smeplass, S., Eds.; Norwegian Concrete Association: Oslo, Norway; pp. 823–832. ISBN 9788291341378.
80. Helland, S.; Maage, M. Strength Loss in Un-remixed LWA-Concrete. In *Proceedings of the International Symposium on Structural Lightweight Aggregate Concrete, Sandefjord, Norway, 20–24 June 1995*; Holand, I., Hammer, Tor, A., Fluge, F., Eds.; Norwegian Concrete Association: Oslo, Norway, 1995; pp. 533–540. ISBN 8291341079.
81. Maso, J.C.; Alexander, M.G.; Bentur, A.; Massat, M.; Massazza, F.; Mindess, S.; Monteiro, P.J.M.; Odler, I.; Ollivier, J.P.; Pratt, P.L.; et al. *Interfacial Transition Zone in Concrete-State-of-the-Art Report Prepared by RILEM Technical Committee 108-ICC.*; E & FN SPON: London, UK, 1996; Volume 11.
82. Mehta, P.K.; Monteiro, P.J.M. Effect of Aggregate, Cement and Mineral Admixtures on the Microstructure of the Transition Zone. *MRS Online Proc. Libr. Arch.* **1987**. [CrossRef]
83. Zhang, M.-H.; Gjørv, O.E. Penetration of cement paste into lightweight aggregate. *Cem. Concr. Res.* **1992**, *22*, 47–55. [CrossRef]
84. Sarkar, S.L.; Satish, C.; Leif, B. Interdependence of microstructure and strength of structural lightweight aggregate concrete. *Cem. Concr. Compos.* **1992**, *14*, 239–248. [CrossRef]
85. Narattha, C.; Chaipanich, A. Thermal analysis and phase formation of eco-friendly cold-bonded high-calcium fly ash–calcium hydroxide lightweight aggregate at various curing time. *J. Therm. Anal. Calorim.* **2019**, *138*, 2123–2130. [CrossRef]
86. Ul Rehman, M.; Rashid, K.; Ul Haq, E.; Hussain, M.; Shehzad, N. Physico-mechanical performance and durability of artificial lightweight aggregates synthesized by cementing and geopolymerization. *Constr. Build. Mater.* **2020**, *232*, 117290. [CrossRef]
87. Weber, S.; Reinhardt, H.-W. A Blend of Aggregates to Support Curing of Concrete. In *Proceedings of the International Symposium on Structural Lightweight Aggregate Concrete, Sandefjord, Norway, 20–24 June 1995*; Holand, I., Hammer, Tor, A., Fluge, F., Eds.; Norwegian Concrete Association: Oslo, Norway, 1995; pp. 662–671. ISBN 8291341079.

88. Lura, P. Autogenous Deformation and Internal Curing of Concrete. Ph.D. Thesis, Technische Universiteit Delft, Delft, The Netherlands, 2003; p. 208.
89. Ferrara, L.; Cortesi, L.; Ligabue, O. Internal Curing of Concrete with Presaturated LWA: A Preliminary Investigation. In Proceedings of the ACI SP 305-Durability & Sustainability of Concrete Structures, Bologna, Italy, 1–3 October 2015; Chiorino, M.A., Coppola, L., Mazzotti, C., Realfonzo, R., Riva, P., Eds.; ACI Italian Chapter: Bologna, Italy, 2015; Volume 305, pp. 12.11–12.12.
90. Bogas, J.A.; Gomes, M.G.; Real, S. Capillary absorption of structural lightweight aggregate concrete. *Mater. Struct.* **2015**, *48*, 2869–2883. [CrossRef]
91. Helland, S.; Chia, K.S.; Zhang, M.H.; Weber, S.; Reinhard, H.-W.; Boyd, S.R.; Holm, T.A.; Bremner, T.W.; Thomas, M.D.A.; Sugiyama, T.; et al. Bremner Symposium on High-Performance Lightweight Concrete. In Proceedings of the ACI SP 212-Sixth CANMET/ACI International Conference on Durability of Concrete, Thessaloniki, Greece, 1–7 June 2003; p. 1161. [CrossRef]
92. Holm, T.A.; Bremner, T.W.; Vaysburd, A. Carbonation of Marine Structural Lightweight Concretes. In Proceedings of the ACI SP 109-2 International Conference on Performance of Concrete in Marine Environment, St. Andrews, NB, Canada, 21–26 August 1988; pp. 667–676. [CrossRef]
93. Thienel, K.-C.; Schmidt-Döhl, F.; Feldrappe, V. In-Situ Tests on Existing LWAC Structures. In *Proceedings of the Second International Conference on Structural Lightweight Aggregate Concrete, Kristiansand, Norway, 18–22 June 2000*; Helland, S., Holand, I., Smeplass, S., Eds.; Norwegian Concrete Association: Oslo, Norway, 2000; pp. 912–921. ISBN 9788291341378.
94. Monteiro, P.J.M.; Maso, J.C.; Ollivier, J.P. The aggregate-mortar interface. *Cem. Concr. Res.* **1985**, *15*, 953–958. [CrossRef]
95. Xie, P.; Beaudoin, J.J. Modification of transition zone microstructure —silica fume coating of aggregate surfaces. *Cem. Concr. Res.* **1992**, *22*, 597–604. [CrossRef]
96. Goldman, A.; Bentur, A. Bond Effects in High-Strength Silica Fume Concretes. *ACI Mater. J.* **1989**, *86*, 440–447. [CrossRef]
97. Thienel, K.-C. Gefügedichter Leichtbeton-Charakteristische Eigenschaften und Anwendungen. In Proceedings of the Schwenk BetonSeminar, Leipzig, Germany, 2 January 2016; p. 28.
98. Bogas, J.A.; Gomes, A. Compressive behavior and failure modes of structural lightweight aggregate concrete–Characterization and strength prediction. *Mater Design* **2013**, *46*, 832–841. [CrossRef]
99. Siebel, E. Verformungsverhalten, Energieaufnahme und Tragfähigkeit von Normal- und Leichtbeton im Kurzzeitdruckversuch. In *Schriftenreihe der Zementindustrie*; Zementwerke, V.D., Ed.; Beton-Verlag: Düsseldorf, Germany, 1989; Volume 50, p. 120.
100. Lusche, M. *Beitrag zum Bruchmechanismus von auf Druck beanspruchtem Normal- und Leichtbeton mit geschlossenem Gefüge*; Beton-Verlag: Düsseldorf, Germany, 1972; Volume 39, p. 114. ISBN 3764000805.
101. Baker, A.L.L. A criterion of concrete failure. *Proc. Inst. Civil Eng.* **1970**, *45*, 269–278. [CrossRef]
102. Bogas, J.A.; Ferrer, B.; Pontes, J.; Real, S. Biphasic Compressive Behavior of Structural Lightweight Concrete. *ACI Mater. J.* **2017**, *114*, 49–56. [CrossRef]
103. Chen, H.J.; Yen, T.; Lia, T.P.; Huang, Y.L. Determination of the dividing strength and its relation to the concrete strength in lightweight aggregate concrete. *Cem. Concr. Compos.* **1999**, *21*, 29–37. [CrossRef]
104. Sim, J.-I.; Yang, K.-H.; Kim, H.-Y.; Choi, B.-J. Size and shape effects on compressive strength of lightweight concrete. *Constr. Build. Mater.* **2013**, *38*, 854–864. [CrossRef]
105. Siebel, E.; Wischers, G. Verformungsverhalten und Energieaufnahme von Normal- und Leichtbeton im Kurzzeitdruckversuch. *Beton* **1989**, *39*, 303–307.
106. Kung, L.; Shu, K.L.; Qing, S.M.; Sheng, S.X.; Xiu, L. Research on several physico-mechanical properties of lightweight aggregate concrete. *Int. J. Lightweight Concr.* **1980**, *2*, 185–191. [CrossRef]
107. ÖNORM B4710-1. *Beton Teil 1: Festlegung, Herstellung, Verwendung und Konformitätsnachweis*; Austrian Standards: Wien, Austria, 2007; p. 160.
108. NBN B 15-001. *Concrete-Specification, Performance, Production and Conformity + Belgian Supplement to NBN-EN 206*; Bureau voor Normalisatie: Brussel, Belgium, 2012; p. 123.
109. DIN EN 1992-1-1/NA. *Nationaler Anhang-National Festgelegte Parameter-Eurocode 2: Bemessung und Konstruktion von Stahlbeton- und Spannbetontragwerken–Teil 1-1: Allgemeine Bemessungsregeln und Regeln für den Hochbau*; Beuth-Verlag: Berlin, Germany, 2013; p. 97.

110. NEN-EN 206 + NEN 8005 nl. In *Concrete-Specification, Performance, Production and Conformity + Dutch Supplement to NEN-EN 206*; Koninklijk Nederlands Normalisatie Instituut: Delft, The Netherlands, 2016; p. 123.
111. BS 8500-2. *Concrete. Complementary British Standard to BS EN 206. Specification for Constituent Materials and Concrete*; British Standards Institution: London, UK, 2015; p. 48. [CrossRef]
112. CEB-FIP. *Model Code 90*; Thomas Telford Services Ltd.: London, UK, 1991; ISBN 978-0-7277-1696-5.
113. Fib Task Group 8.1. *Lightweight Aggregate Concrete (Bulletin 8)*; International Federation for Structural Concrete (fib): Lausanne, Switzerland, 2000; ISBN 2-88394-048-7.
114. Thienel, K.-C. Verification of Conversion Factors used for Compressive Strength Values obtained for Structural Lightweight Concrete. In Proceedings of the fib Symposium 2017 High Tech Concrete: Where Technology and Engineering Meet, Maastricht, The Netherlands, 12–14 June 2017; pp. 1636–1644. [CrossRef]
115. Karamloo, M.; Roudak, M.A.; Hosseinpour, H. Size effect study on compressive strength of SCLC. *Comput. Concr.* **2019**, *23*, 409–419. [CrossRef]
116. DIN EN 12390-2. *Prüfung von Festbeton-Teil 2: Herstellung und Lagerung von Probekörpern für Festigkeitsprüfungen; Deutsche Fassung (Testing Hardened Concrete-Part 2: Making and Curing Specimens for Strength Tests; German Version of EN 12390-2)*; Beuth-Verlag: Berlin, Germany, 2019; p. 8.
117. Herrnkind, V.; Scholz, S.G. Berücksichtigung des Einflusses der unterschiedlichen Lagerungsarten „trocken" und „feucht" auf die Ergebnisse der Druckfestigkeitsprüfungen. *Beton* **2008**, *58*, 164–167.
118. Grube, H.; Herold, W. Der Beton der Rheinbrücke Köln-Deutz. *Beton Inf.* **1979**, *19*, 4.
119. Holm, T.A.; Bremner, T.W.; Newman, J.B. Concrete Bridge Decks: Lightweight Aggregate Concrete Subject to Severe Weathering. *ACI Concr. Int.* **1984**, *6*, 49–54.
120. Roberts, J.E. Lightweight Concrete Bridges for California Highway System. In Proceedings of the ACI SP 136-Structural Lightweight Aggregate Concrete Performance, Detroit, MI, USA, 14 November 1991; pp. 25–272. [CrossRef]
121. Manhout, J.H.J. Lightweight Concrete in Bridges. In *Structural Lightweight Aggregate Concrete*; Clarke, J.L., Ed.; Blackie Academic & Professional: Glasgow, Scotland, 1993; pp. 150–167.
122. Johnson, H.; Helland, S.; Heimdal, E. Construction of the Støvset free cantilever bridge and the Nordhordlandcable stayed bridge. In *Proceedings of the International Symposium on Structural Lightweight Aggregate Concrete, Sandefjord, Norway, 20–24 June 1995*; Holand, I., Hammer, Tor, A., Fluge, F., Eds.; Norwegian Concrete Association: Oslo, Norway, 1995; pp. 373–379. ISBN 8291341079.
123. Lange, C.; Riutort, T.; Lebris, J. Lightweight concrete for a cable-stayed bridge-The "Iroise" bridge in Brest. In *Proceedings of the International Symposium on Structural Lightweight Aggregate Concrete, Sandefjord, Norway, 20–24 June 1995*; Holand, I., Hammer, Tor, A., Fluge, F., Eds.; Norwegian Concrete Association: Oslo, Norway, 1995; pp. 287–298. ISBN 8291341079.
124. Daly, A.F. Use of Lightweight Aggregate Concrete in Bridges. In *Proceedings of the Second International Conference on Structural Lightweight Aggregate Concrete, Kristiansand, Norway, 18–22 June 2000*; Helland, S., Holand, I., Smeplass, S., Eds.; Norwegian Concrete Association: Oslo, Norway, 2000; pp. 345–354. ISBN 9788291341378.
125. Fergestad, S.; Jordet, E.A. The Economical Potential of LWAC in 4 Different Major Bridges. In *Proceedings of the Second International Conference on Structural Lightweight Aggregate Concrete, Kristiansand, Norway, 18–22 June 2000*; Helland, S., Holand, I., Smeplass, S., Eds.; Norwegian Concrete Association: Oslo, Norway; pp. 355–364. ISBN 9788291341378.
126. Fluge, F.; Markey, I.F.; Hasselø, J.A.; Sletten, G.I.; Espeldid, B. Durability Surveillance of Bergsøysundet Bridge. In *Proceedings of the Second International Conference on Structural Lightweight Aggregate Concrete, Kristiansand, Norway, 18–22 June 2000*; Helland, S., Holand, I., Smeplass, S., Eds.; Norwegian Concrete Association: Oslo, Norway; pp. 874–883. ISBN 9788291341378.
127. Melby, K. Use of High Strength LWAC in Norwegian Bridges. In *Proceedings of the Second International Conference on Structural Lightweight Aggregate Concrete, Kristiansand, Norway, 18–22 June 2000*; Helland, S., Holand, I., Smeplass, S., Eds.; Norwegian Concrete Association: Oslo, Norway, 2000; pp. 47–56. ISBN 9788291341378.
128. Rosseland, S.; Thorsen, T.A. The Stolma Bridge-World Record of Free Cantilevering. In *Proceedings of the Second International Conference on Structural Lightweight Aggregate Concrete, Kristiansand, Norway, 18–22 June*

2000; Helland, S., Holand, I., Smeplass, S., Eds.; Norwegian Concrete Association: Oslo, Norway, 2000; pp. 406–415. ISBN 9788291341378.
129. Cousins, T.; Roberts-Wollmann, C.; Brown, M.C. *High-Performance/High-Strength Lightweight Concrete for Bridge Girders and Decks*; Board, T.R., Ed.; National Cooperative Highway Research Programm: Washington, DC, USA, 2013; Volume 733, p. 91. ISBN 978-0-309-25888-3.
130. Gjerde, T. *Structural Lightweight-Aggregate Concrete (LWA-Concrete) for Marine and Offshore Applications*; Norwegian Contractors: May, Norway, 1982; p. 156.
131. Erlien, O. Heidrun TLP. Utilization of High Strength LWA-Concrete. In *Proceedings of the International Symposium on Structural Lightweight Aggregate Concrete, Sandefjord, Norway, 20–24 June 1995*; Holand, I., Hammer, T.A., Fluge, F., Eds.; Norwegian Concrete Association: Oslo, Norway, 1995; pp. 337–348. ISBN 8291341079.
132. Fernandes, J.F.; Bittencourt, T.; Helene, P. A review of the application of concrete to offshore structures. In Proceedings of the ACI SP 253-Fifth ACI/CANMET/IBRACON International Conference on High-Performance Concrete Structures and Materials, Manaus, Brazil, 18–20 June 2008; pp. 377–392. [CrossRef]
133. Dilli, M.E.; Atahan, H.N.; Şengül, C. A comparison of strength and elastic properties between conventional and lightweight structural concretes designed with expanded clay aggregates. *Constr. Build. Mater.* **2015**, *101*, 260–267. [CrossRef]
134. Yang, K.-H.; Kim, G.-H.; Choi, Y.-H. An initial trial mixture proportioning procedure for structural lightweight aggregate concrete. *Constr. Build. Mater.* **2014**, *55*, 431–439. [CrossRef]
135. Suraneni, P.; Anleu, B.P.C.; Flatt, R.J. Factors affecting the strength of structural lightweight aggregate concrete with and without fibers in the 1200–1600 kg/m^3 density range. *Mater. Struct.* **2016**, *49*, 677–688. [CrossRef]
136. Filipaj, P. *Architektonisches Potential von Dämmbeton*; Vdf Hochschulverlag AG: Zürich, Switzerland, 2006; p. 106. ISBN 978-3-7281-3056-3.
137. Hückler, A.; Schlaich, M. Zur Biegung von Infraleichtbetonbauteilen–Werkstoff-, Verbund-, Trag- und Verformungsverhalten. *Beton Stahlbetonbau* **2017**, *112*, 282–292. [CrossRef]
138. Schlaich, M.; Hückler, A. Infraleichtbeton: Reif für die Praxis. *Beton Stahlbetonbau* **2017**, *112*, 772–783. [CrossRef]
139. Zareef, M.A.M.E. Conceptual and Structural Design of Buildings made of Lightweight and Infra-Lightweight Concrete. Ph.D. Thesis, Technische Universität Berlin, Berlin, Germany, 2010; p. 119.
140. *Leichtbeton mit Geschlossenem Gefüge nach DIN EN 206-1 in Verbindung mit DIN 1045-2 "Liapor-Konstruktionsleichtbeton"*; Deutsches Institut für Bautechnik: Berlin, Germany, 2011; p. 7.
141. *Wände aus Leichtbeton mit Haufwerksporigem Gefüge nach DIN 4232:1987-09 "Haufwerksporiger Liapor-Leichtbeton"*; Deutsches Institut für Bautechnik: Berlin, Germany, 2011; p. 7.
142. Real, S.; Bogas, J.A.; Gomes, M.D.G.; Ferrer, B. Thermal conductivity of structural lightweight aggregate concrete. *Mag. Concr. Res.* **2016**, *68*, 798–808. [CrossRef]
143. Thienel, K.-C. Structural lightweight concrete for external walls–A challenge between the poles of improved thermal insulation and fair faced concrete (Легковесный конструкционный бетон для наружных стен-задача между полюсами из улучшенной теплоизоляции иоблицовочного бетона). *Cement. Concrete. Dry Mix.* **2018**, *50*, 18–29.
144. Deutscher Beton- und Bautechnik-Verein, e.V. *Merkblatt "Sichtbeton" (Leaflet-Exposed Concrete)*; Deutscher Beton- und Bautechnik-Verein e.V.: Berlin, Germany, 2015; p. 53.

© 2020 by the authors. Licensee MDPI, Basel, Switzerland. This article is an open access article distributed under the terms and conditions of the Creative Commons Attribution (CC BY) license (http://creativecommons.org/licenses/by/4.0/).

7.2 Challenges on pumping infra-lightweight concrete based on highly porous aggregates

Reprint:

Published in “Journal of Building Engineering”

Volume 65, 105761; doi: 10.1016/j.jobe.2022.105761

Authors: T. Haller, N. Beuntner, H. Gutsch, K.-Ch. Thienel

Journal of Building Engineering 65 (2023) 105761

Contents lists available at ScienceDirect

Journal of Building Engineering

journal homepage: www.elsevier.com/locate/jobe

Challenges on pumping infra-lightweight concrete based on highly porous aggregates

Timo Haller *, Nancy Beuntner, Henrik Gutsch, Karl-Christian Thienel

Universität der Bundeswehr München, Fakultät für Bauingenieurwesen und Umweltwissenschaften, Institut für Werkstoffe des Bauwesens, Werner-Heisenberg-Weg 39, 85579, Neubiberg, Germany

ARTICLE INFO

Keywords:
Infra-lightweight concrete
Ultra-lightweight concrete
Lightweight concrete
Lightweight aggregate
Concrete pumping
Fresh properties
Hardened properties
Expanded glass

ABSTRACT

Infra-lightweight concrete (ILC) is the latest step in the development lightweight concrete mainly for the use in monolithic exterior walls. By optimizing the balance between reduced density, sufficient strength and the lowest possible thermal conductivity, ILC offers a competitive alternative to multilayer wall structures commonly used today. Pumping of fresh concrete is becoming increasingly important owing to further rationalization on the construction site and the increasing use of ready-mix concrete. However, pumping lightweight concretes is often associated with difficulties. This article presents the first study ever on pumpability of a record breaking ILC, using some of the most common concrete pumps. Therefore, an experimental study was carried out to determine whether the pressurization of the fresh concrete in the course of the pumping process influences fresh and hardened ILC properties. Based on the results, it can be concluded that ILC can be pumped. The delivery principle of the pumps has a particular influence on fresh ILC properties, especially in terms of abrasive stress on the porous aggregates and workability. No significant negative influences on hardened concrete properties were detected. Classification of the ILC can be accomplished in the same density and strength class before and after pumping. The study highlights challenges of pumping ILC with highly porous aggregates and provides practical approaches to its realization.

1. Introduction

1.1. Lightweight and infra-lightweight concrete

Lightweight concretes are not a recent achievement of concrete technology. Since ancient times, lightweight concrete has been known and used extensively [1]. The low density is the most obvious characteristic that distinguishes lightweight concretes from normalweight concrete. Its reduced density is achieved by introducing a porous system, whether by lightweight aggregate (structural lightweight concrete (LC)), pore inclusions in the binder paste (aerated or foamed lightweight concrete) or the formation of interstitial voids due to omitting fine aggregates (no-fines lightweight concrete). In addition, combinations of these methods are also possible [2]. Based on these compositional options, there is a variety of definitions for lightweight concretes that can be further differentiated in terms of density, strength, and types of lightweight aggregates used. The use of lightweight aggregates (LWA) goes along with the consideration of density as a primary factor in mix design. Due to the high variety of potentially available LWA [3], lightweight concrete stands out as an extremely versatile building material. Depending on the intended use, LC can be used on the one hand

* Corresponding author.
E-mail address: timohaller@outlook.com (T. Haller).

https://doi.org/10.1016/j.jobe.2022.105761
Received 13 October 2022; Received in revised form 16 December 2022; Accepted 16 December 2022
Available online 17 December 2022
2352-7102/© 2022 Elsevier Ltd. All rights reserved.

primarily for load transfer with the lowest possible density (e.g. offshore structures) or on the other hand primarily as thermal insulation in the form of floor-to-ceiling walls.

In the past two decades, there has been an increasing interest in further reducing concrete density while maintaining the highest possible and sufficient strength [4]. Recently, monolithic structures have gained popularity in Europe with fair-faced concrete in the lowest strength and density classes. Such structures allow the construction of a finished wall in one operation without using additional insulating material or going for multi-layer wall structures [4]. The decision in favor of a monolithic lightweight concrete wall is usually based on the desire to design an individual, easily formable architecture by exploiting the design possibilities of fair-faced concrete. Therefore, constructional design requirements and demands on thermal insulation properties must be met. The current stage of this development includes ILC [2,5–9]. In research projects with similar material approaches, the term ultra-lightweight concrete is also common [10–13]. Consistently, these material approaches apprehend a lightweight concrete below a dry density of 800 kg/m^3. The limit value of 800 kg/m^3 refers to the lower limit for the dry density of LC according to DIN EN 206 [14]. For this reason, the Latin preposition "infra" (eng. "below") has been introduced as a means of differentiation [15].

The mix proportioning of ILC seeks the optimum compromise between reduced density, sufficient strength and the lowest possible thermal conductivity. Lightweight aggregates are the main ingredients in reducing the density of ILC. The LWA occupies more than 70% of the volume in ILC. Depending on the source materials and the production process, the individual lightweight aggregates have varying degrees of interconnectivity of open and closed pores, with a wide pore size distribution [16]. The high porosity of LWA and its accompanying low density is one of the most important factors influencing the development of the mix design [17]. The porous LWA can absorb water from the cement paste and thus lead to stiffening of the fresh concrete. The water absorption of LWA must therefore be taken into account in the mix design by an adjusted water addition or pre-wetting of the LWA [18]. The water absorbed by LWA can be sucked out during later stage of hydration by the increasing capillary action of the hardening cement paste and provide internal curing of the LC [19,20]. A wide range of possible LWA is available for the production of LC. These LWA are of mineral origin according to DIN EN 13055-1 [21] and are either natural materials or manufactured from natural materials, industrial by-products, and recycled source materials. The wide range of possible LWA results in an equally wide variability of the resulting fresh and hardened properties of LC. Thus far, only expanded clay and expanded glass are used for ILC [7,8,10–12,15]. In terms of binder material, cements with low heat of hydration are usually preferred and/or used in combination with fly ash, calcined clay, granulated furnace slag or limestone [2]. Due to the low heat capacity and thermal conductivity of ILC, the resulting high hydration temperature developments in the core of the usually relatively thick components (50–60 cm) should be avoided [7,22]. Admixtures established for normal concrete can also be used for ILC as well. It is generally assumed, that due to the density difference of its constituents (especially binder and LWA), ILC is prone to segregation and bleeding [7]. Therefore, there is particular interest in admixtures that control the balance between the LWA and the binder particles and the finely distributed air bubbles in the cement paste, as well as to ensure suitable workability. The admixtures most commonly used in ILC are therefore superplasticizers, stabilizers and/or air entraining agents [7].

Due to the building physics requirements of the Energy Conservation Ordinance for new and renovated buildings in Germany [23], monolithic lightweight concrete exterior walls with adequate wall thicknesses cannot be achieved at present within the limits of the standard for structural lightweight concrete (DIN EN 206 [14] and DIN EN 1992 [24]). The necessary further reduction of the concrete density is significantly below the normative range of LC. A new approach is therefore being pursued at the Universität der Bundeswehr München in cooperation with several industrial partners. It follows the observation, that due to its high porosity of more than 10 vol.-%, the ILC cannot hold as structural LC [25]. ILC is rather similar in its specific material characteristics and mix design proportions to lightweight aggregate concrete (LAC), which offers an existing structural design system for precast elements in DIN EN 1520 [26]. This design system forms the basis for the adaptation of the standard for ready-mix concrete, including the development of rules for the conformity on site. This implementation is already part of several project-related approvals [27] and shall be transferred into a Technical Approval [2].

The steadily increasing demand for ILC, an emerging material that is not regulated by standards thus far, makes it essential to resolve important questions posed by planners and close remaining research gaps. In this context, the progressing rationalization of the construction process and the optimization of concrete handling on construction sites represent a consistent development step for ILC.

1.2. Pumping of LC

Pumping is one of the most common methods for placing fresh concrete on the construction site and is essential to the modern construction process [28,29]. Continuous development of machine and construction technology enables time- and labor-efficient handling of fresh concrete even in confined conditions [30–32]. Properties of the fresh concrete must be considered for successful pumping operations in addition to external influences of the construction site (e.g. pipeline geometry and length) and the pumping equipment (pumping volume and pressure capacities) [33]. This requires in general a sufficient segregation resistance of the concrete [33–36]. Although it is not a measurable physical quantity, the term pumpability has been established in the literature to describe the ability to pump concrete through pipelines without affecting the fresh and hardened concrete properties [17,29–34,36,37]. From a concrete technological point of view, segregation resistance, bleeding resistance and fluidity can be specified as essential characteristics for pumpability [33]. These characteristics are closely related to rheological properties of fresh concrete, or in particular the lubricating layer that forms between the pipeline wall and the core concrete [33,34]. During the pumping process, the fresh concrete is forced at high pressure through pipelines made of steel or other abrasion-resistant hoses. Concrete with suitable material properties can withstand the various dynamic shear stresses occurring during the pumping process [30]. It has been shown conclusively that the aggregates inside the fresh concrete form the shape of a plug in the center of the pipe, while an easily deformable lubricating layer develops on the inner surface of the pipeline [30,31,38–41]. The latter consists mainly of cement, water, fine aggregate, as well as additives and admixtures. The lubricating layer determines the pressures required for suitable pumpability [31,38,42]. The

deformation behavior of the fresh concrete under pressure within the pipeline results from the rheological properties of the fresh concrete. Various guidelines have been developed to facilitate the selection of the pump and the pipeline system and to avoid injuries and casualties, taking into account the external factors, as well as the interrelations between rheological properties and pumping [29,36,37]. However, pumping of lightweight concretes with porous aggregates is not possible by solely following practical knowledge in developing a mix design or predicting pressure conditions. Rather, precise trials with the intended pumping equipment are highly recommended unless prior experience or mixture analysis can provide satisfactory assurance of pumpability [36,37]. This applies in particular for lightweight concrete [17,43].

In contrast to normalweight concrete, some transport phenomena must be considered when pumping LC. In 2000 the project "Economic Design and Construction with Lightweight Aggregate Concrete" highlighted three major challenges in the pumping process of lightweight concrete [17]:

1. Due to the pressurization of the fresh concrete during the pumping process, water and cement paste can be pressed into the highly porous LWA. This initially reduces the flowability of the fresh concrete and subsequently leads to increased friction on the inner walls of the pipeline.
2. The volume of the fresh concrete may be reduced by the amount of water forced into the LWA. The fresh concrete thereby behaves compressible and elastically during the pumping process. The pressure applied to the fresh concrete can thus not be transmitted over the entire delivery line.
3. The air compressed inside the LWA during the pumping process leads to an overpressure in the LWA pores. As soon as the pump pressure decreases, the compressed air expands and pushes the water within the LWA out again. This can lead to segregation in the fresh concrete, as well as to a disturbed interfacial transition zone between the LWA and the matrix in the hardened concrete.

The first two transport phenomena can result in segregation and reduced workability of the fresh lightweight concrete. Furthermore, the changed rheological properties and non-homogeneous pressure conditions can lead to blockage of the pipeline. The aforementioned effects of the third point can lead to structural damage, as well as reduced strength- and durability-properties of the hardened LC. This factor is taken into account in DIN EN 13670 [44] "Execution of concrete structures" which demands that no significant negative effects on the hardened concrete strength occur as a result of the pumping process. A quantification of the extent of this effect is given by [17] with a maximum strength reduction down to 90% of the initial strength. The use of presaturated LWA can minimize or even eliminate the aforementioned transport processes [17,36,37], but is accompanied by negative effects like an increasing complexity of logistics, increased concrete density, increased moisture content of the hardened LC and an associated increase in thermal conductivity and a decreasing resistance against freezing and thawing [2,17,45,46].

One of the fundamental difficulties for the theoretical design and practical implementation of pumping projects with LC is the lack of information for the practical adjustment of the pumping equipment and its operation, as well as the adjustment of a suitable mix design. The expertise for pumping LC is considered a competitive advantage and thus is often withheld by manufacturers [17]. For these reasons, the pumpability of lightweight concrete in general is often associated with difficulties [16,17,30,47–49]. In the case of very light LC, such as the ILC, the pumpability is also considered to be partly off-target due to the aforementioned challenges [6,50]. Such thinking is reasonable since ILC lacks for instance fine particles which would ensure the lubrication of the pipeline walls. Pumping of ILC would mean a lot to its practical application on site since it will ease the concreting job.

From this perspective, this paper describes the first comprehensive study of ILC pumpability. Therefore, an ILC was pumped under site conditions using three of the most common pump types on the market, namely a piston pump, an eccentric screw pump, and a rotor pump. A primary objective of this study was to demonstrate the pumpability of ILC in general and secondly, to evaluate how the applied pressure affects fresh and hardened properties of an ILC made with a highly porous matrix. In addition to common investigation methods of LC, a main focus was on the impact on the LWA used, which are thought of being more sensitive in the course of the pumping process due to their comparatively low mechanical resistance. This uncharted area was addressed by analyzing the particle size distribution of the LWA used before and after pumping. Against this background, the characteristic differences in the mode of the pumps are highlighted.

Table 1
Summary of the characteristic material properties of the ILC's used.

Maximum grain size [mm]	4
Compaction class (DIN EN 206 [14])	C4
Strength Class (DIN EN 1520 [26])	LAC 4
Characteristic compressive strength [N/mm^2]	5 N/mm^2
Density class (DIN EN 1520 [26])	0.6
Characteristic dry density [kg/m^3]	570
Flexural strength [N/mm^2]	0.9
Modulus of elasticity [N/mm^2]	3900
Thermal conductivity $\lambda_{10,dry}$ (DIN EN 12664 [51]) [W/(m•K)]	0.125
Thermal conductivity $\lambda_{23/80}$ (DIN EN 12664 [51]) [W/(m•K)]	0.143

2. Experimental program

2.1. Materials and mixture design

In terms of its mechanical properties, density and mix design, the ILC (commercially available as Holcim ThermoPact) used corresponds to a lightweight aggregate concrete (LAC) in accordance with DIN EN 1520 [26]. In deviation from this standard, the ILC is a ready-mixed cast-in-place concrete. The characteristic material properties of the ILC are summarized in Table 1. The ILC complies with strength class LAC 4. It has a declared density class 0.6 and has a thermal conductivity according to DIN EN 12664 [51] of $\lambda_{10,dry} = 0,125$ W/(m•K). Several buildings were executed with this ILC in Germany [2]. The LWA was expanded glass in accordance with DIN EN 13055-1 [21] in fractions 1–2 mm and 2–4 mm. The LWA properties are summarized in Table 2. The LWA were used dry without any prewetting. The binder consisted mainly of blast-furnace slag cement CEM III/A 42.5 N according to DIN EN 197-1 [52]. Condensed silica fume in suspension according to DIN EN 13263-1 [53] served as supplementary cementitious material. The silica fume suspension has a solids content of 50 wt.-%, whereby the water content of the suspension is directly accounted to the mixing water in the ILC composition. Further, micro-polymer fibers according to DIN EN 14889-2 [54] were used. A polycarboxylate ether-based superplasticizer and an air-entraining agent served as admixtures. The mix design, the mixing procedure and the properties of the ILC correspond essentially to those of other ILC's known from literature and described in section 1.1. This applies in particular to the dry density and compressive strength, which are decisive for the classification of ILC. Differences are mainly related to the type of LWA used.

The use of ILC in construction projects often fails because concrete producers willing and able to supply ILC cannot be found in the vicinity of the construction site. Common concrete plants are often not equipped to produce LC or even ILC, or do not have enough storage capacity for the required LWA [2]. Nevertheless, to meet the increasing demand, ILC can be produced on site under controlled conditions using a customized mobile mixing plant (Fig. 1). The ILC investigated in this study was produced using this truck-mounted plant. The large-scale pumping operations were video documented [56].

2.2. Pumping equipment

Various pump types are available for pumping fresh concrete. In the present study, three concrete pumps (Putzmeister Holding GmbH) with different pumping methods were used:

1) TP_K: Piston pump P720 TD

TP_K is a hydraulically operated axial two-cylinder piston pump. The two pistons operate in reciprocating motion. The movement of the pistons creates a pressure difference in the pipeline. The stroke movement to bottom dead center draws the fresh concrete from the suction pont. With the subsequent, opposite piston movement, a hydraulic swing arm opens the connection to the discharge pont, allowing the fresh concrete to enter the pipeline.

2) TP_S: Eccentric screw pump FHS 250

The eccentric screw pump TP_S conveys the fresh concrete via a helical displacement body (rotor) rotating in a static, rubbery-elastic element (stator). A cardan shaft moves the rotor through a coupling rod. Radially moving spaces remain between the rotor and the stator, which continuously convey the concrete from the suction port to the discharge pont by means of the rotational movement of the rotor.

3) TP_P: Rotor pump Pumi

The rotor pump TP_P conveys the concrete by external deformation of a flexible hose. Pressure rollers clamp the pump hose and move along the hose through a rotor in a radial action system. The pressure rollers clamp the hose and continuously drive the fresh concrete from suction to the discharge pont by the rotating movement. After passing the pressure rollers, the hose opens again to its initial state due to its elasticity, whereby further concrete is sucked in.

Fig. 2 shows the three pumps with their delivery system depicted schematically. Table 2 summarizes the essential parameters of the pumping process for the respective pumps.

For each pump a concreting operation of 4 m^3 was provided. Fresh ILC samples were taken for fresh concrete tests and specimens cast before (reference) and after (TP_K, TP_P, TP_S) the pumping to produce samples which allowed a comparison of the different pumping methods. The pressure during each pumping job was recorded. Information about the pumps and the pressure during the trials are provided in Table 3.

Table 2
Physical properties of expanded glass aggregates.

Aggregate type	Shape	Crushing resistance[a] [N/mm^2]	Particle density[b] [kg/m^3]	Water absorption[b] [wt.%]
Liaver 1–2 mm	Rounded	2.4	356	20.6
Liaver 2–4 mm	Rounded	2.2	342	20.7

[a] Manufacturers data.
[b] Measured according to DIN EN 1097-6 [55].

Fig. 1. Truck-mounted concrete plant for ILC ready for the test.

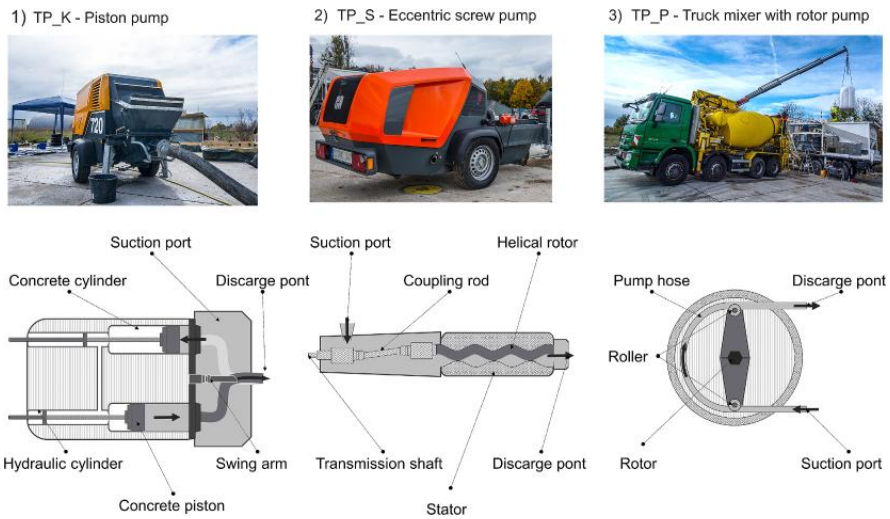

Fig. 2. Schematic representation of the transportation principle of the concrete pumps used 1) TP_K piston pump, 2) TP_S eccentric screw pump, 3) TP_P rotor pump.

Table 3
Summary of the technical parameters of the concrete pumps and equipment used for the pumping operations.

	TP_K	TP_S	TP_P
Type of pump	Piston pump	Eccentric screw pump	Rotor pump
Pipe diameter [mm]	100	100	125
Pipe length [m]	13	13	20
Material pressure [MPa]	20% load ≈ 0.2–0.3 40–50% load ≈ 0.2–0.5	20% load ≈ 0.5 50% load <1.0 100% load >1.0	0.2–0.5 with air inlet 0.7–1.5 without air inlet
Peak pressure [MPa]	0.5	1.0–1.5	2.0

2.3. Test methods

2.3.1. Fresh concrete properties and density

Consistency of the fresh concrete was characterized via slump flow according to DIN EN 12350-2 [57] and the degree of compactability was obtained according to DIN EN 12350-4 [58]. The air content of the fresh concrete was determined by means of the pressure equalization method according to DIN EN 12350-7 [59]. The specimens were not compacted for the hardened concrete tests. For all specimens fresh concrete density was determined according to DIN EN 12350-6 [60]. Hardened concrete density was measured according to DIN EN 12390-7 [61] before any mechanical test.

2.3.2. Mechanical properties

Compressive strength was tested after 28 days on at least six 150 mm cubes per series following DIN EN 1354 [62]. To determine the flexural strength, three beams 100 × 100 × 500 (mm) with 300 mm span were tested per series in a four-point bending test after 28 days according to DIN EN 1521 [63]. Modulus of elasticity was determined according to DIN EN 1352 [64] on cylinders (h/d = 300/150 mm) after 28 days. Besides the reference all samples were cast after the successful pumping process.

2.3.3. Oven dry density and thermal conductivity

Dry density was tested according to DIN EN 992 [65]. Thermal conductivity was obtained by means of the transient plane source method (Hot Disk TPS 2200, Gothenburg, Sweden) in accordance with DIN EN ISO 22007-2 [66]. Prior to the measurement, the specimens were dried carefully to mass constancy and then allowed to cool down to a temperature of 23 °C. During the cooling process, the samples are stored in an airtight container filled with silica gel for drying. The thermal conductivity was determined on three different specimens each and on different specimen sides. Thermal conductivity measurements which shall be used to obtain design values of thermal conductivity must be accomplished using the reference method [51].

2.3.4. Particle size distribution

Particle size distribution of the LWA used was analyzed by photo-optical particle characterization BeVision D2 (3P Instruments GmbH & Co. KG, Odelzhausen, Germany) which photographs and analyzes particles in the particle size range from 30 μm to 10 mm with two digital cameras working in parallel. Each measurement of a sample was performed at least twice and verified for successful reproducibility. The particle size distribution was determined on the LWA as-delivered ($delivered_{LWA}$) as well as on the LWA taken form the mixes before ($reference_{LWA}$) and after the pumping process (TP_K_{LWA}, TP_S_{LWA} and TP_P_{LWA}). The LWA was recovered from the mixes by sieving and subsequent washing. The difference between the particle size distributions before and after pumping is qualitatively evaluated by common metric functions, which represent the measure of error between paired continuous observations. As an example, a single error between the particle size distributions of $delivered_{LWA}$ and $reference_{LWA}$ (after concreting and before pumping) is highlighted in orange in Fig. 3. The applied error measures (RMSE, MAE and MAPE) for the difference between the particle size distributions are determined as follows:

$$Root\ Mean\ Square\ Error\ (RMSE) = \sqrt{\frac{1}{n}\sum_{i=1}^{n}(y_i - \widehat{y}_i)^2} \tag{1}$$

$$Mean\ Absolute\ Error\ (MAE) = \frac{1}{n}\sum_{i=1}^{n}|y_i - \widehat{y}_i| \tag{2}$$

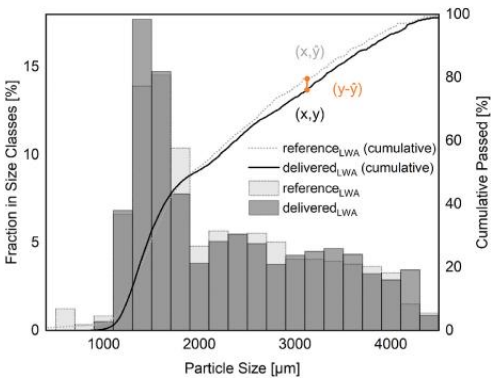

Fig. 3. Particle size distribution of reference LWA ($reference_{LWA}$) compared to as-delivered LWA ($delivered_{LWA}$) with relative proportions in 20 size classes in a particle size range from 400 to 4500 μm.

$$Mean\ Absolute\ Percentage\ Error\ (MAPE) = \left(\frac{1}{n}\sum_{i=1}^{n}\frac{|y_i - \widehat{y}_i|}{|y_i|}\right) \bullet 100 \quad (3)$$

Fig. 3 provides the cumulative distribution function of all measured particles for as delivered LWA ($delivered_{LWA}$) and $reference_{LWA}$, as well as the relative proportions in 20 size classes in a particle size range from 400 to 4500 μm.

3. Results and discussion

3.1. Characteristics of the pumping equipment

For each pump, different pumping runs were conducted with different pumping pressures, equipment adjustments, as well as partial adjustments of water and admixtures. The following characteristics were observed for the respective pump types:

Piston pump TP_K: The cyclic material transport of the piston pump may cause a strong reduction of the consistency of the fresh concrete. It can be assumed that part of the aerated cement paste suspension is pressed into the porous LWA due to the pressurization of the fresh concrete. At the same time, it is possible that the pistons of the pump generate a negative pressure, which extracts water from the fresh concrete. Both effects are largely determined by the applied pump pressure. The negative pressure generated can be reduced by shorter strokes of the cylinder. The fresh concrete could be pumped successfully using the piston pump by adding water to the fresh concrete as well as slowly and steadily increasing the pump strokes.

Eccentric screw pump TP_S: The eccentric screw pump is characterized by a continuous transport of the fresh concrete. The applied pumping pressures have a more pronounced influence on the rheological properties of the fresh concrete compared to the other pump types. At low pressures (<0.5 MPa), the pipeline was filled only partially and apparent segregation between floating LWA and cement paste settling as a sliding film was observed. High pumping pressures (>1.0 MPa) quickly led to a significant reduction in the flowability of the fresh concrete. In addition, a partial collapse of the normally finely dispersed air bubbles originating from the artificially entrained air was observed, resulting in larger unstable air bubbles in the fresh concrete. In the given test setup, pump pressures between 0.5 and 1.0 MPa provided a sufficient consistency and workability for sampling and subsequent investigations.

Rotor pump TP_P: Analogous to the screw pump, the rotor pump transports continuously the fresh concrete. A special feature of the rotor pump used is the possibility of introducing throttled air into the suction channel via a small tube. In the given test setup, the small tube could be controlled manually by the filling height of the feed hopper. Without the additional manual air supply, pressure in the pump went up as high as 0.7 and 2.0 MPa, which slowed down the driving rotor and prevented almost the delivery of the fresh concrete. Continuous air supply, on the other hand, kept material pressures in the pipeline low between 0.2 and 0.5 MPa. The delivery of the fresh concrete with controlled air supply took place continuously and comparatively fast with a delivery rate of about 1 m^3 in 8 min, which corresponds to about 7.5 m^3/h.

The successfully pumped fresh concrete can be seen in Fig. 4, as well as in the video documentation [56].

3.2. Fresh concrete properties

3.2.1. Influence of pumping technology on the LWA particle size distribution

LWA can occupy more than 70% of the volume in ILC. Therefore, the characteristic material properties of the LWA significantly determine the properties of the fresh and hardened concrete. With regard to the pumpability of ILC, the water absorption of the LWA under pressure, as well as the abrasion resistance of the LWA are the main issues. Exceeding the particle strength and the associated destruction of the LWA can reduce strength of the hardened concrete, as well as leading to an increased water absorption and thus altered workability of the fresh concrete. Fig. 5 compares the particle size distributions of the LWA after pumping (TP_K_{LWA}, TP_S_{LWA} and TP_P_{LWA}) with the particle size distribution of the reference before pumping ($reference_{LWA}$). Table 4 provides the associated characteristic parameters of the particle size measurement, as well as the statistical evaluation of the deviation between the pumped samples and $reference_{LWA}$.

The distribution functions in Fig. 5 as well as the parameters provided in Table 4 reveal consistently the influence of the pumping process on the LWA. First, the particle size distributions of the pumped LWA's (TP_K_{LWA}, TP_S_{LWA}, TP_P_{LWA}) is shifted towards finer particle sizes. The finding suggest that mechanical abrasion within the pumps grinds to a certain extend the LWA particles. The different types of pumps yield quantitative differences in terms of the degree of refinement of the particle size distribution. In Table 4 the statistical parameters RMSE, MAE and MAPE identify the largest deviation from $reference_{LWA}$ for pumping with the screw pump

Fig. 4. Continuous flow of pumped ILC without segregation of the material or clogging of the pipeline.

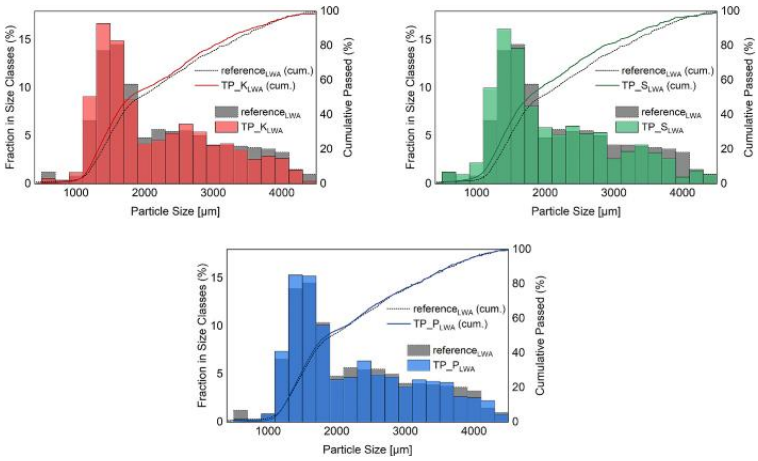

Fig. 5. Particle size distribution of LWA (TP_K_{LWA}, TP_S_{LWA}, and TP_P_{LWA}) after pumping compared to the reference LWA before pumping (reference$_{LWA}$) with relative proportions in 20 size classes in a particle size range from 400 to 4500 µm.

Table 4
Parameters of the particle size measurement of the LWA with statistical evaluation of the deviation of the cumulative distribution function of reference$_{LWA}$ compared to the pumped samples.

Parameter	Sample				
	delivered$_{LWA}$	reference$_{LWA}$	TP_K_{LWA}	TP_S_{LWA}	TP_P_{LWA}
D_{10} [µm]	1255	1250	1206	1168	1239
D_{50} [µm]	1926	1938	1770	1754	1844
D_{90} [µm]	3754	3633	3470	3416	3613
RMSE	–	–	3.37	4.92	0.72
MAE	–	–	2.81	4.24	0.56
MAPE	–	–	9.85	37.1	4.24

(TP_S_{LWA}). The differences in the grading curves are less pronounced between reference$_{LWA}$ and the piston pump (TP_K_{LWA}). The grading curve of the LWA after the rotor pump (TP_P_{LWA}) exhibits only marginal deviations from reference$_{LWA}$. The results indicate a significant influence of the different operating modes of the pump types on the degree of abrasion. While the mode of operation of the piston and rotor pump with their hardly existing gaps between the moving components may provide for abrasion of the aggregate against each other, the screw pump by its design damages the aggregate in the gap between the rotor and the stator. This is indicated in particular by the comparatively high proportion of particles below 1 mm. An increase in the sealing gap between the rotor and stator (see Fig. 2) can possibly reduce in abrasive damage to the LWA. The somewhat finer grading curve of the piston pump can be caused by the removal of water from the mixture, which results in a lack of or at least a stiffer surrounding cement paste between the particles and increases abrasion. The conveying by the rotor pump caused negligible abrasion of the sensitive LWA.

3.2.2. *Fresh density and workability*

The mix design of the ILC focuses on the optimum compromise between reduced density, adequate strength and the lowest thermal conductivity possible. For this reason, the effects of the pumping process on the concrete density are essential for deciding on the suitability of the placement method since changes in density can significantly alter other properties such as strength and durability. In

Table 5
Summary of the determined fresh concrete properties of the ILC.

Property	Reference	TP_K	TP_S	TP_P
Fresh density [kg/m^3]	694	705	723	730
Hardened density [kg/m^3]	681	690	709	715
Dry density[a] [kg/m^3]	570	563	578	586
Slump flow [mm]	490	430	360	480
Degree of compactability [−]	1.0	1.0	1.0	1.0
Air content [Vol.-%]	24	25	22	24

[a] Determined after 28 days.

addition, due to the possible increased water absorption of the LWA in the course of the pumping process, the influence on the workability of the fresh concrete is of particular interest. Table 5 exhibits the results of the fresh concrete tests.

Fig. 6 highlights changes in fresh concrete density, slump flow and water content in comparison to the reference before the pump.

It is apparent from Fig. 6 that the fresh concrete density slightly increases after pumping for all pumps compared to the reference. This can be attributed essentially to the reduction in the volume of the fresh concrete due to the water squeezed into the LWA, as described in Section 2. The reduction in volume increases the fresh concrete density. Furthermore, due to the applied pressure, as well as the reduced availability of free water in the fresh concrete, the artificially entrained air voids can be reduced or even destroyed. This effect yields a further increase in the fresh concrete density after the pumping process.

When evaluating the workability, Fig. 6 exhibits a reduced slump flow after every pumping operation compared to the reference. The results also suggest that the operating principle of the pumps has a significant influence on the extent of this reduction. While TP_P remains with a reduction of approx. 3% in slump flow within the range of the repeatability for the test method [57], TP_S and TP_K suffer a significant reduction of the slump flow with approx. 30% and 12%, respectively. The loss in slump flow can be attributed to the water squeezed into the LWA due to the high pressure applied by the pumps. This argument is supported by the increased water content when determining the dry density of the pumped specimens. The higher water uptake of the LWA due to the applied pressure reduced the amount of water in the cement paste and results in a stiffer, less flowable fresh concrete. Additionally, the damage of LWA due to the pumping process can also be attributed to the decline in slump flow and the increase in density of fresh concrete. As described in Section 4.2.1, the coarser LWA fractions are particularly affected by the abrasive stress during the pumping process. The shift of the particle size distribution to a finer distribution and the associated increase of the fines content led to a higher water demand, as well as a reduced porosity of the damaged LWA. The reducing impact of a finer particle size distribution (see Fig. 5 and Table 4) on slump flow (see Fig. 6) can be observed in particular for TP_K and TP_S. In contrast, TP_P with a particle size distribution close to the reference hardly experiences a reduction of the slump flow. In the case of TP_K, the cyclic operation of the pistons can be considered as an additional reason for the reduced workability. As already mentioned in Section 4.1, the movement of the pistons generates a negative pressure, which can suck water from the fresh concrete into the LWA and thus reduces the flowability. When considering the absolute values of the slump flow for judging the consistency, the low density of the ILC must be taken into account in comparison with other concretes. The weight of the fresh concrete as the driving force of this test differs significantly from conventional concretes and results must therefore be evaluated differently when assessing workability. For this reason, the compaction class C4 was introduced in DIN 1045-2 [67] and later in DIN EN 206 [14] for the evaluation of the workability of LC according to DIN EN 12350-4 [58]. For each test run, a degree of compactability of 1.00 could be obtained to classify the ILC as C4. No difference was found in the compactability between the pumped samples and the reference.

For the mix design of LC, the volumetric share of the components is of major importance. The determination of the air content, which is necessary for this purpose, is therefore essential for a correct mix design. The determination of the air void content by means of pressure method cannot provide exact results, since a distinction between air voids in cement paste and air filled pores in the LWA is impossible. However, due to the good reproducibility of the test results, a qualitative comparison between the different pumping operations and the reference can be made (see Table 5). The test results suggest that none of the pumping operations caused significant differences in air void content.

3.3. Hardened concrete properties

In contrast to normalweight concrete, the LWA plays a predominant role with regard to the stress transfer in the hardened LC and ILC. While in normalweight concrete the mortar matrix determines the concrete strength, the porous and thus less stiff LWA can be decisive for the strength [2]. Therefore, the transport mechanisms in fresh concrete during pumping described in Section 2 and partially observed in Section 4.1 are suspected to cause structural damage, reduced strength, and reduced durability properties of the

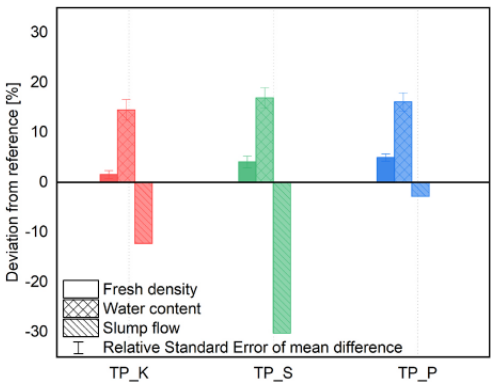

Fig. 6. Deviation in fresh concrete density, slump flow and water content of the ILC as a function of pump type compared to the reference.

hardened ILC. The results of the hardened concrete tests obtained in the course of this study are summarized in Table 6.

Compressive strength plays a major role for ILC. As described in Section 1, ILC is intended to be used for monolithic exterior walls that are mainly loaded with normal forces. Therefore, the correlation of compressive strength to dry density is often used to evaluate the performance of ILC. The test results of the present study are provided in Fig. 7 along with data obtained for project related approvals over the last five years from structures built with this particular ILC [68].

Apparently, the data obtained for pumped ILC's in Fig. 7 lie within the range of dry density and compressive strength values which was thus far determined for previously built structures [68]. Based on these data, the same strength class (LAC 4) and dry density class (600 kg/m^3) were achieved and the classification (see Table 1) could be maintained for future construction projects using pumped ILC.

It can be seen from Figs. 7 and 8 and the data provided in Table 6, that the average compressive strength was higher for the pumped specimens compared to the reference.

A more detailed view reveals further differences between the reference and the samples produced with pumped ILC. TP_P in particular shows a significant increase in average compressive strength of around 14% compared with the reference. A possible reason is the reduced water/binder ratio, which results from the water being pressed into the LWA during pumping. This goes along with the higher fresh density for TP_P (see Table 5). As a further explanation, an increased homogeneity of the fresh concrete can be assumed for TP_K and TP_P after the pumping process. Fig. 8 visualizes the lower scatter of the determined compressive strength values compared to the reference supports this assumption. In contrast, TP_S has a much higher scatter which can be attributed to the higher variation in density, as depicted in Fig. 7.

The test results of flexural strength and modulus of elasticity summarized in Table 6 suggest a comparable material behavior and no major impact nor due to the type of pump nor the pumping process as such.

Thermal conductivity of the ILC is determined by the pore volume and pore size distribution in the hardened concrete. These properties are reflected to a certain extend in the dry density. If pores are enlarged or destroyed by the pumping process, e.g., by the abrasive action on the porous LWA or by suppressing the formation of entrained air voids, the thermal conductivity could increase. Table 6 shows that no particular increase in thermal conductivity can be observed due to the pumping process. As expected, the thermal conductivity is closely related to the dry density. Values of thermal conductivity presented for the tests at hand were obtained using transient plane source method [66]. This procedure yield deviating results from the reference method [51]. Nevertheless, for comparison purposes, as well as for evaluating the influence of the pumping process, this alternative measurement method is well suited.

As described in Section 1, the ILC is currently used primarily for fair-faced monolithic exterior walls, which is why the surface quality of the ILC is of particular importance to architects and principals. From the concrete technological point of view, structural problems of hardened concrete may become apparent. Thus steles with different casting surfaces and dimensions of 600 × 400 × 1100 (mm) were produced as part of the study and are presented in Fig. 9. No sedimentation, no cracks and no other structural flaws are visible for any pumped concrete. The surface quality corresponds to the characteristic appearance of ILC.

4. Conclusion

The present study was designed to prove the pumpability of ILC and to determine the effects of pumping on fresh and hardened concrete properties. This was accomplished using three of the most common concrete pump types. Important conclusions drawn from this study include:

1) All three types of concrete pump tested (piston pump, eccentric screw pump and rotor pump) were able to convey ILC with partial adjustment of pumping equipment. The cyclic material transport of TP_K was found to be disadvantageous compared to the continuous advance of TP_S and TP_P with regard to the initiation of the pumping process. In a comparison of the pumps, TP_S let to relatively large variations in density and strength. TP_P had the least influence with regard to the fresh concrete data. The mechanical properties of TP_P stayed in the range of the reference. For all pump types, it can be noted equally that excessive pressure increase usually leads to clogging of the pipelines. For all pump types, it was found that comparatively lower delivery pressures (<0.5–1 MPa) enabled a pumping process without blockage. In addition, process optimization options for all pumps were identified, such as piston stroke and position (TP_K), increase in the sealing gap between the rotor and stator (TP_S) and adjustable air supply in the suction port (TP_P).
2) The analysis of the particle size distribution showed an abrasive damage of the LWA due to the pumping. Here, TP_S caused the greatest damage to the. In contrast, TP_K led only to minor damage and almost no influence could be observed for TP_P. The results indicate that the abrasive damage has a particular impact on the fresh concrete properties.
3) For all concrete pumps, a slight increase between 2 and 5% could be observed of the fresh concrete density compared to the reference. The increase in the fresh concrete density is not reflected in the hardened concrete properties or the classification of the ILC. The increase of the fresh concrete density can be explained by a partial penetration of water or cement paste into the porous LWA because of the applied pump pressure.
4) Pumping reduced the workability of the fresh concrete expressed as slump, especially for TP_K and TP_S. In contrast, pumping with TP_P yields similar results as the reference. Nevertheless, all pumped ILC maintained a compactability of 1.00.
5) Predicting and optimizing the rheological parameters of the ILC, taking into account the boundary conditions of the construction site as well as the pumping equipment, is essential for conducting successful pumping runs. In general, it can be stated that workability needs to be of a high order and can be maintained after the pumping process.

Table 6
Summary of the determined hardened concrete properties of the ILC.

Property	Reference	TP_K	TP_S	TP_P
Compressive strength[a] [N/mm^2]	6.81	7.23	7.01	7.78
Flexural strength[a] [N/mm^2]	0.98	0.99	1.09	0.90
Modulus of elasticity[a] [N/mm^2]	3367	3379	3289	2960
Thermal conductivity [W/(m•K)]	0.154	0.152	0.155	0.167

[a] Properties determined after 28 days.

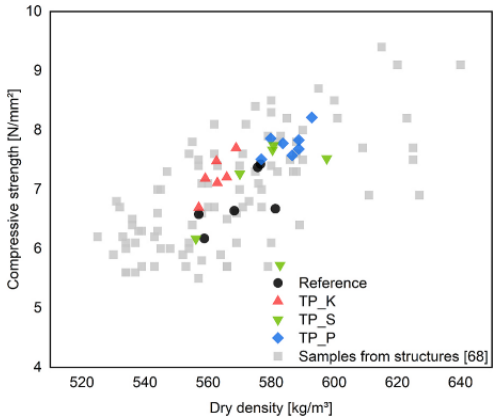

Fig. 7. Compressive strength values of this study compared with data obtained from previously built structures [68].

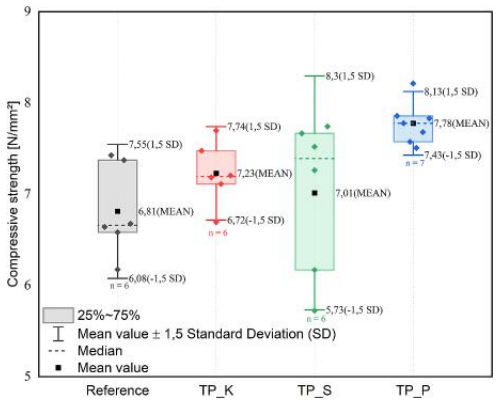

Fig. 8. Compressive strength of ILC after pumping compared to reference with consideration of the statistical variations.

6) The results of the mechanical examinations revealed no damage by pumping to the finished hardened ILC structure. In contrast, an improvement in mechanical properties was observed, such as in compressive strength. The original classification as LAC 4/0.6 can be maintained.

Pumping of ILC can be accomplished if a good mix design is available and competent personnel with previous experience accompanies the pumping on the construction site. In addition, representative pre-tests with the envisaged equipment and application-related expectation values such as required flow rate or pumping distance and height are highly recommended.

CRediT authorship contribution statement

Conceptualization – Timo Haller, Data curation – Timo Haller, Henrik Gutsch, Investigation – Timo Haller, Henrik Gutsch,

Fig. 9. Surface quality of pumped ILC with different casting surfaces.

Methodology – Timo Haller, Nancy Beuntner, Project administration – Nancy Beuntner, Supervision – Nancy Beuntner, Karl-Christian Thienel, Writing - original draft – Timo Haller, Writing - review & editing – Nancy Beuntner, Karl-Christian Thienel.

Declaration of competing interest

The authors declare that they have no known competing financial interests or personal relationships that could have appeared to influence the work reported in this paper.

Data availability

Data will be made available on request.

Acknowledgement

This research did not receive any specific grant from funding agencies in the public, commercial, or not-for-profit sectors. The authors gratefully like to thank Björn Callsen (Holcim (Deutschland) GmbH) for his long-term collaboration and numerous discussions on the science and technology of infra-lightweight concrete as well as for organizing and providing the truck-mounted concrete plant and materials for the study. Contributions of Putzmeister Holding GmbH for provision and handling of the pumping equipment are highly appreciated. In addition, the authors want to thank our group members from the Institute for Construction Materials for their support in carrying out the pumping tests.

References

[1] Expanded Clay, Institute Slate, Lightweight Concrete History Applications Economics, Expanded Clay and Slate Institute (ESCSI), Salt Lake City, Utah, 1971.
[2] K.-C. Thienel, T. Haller, N. Beuntner, Lightweight concrete—from basics to innovations, Materials 13 (5) (2020) 1120.
[3] E.L. Sveindottir, M. Maage, S. Poot, E.A. Hansen, H.W. Bennenk, S. Helland, G. Norden, E. Kwint, A. Milencovic, S. Smeplass, F. Tarquis, I. Holand, B. Price, K. van Breugel, K.-C. Thienel, Light weight aggregates - datasheets, in: J.P.G. Mijnsbergen (Ed.), EuroLightCon - Economic Design and Construction with Light Weight Aggregate Concrete, the European Union – Brite EuRam III, 1997, p. 132. Gouda.
[4] K.-C. Thienel, M. Peck, Die renaissance leichter betone in der Architektur, Zement + Beton (4) (2010) 2–9.
[5] M.A.M. El Zareef, Conceptual and Structural Design of Buildings Made of Lightweight and Infra-lightweight Concrete, Fakultät VI – Planen Bauen Umwelt, Technische Universitat Berlin, Berlin, 2010, p. 119.
[6] C. Lösch, P. Rieseberg, M. Schlaich, R. Leibinger, Building with Infra-lightweight Concrete, De Gruyter, 2020.
[7] M. Elshahawi, A. Hückler, M. Schlaich, Infra Lightweight Concrete: A Decade of Investigation (A Review), Structural Concrete, 2020 n/a.
[8] A. Hückler, M. Schlaich, Zur Biegung von Infraleichtbetonbauteilen – werkstoff-, Verbund-, Trag- und Verformungsverhalten, Beton- Stahlbetonbau 112 (5) (2017) 282–292.
[9] J. Schulze, W. Breit, Experimentalgebäude aus Infraleichtbeton – monolithisch und hochwärmedämmend, Beton- Stahlbetonbau 111 (6) (2016) 377–384.
[10] A.E. Schließer, Warmbeton - Mischungsentwicklung mit verbesserter Übertragbarkeit in den Realmaßstab, Fakultät Bau- und Umweltingenieurwissenschaften, Universität Stuttgart, Stuttgart, 2019, p. 197.
[11] P. Spiesz, M. Hunger, Structural Ultra-lightweight Concrete – from Laboratory Research to Field Trials, 11th High Performance Concrete Conference, Tromso, Norway, 2017, p. 10.
[12] Q.L. Yu, P. Spiesz, H.J.H. Brouwers, Ultra-lightweight concrete: conceptual design and performance evaluation, Cement Concr. Compos. 61 (2015) 18–28.
[13] P. Sikora, T. Rucinska, D. Stephan, S.-Y. Chung, M. Abd Elrahman, Evaluating the effects of nanosilica on the material properties of lightweight and ultra-lightweight concrete using image-based approaches, Construct. Build. Mater. 264 (2020), 120241.
[14] DIN EN 206, Beton – Festlegung, Eigenschaften, Herstellung und Konformität (Concrete - Specification, performance, production and conformity), Beuth Verlag GmbH, Berlin, Germany, 2021, p. 105.
[15] M. Schlaich, M.E. Zareef, Infraleichtbeton (Infra-Lightweight concrete), Beton- Stahlbetonbau 103 (3) (2008) 175–182.

[16] T. Faust, Leichtbeton im Konstruktiven Ingenieurbau, Ernst & Sohn, Berlin, 2003.
[17] G. Norden, K.-C. Thienel, Pumping of lightweight aggregate concrete based on expanded clay in Europe, in: J.P.G. Mijnsbergen (Ed.), EuroLightCon - Economic Design and Construction with Light Weight Aggregate Concrete, the European Union – Brite EuRam III, 2000, p. 67. Gouda.
[18] J.A. Bogas, M.G. Gomes, S. Real, Capillary absorption of structural lightweight aggregate concrete, Mater. Struct. 48 (9) (2015) 2869–2883.
[19] A.M. Vaysburd, Durability of lightweight concrete and its connections with the composition of concrete, design and construction methods, in: T.A. Holm, A. M. Vaysburd (Eds.), ACI SP 136 - Structural Lightweight Aggregate Concrete Performance, American Concrete Institute, Detroit, Michigan, 1992, pp. 295–318.
[20] ESCSI, Internal Curing Using Expanded Shale, Clay and Slate Lightweight Aggregate, Clay & Slate Institute, Salt Lake City, UT, 2006. Publication #4362, Expanded Shale.
[21] DIN EN 13055-1, Leichte Gesteinskörnungen Teil 1: Leichte Gesteinskörnungen für Beton, Mörtel und Einpressmörtel (Lightweight aggregates — Part 1: Lightweight aggregates for concrete, mortar and grout), Beuth-Verlag GmbH, Berlin, Germany, 2002, p. 39.
[22] M. Schnellenbach-Held, M. Held, Hochfester konstruktions-leichtbeton, baukultur : technik, wissenschaft, kunst, umwelt, SH 2 (1997) 24–26.
[23] Bundesregierung, Zweite Verordnung zur Änderung der Energieeinsparverordnung, Bundesregierung (2013) 90. Berlin, Germany.
[24] DIN EN 1992-1-1, Eurocode 2, Design of Concrete Structures - Part 1-1: General Rules and Rules for Buildings, 2011, p. 241.
[25] Deutsches Institut für Bautechnik, Herstellung und Verwendung von Schaumbeton (Production and use of foamed concrete), DIBt Mitteilungen 33 (6) (2002) 185.
[26] DIN EN 1520, Vorgefertigte Bauteile aus haufwerksporigem Leichtbeton und mit statisch anrechenbarer oder nicht anrechenbarer Bewehrung (Prefabricated reinforced components of lightweight aggregate concrete with open structure with structural and non-structural reinforcement), Beuth Verlag GmbH, Berlin, Germany, 2011, p. 119.
[27] HOLCIM GmbH, Außenwände aus hochwärmedämmendem, haufwerksporigem Infraleichtbeton LAC4 (Exterior walls made of highly thermal insulating, open porous infra-lightweight concrete LAC4), Bayerisches Staatsministerium für Verkehr, Bau und Wohnen, München, 2019, p. 10, 29-4112.55-4-107.
[28] K. Kasten, Ein Verfahren zur Bestimmung der Fließeigenschaften von Dickstoffen in Rohrleitungen, TU Dresden, Dresden, 2009, p. 156.
[29] D. Feys, G.d. Schutter, S. Fataei, N.S. Martys, V. Mechtcherine, Pumping of concrete: understanding a common placement method with lots of challenges, Cement Concr. Res. 154 (2022), 106720.
[30] E. Secrieru, Pumpverhalten moderner Betone – Charakterisierung und Vorhersage, Technische Universität Dresden, 2018.
[31] V. Mechtcherine, V.N. Nerella, K. Kasten, Testing pumpability of concrete using sliding pipe rheometer, Construct. Build. Mater. 53 (2014) 312–323.
[32] H. Li, D. Sun, Z. Wang, F. Huang, Z. Yi, Z. Yang, Y. Zhang, A review on the pumping behavior of modern concrete, J. Adv. Concr. Technol. 18 (6) (2020) 352–363.
[33] W.T. Cui, Q. W, H.-F. Song, Effects of viscosity on pumping concrete behavior using computational fluid dynamics method, ACI Mater. J. 2 (2021) 117–126.
[34] V.N. Mechtcherine, Venkatesh Naidu, Beton-3D-Druck durch selektive Ablage, Beton- Stahlbetonbau 114 (1) (2019) 24–32.
[35] E. Secrieru, Pumping Behaviour of Modern Concretes - Characterisation and Prediction, 2018.
[36] ACI Committee 304, ACI 304.2R-17 Guide to Placing Concrete by Pumping Methods, 2017.
[37] ACI Committee 211, ACI 211.9R-18 Guide to Selecting Proportions for Pumpable Concrete, 2018.
[38] E. Secrieru, J. Khodor, C. Schröfl, V. Mechtcherine, Formation of lubricating layer and flow type during pumping of cement-based materials, Construct. Build. Mater. 178 (2018) 507–517.
[39] R. Browne, P. Bamforth, Tests to establish concrete pumpability, ACI Journal Proceedings 74 (5) (1977) 193–203.
[40] M. Choi, N. Roussel, Y. Kim, J. Kim, Lubrication layer properties during concrete pumping, Cement Concr. Res. 45 (2013) 69–78.
[41] J. Vosahlik, Pumping of Concrete Mixtures: Rheology, Lubrication Layer Properties and Pumping Pressure Assessment, Department of Civil Engineering, KANSAS STATE UNIVERSITY, 2018.
[42] T.T. Ngo, E.H. Kadri, R. Bennacer, F. Cussigh, Use of tribometer to estimate interface friction and concrete boundary layer composition during the fluid concrete pumping, Construct. Build. Mater. 24 (7) (2010) 1253–1261.
[43] S. Smeplass, Moisture in light weight aggregates - practical consequences for the production properties of light weight aggregate concrete, in: S. Helland, I. Holand, S. Smeplass (Eds.), Second International Conference on Structural Lightweight Aggregate Concrete, Norwegian Concrete Association, Kristiansand, Norway, 2000, pp. 844–854.
[44] DIN EN 13670, Ausführung von Tragwerken aus Beton (Execution of concrete structures), Beuth-Verlag, Berlin, Germany, 2011, p. 74.
[45] K.-C. Thienel, Application of lightweight concrete, in: J.A. Øverli, J. Zivkovic (Eds.), Nordic Mini-Seminar: Structural Lightweight Aggregate Concrete, Nordic Concrete Federation, Trondheim, Norway, 2019, pp. 6–9.
[46] G. Norden, K.-C. Thienel, Pumping of lightweight aggregate concrete based on expanded clay in Europe, in: S. Helland, I. Holand, S. Smeplass (Eds.), Second International Conference on Structural Lightweight Aggregate Concrete, Norwegian Concrete Association, Kristiansand, Norway, 2000, pp. 823–832.
[47] S. Chandra, L. Berntsson, Lightweight Aggregate Concrete, first ed., Noyes Publications, Norwich, 2002.
[48] ACI Committee 213, ACI 213R-14 Guide for Structural Lightweight-Aggregate Concrete, American Concrete Institute, Farmington Hills, MI, 2014, p. 53.
[49] M. Haist, V. Mechtcherine, H. Beitzel, H.S. Müller, Retrofitting of building structures using pumpable self-compacting lightweight concrete, in: O. Wallevik, I. Nielsson (Eds.), International RILEM Symposium on Self-Compacting Concrete, 2003, pp. 776–785.
[50] M. Schlaich, A. Hückler, C. Lösch, Infraleichtbeton (ILC), in: K. Bergmeister, F. Fingerloos, J.-D. Wörner (Eds.), Beton-Kalender 2021, Ernst & Sohn GmbH & Co. KG, Berlin, Germany, 2021, pp. 909–952.
[51] DIN EN 12664, Wärmetechnisches Verhalten von Baustoffen und Bauprodukten - Bestimmung des Wärmedurchlasswiderstandes nach dem Verfahren mit dem Plattengerät und dem Wärmestrommessplatten-Gerät - Trockene und feuchte Produkte mit mittlerem und niedrigem Wärmedurchlasswiderstand, 2001.
[52] DIN EN 197-1, Zement - Teil 1: Zusammensetzung, Anforderungen und Konformitätskriterien von Normalzement (Cement - Part 1: Composition, specifications and conformity criteria for common cements), Beuth-Verlag, Berlin, Germany, 2011, p. 8.
[53] DIN EN 13263-1, Silikastaub für Beton – Teil 1: Definitionen, Anforderungen und Konformitätskriterien (Silica fume for concrete – Part 1: Definitions, requirements and conformity criteria), Beuth-Verlag, Berlin, Germany, 2009, p. 22.
[54] DIN EN 14889-2, Fasern für Beton - Teil 2: Polymerfasern - Begriffe, Festlegungen und Konformität (Fibres for concrete Polymer fibres. Definitions, specifications and conformity), Beuth Verlag GmbH, Berlin, Germany, 2006, p. 25.
[55] DIN EN 1097-6, Prüfverfahren für mechanische und physikalische Eigenschaften von Gesteinskörnungen - Teil 6: Bestimmung der Rohdichte und der Wasseraufnahme; Tests for mechanical and physical properties of aggregates - Part 6: Determination of particle density and water absorption, 2013, p. 51.
[56] Medienzentrum Universität der Bundeswehr München, Nachhaltiger Baustoff Infraleichtbeton 2.0 – die Zukunft des Bauens?, 2020. https://www.unibw.de/home/news/infraleichtbeton-2-0-die-zukunft-des-bauens. (Accessed 4 April 2022).
[57] DIN EN 12350-8, Prüfung von Frischbeton - Teil 8: Selbstverdichtender Beton – Setzfließversuch (Testing fresh concrete - Part 8: Self-compacting concrete – Slump-flow test), Beuth-Verlag, Berlin, Germany, 2019, p. 8.
[58] DIN EN 12350-4, Prüfung von Frischbeton - Teil 4: Verdichtungsmaß (Testing fresh concrete – Part 4: Degree of compactability), Beuth-Verlag, Berlin, Germany, 2019, p. 10.
[59] DIN EN 12350-7, Prüfung von Frischbeton - Teil 7: Luftgehalte - Druckverfahren (Testing fresh concrete - Part 7: Air content - Pressure methods), Beuth-Verlag, Berlin, Germany, 2019, p. 26.
[60] DIN EN 12350-6, Prüfung von Frischbeton - Teil 6: Frischbetonrohdichte, Beuth-Verlag, Berlin, Germany, 2011, p. 7.
[61] DIN EN 12390-7, Prüfung von Festbeton - Teil 7: Rohdichte von Festbeton + AC: 2020 (Testing hardened concrete – Part 7: Density of hardened concrete), Beuth-Verlag, Berlin, Germany, 2021, p. 14.
[62] DIN EN 1354, Bestimmung der Druckfestigkeit von haufwerksporigem Leichtbeton, Beuth Verlag GmbH, Berlin, GErmany, 2005, p. 18.
[63] DIN EN 1521, Bestimmung der Biegezugfestigkeit von haufwerksporigem Leichtbeton (Determination of flexural strength of lightweight aggregate concrete with open structure), Beuth Verlag GmbH, Berlin, Germany, 1996, p. 7.

[64] DIN EN 1352, Bestimmung des statischen Elastizitätsmoduls unter Druckbeanspruchung von dampfgehärtetem Porenbeton und von haufwerksporigem Leichtbeton, Beuth Verlag GmbH, Berlin, Germany, 1997, p. 7.
[65] DIN EN 992, Bestimmung der Trockenrohdichte von haufwerksporigem Leichtbeton, Beuth Verlag GmbH, Berlin, Germany, 1995, p. 5.
[66] DIN EN ISO 22007-2, Kunststoffe - Bestimmung der Wärmeleitfähigkeit und der Temperaturleitfähigkeit, Teil 2: Transientes Flächenquellenverfahren (Hot-Disk-Verfahren) (ISO 22007-2:2015); Deutsche Fassung EN ISO 22007-2:2015, Beuth Verlag GmbH, Berlin, Germany, 2015.
[67] DIN 1045-2, Tragwerke aus Beton, Stahlbeton und Spannbeton – Teil 2: Beton – Festlegung, Eigenschaften, Herstellung und Konformität – Anwendungsregeln zu DIN EN 206-1 (Concrete, reinforced and prestressed concrete structures – Part 2: Concrete – Specification, properties, production and conformity – Application rules for DIN EN 206-1), Beuth-Verlag, Berlin, Germany, 2008, p. 62.
[68] T. Haller, K.-C. Thienel, Untersuchungsbericht – G2020143 Untersuchungen Am Infra-leichtbeton „ThermoPact“ - Bauwerkskenndaten, Institut für Werkstoffe des Bauwesens, Universität der Bundeswehr München, Neubiberg, 2020, p. 15.

7.3 Optimized Building Envelope: Lightweight Concrete with Integrated Steel Framework

Reprint:

Published in “Materials”

Materials 2024, 17(6), 1278; doi: 10.3390/ma17061278

Authors: T. Haller, N. Beuntner, K.-Ch. Thienel

materials

MDPI

Article

Optimized Building Envelope: Lightweight Concrete with Integrated Steel Framework

Timo Haller, Nancy Beuntner and Karl-Christian Thienel *

Institut für Werkstoffe des Bauwesens, Fakultät für Bauingenieurwesen und Umweltwissenschaften, Universität der Bundeswehr München, Werner-Heisenberg-Weg 39, 85579 Neubiberg, Germany; timo.haller@unibw.de (T.H.); nancy.beuntner@unibw.de (N.B.)
* Correspondence: christian.thienel@unibw.de

Abstract: This study presents a novel construction method for prefabricated wall elements by integrating a framework made of thin-walled sheet steel profiles into an optimized thermally insulating lightweight aggregate concrete (LAC) building envelope. The load-bearing function of the framework is provided by cold-formed Sigma-profiles, which are spot-welded to non-load-bearing U-profiles at the vertical ends. The LAC shapes the wall and stabilizes the thin-walled steel profiles against buckling, but has no further load-bearing function, thus allowing the reduction of its necessary compressive strength and subsequently minimizing its density. As a result, the LAC exhibits strength and density values well beyond existing standards, providing highly competitive thermal conductivity values that meet today's energy requirements without the need for additional insulation materials. Tailored composite specimens verify the stabilization of load-bearing sheet steel profiles by the LAC, which not only prevents buckling but also increases the load-bearing capacity of the overall system. The feasibility of this approach is validated by the production of two prototypes, each comprising a full-sized wall, in two different precast plants using distinct process technologies.

Keywords: lightweight aggregate concrete; building envelope; integrated sheet steel framework; sustained load

check for updates

Citation: Haller, T.; Beuntner, N.; Thienel, K.-C. Optimized Building Envelope: Lightweight Concrete with Integrated Steel Framework. *Materials* **2024**, *17*, 1278. https://doi.org/10.3390/ma17061278

Academic Editors: Paulo Santos, Jong Wan Hu and Seong Tae Yi

Received: 24 January 2024
Revised: 4 March 2024
Accepted: 6 March 2024
Published: 10 March 2024

Copyright: © 2024 by the authors. Licensee MDPI, Basel, Switzerland. This article is an open access article distributed under the terms and conditions of the Creative Commons Attribution (CC BY) license (https://creativecommons.org/licenses/by/4.0/).

1. Introduction

Concrete and steel are the most important structural building materials, which define our built environment in a variety of design forms and therefore shape our modern social lives. Intensive efforts are being made to develop new construction methods to meet increasing ecologically and economically sensitive demands. Therefore, a new prefabricated construction method for wall elements has been developed. The wall element consists of a framework made of thin-walled sheet steel profiles, which is integrated into a heat-insulating lightweight concrete building envelope. The elements can be produced in a precast concrete plant and assembled on site. Figure 1 shows a schematic representation of the new construction method.

The wall element's primary load-bearing function is accomplished by cold-formed steel profiles. These profiles are vertically aligned in a row with defined spacing and connected at the bottom and top by spot welding to non-load-bearing U-channels. The steel profiles form a framework taking into account the subsequent wall design (e.g., technical installations, window openings, and connection elements) before being placed on the molds for concreting. The concreting is carried out with an optimized lightweight aggregate concrete (LAC). The connection of wall elements can be accomplished by means of the profile joints with mortar filling and additional mechanical joints, which are common in prefabricated construction.

The LAC developed within the scope of this work has a dry density of less than 400 kg/m^3 and a corresponding low strength. Both are clearly below the normative limits of EN 1520 [1], but the new LAC still exhibits a great similarity in terms of material

technology. For the purpose of clear differentiation, the LAC developed in the course of this work will be referred to as LAC+ in the following sections.

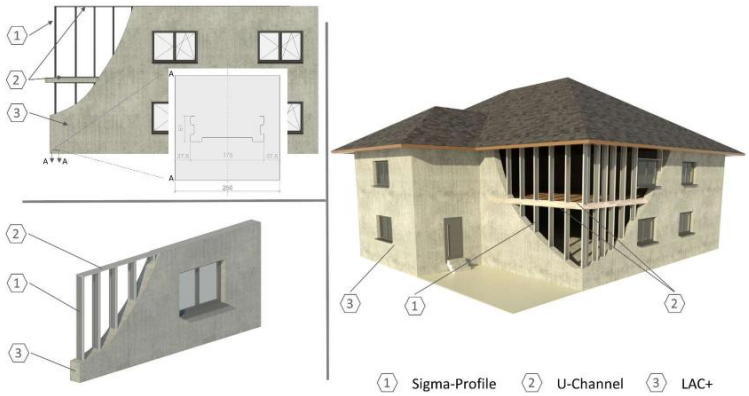

Figure 1. Prefabricated wall construction with sheet steel profile framework in lightweight concrete envelope. (**Top left**) Cross-section with Sigma-Profile. (**Bottom left**) Wall with LAC+ and embedded steel framework. (**Right**) CAD model of the building with new wall elements.

This new approach is designed to utilize LAC+ for its low-density characteristics, which directly influence thermal conductivity. This yields a highly competitive material in terms of energy efficiency, aligning it with increasingly stringent energy-saving regulations in the construction sector. However, as the density decreases, the compressive strength of the LAC+ also decreases. Due to its low compressive strength of around 1 N/mm^2, the LAC+ is unsuitable for traditional load-bearing applications. At this critical point, the sheet steel framework comes into play. It provides the necessary load-bearing capacity of the building envelope, which in turn allows for an intended significant reduction in the required compressive strength of the LAC+. The sheet steel profiles are designed to efficiently utilize the material, resulting in slender profiles, which minimizes their impact on thermal conductivity. When the profiles have significant length (e.g., equal to the wall height), their failure is more likely to occur due to stability issues rather than material failure. In traditional steel construction, lateral bracing, such as cross-bracing, diagonal bracing, or shear walls, can be employed to prevent lateral deflection and ensure stability. In this case, the LAC+ provides this lateral bracing by surrounding the steel profiles and effectively preventing buckling (stability failure), ensuring that the steel profiles offer sufficient load-bearing capacity. This allows us to reduce significantly the required compressive strength of the LAC+ and opens the chance to lower the densities to such an extent that competitive thermal conductivity values unseen for LAC thus far can be achieved for meeting today's energy requirements. The resulting connection between LAC+ and the steel framework must endure, even in the presence of time-dependent deformations, such as shrinkage and creep, or when subjected to sustained loading. This resilience is critical because damage resulting from this deformation has the potential not only to significantly reduce structural stiffness and strength but also to accelerate framework corrosion, thereby significantly impacting the overall durability [2]. The underlying fundamental concept of load transfer and construction methodology is well established for drywall systems, where a metallic framework serves as the primary mechanism for load distribution, while gypsum or wooden oriented strand boards stabilize the framework.

This approach is in line with the increasing stringency of energy saving regulations in the construction sector, which are putting significant pressure on manufacturers of exterior concrete wall elements. These regulations require the achievement of minimum thermal conductivity in order to produce competitive elements for exterior walls. Such

requirements have pushed the application of the material to the limits of its intended use under regulatory conditions. Against this background, the new prefabricated construction method is intended to offer an alternative to satisfy the high market demand for low-cost, fast-to-build, and durable buildings. The low thermal conductivity of the building envelope made of optimized LAC allows for meeting such demands. It is a sustainable solution since it can be separated and recycled easily and completely due to its clear materiality. The new construction method is an innovative solution that optimizes the use of lightweight concrete and steel and combines them in a sustainable way. The benefits of this new wall element design include high thermal insulation, fire resistance, sound insulation, durability, and flexibility. The wall element can be customized to meet different architectural requirements and aesthetic preferences. The prefabrication process reduces labor costs and on-site errors, shortens construction time, and improves safety. The new construction method is suitable for use in multi-story residential buildings as well as industrial or commercial buildings. The construction system could also be used for adding additional floors to buildings. Similar to the currently common construction designs, the low weight ensures comparatively low dead loads of the slabs.

1.1. Background Information on Lightweight Aggregate Concrete (LAC)

The utilization of stationary production methods for concrete components facilitates the standardization and mass production of prefabricated elements, thereby playing a critical role in the industrialization of the construction process [3–5]. The development of standardized elements goes along with the steadily advancing rationalization of the construction process and promises competitive advantages over cast in place concrete construction due to shorter construction times, reduced labor costs, weather-independent production, and high quality assurance [3–5]. Typical applications of the precast construction method in building construction include industrial buildings and warehouses, parking garages, office buildings, hospitals, schools, and multistory residential buildings [3–5]. In structural engineering, precast elements are used in particular when a significant cost advantage can be expected or when the construction conditions at the site cannot be achieved otherwise at a justifiable cost [4]. This applies, for example, to the manufacture of bridges, towers, or masts. Other important product areas include elements for water and wastewater management (e.g., tanks, pipelines, or sewage systems), and elements for traffic infrastructures (e.g., railroad ties, noise barriers, or modular paving) [3–5].

In the course of the 1990s, national standards and regulations were technically revised so that the use of lightweight concrete was standardized on an equal level with normal concrete [6]. Structural lightweight concrete (LC) suitable for reinforced concrete with a closed structure is regulated in EN 1992-1-1 [7] and EN 206 [8]. In addition, lightweight aggregate concrete (LAC) with an open structure for prefabricated reinforced components is covered by EN 1520 [1]. LAC is characterized by voids between aggregates formed by the omission or reduction of individual grain sizes that remain in the structure after compaction. The volume of the cement paste is reduced to such a degree that the aggregates are just pointwise interconnected [9,10]. LAC is produced almost exclusively with coarse lightweight aggregates, which is why the term no-fines is also used synonymously, although low-fines would be more suitable [10]. From the point of view of concrete technology, the structure of the LAC thus differs significantly from that of the dense structural LC. LAC is used to produce wall blocks and load-bearing and insulating wall elements, as well as non-structural components such as noise barriers or drainage concretes [11]. A new market segment opened for LAC wall elements due to the concrete technology available today (e.g., concrete admixtures and agents, as well as the continuous development of manufacturing processes and machine technology), along with the availability of lightweight aggregates (LWA) with particularly low density (e.g., expanded glass). This development allowed for low-density exterior walls to achieve thermal conductivity without the need for additional insulation.

1.2. Research Significance

Despite the widespread use of LAC in various construction applications, the innovative approach lies in its integration with the steel framework to create an energy efficient building envelope. The building envelope requires no additional insulation materials and provides thermal performance that is at least competitive with traditional envelope systems. This unique combination addresses key challenges in the construction industry to reduce energy consumption and improve building performance. This research gap highlights the need to evaluate the potential and suitability of this approach. This study will address the following three key research questions:

1. Feasibility of manufacturing an optimized LAC below the normative limits: A key challenge for manufacturers of precast monolithic walls is to achieve significantly lower thermal conductivity than conventional construction techniques, due to more stringent thermal insulation requirements. The purpose of this question is therefore to examine the feasibility of using a LAC+ with the greatest possible reduction in density and subsequent thermal conductivity while maintaining sufficient strength as a component in a new prefabricated wall system.
2. Assessing the robustness of LAC+ stability across varied conditions: The stability of the LAC+ must be maintained even during time-dependent deformations (e.g., shrinkage and creep) or under continuous loading. In addition, the compatibility of the LAC+ with the conventional compaction techniques used in the precast industry (roller compaction and/or vibratory compaction) should be verified, taking into account the change in consistency caused by the foam and the obstacles created by the steel profiles. This assessment is essential to ensure the quality and structural integrity of the precast elements even under full-scale conditions.
3. LAC+ as structural reinforcement: In this study, LAC+ acts as a critical element in the structural reinforcement, providing lateral bracing to the steel framework. By encasing the steel profiles, LAC+ provides stability and effectively prevents buckling of the integrated steel framework. As a result, a novel testing methodology is used to assess the overall strength and stability of the structure.

To address these research questions, a comprehensive approach was taken. Given the novelty of the LAC+ material technology at the anticipated low density, no previous studies have examined its fundamental material characteristics. Consequently, extrapolating existing standards becomes uncertain. Hence, an experimental investigation was conducted to evaluate the characteristic properties of LAC+. Therefore, three real-scale batches were produced in two precast plants as full-scale trials. Additionally, representative composite specimens were utilized at a smaller scale to demonstrate the capacity of LAC+ in stabilizing the load-bearing sheet steel profiles. Furthermore, prototypes were manufactured as a proof of concept of the potential and suitability of this approach for practical applications. These prototypes consist of full-size wall sections with connection details such as exterior wall joint, transport anchors, and a window opening. The prototypes were manufactured in both partners' precast plants to ensure consistency and reliability.

By implementing this comprehensive approach, this study provides empirical data, practical validation, and prototypes that collectively support the potential application of the new construction method for building envelopes and defines a practical testing methodology to address the unique challenges.

2. Materials and Methods

2.1. Materials

2.1.1. Sheet Steel Profile

In general, different sheet steel profile geometries can be considered for the framework. For the present project, a Sigma-profile was selected as a suitable candidate for the vertical steel profiles of the framework. This profile is commercially available in a wide range of dimensions. A relatively small dimension was chosen to demonstrate suitability in the

lower load range and to limit the required dimensions for the later composite specimens (e.g., concrete cover or required slenderness for buckling). The Sigma profiles are cold-formed symmetrical profiles with parallel flanges and lips. The parallel flanges facilitate easy connection with other elements via welds or bolts, which is particularly useful when used in combination with the U-channel profiles within this project. The lips increase its torsional stiffness and stability. Sigma profiles have high load-bearing capacities and are already used in industrial and non-industrial steel constructions such as warehouses, hangars, and barns [12]. They provide material savings and cost advantages compared to heavy steel profiles due to their low weight, flexibility in the manufacturing process, and easy assembly [12]. They also have good corrosion resistance, which is essential for the present study given the high porosity of the LAC+ used. Additionally, they can be perforated and coated according to the project requirements. Table 1 summarizes the relevant technical parameters for the thin-walled sheet steel profile used.

Table 1. Manufacturer's data for technical parameters of the sheet steel profiles used.

Parameter	Sigma Profile 175/61-1,0
Height [mm]	175
Width [mm]	61
Steel plate thickness [mm]	1.0
Cross-section area [mm^2]	334
Section modulus [mm^3]	18,280
Compressive load capacity [kN]	110
Shear force capacity [kN]	14.2
Bending moment capacity [kNm]	5.9

The profiles are manufactured in accordance with EN 1090-2 [13] in a continuous roll forming process. The raw material of the profiles is a steel strip of grade S320GD according to EN 10346 [14].

2.1.2. LAC+ Raw Material Properties and Mix Design

For the two precast plants involved, the mix design provided in Table 2 was used for the test program. A CEM I 42.5 R (precast plant 1) and a CEM I 52.5 R (precast plant 2) serve as binders. As LWA, expanded clay (Liapor F2.9 E) manufactured by Liapor GmbH & Co. KG (Hallerndorf-Pautzfeld, Germany) and expanded glass (Liaver 2–4 mm) manufactured by Liaver GmbH & Co KG (Ilmenau, Germany) are used in conforming with EN 13055-1 [15], and their physical properties are summarize in Table 3.

Table 2. Mix design composition of the LAC+ for the two precast plants for large-format production.

Material	Precast Plant 1 (Series 2 and 3)		Precast Plant 2 (Series 1)	
	Amount [kg]	Volume [dm^3]	Amount [kg]	Volume [dm^3]
Cement	120 kg	39	120	39
Water	96	96	85	85
Liapor F2.9 E (4/10 mm)	216	920	124	394
Liaver (2/4 mm)	21	109	126	642
Foam	10.8	197	8.65	350
Stabilizer (Sika [1] ST 3)	2	1.9	-	
Accelerator (Daraset [2] 304)	4	1.4	-	

[1] Manufactured by Sika Deutschland GmbH (Stuttgart, Germany). [2] Manufactured by GCP Applied Technologies (Cambridge, MA, USA).

Table 3. Physical properties of the LWA used.

Aggregate Type	Shape	Crushing Resistance [1] [N/mm^2]	Particle Density [1] [kg/m^3]	Water Absorption [1] [wt.-%]
Liaver 2-4	Rounded	1.4	550	11.8
Liapor F2.9 E	Rounded	2.2	342	20.7

[1] Manufacturers data.

In the first step of the mixing process, the LWA is mixed with the specified amount of saturation water and part of the required mixing water. After pre-mixing, the binder, the powdered admixtures, and the additives are added. After a brief homogenization of the components, the remaining mixing water is added. When adding liquid admixtures, care must be taken to ensure that dry LWA in particular does not absorb the admixtures, which would result in reduced effectiveness of the admixtures. Liquid admixtures should therefore be added as the last component. Alternatively, they should be mixed with the remaining mixing water beforehand. After all components have been added, the minimum mixing time should be at least 60 s, depending on the mixing intensity, in order to obtain a uniformly mixed fresh concrete. Finally, the foam is added and mixed for a short period of about 30 s. The mixing process is summarized in Table 4. The mixing process described is an established method for producing lightweight concrete. While there may be different approaches that give similar results, the suitability of each method depends on specific conditions such as the capabilities of the production plant or the saturation options for LWA. For more general information on the production of lightweight concrete, refs. [9,11,16] provide additional insight.

Table 4. Mixing process of LAC+.

Step	Approx. Mixing Time [s]
Mixing of LWA with half of the water	60
Addition of cement and additives	90
Addition of remaining mixing water	60
Addition of foam	30

2.1.3. Manufacturing Process and Porosification

Both precast producers use compulsory mixers with additional agitators to homogenize the fresh concrete. At precast manufacturer 1, the LWA is stored in open boxes and exposed to the weather in the outdoor area of the plant, while at precast manufacturer 2, the LWA is stored in covered silos. Irrespective of the storage situation, both manufacturers must take into account the water absorption of the LWA in their mix design. Another difference between the two manufacturers is the compaction method of the fresh concrete. Whereas precast manufacturer 2 uses vibrating roller compacting, precast manufacturer 1 uses the vibrating or shaking technique for compacting the elements. The compaction technique installed is decisive to the extent of the porosification process of the cement matrix.

Based on preliminary tests on a laboratory scale, various LAC+ formulations were developed and further optimized for the respective production-specific boundary conditions. Balancing the trade-offs between density, strength, and thermal conductivity in LAC+ involved a systematic process of mix design optimization. The first step was to establish a minimum compressive strength requirement of approximately 1 N/mm^2 to ensure sample stability during curing, as this strength threshold was considered sufficient for safe handling and processing within the context of the project and the capabilities of the manufacturers. Once this critical strength parameter was established, the focus shifted to reducing the density of the concrete. The primary approach used was to porosify the binder paste, which significantly improved the thermal insulation properties of LAC+. The exceptionally low density of LAC+ is achieved by introducing fine pores into the binder

paste. The fine pores are created with a foam generator using air, water, and foaming agents. Foam is generated by applying air pressure to a mixture of foaming agent and water in the foam generator. The control of the applied pressure of air and water, as well as the dosage of the foaming agent, defines the properties of the foam produced. The pore structure itself, as well as the shape and distribution of the air bubbles within, significantly determines the properties obtained. In accordance with the desired performance of the concrete, varying proportions and different LWA types were used. In order to achieve the desired material properties, it was first necessary to find a suitable ratio between water and cement, as well as between foam, cement paste, and LWA. This optimization process was carried out to meet stringent energy efficient construction standards whilst ensuring structural stability, resulting in a refined mix design that sets a new standard for competitive lightweight aggregate concrete solutions.

An impression of the manufacturing procedures in the precast plant is given in Figure 2. On the top left side, the framework of steel profiles can be seen, which is rotated later by 90° and placed in a test mold (Figure 2, top right). The interruption of the sigma profile in the middle part serves as a breakthrough and represents a window opening in the later wall system. The adaptation of the framework can be carried out at this point with the same U-profiles used in the framework for the upper and lower closure of the Sigma-profiles.

Figure 2. Manufacturing process of prototype at precast plant. (**Top left**) framework of steel profiles, rotated by 90°; (**Top right**) Partial filling of the formwork with LAC+; (**Bottom**) Filling and compacting of the wall element.

2.2. Experimental Program

Samples for three more comprehensive test series were produced in the precast plants to characterize the LAC+, as well as the construction system. First, two test series (Series 1 and 2) were produced in each precast plant. Based on the results of the first two series of tests, another series of test specimens (Series 3) was fabricated. Cores were drilled from

elements for each series of tests in order to characterize the LAC+ as defined in [1]. The cores have a diameter of 150 mm and a height of 300 mm. They were cut to length and ground plane-parallel before the respective tests.

2.2.1. Mechanical Properties

The compressive strength of LAC+ was determined after 28 days on drill cores (h/d = 300/150 mm) according to EN 1354 [17]. The modulus of elasticity was determined according to EN 1352 [18] on drill cores (h/d = 300/150 mm) after 28 days.

2.2.2. Shrinkage and Creep

Shrinkage and creep deformations were determined on drill cores according to DAfStb booklet 422 [19] in a climate chamber at 20 °C and 65% rel. humidity. For measuring the shrinkage deformation, displacement gauges were attached to three drill cores at a distance of 200 mm on opposite sides and the changes in length were measured at fixed times up to an age of 460 days.

Three drill cores were loaded with a constant creep stress and the deformation measured and recorded for each core using three displacement gauges. The applied creep stress is one third of the average compressive strength after 28 days. The measurements of shrinkage and creep were started at a concrete age of 30 days. The average total deformation of the cores was recorded at specified times up to an age of 460 days.

2.2.3. Dry Density and Thermal Conductivity

The dry density was determined according to EN 992 [20]. Thermal conductivity was measured by means of the transient plane source method (Hot Disk TPS 2200, Gothenburg, Sweden) according to EN ISO 22007-2 [21]. Prior to measurement, the samples were dried to constant mass at 105 °C and then cooled to a temperature of 23 °C. During cooling, the samples were kept in an airtight container filled with silica gel to ensure dry conditions. The thermal conductivity was determined on three different specimens and on different specimen sides in each case.

2.2.4. Coefficient for Long-Term Effects on Compressive Strength

From a practical construction point of view, concrete is subjected to compressive and tensile forces in various structural applications, which can take the form of monotonic, cyclic, or sustained loading [22–25]. Failure of normal concrete is initiated by structural changes in the microstructure, such as cracking [24–28]. However, the characteristics of these structural changes depend on a variety of boundary conditions such as loading rate, water content of the concrete, specimen geometry, or type and direction of loading [25]. Knowledge of the stress-strain relationship and fracture mechanisms is crucial for predicting the behavior of concrete under different loading conditions [22,24–29]. While Rüsch [26,27] carried out important groundwork more than 60 years ago, extensive research has since led to the development of numerous models aimed at predicting stress–strain relationships and also failure states of concrete due to long-term effects. One topic in this context is the study of concrete under sustained loading. In such cases, a critical threshold can be defined as the ratio of the applied compressive stress over a given time period to the reference compressive strength. Once a critical threshold is exceeded, stress-induced structural changes lead to unstable damage progression [23,25–27,30]. A large number of research projects have attempted to establish a relationship between stress level thresholds, age under load, and duration of exposure, using different experimental programs. A comprehensive review of the different considerations and methodologies is provided by [23], where the authors compared six different scientific studies and programs in terms of reference strength, observed threshold, age of testing, duration of testing, and failure under sustained loading. In addition, they proposed a new method for predicting the failure of concrete under different long-term loading patterns based on the results of their

experimental program. Another good review of the different experimental programs with respect to different types of concrete can be found in [25].

Although it has not been possible to derive a uniform experimental program nor a fixed limit, values between 0.70 and 0.90 have generally been determined for the critical stress level thresholds. Building codes, such as Eurocode 2 [7] and Model Code 2010 [31], address this issue through reduction coefficients. For structural lightweight concrete, this reduction coefficient α_{cc} is given in the National Annex (Germany) of Eurocode 2 [7] as 0.85. DIN EN 1520 [1] also recommends a reduction factor of 0.85 for LAC.

It is essential to note that the LAC+ investigated in this project possesses properties that lie outside the scope of these standards, necessitating the demonstration of the validity of these material–technological correlations. Since long-term experimental testing was impractical due to the extended testing duration, a short-term testing method was employed.

Specifically, drill cores were first stored in a standard climate (20 °C, 65% rel. humidity) until an equilibrium moisture content was reached. At 91 days of concrete age, the conditioned test specimens were loaded at a low loading rate (1 N/s) until fracture, meaning that the test specimens were subjected to a steadily increasing continuous load over a duration of approximately 6–7 h per specimen. During the test, inductive displacement transducers in the load direction recorded the deformation. The coefficient for long-term effects on compressive strength is determined by the quotient of the ultimate load achieved in the test and the average compressive strength of the drill core. The tests were carried out representatively for the LAC+ on six cores of Series 3. The test methodology is known from the literature and has been used, for example, to evaluate the sustained load of aerated concrete and normal concrete [24,25]. A similar test program was also carried out on infra-lightweight concrete [32,33], which has some similarities to LAC+ in terms of material technology.

2.2.5. Trials on Composite Specimens

Small-scale composite specimens were designed and fabricated to investigate and demonstrate the stabilizing effect of the LAC+ on the steel sheet profiles in a compression test. The compressive load capacity of the composite specimens is compared with the test results of identical plain steel sheet profiles in a further step.

The vertical sigma profiles are decisive in this context. Due to the slender profile geometry, these profiles can buckle if a certain length is exceeded before the maximum permissible compressive stress of the material is reached. This buckling can be observed already for the specimen lengths tested here. Thus, the vertical sigma profiles need stabilization. The U-profiles at the upper and lower ends are mainly used for load transfer and for easier fixing in the formwork. The composite specimens have a height of 580 mm and a cross-section of approximately 250 × 250 mm^2, which corresponds to a concrete cover of 37.5 mm on the wide side of the Sigma-profile. The sheet steel frames were fixed in specially manufactured formwork and concreted with LAC+ (Series 3) at the precast manufacturer.

3. Results and Discussion

3.1. Hardened Concrete Properties

In general, the optimum compromise between density, strength, and thermal conductivity is at the forefront of LAC+ mix design. Based on the preliminary laboratory tests, the desired material properties are achieved through the systematic use of chemical additives and admixtures, together with adjustments to the material composition and manufacturing process. As the complexity and performance of the material increases, so does the sensitivity of the material's behavior. The type and content of the cement and aggregates, the characteristics of the cementitious foam, the type and concentration of the additives and admixtures, and the timing of their addition have been identified as the main influencing factors. Based on results of initial trials, three larger test series were produced in the precast

plants. Table 5 provides the parameters of the LAC+ for the test series produced in the two precast plants.

Table 5. Overview of the mechanical parameters for three test series of the optimized LAC+.

Parameter	Series 1 (Precast Plant 2)	Series 2 (Precast Plant 1)	Series 3 (Precast Plant 1)
Dry density [kg/m^3]	400	407	358
Thermal conductivity [W/(m·K)]	0.118	0.121	0.092
Mean compressive strength [N/mm^2]	1.12	1.11	1.23
Characteristic compressive strength [1] [N/mm^2]	0.93	0.86	1.15
Modulus of elasticity [N/mm^2]	969	1046	878
Coefficient for long-term effects on compressive strength [-]	-	-	0.81
Shrinkage [2] [mm/m]	-	−0.62	-
Creep [2] [mm/m]	-	−0.96	-

[1] According to EN 1520 [1]. [2] Measurement started 30 days after concreting.

Figure 3 illustrates the relationship between the compressive strength and dry density of the three test series.

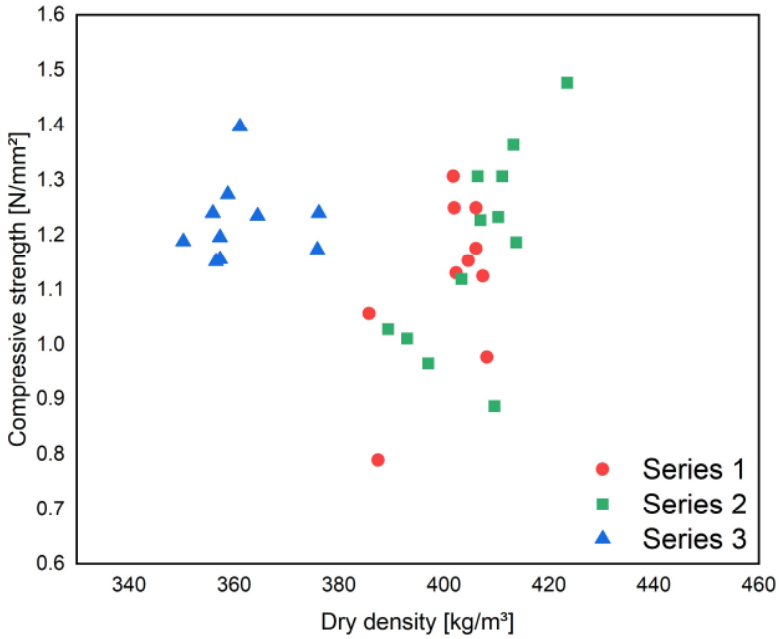

Figure 3. Compressive strength after 28 days for test Series 1, 2, and 3 as a function of the dry density.

The dry densities achieved were around 400 kg/m^3 for the first two test series. The scatter of strength values was significant, reflecting the challenges faced by the precast

plants mentioned earlier. By further optimizing the manufacturing process, the dry density was reduced to 360 kg/m^3 in test Series 3. The variations in dry density are relatively small for all series. The difference between the heaviest and lightest sample is 34, 58, and 22 kg/m^3 for Series 1, 2, and 3, respectively. This fact indicates that the mix design can produce homogeneous and stable concrete even on a factory scale. This was accomplished for the strength values in Series 3 as well. Based on the preliminary laboratory tests, this was initially one of the major uncertainties in mix design.

This uncertainty is due, on the one hand, to the specific nature of the LAC mix design and, on the other hand, to the degree of porosification of the paste between the LWA. With regard to the specific nature of LAC, it should be noted that the optimum water/binder ratio is only within a narrow range. Depending on the chosen LWA composition, a too high water to binder ratio will result in the cement paste draining from the surface of the LWA during compaction, while a too low water to binder ratio may result in adhesive agglomeration of the LWA [9]. With regard to the porosification of the paste between the LWA, it is essential that the foam maintains its quality and quantity in a stable manner. The additives used to produce the foam are usually very sensitive to variations in dosage, temperature, and mixing time. This becomes obvious, for example, in the pore structure of the artificial air pores. Other studies have shown that as the density of the foam decreases and mixing time increases, larger pore diameters are formed which tend to collapse during compaction [10] or result in reduced compressive strength of the hardened concrete [34]. Another special consideration when porosifying the paste is that only the voids between the LWA are filled. While too little foam will only result in inadequate filling of the voids between the LWA, too much foam would cause the LWA to simply float in the foam, and the load transfer along the LWA, which is characteristic of LAC, would no longer be ensured. This effect can be seen in Figure 4. While the left cross-section shows only partial porosification of the matrix (structure very close to conventional no-fines LAC), the right cross-section shows a correct and complete porosification of the paste filling the voids between the LWA.

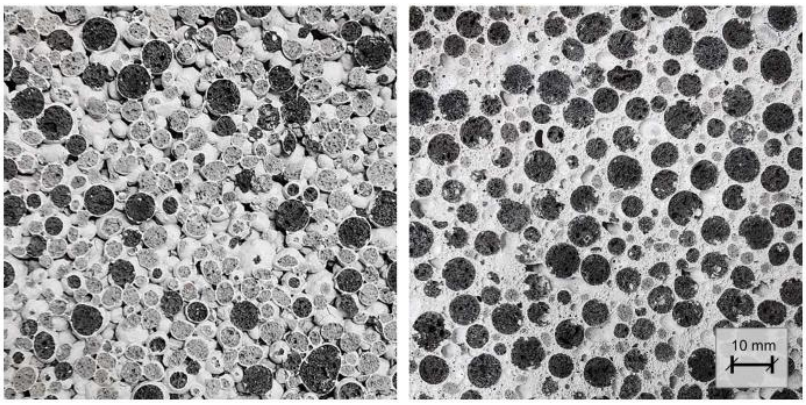

Figure 4. Series 3 (**right**) demonstrates significantly higher porosity compared to Series 2 (**left**), while Series 2 closely resembles typical lightweight aggregate concrete (LAC) in terms of its open-pore structure.

This fine tuning of the porosification determines the density, which is directly linked to the thermal conductivity, as well as the compressive strength of the LAC+, and thus the structural design of the components. In this context, a significant goal of the optimization of the LAC+ is achieving the lowest possible density and thus thermal conductivity. However, a reduction in these parameters is accompanied by a reduction in compressive strength. Further, the strength of the LAC+ must be sufficient to adequately stabilize the steel

sections of the structure. A detailed overview of the compressive strength achieved for the optimized test series produced in the precast plants can be found in Figure 5.

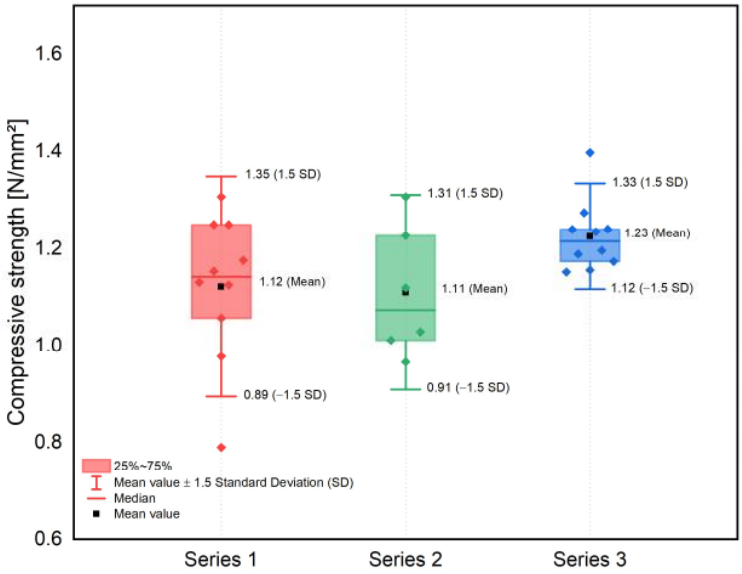

Figure 5. Compressive strength after 28 days of the LAC+ series with consideration of the statistical variations.

The test results yield a compressive strength of the LAC+ of approx. 1.1 N/mm^2. Furthermore, the statistical indicators for the quality control of concrete production were found to lie within the usual scatter range for LAC and confirm the previously formulated assumption of successful adjustment of the porosification of the paste between the aggregates. Series 3 exhibits a slightly higher compressive strength although its dry density is approximately 40 kg/m^3 lower than the other series. Series 3 is an improvement of Series 1 and the higher compressive strength is probably due to a better match between foam and fresh concrete in the mix design (cf. Figure 5) and training of the personnel involved in the precast plant.

The porosification and volume of the hardened cement paste also affect the modulus of elasticity. According to the standard (DIN EN 1520 [1]), the modulus of elasticity can be estimated empirically from the dry density and characteristic compressive strength. For the present test series 1, 2, and 3, the estimated moduli of elasticity are 1016 N/mm^2, 1106 N/mm^2, and 1240 N/mm^2, respectively. The experimentally determined moduli of elasticity (cf. Table 3) are consistently lower than the estimated values. This discrepancy can be attributed, in part, to the porosity of the hardened cement paste, as the reduced stiffness of the cement paste can lead to decreased resistance to deformation. It is important to consider the significant variability in the stiffness of different LWAs as well. In this context, it should be noted that the normative and empirical determination of the modulus of elasticity applies to all LWA approved by this standard. Therefore, the estimation reflects an average relationship and does not account for the specific characteristics of individual LWAs.

3.2. Compressive Strength Capacity under Sustained Loading

Strength under sustained compressive loading is an important parameter for the design and performance of LAC+. It reflects the ability of the material to resist defor-

mation and prevent cracking under long-term service conditions. In general, the compressive strength capacity under sustained loading can be understood as an elementary microstructural threshold above which irreversible and unstable damage progression must be expected. For safe material utilization and saving of resources, a realistic coefficient for long-term effects on compressive strength must therefore be determined for the LAC+.

Figure 6 illustrates the variation in mean relative load capacity, defined as the ratio of the sustained compressive strength to the average compressive strength at 28 days, with respect to longitudinal deformations. The corresponding individual stress–strain curves are provided individually on the left.

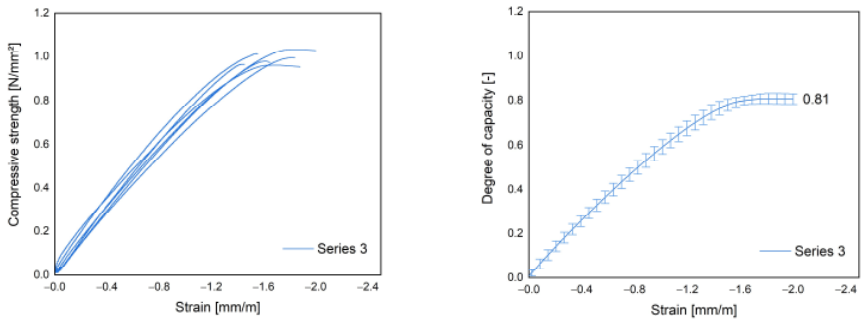

Figure 6. (**Right**) Relative load capacity ($\sigma_{sustained}/\sigma_{28days}$) of the compressive strength under sustained loading. (**Left**) Corresponding stress–strain curves for test Series 3 under sustained loading.

The experimentally determined threshold for sustained loading is 81% for test series 3. This value is comparable to the known α_{cc} for long-term effects on compressive strength for lightweight concrete (according to Eurocode 2: 85% [7], cf. Section 2.2.4) and the one for LAC (85%) according to the DIN EN 1520 [1]. The normative and generalized determination of the reduction factor α_{cc} would overestimate the long-term performance of LAC+. This is confirmed by research conducted by Empelmann [35], who concluded that α_{cc} does not always provide conservative results. Furthermore, the relationship between longitudinal deformation and applied stress is very similar in the lower stress range and only deviates more strongly at higher compressive stresses. This behavior is known from concretes and speaks for a homogeneous load transfer of the optimized LAC+.

3.3. Shrinkage and Creep of the LAC+

Time-dependent deformations can occur due to load-independent processes such as shrinkage or load-dependent processes such as creep [36]. Minimizing the deformations of the LAC+ is essential to minimize cracking, to restrain stresses, and to ensure a permanent bond between the LAC+ and the steel framework. Unlike normal concrete, the time-dependent deformations of LAC+ are largely determined by the aggregate used, although they do not show time-dependent behavior themselves [37]. The main influencing parameters of the LWA are their low density and the associated modulus of elasticity as well as their porosity and stage of water saturation. There is not a wide range of published empirical values for the deformation properties of LAC with a porosified matrix, especially for the present density ranges. Thienel [10] found that the shrinkage values of a LAC without fines and a properly manufactured LAC with a porosified matrix are similar, and at a density of 600 kg/m^3 are approximately 0.6 mm/m. Thienel [10] also observed that a LAC with a porous matrix exhibited higher specific creep values as compared to a conventional LAC. However, the risk of shrinkage cracking was reduced due to the high relaxation potential of the LAC. DIN EN 1520 [1] suggests using 0.75 mm/m for drying shrinkage in an environment with 45 $\pm$ 5% rel. humidity. Figure 7 shows the shrinkage and creep deformation curves for test Series 2 over time.

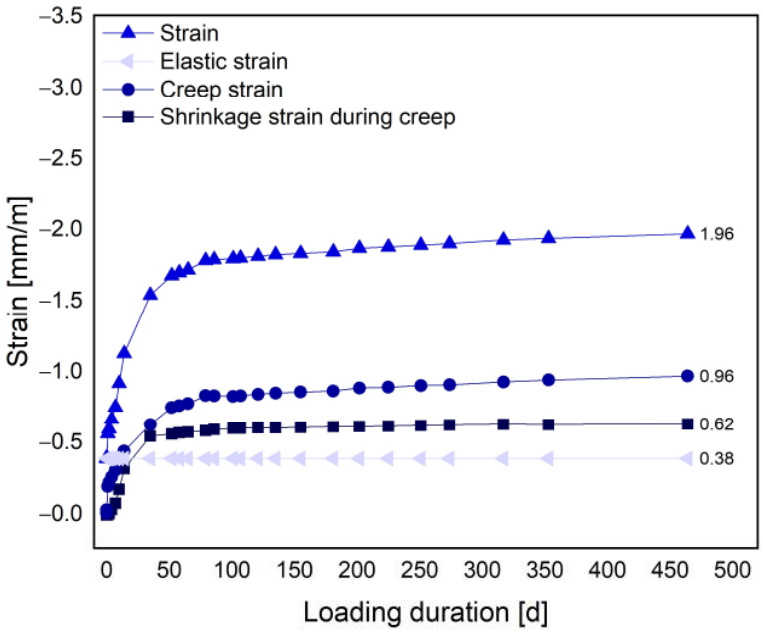

Figure 7. Strains during shrinkage and creep for test Series 2.

The shrinkage deformation curves in Figure 7 are comparable with normal LAC. The results determined within the scope of the present tests are thus within the expected results. However, it must be noted in this comparison that the age of removal differs from the one set in [38]. In relation to the residual stress resulting from shrinkage deformation in precast concrete elements, it should also be noted that a significant portion of the deformation can be alleviated during the curing process in the precast plant and thus before installation on site.

3.4. Trials on Composite Specimens

The composite specimens consist of a sheet steel framework embedded in the LAC+. The successful integration of the sheet steel framework into the LAC+ is critical to the overall development of the wall component. The framework of sheet steel profiles fulfils the load-bearing tasks of the component in the wall. The surrounding LAC+ prevents buckling of the steel profiles and thus yields sufficient load-bearing capacity. As there are no standardized test procedures for this new precast construction method, an individual test program was developed for the composite components (cf. Chapter 2.3). For this purpose, the load-bearing behavior of a plain steel profile is compared with that of an identical steel profile embedded in the LAC+. Figure 8 shows the specimens in comparison. The left half shows the plain steel profile, while the right half shows the composite specimen. The buckling failure of the plain steel frame is obvious. In contrast, the embedded steel frame exhibits no such deformation. Here, the failure was caused by spalling of the LAC+ which subsequently destabilized the steel frame and led to failure. The upper half of the photos shows the specimens before the test, while the lower half shows the specimens after the test.

Figure 8. Comparison of test specimens for the composite system. On the left: plain steel profiles connected to horizontal U-profiles at the top and bottom by spot welding. On the right: identical steel profiles embedded in the LAC+. Compression tests for sheet steel profiles (**left**) versus composite specimens (**right**) before (**top**) and after (**bottom**) the test.

In Figure 9, the results of the compression tests are summarized for the plain steel frames in a Box–Whisker diagram on the left side, while the corresponding load-displacement diagrams are shown on the right side.

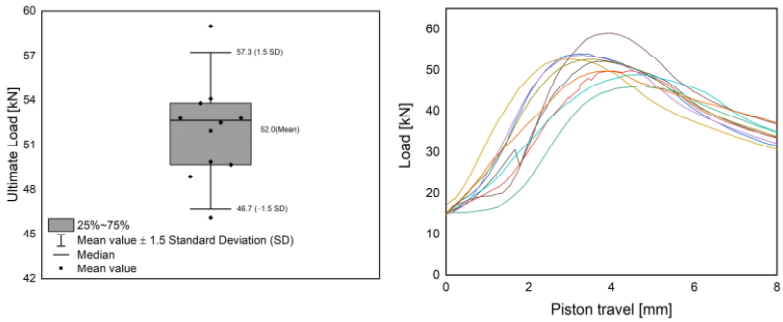

Figure 9. Box–Whisker diagram for compression test of sheet steel profile (**left**) with corresponding load-displacement diagrams (**right**).

The results of the compression tests on the sheet steel profiles confirm that the designed specimen type is suitable for the chosen test setup. The results in the compression test are reproducible and show only minor deviations from the mean value. The average ultimate load of the plain steel profiles is 52 kN and thus well below the value that can theoretically be achieved by material failure. Otherwise, buckling values of around 110 kN would have been expected (cf. Table 1). Thus, the test setup successfully triggers a stability failure of the profile. Figure 10 exhibits the results of the compression tests for the composite specimens.

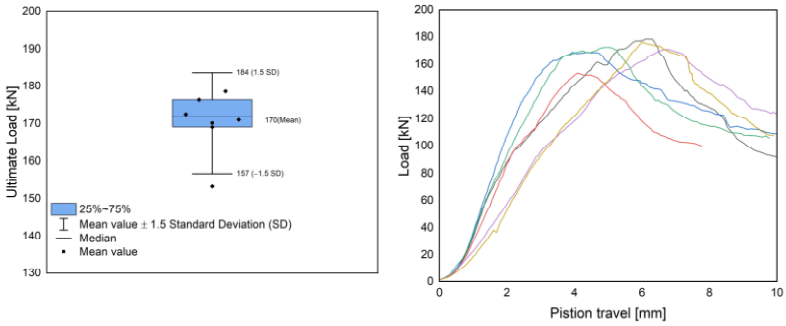

Figure 10. Box–Whisker diagram for compression test of composite specimens with LAC+ from Series 3 (**left**) with corresponding load-displacement diagrams (**right**).

The results of the experimental investigation show that the use of LAC+ as an embedding material for steel sheet profiles can significantly improve their load-bearing capacity. The composite specimens exhibited an ultimate load of 170 kN, which is more than three times that of the plain steel sheet profile (52 kN) and more than 50% higher than the maximum compressive load capacity specified by the manufacturer (110 kN, cf. Table 1). This indicates that the bond between the sheet steel profile and the LAC+ was effective in transferring the load from the sheet steel profile to the concrete section and preventing stability failure due to buckling. However, it should be noted that these results are based on a limited data set and do not allow for generalization or the derivation of design formulae to calculate the compressive capacity of composite specimens with different concrete qualities, profile geometries and types, and concrete coverings. Further research is needed to investigate these variables and to extend the test program to include strength tests on mock-up walls, which would better reflect the actual behavior of composite elements in structural applications. A possible reference for such a test program could be DIN EN 1520 Annex B (design of components based on tests) [1] or ASTM E72 [39], which provides standard methods for conducting strength tests on structural panels.

3.5. Implementing Laboratory Findings in Production: Demonstrator

In general, there are significant challenges in ensuring the applicability of laboratory tests to full-scale production in manufacturering plants. One notable difference is the controlled environment of laboratories, with optimum humidity and temperature conditions, and calibrated and more precisely controllable instruments (e.g., mixing energy and time). However, when testing on a larger scale, such as in production plants, there are unique considerations for lightweight concrete. These may include the need for specialized equipment, such as foam generators, to accommodate complex mix designs. In addition, factors such as saturation of LWA, which can be controlled precisely in the laboratory, need to be taken into account, whereas in concrete plants with open storage and weathering, greater variations are to be expected. In addition, the development of heat of hydration becomes more of an issue with larger samples, such as wall elements, where heat dissipation is less efficient compared to smaller laboratory samples.

In the context of the research presented, there are also a number of considerations that need to be taken into account when handling the samples, given the exceptionally low strength of the concrete. The performance of a structural component is influenced by various factors, including the composite effect between the LAC+ and the steel framework. However, the transfer of shear forces, as well as the introduction of local compressive and tensile forces, are crucial for the overall performance of the component. To introduce these local loads into the construction system, connection and anchorage elements are used. During the transportation, lifting, and assemblage of individual precast elements,

there is a risk of introducing large and variable loads into the component. Hence, careful consideration must be given to the design and implementation of these elements to ensure the safe and efficient functioning of the component. The implementation and handling of the adapted connecting elements was tested exemplarily on the prototypes. Figure 11 gives an impression.

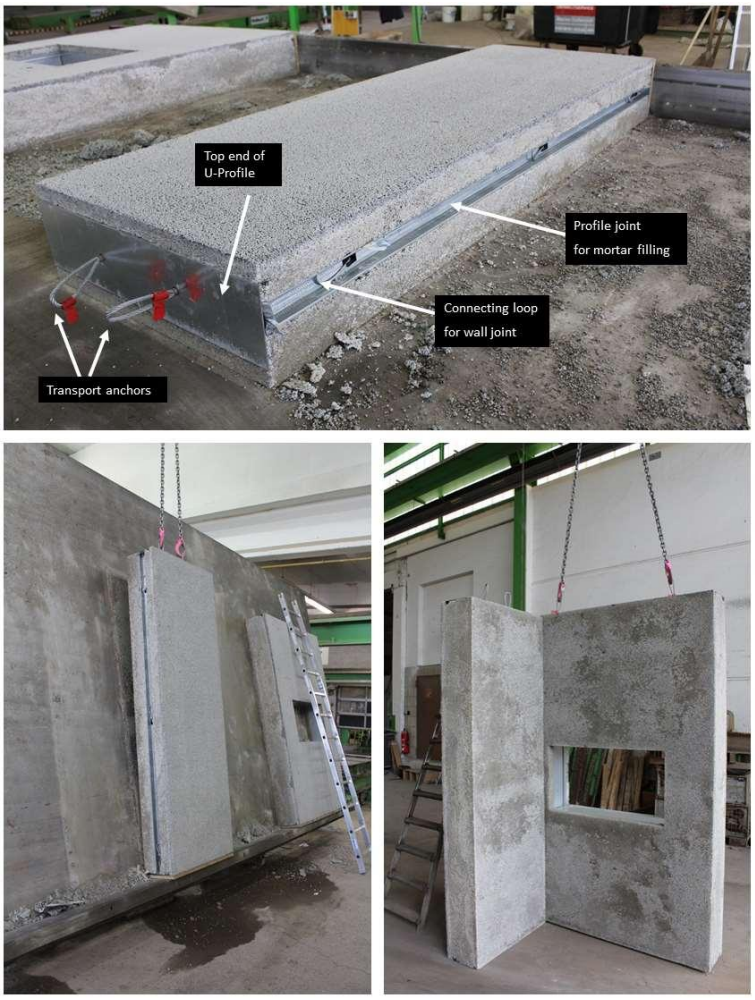

Figure 11. Connecting and anchoring elements for transporting, lifting, and connecting the individual precast elements.

The feasibility of the proposed new construction method, through the successful translation of laboratory findings into production, offers an efficient use of building materials with improved energy efficiency in the building environment, striving towards sustainable building practices. As a result, the proposed building envelope does not require additional insulation materials and provides thermal performance that is at least competitive with traditional envelope systems.

4. Conclusions

This study aimed at presenting a novel construction method for prefabricated wall elements, in which a filigree steel framework takes over the load-bearing function, and a tailor-made LAC provides thermal insulation and stability. To accomplish this, the properties of LAC were optimized, with the objective of achieving the lowest possible density and thermal conductivity while maintaining sufficient strength to prevent framework stability failure. The optimized LAC+ was intended to create a building envelope that complies with current energy regulations without requiring additional insulation. The successful development of the novel construction method was validated in cooperation with two precast plants, demonstrating the transfer of laboratory findings to the real scale. The main findings can be summarized as follows:

1. The mechanical properties of the potential LAC+ candidates were fundamentally characterized on the basis of three extensive real-scale batches. A notable result of this characterization was the remarkable reduction in compressive strength to as low as 1.1 N/mm^2. This reduction in compressive strength created a pathway for density reduction, ultimately achieving densities as low as 360 kg/m^3. This in turn led to the achievement of competitive thermal conductivity values as low as 0.09 W/(m·K). The porosification of the matrix between the LWA grains plays a special role in the successful transition from laboratory to real scale.
2. Short-term tests with a low loading rate revealed a reduction coefficient of 0.81 to account for the reduced compressive strength of the LAC+ under sustained loading. This result is comparable to the factor 0.85 proposed for LAC in DIN EN 1520 [1].
3. Composite specimens, which represent a wall section with a vertical sheet steel profile embedded in the LAC+, were tested to demonstrate the ability of the LAC+ to stabilize thin-walled sections against buckling. The mechanical performance of the framework was significantly increased with the use of LAC+.
4. Based on the obtained mechanical properties of the LAC+ and the composite tests, two prototypes were produced in precast plants of project partners. The design of the prototypes represents wall sections in original size and takes into account a connection detail (outer wall joint) and anchors (transport anchors), as well as a window opening. The experimental tests have thus been successfully transferred to the real scale.

For developing a comprehensive design concept for wall elements, it is necessary to conduct further tests that consider various profile types and cross-section geometries. Additionally, it is important to perform tests with various concrete covers and on the effective cross-section of the LAC+ within the wall element. These tests will provide insights into the behavior of the proposed construction method under different conditions and will support the development of an optimized design approach that meets the required performance criteria.

Author Contributions: Conceptualization, T.H. and K.-C.T.; methodology, T.H. and K.-C.T.; software, T.H.; validation, T.H., N.B. and K.-C.T.; formal analysis, T.H. and K.-C.T.; investigation, T.H. and K.-C.T.; resources, N.B. and K.-C.T.; data curation, T.H. and N.B.; writing—original draft preparation, T.H.; writing—review and editing, T.H., N.B. and K.-C.T.; visualization, T.H.; supervision, N.B. and K.-C.T.; project administration, T.H. and N.B.; funding acquisition, N.B. and K.-C.T. All authors have read and agreed to the published version of the manuscript.

Funding: This research was funded by the German Federal Ministry for Economic Affairs and Climate Action through the ZIM program (Zentrales Innovationsprogramm Mittelstand, project number ZF4416002HF8).

Institutional Review Board Statement: Not applicable.

Informed Consent Statement: Not applicable.

Data Availability Statement: Data are contained within the article.

Acknowledgments: The authors express their gratitude to their project partners at the Institut für Werkstoffe im Bauwesen, TU Darmstadt for their fruitful cooperation, and the two precast plants, Fensterle Beton- und Fertigteilwerk GmbH and Franz Carl Nüdling Basaltwerke GmbH + Co. KG, for their help, support, and engagement in producing the elements.

Conflicts of Interest: The authors declare no conflicts of interest. The authors declare that this study received funding from Fensterle Beton- und Fertigteilwerk GmbH and Franz Carl Nüdling Basaltwerke GmbH + Co. KG. The funders had no role in the design of this study, in the collection, analyses, or interpretation of data, in the writing of the manuscript, or in the decision to publish the results.

References

1. *DIN EN 1520*; Vorgefertigte Bauteile aus Haufwerksporigem Leichtbeton und mit Statisch Anrechenbarer Oder Nicht Anrechenbarer Bewehrung (Prefabricated Reinforced Components of Lightweight Aggregate Concrete with Open Structure with Structural and Non-Structural Reinforcement). Beuth Verlag GmbH: Berlin, Germany, 2011; p. 119.
2. Li, D.; Nie, J.-H.; Wang, H.; Yan, J.-B.; Hu, C.-X.; Shen, P. Damage location, quantification and characterization of steel-concrete composite beams using acoustic emission. *Eng. Struct.* **2023**, *283*, 115866. [CrossRef]
3. Wu, G.; Feng, D.C.; Wang, C.L. *Novel Precast Concrete Structure Systems*; Springer: Singapore, 2023.
4. Bauer, H. *Baubetrieb I: Einführung, Rahmenbedingungen. Bauverfahren*; Springer GmbH: Berlin/Heidelberg, Germany, 1992.
5. Madireddy, H.; Naganathan, S.; Mahalingam, B. A Review on Precast Concrete Construction. In *Sustainable Practices and Innovations in Civil Engineering. Lecture Notes in Civil Engineering*; Naganathan, S., Mustapha, K.N., Palanisamy, T., Eds.; Springer: Singapore, 2021; pp. 77–113.
6. Thienel, K.-C. *Leichtbeton im Hochbau—Woher Kommen Wir und Wo Geht die Reise Hin? Leichtbeton*; InformationsZentrum Beton GmbH: Heilbronn, Germany, 2019; p. 7.
7. *DIN EN 1992-1-1*; Eurocode 2: Design of Concrete Structures—Part 1-1: General Rules and Rules for Buildings. Beuth Verlag GmbH: Berlin, Germany, 2011; p. 241.
8. *DIN EN 206*; Beton—Festlegung, Eigenschaften, Herstellung und Konformitat (Concrete—Specification, Performance, Production and Conformity). Beuth Verlag GmbH: Berlin, Germany, 2021; p. 105.
9. Chandra, S.; Berntsson, L. *Lightweight Aggregate Concrete*, 1st ed.; Noyes Publications: Norwich, UK, 2002.
10. Thienel, K.-C. Precast elements of lightweight concrete with a porous matrix. *BFT Int.* **2000**, *66*, 62–72.
11. Thienel, K.-C.; Haller, T.; Beuntner, N. Lightweight Concrete—From Basics to Innovations. *Materials* **2020**, *13*, 1120. [CrossRef] [PubMed]
12. Öztürk, F.; Mojtabaei, S.M.; Şentürk, M.; Pul, S.; Hajirasouliha, I. Buckling behaviour of cold-formed steel sigma and lipped channel beam–column members. *Thin-Walled Struct.* **2022**, *173*, 108963. [CrossRef]
13. *DIN EN 1090-2*; Ausführung von Stahltragwerken und Aluminiumtragwerken—Teil 2: Technische Regeln für die Ausführung von Stahltragwerken (Execution of Steel Structures and Aluminium Structures—Part 2: Technical Requirements for Steel Structures). Beuth-Verlag GmbH: Berlin, Germany, 2018; p. 214.
14. *DIN EN 10346*; Kontinuierlich Schmelztauchveredelte Flacherzeugnisse aus Stahl zum Kaltumformen—Technische Lieferbedingungen (Continuously Hot-Dip Coated Steel Flat Products for Cold Forming—Technical Delivery Conditions). Beuth-Verlag GmbH: Berlin, Germany, 2015; p. 44.
15. *DIN EN 13055-1*; Leichte Gesteinskörnungen Teil 1: Leichte Gesteinskörnungen fur Beton, Mörtel und Einpressmörtel (Lightweight Aggregates—Part 1: Lightweight Aggregates for Concrete, Mortar and Grout). Beuth-Verlag GmbH: Berlin, Germany, 2002; p. 39.
16. Bogas, J.A.; Gomes, A. A simple mix design method for structural lightweight aggregate concrete. *Mater. Struct.* **2013**, *46*, 1919–1932. [CrossRef]
17. *DIN EN 1354*; Bestimmung der Druckfestigkeit von Haufwerksporigem Leichtbeton. Beuth Verlag GmbH: Berlin, Germany, 2005; p. 18.
18. *DIN EN 1352*; Bestimmung des Statischen Elastizitätsmoduls unter Druckbeanspruchung von Dampfgehärtetem Porenbeton und von Haufwerksporigem Leichtbeton. Beuth Verlag GmbH: Berlin, Germany, 1997; p. 7.
19. Buntke, N. *Heft 422 Prüfung von Beton—Empfehlungen und Hinweise als Ergänzung zu DIN 1048 (Testing of Concrete—Recommendations and Advises in Addition to DIN 1048)*; Deutscher Ausschuss für Stahlbeton: Berlin, Germany, 1991; p. 53.
20. *DIN EN 992*; Bestimmung der Trockenrohdichte von haufwerksporigem Leichtbeton. Beuth Verlag GmbH: Berlin, Germany, 1995; p. 5.
21. *DIN EN ISO 22007-2*; Kunststoffe—Bestimmung der Wärmeleitfähigkeit und der Temperaturleitfähigkeit, Teil 2: Transientes Flächenquellenverfahren (Hot-Disk-Verfahren) (ISO 22007-2:2015); Deutsche Fassung EN ISO 22007-2:2015. Beuth Verlag GmbH: Berlin, Germany, 2015.
22. Sadeghi, K.; Muhammad, S.M.; Sofy, S.A. Constitutive Laws for Compression Concrete under Monotonic and Cyclic Loading: Characteristic Models. *Acad. Res. Int.* **2018**, *9*, 11–23.
23. Tasevski, D.; Ruiz, M.F.; Muttoni, A. Compressive Strength and Deformation Capacity of Concrete under Sustained Loading and Low Stress Rates. *J. Adv. Concr. Technol.* **2018**, *16*, 396–415. [CrossRef]

24. Raue, E.; Tartsch, E. Bewertung der Dauerstandfestigkeit von Porenbeton und Normalbeton auf der Basis von Kurzzeitversuchen. *Mauerwerk* **2006**, *10*, 140–148. [CrossRef]
25. Tartsch, E. *Bewertung der Dauerstandfestigkeit von Dampfgehartetem Porenbeton auf der Grundlage von Kurzzeitversuchen*; Fakultat Bauingenieurwesen, Bauhaus-Universitat Weimar: Weimar, Germany, 2008.
26. Rüsch, H. Physikalische Fragen der Betonprüfung. *Zement-Kalk-Gips* **1959**, *12*, 1–9.
27. Rüsch, H. Researches Toward a General Flexural Theory for Structural Concrete. *ACI J. Proc.* **1960**, *57*, 1–28.
28. Rüsch, H.; Sell, R.; Rasch, C.; Grasser, E.; Hummel, A.; Wesche, K.; Flatten, H. *Festigkeit und Verformung von Unbewehrtem Beton unter konstanter Dauerlast*; Deutscher Ausschuss für Stahlbeton: Berlin, Germany, 1968; Volume 198, pp. 1–58.
29. Schickert, G. *Schwellenwerte Beim Betondruckversuch: Bericht/Erstattet von Gerald Schickert*; Deutscher Ausschuss für Stahlbeton: Berlin, Germany; Ernst: Berlin, Germany, 1980; Volume 312.
30. Rüsch, H.; Jungwirth, D. *Stahlbeton—Spannbeton. Berücksichtigung der Einflüsse von Kriechen und Schwinden auf das Verhalten der Tragwerke*; Werner-Verlag: Düsseldorf, Germany, 1976.
31. Walraven, J.E. *Model Code 2010—Final Draft*; Internation Federation for Structural Concrete (FIB): Lausanne, Switzerland, 2012; Volume 1, p. 350.
32. Schlaich, M.; Hückler, A.; Lösch, C. Infraleichtbeton (ILC). In *Beton-Kalender 2021*; Bergmeister, K., Fingerloos, F., Wörner, J.-D., Eds.; Ernst & Sohn GmbH & Co. KG: Berlin, Germany, 2021; pp. 909–952.
33. Schlaich, M.; Hückler, A. Infraleichtbeton bietet die architektonische Freiheit für ein neues einfaches und baukulturell wertvolles Bauen. Monolithische recycelbare tragende Wärmedämmungen als echte Alternative zu mehrschichtigen Wandsystemen. *Der Prüfingenieur* **2020**, *56*, 58–66.
34. Chung, S.-Y.; Kim, J.-S.; Han, T.-S.; Stephan, D.; Kamm, P.H.; Elrahman, M.A. Characterization of foamed concrete with different additives using multi-scale micro-computed tomography. *Constr. Build. Mater.* **2022**, *319*, 125953.
35. Empelmann, M.; Javidmehr, S. Anwendungsgerechte Bestimmung des αcc-Beiwerts. *Beton- und Stahlbetonbau* **2020**, *115*, 560–565. [CrossRef]
36. Faust, T. *Leichtbeton im Konstruktiven Ingenieurbau*; Ernst & Sohn: Berlin, Germany, 2003.
37. Schmidt-Döhl, F.; Thienel, K.-C. *Messung des Schwindens von Leichtbetonzuschlag aus Blähton mit Einer Mikroskopischen Methode (Measurement of Shrinkage of Lightweight Concrete Aggregate from Expanded Clay Using a Microscopic Method)*; Forschungsarbeiten 1995–1999; Institut für Baustoff, Massivbau und Brandschutz: Braunschweig, Germany, 1999; pp. 95–96.
38. *DIN EN 1355*; Bestimmung der Kriechverformung unter Druckbeanspruchung von Dampfgehärtetem Porenbeton und von Haufwerksporigem Leichtbeton. Beuth Verlag GmbH: Berlin, Germany, 1997; p. 7.
39. *ASTM E72-15*; Standard Test Methods of Conducting Strength Tests of Panels for Building Construction. ASTM International: West Conshohocken, PA, USA, 2015; p. 13.

Disclaimer/Publisher's Note: The statements, opinions and data contained in all publications are solely those of the individual author(s) and contributor(s) and not of MDPI and/or the editor(s). MDPI and/or the editor(s) disclaim responsibility for any injury to people or property resulting from any ideas, methods, instructions or products referred to in the content.

7.4 Renewable construction with lightweight concrete – Reclaimed recycled material system with CO_2-absorption

Reprint:

Published in “Construction and Building Materials”

Volume 466, 140339; doi: 10.1016/j.conbuildmat.2025.140339

Authors: T. Haller, S. Scherb, N. Beuntner, K.-Ch. Thienel

Construction and Building Materials 466 (2025) 140339

Contents lists available at ScienceDirect

Construction and Building Materials

journal homepage: www.elsevier.com/locate/conbuildmat

Renewable construction with lightweight concrete – Reclaimed recycled material systems with CO_2-absorption

Timo Haller *, Sebastian Scherb, Nancy Beuntner, Karl-Christian Thienel

Universität der Bundeswehr München, Fakultät für Bauingenieurwesen und Umweltwissenschaften, Institut für Werkstoffe des Bauwesens, Werner-Heisenberg-Weg 39, Neubiberg 85579, Germany

ARTICLE INFO

Keywords:
Recycled concrete
Lightweight concrete
Infra-lightweight concrete
CO_2 absorption
Carbonation
Construction and demolition waste

ABSTRACT

The conservation of natural resources and the effective reduction of CO_2 emissions are critical goals for the cement and concrete industries. This study addresses the end-of-life scenario for lightweight concretes by presenting a strategy to recycle the most challenging type, Infra-Lightweight Concrete. The current version of the German standard for concrete, DIN 1045 (2023), does not permit the use of recycled materials in Lightweight Concretes. The objective of this study is to investigate the potential of Infra-Lightweight Concrete elements to be recycled into Recycled Lightweight Concrete Aggregates through mechanical processing and screening. Subsequently, these Recycled Lightweight Concrete Aggregates are used to produce Recycled Infra-Lightweight Concrete, which aims to replicate the properties of the original Infra-Lightweight Concrete. Key testing methods were employed to characterize Recycled Lightweight Concrete Aggregates and Recycled Infra-Lightweight Concrete, including density, water absorption, compressive strength, thermal conductivity, and CO_2 absorption. The study shows that Recycled Lightweight Concrete Aggregates exhibit an agglomerate structure, which significantly affects key parameters like density and water absorption, both essential for successful integration into new concrete mix designs. Recycled Lightweight Concrete Aggregates exhibited consistent strength potential across different batches of recycled material within a simple and reproducible method, particularly suitable for recycling Lightweight Concretes. Additionally, Recycled Lightweight Concrete Aggregates demonstrated substantial CO_2 absorption potential, with maximum CO_2 uptake values ranging from 123 to 138 kg per ton of Recycled Lightweight Concrete Aggregate after 10 days of conditioning in a controlled environment containing 0.5 % CO_2 by volume. Recycled Infra-Lightweight Concrete produced from Recycled Lightweight Concrete Aggregates exhibited similar strength, modulus of elasticity, and thermal conductivity as the original Infra-Lightweight Concrete. Notably, despite a 32 % increase in dry density, the thermal conductivity of Recycled Infra-Lightweight Concrete only increased by 3.3 %, indicating nearly identical performance properties to Infra-Lightweight Concrete. In conclusion, monolithic wall elements can be constructed using only Recycled Lightweight Concrete Aggregates while maintaining similar performance parameters. This approach promotes material circularity, reduces CO_2 emissions, and validates the structural performance of recycled lightweight concrete, thereby contributing to more sustainable construction practices.

1. Introduction

Modern life in the 21st century takes place in the built environment and is shaped by concrete and steel. The construction efforts required for expansion and maintenance in the building sector consume vast amounts of natural resources and are accompanied by high CO_2 emissions. New strategies are needed to make the construction sector more sustainable and to meet increasing environmental demands.

The reuse of construction and demolition waste (CDW) is crucial for promoting material circularity in the construction industry. Numerous studies highlight CDW as the largest global waste source, with its volume increasing annually [1–5]. Despite efforts to reuse CDW, most of it is disposed of in landfill sites or downgraded to be used in earthworks and road construction [6–9]. Currently, only a small fraction of CDW is reused as recycled concrete aggregate (RCA) in concrete production. In Germany, for instance, this fraction is less than 1 % of the total aggregate used for concrete production [5].

* Corresponding author.
E-mail addresses: timo.haller@unibw.de (T. Haller), sebastian.scherb@unibw.de (S. Scherb), nancy.beuntner@unibw.de (N. Beuntner), christian.thienel@unibw.de (K.-C. Thienel).

https://doi.org/10.1016/j.conbuildmat.2025.140339
Received 15 August 2024; Received in revised form 16 January 2025; Accepted 5 February 2025
Available online 8 February 2025
0950-0618/© 2025 The Author(s). Published by Elsevier Ltd. This is an open access article under the CC BY license (http://creativecommons.org/licenses/by/4.0/).

Nomenclatures

(CDW)	Construction and Demolition waste
(RCA)	Recycled Concrete Aggregate
(LC)	Lightweight Concrete
(LWA)	Lightweight Aggregates
(ILC)	Infra-Lightweight Concrete
(LAC)	Lightweight Aggregate Concrete
(RILC)	Recycled Infra-Lightweight Concrete
(RLCA)	Recycled Lightweight Concrete Aggregate
(ITZ)	Interfacial Transition Zone
(TGA)	Thermogravimetric Analysis
(FTIR)	Fourier Transformed Infrared Spectroscopy

The recycling of ordinary concrete has been extensively researched over the last few decades and has now been put into practice. CDW can originate from various sources and is classified into six categories according to EN 933–11 [10]. Recycled concrete is the dominant component of type 1 and type 2 RCA according to DIN 4226–101 [11]. RCA can replace up to 25 % by volume of the total aggregate for concrete grades $\leq$ C50/60 in concrete class BK-N [12]. A major challenge with coarse RCA is the adhesive mortar, which is typically weaker than the original aggregate, leading to a higher water demand and lower density of RCA compared to normalweight virgin aggregate [6,13,14].

For Lightweight Concrete (LC) using Lightweight Aggregates (LWA), the recycling scenario is different. According to DIN 1045–2 [12], the use of RCA derived from LC in structural concrete is limited to less than 10 % for type 1 and less than 30 % for type 2 RCA. Moreover, RCA cannot be used for producing LC itself, and RCA with a dry density lower than 2000 kg/m^3 is not permitted for sole use in recycled concrete [12]. The latter restriction applies to the very light LC`s popular today, which are used in producing monolithic fair-faced wall elements in the lowest strength and density classes. These constructions enable the creation of finished walls in a single operation and do not require any additional insulation materials or multi-layer wall assemblies. Consequently, these structures must meet both constructional design criteria and thermal insulation requirements.

Infra-Lightweight Concrete (ILC) represents the latest stage of this development [15–19]. The mix design of ILC aims to achieve a balance between reduced density, adequate strength, and minimal thermal conductivity. Mechanically and in terms of density and mix design, ILC aligns with lightweight aggregate concrete (LAC) as defined in DIN EN 1520 [20], but it deviates by being a ready-mixed, cast-in-place concrete. This approach has already received several project-specific approvals [15] and is scheduled for formal introduction by the German Committee for Reinforced Concrete (Deutscher Ausschuss für Stahlbeton e.V.) for construction use. The monolithic structure of ILC is predestined for recycling and reuse strategies, as it does not require the separation of different materials prior to recycling, which is a common challenge for multi-layer construction components [9,18]. Given the suitability of ILC and its the lack of consideration in current standards, this study aims to present a methodology for recycling and reuse of ILC, promoting circular economy and CO_2 reduction strategies.

The objective of this study is to demonstrate the feasibility of recycling ILC by producing Recycled Infra-Lightweight Concrete (RILC) using Recycled Lightweight Concrete Aggregates (RLCA) as the sole aggregate source. Additionally, the study seeks to highlight the CO_2 absorption potential of RLCA, attributed to their favorable characteristics.

The study involves characterizing RLCA processed from virgin ILC and subsequently producing and characterizing RILC made from RLCA. The study addresses the following three key research questions:

1. Identifying the key material characteristics of RLCA: RLCA material properties are crucial for the properties of the concretes produced from them. Determining density and water absorption is essential for successfully integrating RLCA into RILC mix design. A method for assessing the uniformity of mechanical performance of RLCA is introduced to account for variations in RLCA.
2. Evaluating the performance of RILC made from RLCA: The study aims to produce RILC solely from RLCA, replicating the properties of the original concrete. This approach allows for a comprehensive comparison with benchmark ILC, evaluating property degradation through recycling, and suitability for repeated recycling loops. The quality of RILC is assessed using standard LC testing methods (density, strength, thermal conductivity) and additional properties influenced by RLCA (initial drying shrinkage, modulus of elasticity, sustained loading).
3. Assessing RLCA`s potential for CO_2 mineralization: RLCA offers favorable characteristics for targeted carbonation, including higher proportion and porosity of carbonatable material. The study quantifies CO_2 uptake of recycled material from ILC elements. The degree of CO_2 uptake is measured under elevated CO_2 concentration in a controlled environment using a combination of thermogravimetric analysis (TGA) and coupled Fourier transformed infrared spectroscopy (FTIR). The study takes into account the initial carbonation status achieved under natural conditions, the total CO_2 uptake potential and the proportion of carbonatable material in the RLCAs.

This study responds to the urgent global need to mitigate climate change and the transition to more sustainable construction practices, making it a crucial step towards a more sustainable future.

2. Concepts for recycling and carbonation of ILC

2.1. Recycling of lightweight concretes

Internationally, recycled aggregate for LC mainly refers to the use of recycled organic materials replacing traditional mineral LWA (e.g. pumice, expanded clay or expanded glass [21–25]). When authors refer to recycled mineral LWA, it is predominantly expanded glass made from recycled glass [26–28], which is already covered by DIN EN 13055–1 [29], which considers it being a manufactured, not a recycled, LWA. Studies on recycled aggregates of mineral origin and its use in lightweight concretes focused on autoclaved aerated concrete fragments [30–32] or processed CDW, such as bricks [33] or concrete powder [34]. The latter is either cold-bound [35] or mixed with an expansion agent before being granulated and subsequently burned in a kiln [36,37].

Information on recycled concrete using RLCA originating from lightweight concretes is limited. Existing studies aim to reduce natural resource consumption and examine the effects on RLCA and/or LC.

A report [38], funded by the European Union under the Brite EuRam III program, investigated the use of RLCA as aggregate in recycled concrete. It found that RCLA met environmental standards in leaching test and could be used to produce grade B35 concrete (in current standards (EN 206 [39] and DIN 1045–2 [12])), this corresponds to a classification of C30/37 concrete). However, RLCA-based concrete required more cement and had a density approximately 200 kg/m^3 lower than gravel concrete.

Kümmel [40] evaluated the recycling potential of LC based on technical, ecological, and economic criteria, showing that RLCA can be used effectively in recycled concrete. The study noted a high flakiness and unfavorable shaped RLCA when using a jaw crusher for processing. In contrast to RCA, the particle density of RLCA decreases with increasing particle size. Adjustments in the mix design were suggested due to the increased water absorption of RLCA. Satisfactory compressive strength was found, meeting structural requirements. In addition, a reduced modulus of elasticity was observed, attributed to the weaker interfacial transition zone (ITZ) and higher shrinkage and creep values

due to higher porosity and the presence of cracks in RLCA.

Bogas et al. [41,42] produced recycled concrete with RLCA originating from LC and LAC and investigated various durability properties including drying shrinkage, capillary and immersion water absorption, carbonation, and chloride penetration resistance. Recycled concrete mixtures with varying RLCA content were tested, showing up to 60 % higher particle density of the RLCA, resulting in higher strength along with a 10 % increase in density. The findings indicated that the durability properties of the recycled concretes generally decline with an increase in the RLCA replacement ratio. Contrary to Kümmel [40], they found a higher modulus of elasticity, attributed to the higher stiffness of RLCA compared to original LWA.

Huang et al. [43] proposed a novel approach to recycle end-of-life LC by applying freezing and thawing cycles to separate the components of LC without significant damage. LC was collected from the Nanjing Yangtze River Bridge. The recycled materials included recycled powder, recycled fine aggregate and RLCA. The RLCA exhibited a dry density similar to the original LWA, but lower water absorption due to old paste coverage. Recycled concrete mixes with replacement rates of RLCA of 10 %, 20 %, and 30 % were produced. While 10 % and 20 % replacement rates yielded no significant change in compressive strength after 28 days, a 30 % replacement rate resulted in a 14 % increase in compressive strength after 28 days. Microstructural analysis revealed the strongest ITZ between new paste and RLCA without old paste and the weakest between new paste and RLCA covered with old paste.

The type and properties of LWA are the dominant factors influencing the properties of any lightweight concrete. Although LWA`s yield the unique properties of lightweight concretes, they also pose challenges for. When normalweight concrete is crushed, the fracture pattern follows the weakest links, typically the ITZ and voids, resulting in RCA predominantly composed of normalweight particles with adherent mortar. The shape of RLCA depends on factors like the type of crusher used [44]. The density of RCA is lower than that of the original aggregate used due to the lower density of the adherent paste, with particle density increasing with RCA particle size. On the other hand, water demand decreases since the percentage of adherent mortar and paste is lower for coarser RCA [13,44,45]. In contrast, well-designed LC lacks an ITZ [46], causing cracks to run through the LWA during crushing. As a result, RLCA forms agglomerates consisting of LWA and adherent mortar, driving its properties and distinguishing it significantly from RCA [40,41].

2.2. Carbonation of RCA

From a technical perspective, the carbonation of RCA during recycling and reuse strategies is of great interest. The underlying process of carbonation is the transformation of calcium hydroxide into calcium carbonate [47,48]. According to the cement and concrete industry`s carbon neutrality roadmaps [49], by 2050, approximately 51 kg of CO_2 per ton of cement paste is expected to be re-absorbed through carbonation [5,49]. After concrete structures are demolished CO_2 uptake increases significantly due to the greater surface area exposed to carbonation during crushing and further processing [50,51]. Integrating RCA carbonation into the life cycle assessments can reduce the carbon footprint of concrete. In literature, the targeted carbonation of RCA is also referred to as CO_2 mineralization, CO_2 curing or Forced Carbonation. The most important factor for carbonation of RCA is the type of material used, including the content of carbonatable material (e.g. non-hydrated cement residues, calcium hydroxide, calcium silicate hydrates, sulfate-free and sulfate-containing aluminate hydrates [9]), initial carbonation progress status, porosity and particle size [51].

Different methods have been investigated to understand and improve RCA carbonation. Poon [51] modeled CO_2 uptake for various ambient conditions like temperature and relative humidity as well as CO_2 related conditions like CO_2 concentration, pressure conditions and exposure time. Other studies have explored pretreatment methods of RCA to accelerate the carbonation of RCA, including varying the media in which RCA is exposed to CO_2, such as different gases (e.g. biogenetic CO_2 [52] or aqueous medium [53]), pressure chambers, flow containers [51], or under hydrothermal conditions in a pressurized autoclave [9] or in combination with technological integration in cement plants [54,55]. Pre-soaking RCA in solutions, slurries, or emulsions has been investigated by [56,57].

The improvement of physical properties of RCA through carbonation have also been examined in studies. Most of the efforts focus on reducing the water absorption and either removing or strengthening the adherent cement paste [56]. These improvements are largely contributed to the densification during carbonation of the adherent cement paste, where $CaCO_3$ microcrystals fill the pores of RCA [6,56–58]. Infante Gomes et al. [59] summarized the influence of CO_2 curing on the properties of carbonated RCA`s across several studies. Another area of improvement is enhancing the reactivity of recycled fines for use as supplementary cementitious materials [60,61].

Despite these efforts, only few studies focused on the experimental determination of CO_2 uptake potential of RCA for use in concrete in life cycle assessments. Table 1 summarizes relevant studies on CO_2 uptake by RCAs under various carbonation conditions. Databases were searched for research specifically focused on CO_2 uptake using thermogravimetric experimental setups. The summary aims to provide an overview of the CO_2 uptake of RCA`s and offer reference values for classifying the measurements presented in this study.

The different approaches to determine CO_2 uptake, as well as the varying types of RCA (particularly regarding carbonatable material content, initial carbonation progress status, and porosity) pose a challenge for the comparison of CO_2 uptake across different RCA`s. However, the targeted carbonation of RCA has been demonstrated to be feasible on an industrial scale [54,55], making it a promising technique for application on lightweight concretes.

3. Materials and methods

3.1. ILC

The ILC used in this study (ILC_{Origin}) was designed for fair-faced external walls, combining structural and thermal insulation requirements in a monolithic component [15,19]. ILC_{Origin} was produced as part of a study into the pumpability of ILC [67], where its characteristic properties were determined. These properties are summarized in Table 8 and will serve as the reference for analyzing the RILC developed in this study

ILC_{Origin} belongs to strength class LAC 4 and density class 0.6 according to EN 1520 [20]. The LWA used in ILC_{Origin} were expanded glass in 1–2 mm and 2–4 mm fractions, according to DIN EN 13055–1 [29]. The binder is composed of slag cement CEM III/A 42.5 N according to EN 197–1 [68] and condensed silica fume in suspension according to EN 13263–1 [69]. The water content of the silica fume suspension was accounted for in the mix design. Additives include a polycarboxylate ether based superplasticizer, an air entraining agent and micropolymer fibers according to EN 14889–2 [70].

ILC_{Origin} was then recycled into RLCA to explore its potential for reuse in producing new concrete.

3.2. Recycling process of ILC_{Origin} into RLCA

To produce RLCA, larger elements of ILC_{Origin} (4×2×0.5 m) were manually crushed, followed by further mechanical crushing using a laboratory jaw crusher. The process reduced the particle size to approximately < 32 mm. The crushed material was then screened into particle size groups: < 1 mm ($RLCA_{fine}$), 1–2 mm ($RLCA_{1–2}$), 2–4 mm ($RLCA_{2–4}$), 4–8 mm ($RLCA_{4–8}$) and 8–16 mm ($RLCA_{8–16}$). Fig. 1 shows an example of the particle size distributions, illustrating how adjusting the jaw crusher`s settings impacts the size of the particles. However, for this study, the focus was not on fine-tuning the crushing process but on assessing the general suitability of RLCA for concrete production.

Table 1
Summary of CO2 uptake studies on RCA under different carbonation conditions.

Reference	Type of Material	CO_2 Exposure	CO_2 Uptake [kg CO_2 /t_{RCA}]	Determination of CO_2 uptake	Climate	Special observations
Kikuchi and Kuroda [50]	Old demolished concrete, Recycled crusher-run stone, New lab mortar	Natural carbonation	~11	TGA + insoluble residue test	20 °C / 65 % RH -pre-conditioning by applying dried and alternating wet and dry condition	-Reduced overall CO_2 emissions in concrete life cycle by 5.5 % -Alternating wet and dry conditions greatly increased CO_2 uptake
Xuan et al. [58]	Old demolished concrete, Recently crushed concrete, New lab concrete	Pressurized carbonation chamber (0.1 and 5 Bar), 100 % CO_2 concentration for 24 hours	4.9–8.1	TGA	Not specified -pre-conditioning at 25 ± 3 °C / 50 ± 5 % RH, corresponding to moisture content of RCA in range of 40–70 %	-Higher CO_2 uptake with finer aggregates -Physical and mechanical properties of RCA`s were improved
Fang et al. [51]	Demolished concrete, Old lab concrete	a) Flow-through carbonation (Flow rate of 1 – 10 l/min), varying CO_2 concentrations for 24 hours b) Pressured carbonation chamber (0.1 Bar), 100 % CO_2 concentration for 24 hours	~6.5 (Flow through) ~28–37 (Pressured chamber)	TGA	25 °C / 50 ± 5 % RH	-Flow-through carbonation method is less efficient than the pressured carbonation method
Sereng et al. [62]	Old demolished concrete, Recent crushed concrete, Lab concrete	Carbonation chamber, 15 or 100 % CO_2 concentration	~8.6–20.4 (Crushed concrete) 49.9 (Lab concrete)	TGA + mass control	20 °C / 65 % RH	-Study is part of large-scale "FastCarb" project on optimization of CO_2 uptake -Elevated temperatures improve CO_2 uptake by enhancing diffusion through RCA`s
Leemann et al. [63]	Demolished concrete	Flow-through carbonation at atmospheric pressure, 100 % CO_2 concentration for 70 minutes	10–21	Mass change corrected for moisture loss and CO_2 vs air mass differences	Not specified -pre-conditioning at 80 °C, then water sprinkling corresponding to moisture content of RCA in range of 30–200 %	-RCA tends to absorb more CO_2 at lower water contents (30 % of water absorption) compared to higher values (60–200 %)
Kaddah et al. [64]	RCA, Mortar spheres (model material)	Carbonation chamber, 15 % CO_2 concentration, for four days	~6.5–12.2 (RCA) ~51.6–70.6 (Mortar spheres)	TGA + mass control	20 °C / 65 % RH	-Pre-existing natural carbonation in RCA reduces further CO_2 uptake
Dündar et al. [65]	RCA	Carbonation chamber, 15 % CO_2 concentration Pressure varied between 1 and 3 bar Duration varied between 2 and 120 hours	~3.7–7.4	TGA	Varied 50–90 °C 50–90 % RH	-As RCA size increases, pressure increase is beneficial -RCAs showed improved microstructure,as well as physical and mechanical aspects
Bastos et al. [66]	CDW, Mixed recycled aggregates, Lab concrete	Carbonation chamber, 25 % CO_2 concentration for 24 hours	6–41 (CDW), 7–18 (Mixed recycled aggregates), 49 (Lab concrete)	TGA	23 °C / 60 % RH -pre-conditioning at 60 °C	-Acid attack occurs with longer carbonation times, promotes dissolution of $CaCO_3$, reducing the potential for CO_2 capture

3.3. Testing and application of RLCA in RILC

Following the mechanical processing, an experimental program was applied to determine the key material properties of RLCA. These properties are critical for replicating the mix design of ILC_{Origin} in the production of RILC. A summary of the testing methods for both RLCA and RILC is provided in Table 2 and a schematic principle of the study is shown in Fig. 2.

3.4. Experimental program for RLCA

This section outlines the experimental program designed to evaluate the properties of RLCA, focusing on density and water absorption, which are critical for mix design in RILC.

3.4.1. Density and water absorption of RLCA

All tests were performed on three samples for each particle size group. The particle density and water absorption properties were determined using the pycnometer method in accordance with EN 1097–6 [72]. For finer particles (<1 mm), the density and water absorption were assessed following DIN EN 1097–6 (Annex D) [72], which is suitable for light, open porous aggregates with a predominant particle content of less than 1 mm and more than 50 % by weight. These parameters are determined both, on oven-dried material dried (105 ± 5) °C and on material exposed to laboratory conditions (20 ± 5 °C and 65 ± 5 % RH).

The bulk density is determined in accordance with DIN EN 1097–3 [71], and this parameter was tested only on material exposed to laboratory conditions (20 ± 5 °C and 65 ± 5 % RH). Fig. 3 illustrates the cross section of a cut cylinder (left) and LWA particle after processing of ILC in jaw crusher (right).

3.4.2. Uniformity control of RLCA's mechanical properties

The recycling process can lead to variations in RLCA properties, such as density, water absorption and particle strength. To assess how these variations affect concrete properties - specifically density and compressive strength- compressive strength tests were performed on a standard concrete mix. For this purpose, a volumetric mixture of RLCA

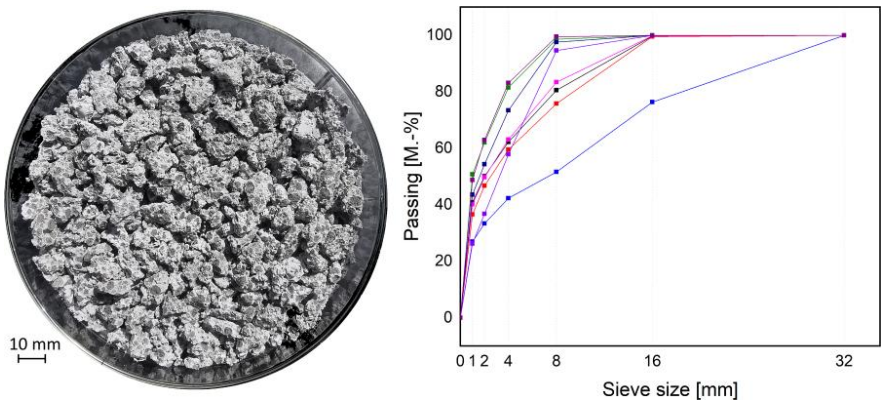

Fig. 1. Left: Particle size group $RLCA_{2-4}$. Right: Volumetric passing of the RLCA (> 1 mm) after preparation by the jaw crusher. The curves shown differ in the setting of the distance between the jaws of the laboratory jaw crusher used.

Table 2
Test program for RLCA and RILC performance parameters.

Property	Testing method
RLCA	
Bulk Density [kg/m³]	EN 1097–3 [71]
Particle Density [kg/m³]	EN 1097–6 [72]
Water Absorption [wt%]	EN 1097–6 [72]
Uniformity of strength potential [N/mm²]	DIN 4226–3 1983 [73]
CO_2-Absorption [kg CO_2/ton RLCA]	Based on [58,62]
RILC	
Fresh Density [kg/m³]	EN 12350–6 [74]
Plastic Shrinkage [mm/m]	Based on [75,76]
Dry Density [kg/m³]	EN 992 [77]
Compressive Strength [N/mm²]	EN 1354 [78]
Thermal Conductivity [W/(m•K)]	EN ISO 22007–2 [79]
Sustained Loading [-]	Based on [80]
Modulus of Elasticity [N/mm²]	EN 1352 [81]

was prepared according to grading curve B16 (DIN 1045–2 [12]). The mixture for one cubic meter of compacted concrete included 350 kg of CEM III B 42.5 N, with an effective water/cement ratio of 0.50. The RLCA water absorption, as described in section ↱3.4.1, was taken into account. The mix composition for the uniformity test is summarized in Table 3. Compressive strength test were performed after 28 days on 100x100x100 mm cubes in accordance with EN 1354 [78]. To assess the variations in RLCA properties due to recycling of different elements, four separate concrete operations were conducted, with at least six cubes tested for each operation. This approach minimizes the influence of irregularly shaped particles on the results, which could arise with other methods, as reported by Thienel [82]. However, it is important to note that while mix design is robust and allows for the widest possible range of RLCA, it is not optimized for specific concrete properties. The procedure is based on a method outlined in DIN 4226–3 [73] previously used for factory control of LWA in LC with strength classes LB 8 (characteristic cube strength 8 N/mm²) [83] and above. This test effectively detects variations in the RLCA properties with minimal effort, ensuring consistent quality of the RILC, which is produced using the tested RLCA.

3.5. Experimental program for RILC

This section outlines the experimental program conducted to produce and evaluate RILC using RLCA. The primary objective was to optimize the mix design to replicate the properties of the original concrete (ILC_{Origin}) while addressing expected differences in strength and density. The goals were to achieve the same strength class ILC_{Origin} and to maintain a comparable density levels.

3.5.1. Mix design optimization, density control and thermal conductivity

Based on RLCA characterization described in section ↱3.4, RILC is produced with a mix design intended to reproduce the properties of the original concrete (ILC_{Origin}). The mix design includes only RLCA as aggregates, comprising 54 % by volume of RILC. Specifically, the mix included 315 kg of CEM III A 42.5 N per cubic meter of compacted concrete, with an effective water/binder ratio of 0.44. The mix composition for producing 1 m³ of RILC is summarized in Table 4 and the mixing regime is detailed in Table 5.

The theoretical mix design is validated by determining the fresh concrete density and the yield. Fresh concrete density is determined in accordance with EN 12350–6 [74] on all test specimens produced to characterize the mechanical properties of RILC. The yield is calculated by determining the volume of fresh concrete produced from a given batch of materials according to ASTM C138/C138M – 17a [84].

Dry density was measured on 16 cylinders (300 mm height and 150 mm diameter) from six different batches according to EN 992 [77]. Thermal conductivity measurements were performed using the transient plane source method (Hot Disk TPS 2200, Gothenburg, Sweden) according to EN ISO 22007–2 [79]. First, samples were dried to a constant mass at 105 °C and then allowed to cool to 23 °C in an airtight container filled with silica gel to ensure dry conditions. Thermal conductivity was measured on four separate cubes.

3.5.2. Plastic shrinkage

Plastic shrinkage of the fresh concrete was measured using a shrinkage cone paired with a laser beam for contactless deformation measurement. This method allows for immediate assessment of shrinkage strain after placing the concrete in the cone.

The shrinkage cone has a volume of 682 cm³ and a height of 125 mm. Approximately 5 minutes after mixing, the fresh concrete is poured into the shrinkage cone. In total, two measurements were performed on fresh concrete samples. The settlement of the concrete surface was recorded every 150 seconds for 72 hours. The shrinkage strain was calculated using the formula $\Delta h/h$, where Δh is the change in height and h is the initial height of the concrete in the cone.

Kucharczyková et al. [75] describe a similar measurement procedure for the early age shrinkage of cement composite. Deviating from this, no reflector was used for distance tracking, as this reflector would sink into the fresh concrete due to of its low density. Greim [76] provides further

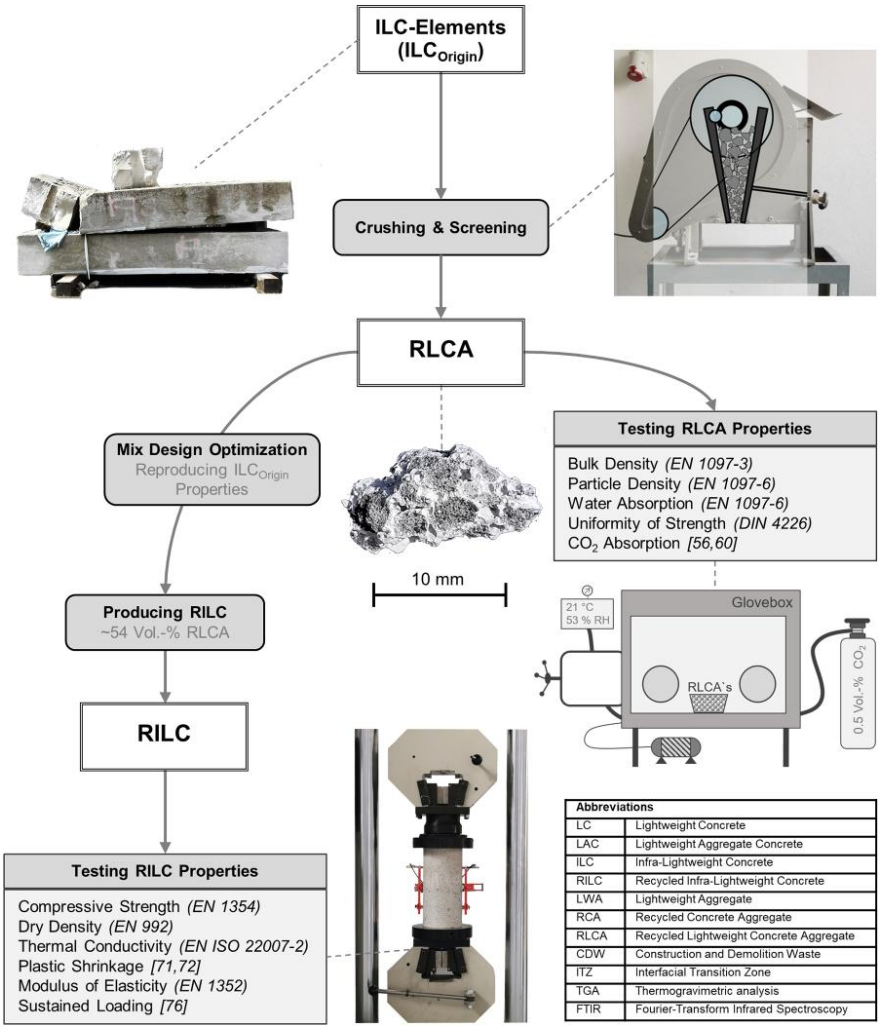

Fig. 2. Schematic representation of the study methodology. The study involves the characterization of RLCA processed from conventional ILC (ILC$_{Origin}$) and the subsequent preparation and characterization of RILC made from RLCA.

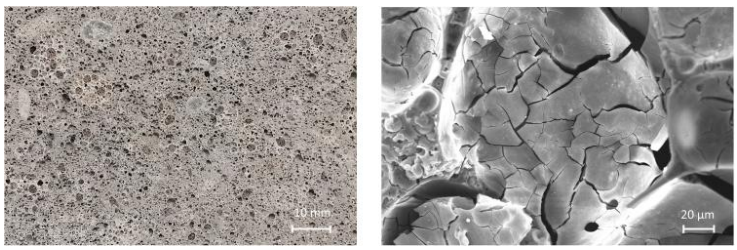

Fig. 3. Cross section of cut cylinder (left) and Scanning Electron Microscope image of shattered LWA after processing in jaw crusher (right).

Table 3
Mix design composition for 1 m^3 for uniformity control of RLCA mechanical properties.

Material	Amount [kg]	Volume [m^3]
$RLCA_{8–16\ mm}$	128	0.161
$RLCA_{4–8\ mm}$	107	0.134
$RLCA_{2–4\ mm}$	89	0.094
$RLCA_{1–2\ mm}$	67	0.067
$RLCA_{fine}$	317	0.241
Cement (CEM III A 42.5 N)	350	0.117
$Water_{total}$	356	0.356
$Water_{effective}$	177	0.177

Table 4
Mix design composition for production of 1 m^3 RILC.

Material	Amount [kg]	Volume [m^3]
$RLCA_{8–16\ mm}$	151	0.191
$RLCA_{4–8\ mm}$	127	0.159
$RLCA_{2–4\ mm}$	105	0.111
$RLCA_{1–2\ mm}$	79	0.079
Cement (CEM III A)	315	0.105
Silica Fume	24	0.020
$Water_{total}$	264	0.264
$Water_{effective}$	150	0.150
Air	-	0.185
Superplastizicer (SP)	1.6	-
Air entraining agent (AEA)	0.5	-
Stabilizer	1.3	-

Table 5
Mixing process for production of RILC.

Step	Approx. mixing time [s]
Mixing of RLCA with half of the water	30
Addition of Cement	45–60
Addition of remaining mixing water	60–90
Addition of Silica Fume, SP and AEA	180
Addition of Stabilizer	60

information on the technical details of the shrinkage cone.

3.5.3. Mechanical properties of RILC

Cylinders (300 mm height and 150 mm diameter) were produced across different concrete batches to determine the mechanical performance of RILC. Prior to testing, cylinder surfaces were ground plane-parallel. Compressive strength was determined after 28 days on cylinders according to EN 1354 [78]. Deformations during the test were monitored using two displacement sensors (DD1, Hottinger Brüel & Kjaer GmbH, Darmstadt, Germany) positioned on two opposite longitudinal sides of the cylinders, with a measuring distance of 150 mm to record the stress-strain relationship.

The modulus of elasticity was determined on cylinders (300 mm height and 150 mm diameter) after 28 days in accordance with EN 1352 [81].

The influence of sustained load on compressive strength was examined using seven additional cylinders (300 mm height and 150 mm diameter). These specimens were subjected to a low loading rate (4.2 N/s) at 28 days of concrete age until failure. Additionally, two displacement transducers (DD1, Hottinger Brüel & Kjaer GmbH, Darmstadt, Germany) were used to record the deformation on two opposite longitudinal sides of the cylinders, with a measuring distance of 150 mm, to accurately capture the strain during loading. After approximately 6 hours under the steadily increasing load, the specimens failed. The coefficient α was calculated by dividing the ultimate load achieved in the test by the average compressive strength of the RILC after 28 days. The methodology is well known from the literature and has been used, for example, to evaluate the sustained loading behavior and to estimate the reduction coefficient α of concrete with similar material behavior, such as ILC [18,85] and LAC with porosified matrix [80]. Furthermore, the values of coefficient α obtained from the tests are compared to those suggested by building codes, such as Eurocode 2 [86] (for LC; $\alpha = 0.85$), Eurocode 2 National Annex (Germany) [87] (for LC; $\alpha = 0.75–0.8$) or EN 1520 [20] (for LAC; $\alpha = 0.85$ in case of uniform compression or 0.8 when a decreased compression zone width is expected). This comparison helps confirm that the material behavior of RILC is comparable to that of the original concrete. The same procedure for determining coefficient α was also performed for ILC_{Origin}.

3.6. CO_2 absorption capacity of RLCA

The CO_2 absorption capacity of RLCA was investigated using a combination of TGA (Netzsch STA 449 F3 Jupiter, Selb, Germany) and FTIR (ThermoFisher Scientific Nicolet iS10). This approach allows a distinction between weight losses associated with H_2O and CO_2, which occur partly in parallel over the temperature range between 300 and 550 °C (see Appendix A. – TGA). Three samples of different grain sizes ($RLCA_{fine}$, $RLCA_{2–4}$ and $RLCA_{8–16}$) were first conditioned in a glovebox under a controlled nitrogen atmosphere (21 °C and 53 ± 5 % relative humidity) to stabilize their initial mass.

After conditioning, the samples were exposed to a nitrogen atmosphere containing 0.5 % CO_2 by volume for 10 days - this duration was sufficient to reach the point where no further CO_2 uptake could be measured. Coupled TGA-FTIR analysis were performed on samples at four time points: after conditioning (0 days) and after 3, 7 and 10 days of CO_2 exposure.

For TGA analysis, 200 mg of each crushed sample were heated from room temperature to 1000 °C at a rate of 10 K/min. The gas released during heating was transported through a heated pipe for FTIR analysis. The conditioned samples represent the carbonation status of ILC_{Origin} and served as the starting point for investigating the carbonation potential of RLCA. Until this point, carbonation of ILC elements had occurred under natural conditions over a duration of approximately 32 months.

Mass loss of CO_2 was recorded individually, accounting for the overlap with H_2O in the temperature range of 300 °C to 1000 °C (see Appendix A. – TGA), assuming it is related to CO_2 release from calcium carbonate [58,88,89].

The maximum CO_2 absorption capacity of the RLCA was calculated following a method of Greve-Dierfeld et al. [90], based on the CaO content of the different RLCA. To determine the CaO content, chemical analysis (see Table 6) was performed using inductively coupled plasma optical emission spectroscopy (ICP) after melt fusion, as described by Scherb et al. [91]. This analysis was essential to estimate the amount of carbonatable material in RLCA.

The potential available CaO for carbonation ($m_{CaO\text{-}CO2}$) was calculated using Eq. (1), which subtracts the CaO content of the LWA ($m_{CaO\text{-}LWA}$) and calcium sulfate ($m_{CaO\text{-}Sulfate}$) from the total measured CaO content obtained from the ICP analysis ($m_{CaO\text{-}ICP}$). The LWA content of

Table 6
Chemical composition and loss on ignition (LOI) of the RLCA and the LWA.

Oxides [wt%]	$RLCA_{fine}$	$RLCA_{2–4}$	$RLCA_{8–16}$	LWA
SiO_2	32.5	33.7	34.3	71.0
Al_2O_3	4.4	4.4	4.5	2.0
CaO	28.6	27.4	27.3	9.5
Fe_2O_3	0.7	0.7	0.7	0.5
K_2O	0.6	0.7	0.8	1.0
MgO	2.4	2.4	2.5	2.0
Na_2O	6.0	6.4	6.8	14.0
TiO_2	0.4	0.5	0.5	-
SO_3	2.3	2.2	2.1	-
LOI	22.1	21.6	20.5	< 1

RLCA was estimated based on the Na_2O content, assuming the Na_2O content from the cement was negligible to reflect a worst-case scenario. The CaO content of the calcium sulfate was calculated based on the SO_3 content, since the SO_3 was present as calcium sulfate in the carbonated sample [90,92], making it unavailable for carbonation. The results of the CO_2 uptake calculations are summarized in Table 9 (see Appendix C. – Potential CO_2 uptake).

$$m_{CaO-CO2} = m_{CaO-ICP} - m_{CaO-LWA} - m_{CaO-Sulfate} \quad (1)$$

4. Results and Discussion

4.1. Performance parameter RLCA

Several critical aspects are considered when evaluating the performance parameters of RLCA. These include, firstly, the parameters required for concrete design, namely the particle density and water absorption of RLCA. Secondly, it is important to evaluate the uniformity control of the mechanical properties of RLCA, which ensures uniformity of strength capabilities. The evaluation of CO_2 uptake potential provides a starting point for considering the reabsorption potential in life cycle assessments of concretes. The results are summarized in Table 7.

4.1.1. Density and water absorption of RLCA

Fig. 4 shows the particle density and water absorption of RLCA for different RLCA groups. A distinction is made between storage condition (~ 20 °C / 65 % rel. humidity) and oven dry condition (mass constancy at 105 °C). While the storage condition is particularly relevant to the mix design composition of the RILC, it is to a certain extend comparable to the particle density in a saturated surface dry stage (ρ_{ssd}) [72]. The oven dry condition results serve as reference and allow comparability between RLCA`s of different origins. The particle density of RLCA ranges from 730 to 1590 kg/m^3 . The $RLCA_{fine}$ group deviates significantly from the other RLCA groups, being, on average, at least 500 kg/m^3 denser. This can be attributed to the distinctive agglomerate structure of the RLCA. Larger particle contain a higher proportion of LWAs with relatively low densities, while the $RLCA_{fine}$ fraction contains an increased proportion of crushed LWA, which have a reduced pore volume and thus a higher particle density. As a result, the density decreases with increasing particle size. These observations are consistent with results reported in literature [40–42]. The horizontal dashed lines in Fig. 4 represent the densities of the original LWA used (expanded glass) in ILC_{Origin}. It should be noted that the RLCA`s in the same particle size group ($RLCA_{1-2}$ and $RLCA_{2-4}$) have a higher particle density by a factor of 2.6 and 2.7 respectively. This performance parameter limits the possibility of obtaining the same density of the RILC produced from the RLCA.

The water absorption of the RLCA ranges between 27 % and 60 % by weight. As expected, the values for water absorption of the RLCA are significantly higher in oven dry condition. Notably, the variations in water absorption are significantly higher for RLCA in storage condition, likely due to more variable moisture content. It can be assumed that the RLCA sourced from areas near the surface of ILC_{Origin} elements have undergone more advanced moisture exchange with the ambient air than those from the interior. This difference also depends on the storage conditions - free weathering, for instance, might yield opposite results. These observations are in line with results presented by Smeplass [93], who investigated the water absorption for different initial moisture contents of coarse LWA. Proper consideration of RLCA`s water absorption is crucial, as uncontrolled absorption of water from the concrete matrix can result in the formation of severe microcracks, reducing the achievable strength and compromising durability [15].

Table 7
Summarized results for performance parameters of RLCA.

Parameter	$RLCA_{fine}$	$RLCA_{1-2}$	$RLCA_{2-4}$	$RLCA_{4-8}$	$RLCA_{8-16}$
Bulk density [kg/m^3]	755	350	305	295	300
Particle density (lab condition) [kg/m^3]	1590	1000	940	800	790
Particle density (dry condition) [kg/m^3]	1525	910	835	810	730
Water absorption (lab condition) [wt%]	41	27	27	34	34
Water absorption (dry condition) [wt%]	60	54	50	47	55
CO_2-absorption [kg CO_2/ton RLCA]	138	-	128	-	123
CO_2-absorption potential [kg CO_2/ ton RLCA]	203	-	194	-	193

4.1.2. Uniformity control of RLCA mechanical properties

Compressive strength is a key parameter in concrete technology. Since the strength of LC can be limited by the strength of the LWA used [15], it is important to estimate the strength of the LWA or to ensure uniformity of strength potential. In the context of concrete recycling, this applies to ensuring uniformity of the strength potential of RLCA in different batches of recycled material (ILC_{Origin}).

Fig. 5 shows the relationship between dry density and compressive strength (Fig. 5 left) for four concreting operations (G0 – G3) using RLCA. Fig. 5 (right) provides the corresponding statistical variation within these defined mix designs. The results indicate comparable mean compressive strengths between 11.6 and 14.9 N/mm^2 across the four operations, with a range of 3.3 N/mm^2. The variation within each batch is relatively small with a standard deviation between 0.5 and 0.9 N/mm^2 and coefficients of variation between 0.03 and 0.08. Therefore, the RLCA can be expected to have a consistent strength capability. Furthermore, the compressive strength values achieved with RLCA are higher than the values of ILC_{Origin} (6.8 N/mm^2, see Table 8), from which the RLCA is derived. This indicates that the strength of RILC is not limited by the strength of the original ILC, allowing the RLCA to be used for different strength and density classes broadening recycling and reuse strategies for ILC`s.

4.2. Performance parameter of RILC

Design and performance characteristics need to be verified to ensure the material`s suitability for structural applications. First, the basic material properties typical for LC design are assessed using standardized testing methods. Next, parameters that may be unfavorably affected by the unique properties of the RLCA are investigated. In this study, these parameters are identified as plastic shrinkage, modulus of elasticity and sustained loading. Evaluating them is crucial to validate the efficiency of the recycling process and to compare performance parameters with benchmark ILC (ILC_{Origin}).

The performance parameters obtained for ILC_{Origin} and RILC, along with the percentage change in these parameters, are summarized in Table 8. Fig. 6 provides a microstructural view of RILC as observed under a scanning electron microscope. The image highlights the RLCA embedded within the newly formed cement paste.

The agglomerate structure of the RLCA (highlighted in the yellow circle) is clearly visible within the new cement paste of the RILC. Fig. 6 (1−4) highlights key features of RILC`s microstructure. (1) The pores within the RLCA predominantly exhibit a compact appearance of the expanded LWA from ILC_{Origin}, with no visible hydrate or carbonated phases. Several microcracks are evident within the RLCA, caused by the mechanical fragmentation process using a jaw crusher. (2) Newly formed calcium silicate hydrate needles are visible within the pores of the cement paste. (3&4) Pores of the ITZ between RLCA and cement paste forming a bridge between (3) the inside of the RLCA and (4) the area directly outside the RLCA. The pores exhibit the formation of new hydration products on the RLCA surfaces. In (3), calcium silicate hydrate phases appear to infiltrate the RLCA`s pores from the bottom left, while

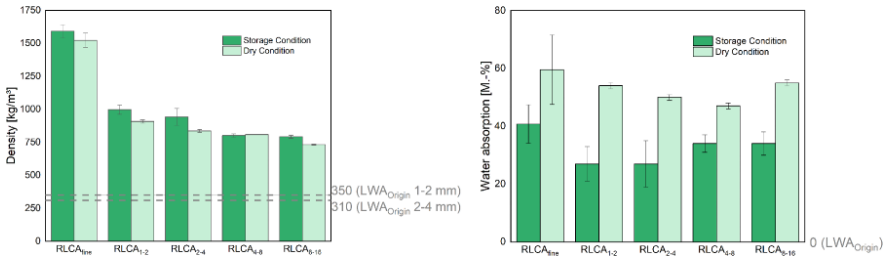

Fig. 4. – Particle density and water absorption of RLCA subdivided in grain fractions. Particle density of origin ILC's aggregates used (expanded glass) is given to illustrate the increase in density. Differentiation between storage condition (~ 20 °C / 65 % rel. humidity) and oven dry condition (mass constancy at 105 °C).

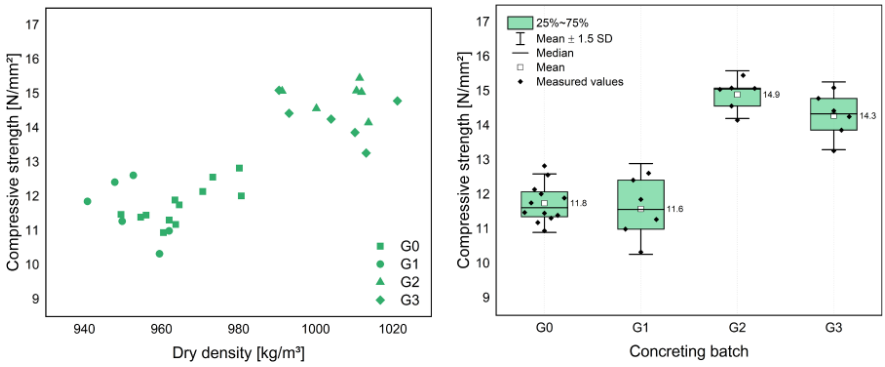

Fig. 5. Left: Compressive strength of four concreting operations in relation to dry density. Right: Compressive strength and statistical variation of these four concreting operations to assess uniformity of strength potential of RLCA within different charges of recycling material (recycled ILC).

Table 8
Summarized results for performance parameters of RILC and ILC$_{Origin}$.

Property	ILC$_{Origin}$	RILC	Change in RILC vs. ILC$_{Origin}$ [%]
Plastic Shrinkage [mm/m]	−0.96	−0.87	−9.4
Dry Density [kg/m³]	570[a]	750	31.6
Compressive Strength [N/mm²]	6.8[a]	7.1	4.4
Thermal Conductivity [W/(m•K)]	0.154[a]	0.159	3.3
Modulus of Elasticity [N/mm²]	3370[a]	3750	11.4
Sustained Loading [-]	0.84	0.80	−4.8

[a] Values determined in [67]

in (4) newly formed pores directly connected to the ITZ show the embedding of RLCA in RILC.

Overall, these agglomerates contain a higher amount of adhered cementitious material compared to RCA derived from normalweight concrete. This higher adherence contributes to the unique properties observed in RILC. Surrounding the RLCA is a distinct compacted ring, denser than the surrounding hardened cement paste, indicating a good embedding of the RLCA in the RILC cement matrix. This densification can be attributed to adsorption effects and the formation of new hydrate phases between the RLCA and the cement paste, leading to improved interfacial bonding and reduced porosity in this region.

4.2.1. *RILC - mix design optimization, density control and thermal conductivity*

Fig. 7 outlines the mix design methodology. In LC, the declaration of the volumetric mix design often lags information about air void content, as reported by Thienel et al. [15]. Unlike normalweight concrete, verifying the calculated air volume in LC is challenging, as the commonly used technique of air control by pressure method [94] is not suitable, since it cannot distinguish between air voids in the paste and porous LWA [15]. In addition, variations in RLCA density and water absorption, as well as the efficiency of the air entraining agent in creating fine dispersed pores in the new binder paste combined with the mixing and compaction technology used, make it challenging to achieve reliable mix design. Therefore, it is crucial to evaluate both the measured and calculated fresh density, as well as to control the yield (volume of concrete produced from a mixture of predetermined proportions of constituents [84]). Fig. 7 (left) shows the measured fresh density and yield for nine concreting batches in the RILC test series. The calculated air content is 18.5 % per cubic meter (see Table 4), resulting in a calculated fresh density of 1088 kg/m³ . The results show a measured mean fresh density of the nine concreting batches of 1078 kg/m³ , with a maximum deviation of 77 kg/m³ for a single sample from the calculated value. This is within the normative limits for similar types of concrete (e.g. LAC according to EN 1520 [20]), emphasizing the robustness of the mix design.

The measured yield in the RILC test series ranges from 92 % to 102 % of the calculated volume, with variations likely due to the variability in density and moisture content of RLCA. Regular control of measured and calculated density and yield is important to avoid errors in concrete

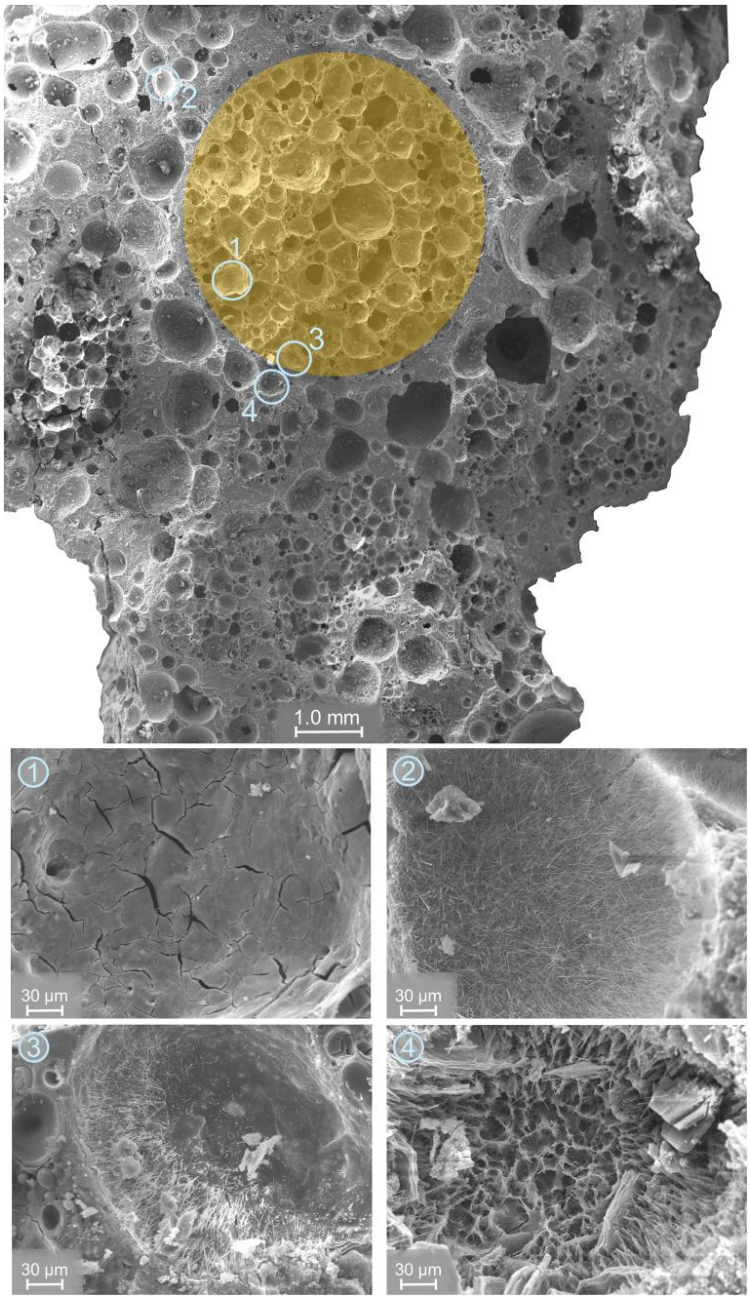

Fig. 6. Microstructure of RILC in newly formed cement paste under a scanning electron microscope. Left: Stage Scan of RILC, the yellow circle shows RLCA with a dense ITZ. Right: (1) Pore inside RLCA. (2) Pore inside the new cement paste. (3&4) Pores of the ITZ between RLCA and cement paste forming the bridge between (3) inside the RLCA and (4) directly outside the RLCA.

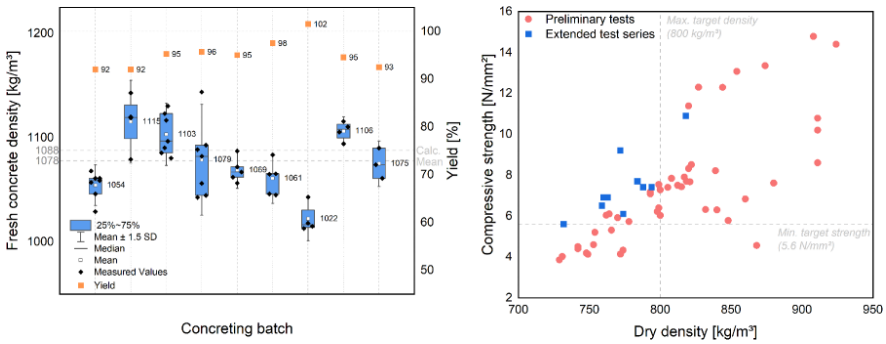

Fig. 7. Results for mix design optimization for production of RILC aiming to reproduce ILC_{Origin}. Left: Fresh concrete density with reference to calculated density and average density over all concrete batches, second y-axis is giving yield of RILC for each concrete batch. Right: Relationship between dry density and compressive strength on cubes (100 mm) after 28 days for RILC (blue) with reference to preliminary tests (red) for reaching target density and compressive strength to reproduce ILC_{Origin}.

properties and to adjust changes in constituent properties. Fig. 7 (right) illustrates the iterative process of mix design, aimed at reproducing ILC_{Origin} with a maximum target density of 800 kg/m^3 and a minimum target strength of 5.6 N/mm^2. In the RILC test series, the average dry density was measured at 750 kg/m^3 from 16 cylinders, with a coefficient of variation of 0.02. Thermal conductivity, measured on oven-dried material, yielding an average value of 0.159 W/(m•K) based on measurements from four cubes, with a coefficient of variation of 0.06. This represents only a 3.3 % increase in thermal conductivity, which is significantly lower than expected given the 31.6 % increase in dry density compared to ILC_{Origin}. Based on a normative estimate (EN 1520 [20]), a thermal conductivity of 0.205 W/(m•K) would have been expected. Thus, RILC achieves almost the same thermal performance as ILC_{Origin}. The reason for the relatively small increase in thermal conductivity cannot yet be conclusively explained. However, two potential hypotheses are worth investigating to better understand their effects on thermal performance. First, the more porous cement paste matrix in RILC compared to ILC_{Origin}, and second, the effect of partially carbonated RLCA. Additionally, as already observed within the test series for uniformity of strength capabilities (see Fig. 5), the results show that the compressive strength of recycled concrete using RLCA is not limited to the strength of ILC_{Origin}.

4.2.2. Plastic shrinkage

The early age shrinkage strain is of particular interest for the RILC under investigation, since the water migration between RLCA and cement paste is expected to have a major impact on deformation behaviour. Fig. 8 compares the initial plastic shrinkage deformations of RILC (right) with benchmark ILC_{Origin} (left), measured from the fresh state over a period of 72 hours.

The average shrinkage results for ILC and RILC are similar, with values at 72 hours recorded as −0.96 mm/m and −0.87 mm/m, respectively. Most of the deformation occurs within the first 8 hours after water addition, after which remains constant. RILC shows higher variation in shrinkage strain, mainly due to the higher variability in RLCA water absorption compared to the industrial produced LWA used in ILC_{Origin}.

Shrinkage describes time-dependent and load-independent deformations when concrete loses moisture and undergoes volumetric changes due to various mechanisms such as drying, autogenous processes, and carbonation [95]. Especially in constrained conditions these deformations can lead to initiation and propagation of cracking which may provide pathways for water and harmful substances resulting in corrosion of embedded steel, deterioration of concrete and a compromised structural and thermal performance [95,96]. In general, lightweight concretes exhibit higher shrinkage values compared to normalweight concrete [95]. The shrinkage behavior is largely influenced by the properties of the LWA, such as its modulus of elasticity, porosity and stage of water saturation [95–97]. These properties significantly influence the water mitigation between LWA and cement

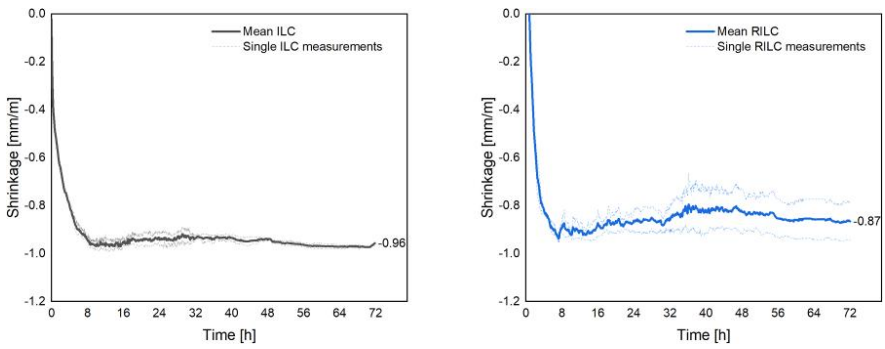

Fig. 8. Plastic shrinkage strain over period of 72 hours for RILC (right) and reference ILC_{Origin} (left).

paste, as well as the LWA`s ability to restrain shrinkage of the surrounding cement matrix.

With reference to this, it can be concluded that similar shrinkage behavior of recycled concrete made from RLCA are expected, as long as additional water uptake is accounted for in a manner similar to LWA measurements as described in section ↱3.4.1.

4.2.3. Mechanical properties of RILC

The mechanical properties of RILC play a crucial role in determining its suitability for structural applications. In LC design, both density and strength are the most important parameters and this applies for RILC as well. Achieving the right balance between reducing density while maintaining sufficient strength is essential. Moreover, for elements where thermal performance is relevant, the relationship between density and thermal conductivity must also be considered.

The following section compares RILC`s mechanical properties to those of other established lightweight concretes, including the reference material $ILC_{Origin}$. The correlation between dry density and compressive strength for RILC is plotted in Fig. 9 (top left). Similar to what is observed for LAC [98] and other LC`s [99], RILC`s compressive strength tends to increase with higher density, as a denser structure generally indicates reduced porosity and better load-bearing capacity. However, several factors must be taken into account when considering the fluctuations in RILC strength. Variations in RLCA density and water absorption impact the resulting density of the hardened RILC and affect the balance between RLCA, cement paste and water. Typically, RLCA with higher particle density and lower porosity will yield higher strength in the hardened concrete. These factors, along with the normal variations in concrete production, compaction and testing, contribute to the observed variability in compressive strength.

Fig. 9 (top right) illustrates the variation in compressive strength, based on tests from nine cylinders across different batches. The mean compressive strength after 28 days is 7.1 N/mm^2, with a standard deviation of 0.9 N/mm^2, which is consistent with LAC`s of similar strength. The characteristic compressive strength, calculated according to EN 1520 [20], is 5 N/mm$^2$, matching the characteristic compressive strength of $ILC_{Origin}$ (see Table 8). Therefore, the study`s objective of achieving the same strength as ILC_{Origin} is accomplished.

Understanding the stress-strain relationship of concrete is essential for assessing load-bearing capacity and deformation, both of which are critical for ensuring structural integrity, optimized design, and effective reinforcement strategies. Fig. 9 (top right) shows RILC`s stress-strain curve under compression, where it initially exhibits linear elastic behavior. Unlike normalweight concrete, RILC shows little plastic deformation, leading to a more sudden failure. Fig. 9 (bottom left) presents decreasing ultimate strain values with decreasing dry density. This trend is also reflected in the normative estimation of the ultimate strain (ε_{cu}), which can be calculated according to EN 1520 [20] using a coefficient (η_1) as a function of the dry density (ρ) using the following formula:

$$\varepsilon_{cu} = 0.0035 \bullet \eta_1 \geq 0.002, \text{with} \eta_1 = 0.4 + 0.6 \bullet \left(\frac{\rho}{2200}\right) \quad (2)$$

The observed lower plastic deformation and reduced ultimate strain were also noted in ILC by Hückler et al. [16]. Therefore, these characteristics are more inherent to very light lightweight concretes rather than direct results of the recycling process or the use of RLCA. Nevertheless, as with ILC, RILC`s lower ultimate strain requires careful design

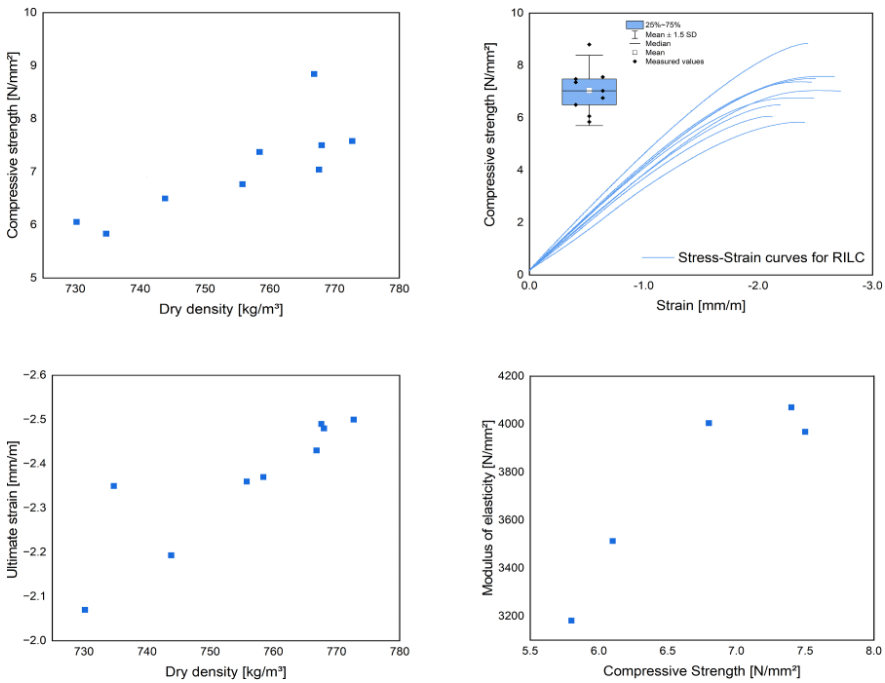

Fig. 9. Compressive strength tests on RILC cyclindirc forms. Top Left: Compressive strength in relation to dry density. Top Right: Stress strain curves and Box-Whiskyer plot for statistical variation of compressive strength reuslts.Bottom Left: Ultimate strain in compression test in relation to dry density. Bottom Right: Modulus of elasticity in relation to compressive strength.

considerations to prevent excessive deformation and brittle failure.

The modulus of elasticity reflects the stiffness of concrete and its ability to deform under stress. Fig. 9 (bottom right) provides the results for RILC`s modulus of elasticity and its relationship with compressive strength, indicating that an increase in compressive strength is accompanied by an increase in the modulus of elasticity. According to EN 1520 [20], the mean modulus of elasticity (E_{cm}) of LAC with dry density of 1400 kg/m^3 or less can be estimated based on mean dry density (ρ) and characteristic compressive strength (f_{ck}) using the following formula:

$$E_{cm} = 10000 \bullet f_{ck}^{\frac{1}{3}} \bullet 0.64 \quad \bullet \left(\frac{\rho}{2200}\right) \tag{3}$$

For the RILC in this study, the estimated modulus of elasticity, calculated according to the given formula, is 3730 N/mm^2. This is very close to the experimentally determined mean value of 3750 N/mm^2, based on five independent measurements with a standard deviation of 385 N/mm^2. It is important to note that the normative and empirical determination of the modulus of elasticity applies to all LWAs approved by this standard, representing an average relationship that does not account for the unique characteristics of individual LWA`s. These results demonstrate that the use of RLCA in RILC can yield moduli of elasticity similar to those LAC using common LWA.

The experimentally determined threshold for sustained loading of both RILC and ILC is shown in Fig. 10. For RILC, the relationship between longitudinal strain and applied stress under sustained loading is linear at lower stress levels but exhibits a slight plasticity as compressive stress increases, eventually leading to an extended plastic deformation plateau. The coefficient α, which accounts for long-term effects on the compressive strength, was found to be 0.80 for RILC and 0.84 for ILC_{Origin}. These values fall within the suggested range of 0.75–0.85, according to Eurocode National Annex [87] for LC and according to DIN EN 1520 [20] for LAC respectively. Consequently, the generalized normative reduction factor α effectively describes the long-term behavior of RILC under compression. However, in some cases, this value may be on the lower side, potentially overestimating the load-bearing capacity. This is consistent with findings reported by Schlaich et al. [18], where a similar experimental program on ILC founded an experimentally determined α value of 0.78 and the authors subsequently recommended using a generalized reduction factor of α = 0.75 for ILC.

Overall, RILC demonstrates uniform load transfer under sustained compression, in line with normative behavior. Nonetheless, applying a more conservative reduction factor α, as proposed by Schlaich et al. for ILC [18], is recommended to ensure reliable long-term performance.

4.3. CO_2 absorption potential of RLCA

The carbonation of RLCA was investigated to understand its CO_2 uptake potential at end-of-life of ILC elements. Fig. 11 shows the CO_2 uptake of the three different RLCA particle size groups after conditioning (0 days) and after 3, 7 and 10 days of controlled CO_2 exposure. The bars on the right sum up the CO_2 uptake of the four different exposure times, with the white bars indicating the remaining carbonation capacity, which decreases from left to right as carbonation progresses. The calculated carbonation capacity (see section ↱3.6 and Table 9, Appendix C. – Potential CO2 uptake) differs only slightly between the RLCA with $RLCA_{fine}$ having the highest value of 203 kg/t, compared to 194 kg/t for $RLCA_{2–4}$ and 193 kg/t for $RLCA_{8–16}$. This indicates just a slight enrichment of the binder in the finer particle size groups, which is plausible due to the random fragmentation of the LWAs and hardened cement paste during recycling.

The 0-day results reveal the CO_2 uptake of ILC_{Origin} under natural conditions before being crushed into RLCA, which is approximately 30 kg/t_{RLCA} for all particle size groups. This supports initial observations on the carbonation behavior of ILC, which has not yet been conclusively clarified for the still young building material, but can be assumed to progress faster than in normalweight concrete as reported by Lösch et al. [100]. Given that RLCA is composed of approximately 46 % LWA and 54 % adhering cement paste by weight (see Table 9, Appendix C. – Potential CO2 uptake), it can be estimated that the cement paste has absorbed around 55 kg of CO_2 through natural carbonation. Against this background, the target value of 51 kg CO_2 per ton of cement paste, as outlined in the carbon neutrality roadmaps for the cement and concrete industry [5,49], seems achievable. Furthermore, the applied methodology effectively assesses the natural carbonation status of the RLCA, which is highly dependent on the microenvironment of the exposed concrete surfaces as reported by Lagerblad [101], making general estimations difficult.

During the first carbonation interval (0–3 d), smaller particles ($RLCA_{fine}$) facilitate a faster CO_2 uptake due to their higher surface area. However, this trend reverses in the second carbonation interval (3–7 d) where $RLCA_{2–4}$ and $RLCA_{8–16}$ reach higher values. Subsequently, in the third carbonation interval (7–10 d), the carbonation slows down significantly, with only slight increases in $RLCA_{8–16}$. Overall, these findings are in line with Fang et al. [51], who observed a higher cement paste content and a faster CO_2 uptake for smaller particle sizes of RCA. However, the enrichment of hardened cement paste in smaller particle sizes is less pronounced for ILC than for normalweight concrete. The total CO_2 uptake for $RLCA_{fine}$ is 138, for $RLCA_{2–4}$ 128 and for $RLCA_{8–16}$ 123 kg/t_{RCLA}, corresponding to relative CO_2 uptakes of 68, 66 and 64 % of their calculated carbonation capacity, respectively. This indicates that

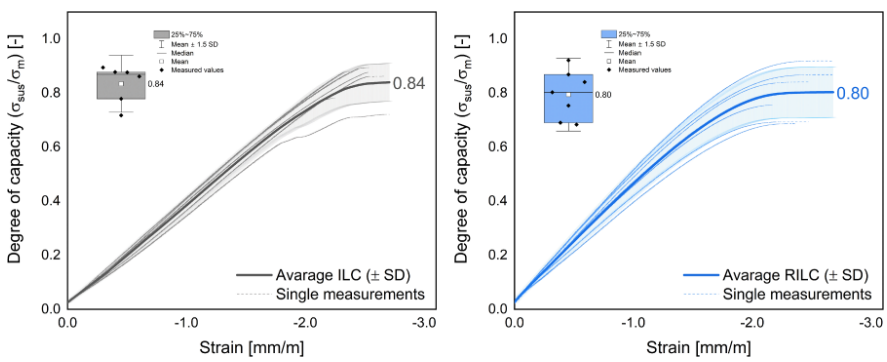

Fig. 10. Relative load capacity ($\sigma_{sustained}/\sigma_{28days}$) of the compressive strength under sustained loading for reference ILC_{Origin} (Left) and RILC (right).

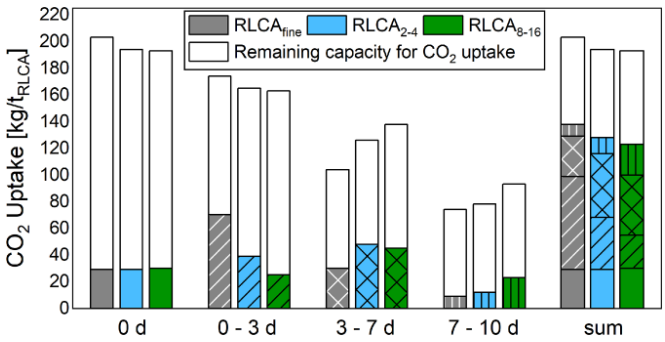

Fig. 11. CO_2 uptake of the three different RLCA after conditioning (0 days, natural carbonation status) and after 3, 7 and 10 days of CO_2 exposure. The bars on the right show the sum of the four different time points.

although initial carbonation is faster in smaller particles, the total CO_2 uptake potential is similar across different particle sizes for RLCA. These observations provide insight into the carbonation that may occur between the demolition, processing and reuse of ILC.

Comparing these results with existing literature is challenging due to differences in carbonation conditions and the distinct properties of normalweight and lightweight concretes. However, reference values by Richter [102] for ILC, with typical volume fractions of cement and LWA, proposes a global warming potential between 255 and 295 kg CO_2-equivalent per cubic meter. For ILC_{Origin}, it can be assumed that approximately 680 kg of RLCA can be recovered from one cubic meter of ILC_{Origin} through recycling, corresponding to a CO_2 recovery of approximately 83 kg per cubic meter, or 30 % of the total greenhouse gas emissions of ILC_{Origin}.

This study provides a general estimate of RLCA`s suitability for targeted carbonation at the end-of-life of ILC elements. The practical application of targeted carbonation will need to consider at which phase of the life cycle the absorbed CO_2 can be credited. According to Lagerblad [101] this could be either during service life of the concrete, after demolition and secondary use or at the end-of-life. Another important consideration is how the RLCA can be specifically carbonated. While this study used a relative low concentration of CO_2 (0.5 % by volume), other studies suggest that CO_2 uptake increases with concentration up to about 10 % by volume [51,62]. Targeted carbonation near cement, concrete or precast plants, where exhaust gases containing approximately 15 % CO_2 by volume, as reported by Sereng et al. [62], could significantly enhance carbonation efficiency.

Overall, RLCAs have significant CO_2 uptake potential, contributing to the sustainability of lightweight concretes. Future research should focus on the practical implementation of RLCA carbonation, investigating different types of lightweight concrete, and integration into life cycle assessments to maximize environmental benefits.

5. Conclusion

The study addresses the significant problem of limited recycling strategies for LC, particularly very light LC like ILC, which are excluded from normative recycling practices. The methodology involved characterizing RLCAs processed from ILC and subsequently producing RILC, aiming to replicate the properties of the original ILC (ILC_{Origin}). This approach promotes material circularity, reduces CO_2 emissions, and validates the structural performance of the recycled material, thereby contributing to more sustainable construction practices. The main findings can be summarized as follows:

1. The RLCA`s exhibit an agglomerate structure, because crushing of LC`s also breaks up the initial LWAs, which is a major difference from recycling of normalweight concrete.
2. Density and water absorption of RLCA are key parameters for successful integration into recycled concrete mix design. RLCA exhibit particle densities ranging from 730 to 1590 kg/m^3 , approximately three times higher than particle densities of the initial LWA within the same size group. Water absorption rates vary between 27 % and 60 % by mass, with higher values observed under oven-dry conditions compared to laboratory conditions. These factors are critical for successful integration into recycled concrete mix design.
3. A simple and reproducible method confirmed the consistent quality and strength potential of RLCA across different batches of recycled material. Notably, the strength of recycled concrete produced from RLCA is not limited to the strength of the original ILC, indicating that reuse according to type is not necessary.
4. RILC produced from RLCA has comparable strength, modulus of elasticity, and thermal conductivity to ILC_{Origin}. Specifically, the same strength classification was achieved, and long-term behavior under compression is expected to follow principles of ILC_{Origin}. The increase in thermal conductivity of RILC was minimal (3.3 %) despite a significant increase in dry density (31.6 %), indicating that RILC maintains almost the same performance properties as ILC_{Origin}. In fact, monolithic wall elements with the same performance parameters could be built solely using RLCA`s.
5. Accelerated carbonation of RLCA led to substantial CO_2 uptake, with smaller particle sizes showing faster initial carbonation. After 10 days of conditioning in a controlled environment containing 0.5 % CO_2 by volume, maximum CO_2 uptake ranged between 123 and 138 kg/t of RLCA. This corresponds to a relative CO_2 uptake of 64–68 % in relation to the calculated total CO_2 uptake potential and an approximate 30 % recapture of the greenhouse gas emissions of ILC_{Origin}. Taking into account the proportion of adherent cement paste in the RLCA, a CO_2 uptake of about 55 kg per ton of cement paste was determined after about 32 months of natural carbonation.

Future research should focus on the integrating different types of lightweight concrete, optimizing carbonation processes for RLCA, and evaluating the practical application of targeted RLCA carbonation in life cycle assessments to maximize environmental benefits.

CRediT authorship contribution statement

Scherb Sebastian: Writing – review &editing, Methodology, Investigation, Data curation. **Haller Timo:** Writing – original draft, Methodology, Investigation, Data curation, Conceptualization. **Thienel**

Karl-Christian: Writing – review & editing, Supervision, Methodology, Conceptualization. **Beuntner Nancy:** Writing – review & editing, Supervision, Methodology, Conceptualization.

Declaration of generative AI and AI-assisted technologies in the writing process

During the preparation of this work, the authors used GPT-3.5 and DeepL in order to improve the language and readability. After using these services, the authors reviewed and edited the content as needed and take full responsibility for the content of the publication.

Declaration of Competing Interest

The authors declare that they have no known competing financial interests or personal relationships that could have appeared to influence the work reported in this paper.

Appendix A. – TGA

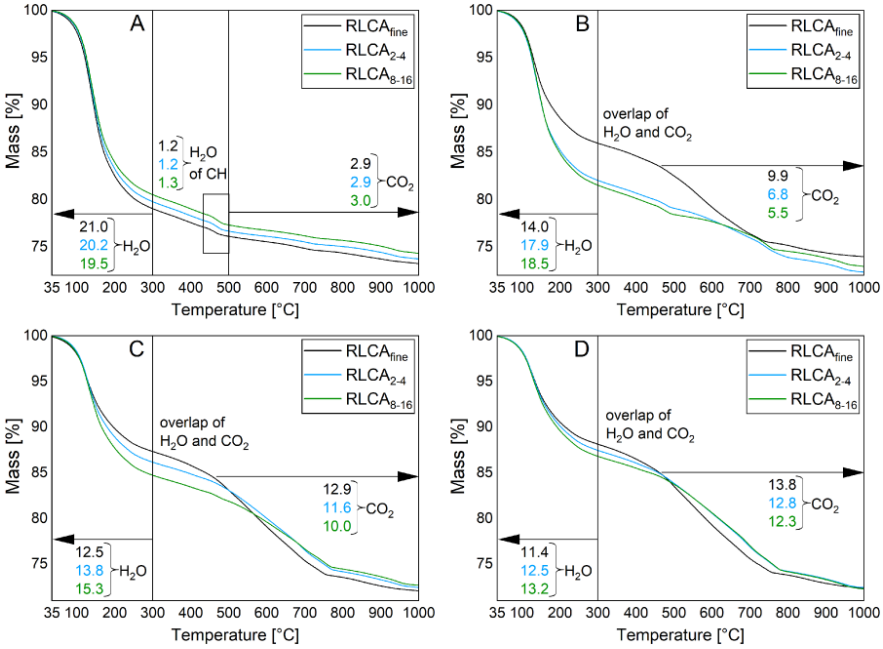

Figure 12 - TGA of the different RLCA after conditioning (0 days, A) and after 3 (B), 7 (C) and 10 days (D) of CO2 exposure. The values of the bound water and CO2 (used for calculation of the CO2 uptake) are added in the figure

Appendix B. – FTIR

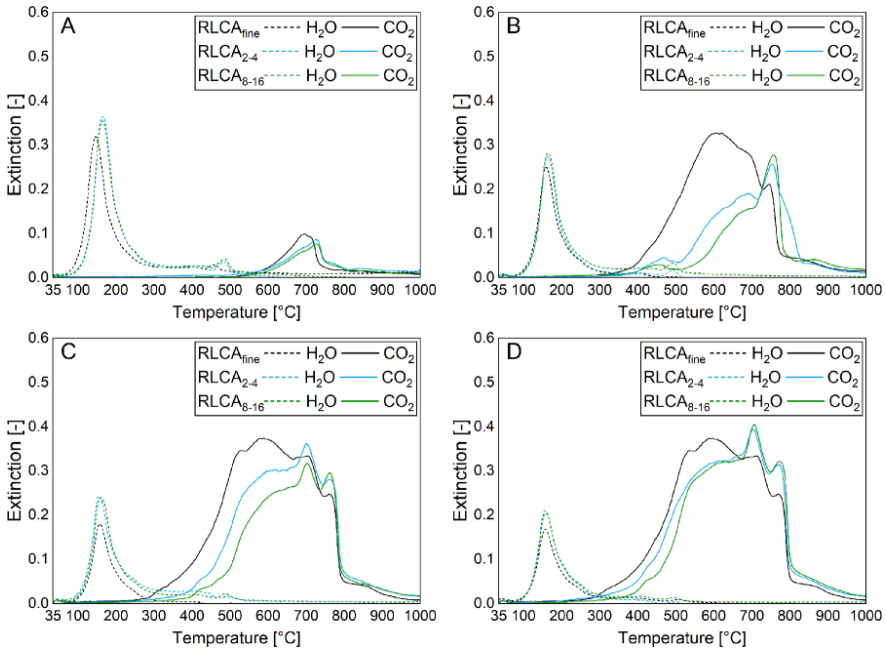

Figure 13 - Extinction of the FTIR signal of the gases released during TGA as a function of temperature after conditioning (0 days, A) and after 3 (B), 7 (C) and 10 days (D) of CO2 exposure. For water, the FTIR band at 1508 cm-1 and CO2 at 2359 cm-1 were used for the evaluation

Appendix C. – Potential CO_2 uptake

Table 9
Potential CO_2 uptake

	$RLCA_{fine}$	$RLCA_{2–4}$	$RLCA_{8–16}$
Amount of LWA in RLCA based on the Na_2O content [wt%]	43	46	48
Residue CaO for CO_2 uptake ($m_{CaO\text{-}CO2}$) [kg/t]	258	247	246
Potential of CO_2 uptake [kg/t]	203	194	193

Data availability

Data will be made available on request.

References

[1] J. Kim, A.M. Grabiec, A. Ubysz, An experimental study on structural concrete containing recycled aggregates and powder from construction and demolition waste, Materials (2022).
[2] J. Kim, Construction and demolition waste management in Korea: recycled aggregate and its application, Clean. Technol. Environ. Policy 23 (8) (2021) 2223–2234.
[3] H. Yang, J. Xia, J.R. Thompson, R.J. Flower, Urban construction and demolition waste and landfill failure in Shenzhen, China, Waste Manag. 63 (2017) 393–396.
[4] A. Müller, , Progresses and challenges in recycling of construction and demolition waste. International Conference of Recycling in Built Environment, RILEM Publications S.A.R.L, Weimar, Germany, 2023.
[5] V. Verein Deutscher Zementwerke e, Ressourcen der Zukunft für Zement und Beton, Düsseldorf, Germany, 2022, p. 56.
[6] M. Zajac, J. Skocek, M. Ben Haha, J. Deja, CO2 Mineralization Methods in Cement and Concrete Industry, Energies 15 (10) (2022) 3597.
[7] A. Saxena, S.S. Sulaiman, M. Shariq, M.A. Ansari, Experimental and analytical investigation of concrete properties made with recycled coarse aggregate and bottom ash, Innov. Infrastruct. Solut. 8 (7) (2023) 197.
[8] S.V. Zito, E.F. Irassar, V.F. Rahhal, Recycled construction and demolition waste as supplementary cementing materials in eco-friendly concrete, Recycling 8 (4) (2023) 54.
[9] A.M. Müller, Isabel, Recycling of Building Materials - Generation - Processing - Utilization, 1 ed, Springer Vieweg, Wiesbaden, 2022.
[10] DIN EN 933-11, Prüfverfahren für geometrische Eigenschaften von Gesteinskörnungen – Teil 11: Einteilung der Bestandteile in grober recyclierter Gesteinskörnung (Tests for geometrical properties of aggregate -Part 11: Classification test for the constituents of coarse recycled aggregate), Beuth Verlag GmbH, Berlin, Germany, 2011, p. 15.
[11] DIN 4226-101, Rezyklierte Gesteinskörnungen für Beton nach DIN EN 12620 – Teil 101: Typen und geregelte gefährliche Substanzen (Recycled aggregates for

concrete in accordance with DIN EN 12620 – Part 101: Types and regulated dangerous substances), 2017, p. 11.
[12] DIN 1045-2, Tragwerke aus Beton, Stahlbeton und Spannbeton – Teil 2: Beton (Concrete, reinforced and prestressed concrete structures – Part 2: Concrete), Beuth-Verlag, Berlin, Germany, 2023, p. 62.
[13] M.S. de Juan, P.A. Gutiérrez, Study on the influence of attached mortar content on the properties of recycled concrete aggregate, Constr. Build. Mater. 23 (2) (2009) 872–877.
[14] J. Scheidt, Einfluss der Wasseraufnahme von rezyklierten Gesteinskörnungen auf den Wasserzementwert von R-Beton, Beton 70 (4) (2020) 2–8.
[15] K.-C. Thienel, T. Haller, N. Beuntner, Lightweight concrete—from basics to innovations, Materials 13 (5) (2020) 1120.
[16] A. Hückler, M. Schlaich, Zur Biegung von Infraleichtbetonbauteilen – Werkstoff-, Verbund-, Trag- und Verformungsverhalten, Beton- und Stahlbetonbau 112 (5) (2017) 282–292.
[17] C. Lösch, A. Hückler, M. Schlaich, Infraleichtbeton, Bauphysik 41 (1) (2019) 1–6.
[18] M. Schlaich, A. Hückler, C. Lösch, Infraleichtbeton (ILC), in: K. Bergmeister, F. Fingerloos, J.-D. Wörner (Eds.), Beton-Kalender 2021, Ernst & Sohn GmbH & Co. KG, Berlin, Germany, 2021, pp. 909-952.
[19] B. Callsen, K.-C. Thienel, Besondere Aspekte bei der Entwicklung und Ausführung eines hochwärmedämmenden Hochleistungs-Leichtbetons mit sehr niedriger Betonrohdichte, Beton 67 (4) (2017) 128–134.
[20] DIN EN 1520, Vorgefertigte Bauteile aus haufwerksporigem Leichtbeton und mit statisch anrechenbarer oder nicht anrechenbarer Bewehrung (Prefabricated reinforced components of lightweight aggregate concrete with open structure with structural and non-structural reinforcement), Beuth Verlag GmbH, Berlin, Germany, 2011, p. 119.
[21] S. Akçaözoglu, C. Ulu, Recycling of waste PET granules as aggregate in alkali-activated blast furnace slag/metakaolin blends, Constr. Build. Mater. 58 (2014) 31–37.
[22] J.M. Abed, B.A. Khaleel, I.S. Aldabagh, N.H. Sor, The effect of recycled plastic waste polyethylene terephthalate (PET) on characteristics of cement mortar, J. Phys.: Conf. Ser. 1973 (1) (2021) 012121.
[23] S.I. Basha, M.R. Ali, S.U. Al-Dulaijan, M. Maslehuddin, Mechanical and thermal properties of lightweight recycled plastic aggregate concrete, J. Build. Eng. 32 (2020) 101710.
[24] S. Talukdar, S.T. Islam, N. Banthia, Development of a lightweight low-carbon footprint concrete containing recycled waste materials, Adv. Civ. Eng. 2011 (2011) 594270.
[25] C. Parra, E.M. Sánchez, I. Miñano, F. Benito, P. Hidalgo, Recycled plastic and cork waste for structural lightweight concrete production, Sustainability 11 (7) (2019) 1876.
[26] A. Petrella, M. Petrella, G. Boghetich, D. Petruzzelli, D. Calabrese, P. Stefanizzi, D. De Napoli, m Guastamacchia, Recycled waste glass as aggregate for lightweight concrete, Proc. Inst. Civ. Eng. - Constr. Mater. 160 (4) (2007) 165–170.
[27] D. Kralj, Experimental study of recycling lightweight concrete with aggregates containing expanded glass, Process Saf. Environ. Prot. 87 (4) (2009) 267–273.
[28] S.-Y. Chung, M. Abd Elrahman, P. Sikora, T. Rucinska, E. Horszczaruk, D. Stephan, Evaluation of the effects of crushed and expanded waste glass aggregates on the material properties of lightweight concrete using image-based approaches, Materials 10 (12) (2017) 1354.
[29] DIN EN 13055-1, Leichte Gesteinskörnungen Teil 1: Leichte Gesteinskörnungen für Beton, Mörtel und Einpressmörtel (Lightweight aggregates — Part 1: Lightweight aggregates for concrete, mortar and grout), Beuth-Verlag GmbH, Berlin, Germany, 2002, p. 39.
[30] A. Wongkvanklom, P. Posi, B. Khotsopha, C. Ketmala, N. Pluemsud, S. Lertnimoolchai, P. Chindaprasirt, Structural lightweight concrete containing recycled lightweight concrete aggregate, KSCE J. Civ. Eng. 22 (8) (2018) 3077–3084.
[31] J. Suchorzewski, N. Chitvoranund, S. Srivastava, M. Prieto, K. Malaga, Recycling potential of cellular lightweight concrete insulation as supplementary cementitious material, in: A. Jóźwiak-Niedźwiedzka, F. Kanavaris, M. Azenha, F. Benboudjema, D. Schlicke (Eds.), International RILEM Conference on Synergising Expertise towards Sustainability and Robustness of Cement-based Materials and Concrete Structures - SynerCrete'23, I, Springer Nature Switzerland, Milos, Greece, 2023, pp. 133–141.
[32] F. Hlawatsch, M. Peters, D. Ufermann-Wallmeier, Leichter Schaumstein aus groben Porenbetongranulaten im zweiten Nutzungszyklus – RC-Schaumstein, ce/Pap. 6 (6) (2023) 867–874.
[33] Y. Zhao, J. Gao, F. Chen, C. Liu, X. Chen, Utilization of waste clay bricks as coarse and fine aggregates for the preparation of lightweight aggregate concrete, J. Clean. Prod. 201 (2018) 706–715.
[34] I. Wichmann, R. Firdous, D. Stephan, Upcycling of demolition material from concrete and brick for the production of cold-bound, alkali-activated lightweight aggregates, Mater. Struct. 56 (7) (2023) 135.
[35] F. Tajra, M.A. Elrahman, D. Stephan, The production and properties of cold-bonded aggregate and its applications in concrete: a review, Constr. Build. Mater. 225 (2019) 29–43.
[36] B. Leydolph, A. Müller, U. Palzer, Sustainability benefits of lightweight concrete: Recycling of lightweight concrete, BFT Int. 82 (2) (2016) 127–129.
[37] A. Mueller, A. Schnell, K. Ruebner, The manufacture of lightweight aggregates from recycled masonry rubble, Constr. Build. Mater. 98 (2015) 376–387.
[38] H.G.A. Kouwenhoven, M.-L. Peters, Economic Design and Construction with Light Weight Aggregate Concrete. Recycling Lightweight Aggregate Concrete, EuroLightCon, European Union – Brite EuRam III, 2000.
[39] DIN EN 206, Beton – Festlegung, Eigenschaften, Herstellung und Konformität (Concrete - Specification, performance, production and conformity), Beuth Verl. GmbH, Berl., Ger. (2021) 105.
[40] J. Kümmel, Ökobilanzierung von Baustoffen am Beispiel des Recyclings von Konstruktionsleichtbeton, Fak. ät Bauing. - und Vermess., Univ. ät Stuttg., Stuttg. (2000) 169.
[41] J.A. Bogas, J. de Brito, J. Cabaço, Long-term behaviour of concrete produced with recycled lightweight expanded clay aggregate concrete, Constr. Build. Mater. 65 (2014) 470–479.
[42] J.A. Bogas, J. de Brito, J.M. Figueiredo, Mechanical characterization of concrete produced with recycled lightweight expanded clay aggregate concrete, J. Clean. Prod. 89 (2015) 187–195.
[43] L. Huang, Z. Yang, Z. Li, Y. Xu, L. Yu, Recycling of the end-of-life lightweight aggregate concrete (LWAC) with a novel approach, J. Clean. Prod. 275 (2020) 123099.
[44] J. de Brito, N. Saikia, Recycled Aggregate in Concrete - Use of Industrial, Construction and Demolition Waste, Springer-Verlag, London, London, 2013.
[45] J. Dahms, G. Brune, Wasseraufnahme und Rohdichte von Betonbruch, Beton 46 (8) (1996) 480–486.
[46] Expanded Clay and Slate Institute, Internal Curing Using Expanded Shale, Clay and Slate Lightweight Aggregate, Publication #4362, Expanded Shale, Clay & Slate Institute, Salt Lake City, UT, 2006..
[47] G.W. Groves, A. Brough, I.G. Richardson, C.M. Dobson, Progressive Changes in the Structure of Hardened C3S Cement Pastes due to Carbonation, J. Am. Ceram. Soc. 74 (11) (1991) 2891–2896.
[48] V.G. Papadakis, C.G. Vayenas, M.N. Fardis, Fundamental modeling and experimental investigation of concrete carbonation, Materials 88 (1991) 363–373.
[49] CEMBUREAU, Cementing the European Green Deal (Brussels), in: C.-T.E. C. Association (Ed.), REACHING Clim. NEUTRALITY Cem. Concr. VALUE CHAIN 2050 (2020) 38.
[50] T. Kikuchi, Y. Kuroda, Carbon Dioxide Uptake in Demolished and Crushed Concrete, J. Adv. Concr. Technol. 9 (1) (2011) 115–124.
[51] X. Fang, D. Xuan, C.S. Poon, Empirical modelling of CO2 uptake by recycled concrete aggregates under accelerated carbonation conditions, Mater. Struct. 50 (4) (2017) 200.
[52] L. Rosa, V. Becattini, P. Gabrielli, A. Andreotti, M. Mazzotti, Carbon dioxide mineralization in recycled concrete aggregates can contribute immediately to carbon-neutrality, Resour., Conserv. Recycl. 184 (2022) 106436.
[53] H.-J. Ho, A. Iizuka, E. Shibata, H. Tomita, K. Takano, T. Endo, Utilization of CO2 in direct aqueous carbonation of concrete fines generated from aggregate recycling: Influences of the solid–liquid ratio and CO2 concentration, J. Clean. Prod. 312 (2021) 127832.
[54] T. Wang, Z. Yi, J. Song, C. Zhao, R. Guo, X. Gao, An industrial demonstration study on CO2 mineralization curing for concrete, iScience 25 (5) (2022) 104261.
[55] L. Izoret, T. Pernin, J.-M. Potier, J.-M. Torrenti, Impact of industrial application of fast carbonation of recycled concrete aggregates, Appl. Sci. (2023).
[56] C. Shi, Y. Li, J. Zhang, W. Li, L. Chong, Z. Xie, Performance enhancement of recycled concrete aggregate – A review, J. Clean. Prod. 112 (2016) 466–472.
[57] K. Ouyang, C. Shi, H. Chu, H. Guo, B. Song, Y. Ding, X. Guan, J. Zhu, H. Zhang, Y. Wang, J. Zheng, An overview on the efficiency of different pretreatment techniques for recycled concrete aggregate, J. Clean. Prod. 263 (2020) 121264.
[58] D. Xuan, B. Zhan, C.S. Poon, Assessment of mechanical properties of concrete incorporating carbonated recycled concrete aggregates, Cem. Concr. Compos. 65 (2016) 67–74.
[59] R. Infante Gomes, C. Brazão Farinha, R. Veiga, J. de Brito, P. Faria, D. Bastos, CO2 sequestration by construction and demolition waste aggregates and effect on mortars and concrete performance - an overview, Renew. Sustain. Energy Rev. 152 (2021) 111668.
[60] J. Skocek, M. Zajac, M. Ben Haha, Carbon Capture and Utilization by mineralization of cement pastes derived from recycled concrete, Sci. Rep. 10 (2020).
[61] A. Gholizadeh-Vayghan, R. Snellings, Beneficiation of recycled concrete fines through accelerated carbonation, Mater. Struct. 55 (7) (2022) 171.
[62] M. Sereng, A. Djerbi, O.O. Metalssi, P. Dangla, J.-M. Torrenti, Improvement of Recycled Aggregates Properties by Means of CO2 Uptake, Appl. Sci. (2021).
[63] A. Leemann, F. Winnefeld, B. Münch, J. Tiefenthaler, Accelerated carbonation of recycled concrete aggregates and its implications for the production of recycling concrete, J. Build. Eng. 79 (2023) 107779.
[64] F. Kaddah, E. Roziere, H. Ranaivomanana, O. Amiri, Complementary use of thermogravimetric analysis and oven to assess the composition and bound CO2 content of recycled concrete aggregates, Dev. Built Environ. 15 (2023) 100184.
[65] B. Dündar, M.S. Tuğluca, H. Ilcan, O. Şahin, M. Şahmaran, The effects of various operational- and materials-oriented parameters on the carbonation performance of low-quality recycled concrete aggregate, J. Build. Eng. 68 (2023) 106138.
[66] D. Bastos, C. Brazão Farinha, C. Maia Pederneiras, R. Veiga, J.A. Bogas, R. Infante Gomes, A. Santos Silva, Pathway to carbon neutrality in the cement industry: CO2 uptake by recycled aggregates from construction and demolition waste, Appl. Sci. (2024).
[67] T. Haller, N. Beuntner, H. Gutsch, K.-C. Thienel, Challenges on pumping infra-lightweight concrete based on highly porous aggregates, J. Build. Eng. 65 (2023) 105761.
[68] DIN EN 197-1, Zement - Teil 1: Zusammensetzung, Anforderungen und Konformitätskriterien von Normalzement (Cement - Part 1: Composition, specifications and conformity criteria for common cements), Beuth-Verlag, Berlin, Germany, 2011, p. 8.

[69] DIN EN 13263-1, Silikastaub für Beton – Teil 1: Definitionen, Anforderungen und Konformitätskriterien (Silica fume for concrete – Part 1: Definitions, requirements and conformity criteria), Beuth-Verlag, Berlin, Germany, 2009, p. 22.
[70] DIN EN 14889-2, Fasern für Beton - Teil 2: Polymerfasern - Begriffe, Festlegungen und Konformität (Fibres for concrete Polymer fibres. Definitions, specifications and conformity), Beuth Verlag GmbH, Berlin, Germany, 2006, p. 25.
[71] DIN EN 1097-3, Prüfverfahren für mechanische und physikalische Eigenschaften von Gesteinskörnungen - Teil 3: Bestimmung von Schüttdichte und Hohlraumgehalt, 1998.
[72] DIN EN 1097-6, Prüfverfahren für mechanische und physikalische Eigenschaften von Gesteinskörnungen - Teil 6: Bestimmung der Rohdichte und der Wasseraufnahme; Tests for mechanical and physical properties of aggregates - Part 6: Determination of particle density and water absorption, Beuth Verlag, Berlin, Germany, 2022, p. 64.
[73] DIN 4226-3, , Zuschlag für Beton - Prüfung von Zuschlag mit dichtem oder porigem Gefüge (Aggregates for concrete, Test. Aggreg. Compact Or. Porous Struct.) (1983) 8.
[74] DIN EN 12350-6, Prüfung von Frischbeton - Teil 6: Frischbetonrohdichte, Beuth-Verlag, Berlin, Germany, 2011, p. 7.
[75] B. Kucharczyková, D. Kocáb, I. Rozsypalová, O. Karel, P. Misák, T. Vymazal, Measurement and evaluation proposal of early age shrinkage of cement composites using shrinkage-cone, IOP Conf. Ser.: Mater. Sci. Eng. 379 (1) (2018) 012038.
[76] M. Greim, Meas. Early Shrinkage Mortars (2011).
[77] DIN EN 992, Bestimmung der Trockenrohdichte von haufwerksporigem Leichtbeton, Beuth Verlag GmbH, Berlin, Germany, 1995, p. 5.
[78] DIN EN 1354, Bestimmung der Druckfestigkeit von haufwerksporigem Leichtbeton, Beuth Verlag GmbH, Berlin, Germany, 2005, p. 18.
[79] DIN E.N. ISO 22007-2, Kunststoffe - Bestimmung der Wärmeleitfähigkeit und der Temperaturleitfähigkeit, Teil 2: Transientes Flächenquellenverfahren (Hot-Disk-Verfahren) (ISO 22007-2:2015); Deutsche Fassung EN ISO 22007-2:2015, Beuth Verlag GmbH, Berlin, Germany, 2015.
[80] T. Haller, N. Beuntner, K.-C. Thienel, Optimized Building Envelope: Lightweight Concrete with Integrated Steel Framework, Materials 17 (6) (2024) 1278.
[81] DIN EN 1352, Bestimmung des statischen Elastizitätsmoduls unter Druckbeanspruchung von dampfgehärtetem Porenbeton und von haufwerksporigem Leichtbeton, Beuth Verlag GmbH, Berlin, Germany, 1997, p. 7.
[82] K.-C. Thienel, Besonderheiten bei Leichtbeton in DIN FB 100. Deutscher Ausschuss für Stahlbeton (Ed.), Heft 526 Erläuterungen zu den Normen DIN EN 206-1, DIN 1045-2, DIN EN 13670, DIN 1045-3, DIN 1045-4 und DIN EN 12620, Beuth Verlag, Berlin, 2011, pp. 80–84.
[83] DIN 4219-1, Teil 1: Leichtbeton und Stahlleichtbeton mit geschlossenem Gefüge - Anforderungen an den Beton, Herstellung und Überwachung, Beuth-Verlag, 1979, p. 4.
[84] A. C138/C138M-17a, Standard Test Method for Density (Unit Weight), Yield, and Air Content (Gravimetric) of Concrete, 2023.
[85] M. Schlaich, A. Hückler, Infraleichtbeton bietet die architektonische Freiheit für ein neues einfaches und baukulturell wertvolles Bauen. Monolithische recycelbare tragende Wärmedämmungen als echte Alternative zu mehrschichtigen Wandsystemen, Der Pr. üfingenieur 56 (2020).
[86] DIN EN 1992-1-1, Eurocode 2: Design of concrete structures - Part 1-1: General rules and rules for buildings, Beuth Verlag GmbH, Berlin, Germany, 2011, p. 241.
[87] DIN EN 1992-1-1/NA, Nationaler Anhang - National festgelegte Parameter - Eurocode 2: Bemessung und Konstruktion von Stahlbeton- und Spannbetontragwerken – Teil 1-1: Allgemeine Bemessungsregeln und Regeln für den Hochbau, 2013, p. 97..
[88] M. Thiery, P. Dangla, P. Belin, G. Habert, N. Roussel, Carbonation kinetics of a bed of recycled concrete aggregates: A laboratory study on model materials, Cem. Concr. Res 46 (2013) 50–65.
[89] S.-C. Kou, B.-j Zhan, C.-S. Poon, Use of a CO2 curing step to improve the properties of concrete prepared with recycled aggregates, Cem. Concr. Compos. 45 (2014) 22–28.
[90] S. von Greve-Dierfeld, B. Lothenbach, A. Vollpracht, B. Wu, B. Huet, C. Andrade, C. Medina, C. Thiel, E. Gruyaert, H. Vanoutrive, I.F. Saéz del Bosque, I. Ignjatovic, J. Elsen, J.L. Provis, K. Scrivener, K.-C. Thienel, K. Sideris, M. Zajac, N. Alderete, Ö. Cizer, P. Van den Heede, R.D. Hooton, S. Kamali-Bernard, S.A. Bernal, Z. Zhao, Z. Shi, N. De Belie, Understanding the carbonation of concrete with supplementary cementitious materials: a critical review by RILEM TC 281-CCC, Mater. Struct. 53 (6) (2020) 136.
[91] S. Scherb, M. Köberl, N. Beuntner, K.-C. Thienel, J. Neubauer, Reactivity of metakaolin in alkaline environment: correlation of results from dissolution experiments with XRD quantifications, Materials 13 (2214) (2020) 18.
[92] C.W. Hargis, B. Lothenbach, C.J. Müller, F. Winnefeld, Carbonation of calcium sulfoaluminate mortars, Cem. Concr. Compos. 80 (2017) 123–134.
[93] S. Smeplass, Moisture in light weight aggregates - practical consequences for the production properties of light weight aggregate concrete, in: S. Helland, I. Holand, S. Smeplass (Eds.), Second International Conference on Structural Lightweight Aggregate Concrete, Norwegian Concrete Association, Kristiansand, Norway, 2000, pp. 844–854.
[94] DIN EN 12350-7, Prüfung von Frischbeton - Teil 7: Luftgehalte - Druckverfahren (Testing fresh concrete - Part 7: Air content - Pressure methods), Beuth-Verlag, Berlin, Germany, 2019, p. 26.
[95] S. Chandra, L. Berntsson, Lightweight Aggregate Concrete, 1st ed., Noyes Publications, Norwich, 2002.
[96] Y. Liu, T. Tafsirojjaman, A.U.R. Dogar, A. Hückler, Shrinkage behavior enhancement of infra-lightweight concrete through FRP grid reinforcement and development of their shrinkage prediction models, Constr. Build. Mater. 258 (2020) 119649.
[97] S. Labbé, M. Lopez, Towards a more accurate shrinkage modeling of lightweight and infra-lightweight concrete, Constr. Build. Mater. 246 (2020) 118369.
[98] K.-C. Thienel, Precast elements of lightweight concrete with a porous matrix, BFT Int. 66 (1) (2000) 62–72.
[99] K.-C. Thienel, M. Peck, Die Renaissance leichter Betone in der Architektur, Zem. + Beton 4 (2010) 2–9.
[100] C. Lösch, P. Rieseberg, M. Schlaich, R. Leibinger, Building with Infra-lightweight Concrete, De Gruyter 2020.
[101] B. Lagerblad, Carbon Dioxide Uptake during Concrete Life Cycle - State of the Art, Swedish Cement and Concrete Research Institute, 2005.
[102] A.R. Richter, Thomas, Zement-Merkblatt Betontechnik B14 - Infraleichtbeton, in: I.B. GmbH (Ed.), 2022..

8 Appendix

A list of all publications prepared and talks given during the doctorate:

2025:

- **Haller, T.**, Scherb, S., Beuntner, N., Thienel, K.-Ch. *"Renewable construction with lightweight concrete – Reclaimed recycled material systems with CO_2-absorption"*. Construction and Building Materials 2025; 466:140339.
- Konferenzartikel 69. Betontage 2025. 11.-13. März, Ulm. **Haller, T.**, Beuntner, N., Thienel, K.-Ch. *„Recycling von Leichtbeton als Baustein für kreislauffähige und CO_2-speichernde Betonsysteme"*.

2024:

- **Haller, T.**, Beuntner, N., Thienel, K.-Ch. *"Optimized Building Envelope: Lightweight Concrete with Integrated Steel Framework"*. Materials 2024; 17(6).
- Vortrag und Konferenzartikel 68. Betontage 2024. 14.-16. Juni 2024, Ulm. **Haller, T.**, Berger, J., Köberl, M., Thienel, K.-Ch. *"Ressourcenschonendes Bauen mit Leicht- und Infraleichtbeton"*.
- Konferenzartikel Fachtagung Betonbau.aktuell. 20.02.2024, Apolda. **Haller, T.**, Beuntner, N., Thienel, K.-Ch. *"Infraleichtbeton – nachhaltig und innovativ"*.

2023:

- **Haller, T.**, Beuntner, N., Gutsch, H., Thienel, K.-Ch. *"Challenges on pumping infra-lightweight concrete based on highly porous aggregates"*. Journal of Building Engineering 2023; 65(5):105761.
- Vortrag 21. International Conference on Building Material ibausil. 13.-15. September 2023, Weimar. **Haller, T.**, Beuntner, N., Gutsch, H., Thienel, K.-Ch. *„Challenges on Pumping Infra-Lightweight Concrete Based on Highly Porous Aggregates"*.

2022:

- Vortrag und Konferenzartikel 66. Betontage 2022. 21.-23. Juni 2022, Ulm. **Haller, T.**, Thienel, K.-Ch. *"Mechanically and thermally optimized building envelope made of no-fines lightweight concrete"*.

2020:

- Thienel, K.-Ch., **Haller, T.**, Beuntner, N. *"Lightweight Concrete—From Basics to Innovations"*. Materials 2020; 13(5):1120.